CRANFIELD INSTITUTE OF TECHNOLOGY

SCHOOL OF MECHANICAL ENGINEERING

PH.D. Thesis

Academic Year 1988-89

RASHID MAHMOOD

STATIC AND DYNAMIC FINITE ELEMENT STRESS ANALYSIS OF LAYERED COMPOSITE PLATES AND SHELLS

Supervisors : DR. A.M.EL-Zafrany

: PROFESSOR R.A.Cookson

External Examiner : Mr. D.A.Thurgood
Chief Mechanical Engineer (rtd)
British Aerospace Dynamics Group

September 1989

TO MY SON FARAN,
WHO HAS BROUGHT
GREATEST HAPPINESS
IN MY LIFE.

ACKNOWLEDGEMENTS

The author is firmly indebted to Pakistan Space and Upper Atmosphere Research Commission for their sponsorship.

The author is extremely grateful to Dr.Zafrany, whose excellent tuition, valuable advice, continous encourgement and productive guidance has a vital role for the accomplishment of the work.

The author is thankful to Professor R.A.Cookson for his help, guidance and kind encouragement.

Finally author appreciate patience, love and kindness of his wife Ghazala shown in the course of this work.

SUMMARY

In this work an attempt has been made to develop theories for finite element static and dynamic stress analysis tailored for use with composite layered plates and shells in this way it was hoped to provide accurate values of the stresses particularly transverse shear stresses through the thickness, and to perform accurate natural frequency analysis by including non-linear effects such as centrifugal stiffening.

Initial derivations were based upon first order facet shell element analysis and first order curved shell element analysis. Subsequently, derivations were produced for higher order element analysis.

A programming package has been developed based upon the above derivations, and containing a banded solver as well as a frontal solver, capable of analysing structures build up from uniform or variable thickness layers and with a multiple number of layers having constant or variable dimension.

Results obtained with the aid of the present package have been compared with results derived from experimental work as well as with results derived from available analytical solutions. Investigations have been carried out for existing compressor blades, made of isotropic material and layered composite material, respectively. The results obtained from the package have been compared with available experimental results produced by RR or carried out at Cranfield. It has been shown that the above mentioned derivations produce comparable results and the package has proved to be reliable and accurate.

NOTATIONS

a	Translational Acceleration
Ω	Rotational Speed
N_i	Lagrangian Shape Function
H_i	Hermiatian Shape Function
ξ, η, ζ	Intrinsic Coordinates
x, y, z	Cartesian Coordinates
$\underline{\delta}$	Nodal Displacement Vector
$\underline{F}$	Nodal Force Vector
u, v, w	Displacement Components
ε_i	Normal Strain in i direction
γ_{ij}	Shear strain in i-j plane
$\underline{\varepsilon}$	Strain Matrix
$\underline{\varepsilon}_{xy}$	In-plane Strain matrix
$\underline{\varepsilon}_s$	Transverse Strain Matrix
$\underline{\sigma}$	Stress Matrix

$\underline{\sigma}_{xy}$ In-Plane stress matrix

$\underline{\sigma}_{s}$ Transverse stress matrix

E_i Young's Modulus in i-direction

G_{ij} Shear Moduli in i-j plane

ν_{ij} Poisson's ratio for transverse strain in the j-direction when stresses in the i-direction

l,m,n Directional Cosines

$\underline{B}$ Strain-Displacement Matrix

$\underline{D}$ stiffness Matrix

$\underline{D}_{11}$ Extensional Stiffness

$\underline{D}_{12}$ Coupling Stiffness

$\underline{D}_{22}$ Bending Stiffness

$\underline{S}$ Compliance Matrix

$\underline{J}$ Jacobian Matrix

ρ Density

U Strain Energy

V Potential Energy

W Work Done by External Loads

KE Kinetic Energy

LIST OF FIGURES

LIST OF TABLES

LIST OF APPENDICES

CONTENTS

CHAPTER THREE

CHAPTER FOUR

CHAPTER FIVE

CHAPTER SIX

CHAPTER SEVEN

CHAPTER EIGHT

CHAPTER 1

INTRODUCTION

1.1 Composite Materials

At their inception fibre-reinforced composites were hailed by the press and the popular scientific journals as a technological breakthrough which was to revolutionise, within a few years, our use of materials in structures and machines. Extravagant claims were made for their outstanding physical properties and low cost. It was predicted that the time was imminent when material properties would be as much subject to design specification as the product of which they were a part.

It was inevitable that with their first major technological setback, that is, their demonstrated unsuitability for use in an exposed application in a modern turbo-jet engine, a reaction should set in. It is arguable that fibre-reinforced composites are as much undervalued now as they were over-sold in the beginning. Over the past few years technological progress has continued quietly to improve the physical properties of composite materials and, equally important, to improve our understanding of how they may be used to greatest effect. At the core of this progress there has been extensive research into the behaviour of composite materials under realistic environmental conditions (corrosive environments, vibrational stress, extreme conditions of loading), and subject to the complex stress fields that occur in such materials due to their configurations, loading conditions and internal physical structure.

The word 'composite' means consisting of two or more distinct parts. Therefore, a composite material is formed when two or more materials are combined so that the properties of the composite are different, and usually better, from those of the individual constituents. The composites may often exhibit qualities that neither constituent possesses.

Composite material is, generally, a combination of fibres, typically glass, carbon or polyaramid embedded in a resin matrix. Fibres are the principal reinforcing or load carrying agent, while the matrix, typically epoxy, polyesters or polymids, are to support and protect the fibres and to provide a means of distributing and transmitting loads between fibres. Strength and stiffness of composites are determined by the orientation of the fibres. Maximum strength is achieved when the fibres are arranged in continuous strands, but the fibres can also be woven or randomly distributed to deal with specific load values to suit performance requirements. The study of composite materials actually involves many topics, such as anisotropic elasticity, strength of anisotropic materials and micromechanics etc.

The advent of fibre-reinforced composites, often referred to as laminates, has been hailed as the biggest technical revolution since the jet engine, because they possess such beneficial properties as high strength-to-weight ratio, stiffness-to-weight ratio, corrosion resistance, wear resistance, fatigue life, dimensional stability, fire resistance, crash-worthiness, and high rigidity. When one adds to these advantageous characteristics and superiority over traditional materials, the fact that most composite have excellent surface finish, low thermal conductivity, low maintenance costs and the

opportunity to reduce through-life costs, it may be seen just why they appear to be so attractive to the practising engineer.

The use of composite materials in the last two decades has increased not only in quantity but also in breadth of application. Applications range from medical devices, sports equipment, appliances, and automobile parts to high performance products such as aircraft, helicopters, satellites, spacecraft and satellite antennas. Growing confidence in composites has seen them spread from engine components and interior furnishings to large scale structural use for wings, tailfins and fuselages where their properties of light weight, high rigidity and excellent surface finish give aerodynamic and structural efficiency at cost-effective prices.

Composites give designers the freedom to optimise material performance in different areas. A single composite can often be used to replace a number of complicated components, hence reducing assembly line costs and so influencing the overall production costs. Complex structures can be fabricated without welding or riveting separate pieces together.

The infinite variable configurations that are now possible with multiple composite lay-ups has meant highly sophisticated optimum design, where the ply stacking sequence, the fibre orientations, and the plate thickness are varied continuously over the structure.

The inherent advantage of fibre reinforced plastic is the possibility of arranging the fibres in such a manner as to optimise the load carrying capacity of the structure.

This purpose may be served by developing arrangements that reduce stress concentrations along the edge of a circular hole in the composite plate.

The skill of designing in composite materials is still relatively young and its potential has not yet been realised fully. Little advantage has as yet been taken of the great variety of fibre arrangements that can be introduced into composite design, a possibility that does not exist with metals which are essentially isotropic.

Trends in the aerospace industry show that the use of advanced composites will continue to grow in this and other sectors. Without doubt, composites will be playing an increasing role throughout industry. The work on composite materials is representative of the progress that is being made in these areas, and indicates the degree to which our understanding of fibre-reinforced composite materials is gradually progressing to a stage at which, perhaps composite materials will eventually fulfil the initial claims that were made for them. Together with ceramics, carbon-carbon, and metal matrix composites, the fibre-reinforced composite form a family of advanced materials that will, in turn, be as significant for industrial progress in the 21st century as was iron and steel in the industrial revolution of the 19th century.

1.2 Finite Element Method

In practice, most engineering problems are too complicated for a closed form mathematical solution. A numerical solution is required for the analysis, and the

most versatile method discovered to date is the finite element method (FEM), which may be defined as a numerical procedure for solving continuum mechanics with an accuracy acceptable to engineers.

In many numerical solutions an adequate model is obtained using a finite number of well defined components, such problems are discrete. In others the subdivision is continued indefinitely, hence, containing an infinite number of elements, such problems are called continuous.

The FEM is a method of approximation for continuum problems where the continuum is divided into a finite number of parts. The behaviour of this discretised continuum is specified by a finite number of parameters and the solution of the complete system, as an assembly of its elements, follows precisely the same rules as those applicable to standard discrete problems.

In structural analysis, the FEM can be understood as an extension of earlier established analytical techniques in which a structure was represented as an assemblage of discrete truss and beam elements. The same matrix algebraic procedures are used, but instead of truss and beam members, finite elements (FEs) are employed to represent regions of plane stress, plane strain, axisymmetric, three dimensional and plate or shell behaviour.

The success of FEM is based largely on the basic FE procedures used: the formulation of the problem in variational weighted residual form, the FE discretisation of this formulation, and the effective solution of the resulting FE equations. The FEM may be divided into various steps. The first step is to determine the element properties from geometry, material and loading conditions. Subsequently, the structure under consideration is divided

into subregions called finite elements (FEs), this process of domain discretisation being known as mesh generation. The FEs are connected at well defined points called nodes. Arrangements of elements and nodes are known as a mesh. Hence a continuum, with an infinite degrees of freedom (DOF) is represented by a discrete model with finite DOF. Moreover, as the number of FEs is increased with reduced dimension, the behaviour of the discrete system converges to that of the continuum system. Further, the position and the elastic properties of each element are defined so that the displacement of each element can be related to the forces on that element, therefore each element has its own identifying number and nodal connection.

The next step in the FEM is the most essential part and the core of the FE program,i.e. the formulation of the global stiffness matrix, which is essentially the assembly of the equations concerning those elements which contribute to a particular node. The global matrix of the structure relates the displacements at the nodal points of each element to the external forces acting on the system. The next step is to insert the boundary conditions into the assembled equations. The system of equations can be solved once the prescribed support displacements have been substituted, hence, reducing the number of equilibrium equations. Numerous solver techniques may be applied for solution of the reduced system of the matrix equation. Thereafter, unknown parameters, i.e., displacement, stresses, and internal forces are found for every node.

The formal presentation of the FEM is attributed to Turner, Clough, Martin and Topp [100], who applied the equations of classical elasticity to plane stress problems.

It was Clough [57] who first used the term 'Finite Element' in his paper 'the FEM in plane stress analysis'. Clough presented the method as an extension of structural analysis techniques to the solutions of problems in continuum mechanics.

During the earlier development of the FEM for structural analysis, almost all emphasis was directed towards the development of effective FE for the solution of specific problems. However, the very broad potential of the method was rapidly recognised and more general techniques for structural analysis were developed while at the same time important applications were found in other fields.

The FEM has evolved over the past 30 years as the most powerful numerical technique for the solution of solid mechanics problems. It has been applied to problems in many disciplines and, indeed, many major advances in structural design, component design, advanced material technology, emerging material technology and aerospace applications (to name a few) would not have been possible without the employment of FE solutions. While much progress has been made and FE analyses are performed routinely today, there are still many new problems to be explored with the aid of this powerful method.

The problem of validation of the results of a FE analysis is a complex one, due to the number of possible factors which can result in an invalid solution. Traditionally new FEs and FE programs have been subjected to tests which validate the theoretical development of the elements and the computer code itself. However, poor modelling can still destroy the solution. For example, excessive discretisation error can result from poor mesh design. Approximation errors also result from the theoretical basis of any particular analysis, such as an

assumption of linear behaviour or from the use of elements based on approximate engineering theories, such as the Kirchhoff hypothesis for thin plates.

Error diagnosis contained in most of the commercial FE systems searches for poor element geometry and senses the presence of round-off error. However, the user is left with the task of assessing the accuracy of the solution given the discretisation and modelling approximations which can be made. In part, this problem can be answered by refining the mesh and increasing the accuracy of the theoretical basis of the analysis, a procedure which can prove to be very expensive.

1.3 Plates and Shells

Plates and shells are respectively initially flat and curved structural elements, for which the thicknesses are much smaller than the other dimensions. Included among the more familiar examples of plates are table tops, street manhole covers, side panels and roofs of building, turbine discs, bulkheads, and tank bottoms. Examples of shells include pressure vessels, aeroplane wings, pipes, the exterior of rockets, missiles, automobile tyres, incandescent lamps, caps, roof domes, factory or car sheds, and a variety of containers. Each of these examples has walls that are curved.

Generally we treat plates by dividing the thickness into two equal components by a plane parallel to the faces. This plane is called the midplane of the plate. The flexural properties of a plate depends greatly upon its thickness in comparison with its other dimensions.

According to a criterion often used to define a thin plate (or for the purpose of technical definition) the ratio of the thickness to the smaller span should be no greater than 1/20.

As long as a curved plate can be viewed as a portion of a shell, the general equations of shells are also applicable to curved plates and vice versa. Again, the thickness of a shell is small in comparison with the other dimensions. As in the treatment of plates, the plane bisecting the shell thickness is called the midsurface. To describe the shape of a shell, we need to know only the geometry of the midsurface and thickness of the shell at each point. Shells of technical significance are often defined as thin when the ratio of thickness to the radius of the curvature is equal to or less than 1/20.

When contemplating the incorporation of plates into a specific design of component or system, it is necessary to determine the most appropriate plate shape and to select the most efficient material in order to resist a given system of forces under specified conditions of operation. A basic understanding of material behaviour and evaluation of most likely mode of failure under anticipated conditions of service are essential for this purpose. The rational design of plates and shells relies greatly upon their stress and deformation analysis.

The analysis of plate/shell structures often embraces two distinct, commonly applied, theories. The first of these, the membrane theory, usually applies to a rather large part of the body. A membrane either flat or curved, is identified as a body of the same shape as a plate or shell, but incapable of conveying moments or shear forces. In other words, a membrane is a two-dimensional analogue of a flexible string. The second, the bending theory, or

general theory, includes the effects of bending. Thus, it permits the treatment of discontinuities in the stress distribution taking place in a limited region in the vicinity of a load or structural discontinuity. However, information relative to membrane stresses is usually of much greater practical significance than the knowledge of the bending stresses. Bending theory generally comprises a membrane solution, corrected in those areas in which discontinuity effects are significant. The goal is thus not the improvement of the membrane solution, rather the analysis of stresses and strains owing to the edge forces or concentrated loading, which cannot be accomplished by membrane theory alone.

It is important to note that the membrane forces are independent of bending and are defined by the conditions of static equilibrium. As no material properties are used in the derivation of these forces, the membrane theory applies to all plates/shells made of any material (e.g., isotropic, anisotropic, homogeneous, non-homogeneous).

The design of the composite plate/shell is usually based on the so-called laminate theory. The theory is often useful in synthesising the overall mechanical properties, e.g. stiffness and compliance, of laminates of either symmetric or general type. The laminate theory takes into account the orthotropic or anisotropic properties of constituent unidirectional lamina and the non-uniform ply stress distribution in the laminate.

Composite plates/shells, made of several plies of fibre-reinforced composite, develop interlaminar stresses which may prove to be critical to the integrity of the structures. These stresses are responsible for delamination and eventual failure of the laminated structure. The most serious problem of stress concentration in a laminate is

the occurrence of the interlaminar shear concentration near to the free edges or in the boundaries of the laminate. This problem, often referred to as the edge effect, is due to heterogeneity of the laminate and therefore, is a material characteristic.

1.4 Work Objectives

The major objective of this work is to develop an efficient finite element static and dynamic stress analysis method program package tailored for use with laminated composite plates and shells. By developing new derivations such as higher order elements, extending existing theories similar to curved shell elements, and including non-linear effects such as centrifugal stiffening, it is hoped to produce a very efficient system. The developed analysis should be capable of calculating very accurate values of the stresses particularly the transverse shear stresses, through the thickness and also calculate accurate natural frequencies of free vibration of stationary and rotating bodies.

Subsequently, the derivations are to be used for the development of a programming package which is to be capable of carrying out the analysis accurately at a fast pace and at low cost. The successful accomplishment of this project will result in reliable results produced in reasonable CPU time. It is also hoped in this thesis to compare the results obtained by the developed theories with experimental results and/or with other available analytical solutions and, thereafter, discuss the verification of the final results.

1.5 Thesis Layout

The major part of this thesis represents a detailed guide for the developed finite element theory and its application. However, chapter two contains a comprehensive literature review on the subject of interest, whilst chapter three contains work on the development of the constitutive equations for laminated composite plates/shells, describing the construction of various stiffness matrices.

Chapters four and five involve derivations for the first order plate and shell elements, respectively, which also include centrifugal stiffening.

Chapter six gives details of original work on the derivation of a high order element for plate analysis, while chapter seven includes the analytical derivation for centrifugal stiffening of the element.

A general description of the present programming package is reviewed in chapter eight. Results and discussion of the validation of the package together with engineering case studies, including some useful experimental work, are summarised in chapter nine, and the final conclusions are summarised in chapter 10.

CHAPTER 2

LITERATURE REVIEW

In recent years, both theory and observations of fibre reinforced composites have advanced dramatically. Review of this subject includes publications on theory by Hashin [1], Sendeckyj [2], and Walpole [3], and on experiments by Bert [4].

In practice, two types of fibre reinforcement occurs: continuous-fibre and short-fibre (chopped fibre). Most studies consider only the first type [5].

Development of advanced reinforcement materials, having high specific strength and stiffness, has provided designers with considerable potential for weight saving. A necessary precursor to the effective design of composite structure is reliable knowledge of strength and stiffness properties. At present, only uniaxial deformation behaviour has been, to some extent, investigated thoroughly [8]. Little relevant data has been collected for more complex forms of deformation [9].

Analysis reported in the literature for layered systems can, for the most part, be divided into two categories [10]. The first is connected with the detailed response of a single layer subjected to idealised loading conditions. Such analysis give insight into the fundamental behaviour of layered systems; this knowledge is a prerequisite for the construction of general composite theories applicable to large scale systems. Both approximate analytical and numerical solutions have been used for the study of single layer configurations (e.g.,see 11,14). The second category is primarily concerned with the overall response of layered structural components and

secondarily with the detailed stress distribution in individual layers.

There are two classical approaches to the finite element (FE) analysis of composite materials [15,16]. They differ in their underlying descriptions of the layered systems, i.e., discrete or composite. In a discrete analysis the detailed inhomogeneous nature of the system is modelled so that all material interfaces fall along element boundaries (thus such elements contain only one type of material). Because of the complicated nature of the layer interaction, in general for this type of modelling, very fine grids are required [16]. An alternative to the discrete representation is to model the layered system as an equivalent homogeneous, orthotropic continuum material [8]. Analysis using such representations are called composite analysis. Because the detailed geometry of the layering is not represented, rather coarse grids may be used [18].

The advantage of discrete analysis is that the local stress and strain states at, and near, the layer interfaces, and at the edges of the body, are directly calculated. The chief disadvantage (often rendering the method entirely impractical) is the excessive computational cost required for the analysis of two- and three-dimensional systems with a large number of layers, and when non-linear or inelastic effects, or both, must be included. The advantage of composite analysis lies in its low computational cost. However, for the class of layered composites of interest here, if certain edge effects are not included, they are of limited value [17, 19].

It has been the objective of a number of investigations to develop extended composite analyses which retain the simplicity and cost effectiveness of conventional composite analyses, whilst maintaining accuracy in predicting local stress states almost as good as for discrete analyses. One procedure is to use an overall crude discrete representation with sub-structuring in critical regions [19]. A second method is to form a composite stiffness matrix by directly adding stiffness matrices for the individual layers occupying the domain of the composite element and for fictitious bond links modelling their interaction [15,18]. A third approach is to model the layered system by a higher order continuum theory capable of accounting for material microstructure [20]. Lastly, several attempts have been made to derive a more comprehensive composite theory by not only satisfying the continuum equations for the heterogeneous (layered) solids in an average sense (usually composite theory), but, in addition, including high order effects (such as first moments etc.) [21].

Because they are well established and understood, the Kirchhoff plate and shell theories have formed the basis for the formulation of plate and shell elements from the beginning. In conjunction with the principle of minimum potential energy, they demand the continuity of the normal slope across the element boundaries for the formulation of conforming plate or shell elements.

A number of articles dealing with transverse shear deformation have appeared in the literature. These include Basset [22], Reissner [23-25], Hildebrand, Reissner and

Thomas [26] and Mindlin [27]. Other references can be found in reference 28. These theories can be classified into two major classes on the basis of assumed fields: (1) stress based theories [23-25] and (2) displacement based theories [21,26].

The stress based theories are derived from an assumed stress field, which are assumed to vary linearly over the thickness of the field. The transverse normal and shear stresses are then derived from the equilibrium equations of the three-dimensional problem in the theory of the elasticity. The governing equations for the theory are derived using a stationary variational theorem. While displacement based theories are derived from an assumed displacement field and the governing equations are derived using the principle of minimum total potential energy.

There are two theories in use that predict the strength of the unidirectional composite material. They are : the maximum strain theory and the quadratic failure criterion [8]. The equations of the maximum strain theory are the equations of the maximum stress theory when Hooke's law is applicable to rupture. This is a non-interactive criterion which also determines the mode of failure. For some materials the maximum strain theory is a reliable measure of strength; and it is worth noting that strain at a point is a measurable quantity, whilst stress is not. The quadratic failure criterion is an interactive failure criterion and the expression includes coefficients of the stress terms which are characteristics of material to be determined by experiment.

A serious failure mechanism for laminated composite materials is edge delamination. Various numerical methods have been used in attempts to calculate the interlaminar stress components that precede delamination in a finite

width angle-ply laminate under uniform axial strain [30-33]. These efforts have resulted in serious discrepancies in the reported behaviour for the interlaminar stress distribution near to an interface corner [33]. For example, a finite difference procedure [31] predicts, tensile interlaminar normal stress at an interface corner, while finite element methods [32,33] predict compressive normal stress in this region. Furthermore, some uncertainty exists regarding the character of the in-plane, interlaminar normal and shearing stress distribution near an interface corner as predicted by FEM [32-34].

The presence of a free edge in composite laminates often gives rise to a complex three-dimensional stress field with steep gradients. It is thought that [35] delamination and matrix microcracking occurring near free edges are due to steep interlaminar stress gradients in the free edge region. A composite laminate is usually modelled as homogeneous anisotropic layers sharing common boundaries between them. In reality, however, there exists a thin soft matrix layer between the plies. Singularities are inherent in the formulation when there is an abrupt change in material property across common boundaries.

For the case of layered composite materials, experimental observations indicate that the failure modes are, in general, either along the interface between the layers or transverse to the layers [35]. The stress singularities at the free edge were investigated and it was shown [36] that, except for certain special combinations of the ply-angles on both sides of the interface, the stresses have the logarithmic singularity at the free edge in addition to the $\bar{r}^{K}(K>0)$ singularity. Moreover, unlike the $\bar{r}^{K}$ singularity whose existence depends on the stacking sequence of the layers and the complete boundary

conditions, the existence of the logarithmic singularity at a point depends only on the ply angles on both sides of the interface. Instead of delamination, a transverse crack may occur in the layer [35].

Recently, a considerable amount of research activity has been devoted to the study of failure mechanisms in composite materials [37]. Failure in these materials often begins as matrix microcracking and delamination. These modes of damage are essentially 3-D in nature and generally caused by interlaminar stresses. Steep stress gradients are encountered in regions such as free edges, ply termination, zones of delamination and voids and holes. An example is the classical finite width free-edge problem [38] associated with a composite laminate in uniform axial extension, a problem which has been studied by many investigators. The analyses are based on the use of the finite difference [38], FE [39], FE including fracture mechanics concepts [39,40], boundary layer [41], energy based approximations [42] and extended Galerkin [43] procedures. Conventional laminate theories are inadequate for this purpose as they are based on global displacement assumptions. Moreover, the interlaminar stresses are often neglected in the initial formulations. Therefore, the final solution cannot yield realistic stress distributions. A survey of these solutions appears in references 42 & 44. With the exception of the results in reference 43, all other solutions are numerical. The presence of stress singularities poses a severe obstacle to the implementation of numerical procedures. As a result, the computed stresses are not universally accurate. Different distributations for the transverse normal stress are reported by several authors for an angle-ply laminate. Reasons for this anomaly are explored at length in reference [33]. Numerical solutions are also not economical. For the accurate determination of the edge stresses, one requires extensive

modelling of the response variables in the edge region. Wang and Crossman [39] employed 16 elements in the thickness direction within each layer in the region of steep stress gradients and a total of 192 elements per layer. Different discretizations were used in reference [40] with a fine mesh having 1833 nodes and 576 elements.

In an earlier study of laminated composites, Pryor and Baker [46] presented a two-dimensional analysis for rectangular plates which included transverse shear deformations. This was accomplished by allowing the normal perpendicular to the middle surface to rotate but still remain straight. In the analysis, the properties of the individual layers with arbitrarily oriented fibres were integrated through the thickness of the plate to give one matrix relating the stress resultants to the deformation states at the middle surface. Comparisons with an elasticity solution for cylindrical bending by Pagano [47] indicate that when there exists a large difference in material properties between layers, the normal to the middle surface is severely distorted and a single straight line rotation through the thickness is not adequate.

To remove the restrictions of one straight line rotation through the plate thickness and the application to rectangular shapes, a curved isoparametric element [48] with cubic displacement expansion in planform, and a linear variation through the thickness, is used [49] for each layer of the laminate. A similar element was developed by Ahmad and co-workers [50] and was applied to isotropic plates and shells by condensing the six degrees of freedom (DOF) on a line through the thickness to five DOF at the middle surface. The DOF associated with change in thickness was replaced by the assumption that the normal stress in the thickness direction must vanish. Comparisons with three-dimensional elasticity solutions are in agreement and

show [49] the necessity for having individual elements for each layer when they have different fibre orientations and when the plates are thick.

The static or dynamic analysis of multi-layer composite laminates using three-dimensional FE models often results in high computational cost because of the large number of DOF pertaining to the formulation scheme. When there is a region of high stress concentration in the laminate, a common approach is to have a finer mesh near the region [34,54]. Consequently, the number of DOF is increased quite substantially. An accurate modelling of structure using the conventional fully assembled 3-D FE will certainly result in enormous computational cost. The necessity to reduce computational cost provides the incentive to formulate the 3-D super element scheme [56] which can reduce substantially the computational cost for analysis of multi-layered laminates. Wang and Crossman [19] also reported a super element scheme for analysis of multi-layer laminates. However, the formulation of their [19] super element is based on classical lamination theory whilst the basis of the formulation [56] of the super-element scheme is 3-D elasticity theory. Super-element schemes can be quite useful for analysis of high stress concentration in a laminate plate, by modelling the immediate region by ordinary elements and rest of the element by super-elements.

The hybrid-stress model is based upon a modified energy principle in which equilibrated stresses within the elements, and elemental displacements at the boundary, are independently interpolated. This model is well suited to the analysis of multi-layered laminated plates as has been demonstrated by a number of studies [58-60]. In studies of single layer hybrid-stress plate elements, including transverse shear effects, [61-63] Spilker and Munir

demonstrated that proper choice of the element spanwise stress distribution would produce an element of correct rank which was free from locking in the thin plate limit. In reference 64, Spilker extended the eight-node single-layer element of reference 62 to a multilayer element, and studied alternative forms of the stress fields within the layer to determine the nature of the constraints for laminated elements in the thin plate limit. A multi-layer element was identified which has behaviour similar to the single-layer element of reference 62. The single layer plate elements of reference 61-63 were subsequently re-examined to determine whether a non-locking element of correct rank could be defined which was naturally invariant with respect to co-ordinate frame translation and rotation. An eight-node isoparametric element (QH3) which satisfies these criteria and which allows for independent layer stress and displacement fields, was identified [65].

The problem of finite width laminates under uniform extensional strain was first analysed by Pipe and Pagano [30]. The formulation was based upon anisotropic elasticity and the solution was obtained using a finite difference scheme. A number of investigations have subsequently been conducted into this problem with a fairly wide range of approaches. Quasi-3D FE approaches which utilise plane strain plate-elements can be found in references [34,40,66]. Hsu and Herakovich [31] have obtained a solution using a perturbation technique. Singular hybrid-stress FE models have been employed by Spilker and Chou [67], and Wang and Yuan [68]. The latter work was based upon the theory of anisotropic elasticity and Lekhnitskii's stress potentials [69]. A fully 3-D formulation with a three-dimensional finite-difference solution scheme was given in reference [70]. Recently a global-local laminate variational model has been proposed

by Soni and Pagano [44]. A review of free edge stress problem, with comparative assessment, can be found in references [66,71,72].

Composite materials and reinforced plastics are increasingly used in automobiles, space vehicles and pressure vessels. With the increased use of fibre reinforced composites as structural elements, studies involving the thermo-mechanical behaviour of shell components made of composite are receiving considerable attention. The majority of the research papers in the open literature on shells is concerned with bending, vibration and buckling of isotropic shells [73]. As composite materials are making their way into many engineering structures, analyses of shells made of such materials become important.

FE analyses of shell structures have in the past [73] used one of the three types of elements: (1) a two dimensional element based on 2-D shell theory; (2) a three-dimensional element based on 3-D elasticity theory of shells; (3) a 3-D degenerated element derived from the 3-D elasticity theory of shells. The 2-D shell theory is derived from the 3-D continuum field equations via simplifying assumptions. These simplifications require the introduction of static and kinematic resultants, which are used to describe the equations of motion. The unavailability of a convenient general non-linear 2-D shell theory makes the 2-D shell element restrictive in its use. The degree of geometric non-linearity included in the 2-D shell element is that of the Von Karman plate theory. In contrast to the 2-D shell theory, no specific shell theory is employed in 3-D degenerated elements; instead, the geometry and the displacement fields are directly discretized, and interpolated, as in the analysis of continuum problems.

The analysis of plate and shell structures by the FE method has been an active area for more than a decade and a half. It has also led to the opening of new avenues of research into the FE theory, such as hybrid methods and isoparametric elements with reduced or selective integration.

There have been numerous developments of refined theories [29,74-76] aimed at capturing the intrinsic behaviour of transverse shear and normal stresses at both lamina interface and free edge. It is emphazied that the reliable and efficient utilisation of these developed formulations, in both linear and nonlinear design analysis, requires substantial research effort [77]. Reliable and efficient numerical methods are required so that they can be practically implemented in the design process. This is especially true when the development is extended to include non-linear analytical capabilities.

Recent refined engineering theories [33,44,78-80] for homogeneous plates and laminated plates provide appropriate models for the ply and sublaminate models, since they incorporate all of the essential physical efforts related to transverse shear strains, transverse normal strain and section warping etc. These efforts which are ignored by classical theories, can be significant in structures constructed of modern composite materials. The theories developed in [33,44,78-80] were applied [37] on a ply-by-ply basis to the free-edge problem and on a sublaminate basis to the compression problem and to the double-lap fracture specimen, and found adequate for predicting the behaviour of individual layers in equilibrium.

Iron and Draper [81] showed that it was impossible to form a Kirchhoff theory conforming triangular plate or shell element with simple nodal connections. To alleviate the problem, efforts were focused on element formulations based on plate and shell theories which relax the Kirchhoff assumptions. In this approach the displacements of the reference surface and rotations of the normals to the reference surface are independently assumed. Melosh [82] employed it for plate bending problems and Utku [83] applied it to shallow shell elements. Later Key and Beisinger [84] developed a quadrilateral element of thin shells. All of these elements, however, inherited problems of excessive stiffness for coarse meshes and slow convergence rates.

To overcome the above disadvantages in an otherwise attractive approach, the imposition of the Kirchhoff hypothesis at a discrete number of points in the structure was proposed and used by Wempner et al.[85]; this scheme later became known as 'discrete Kirchhoff theory (DKT)'. The Kirchhoff assumption is imposed in a discrete way: the rotations are forced to coincide with the first-order derivatives of the lateral deflection at some selected points in the FE.

In DKT the bending energy is calculated from the independently-assumed normal relations. To force the convergence of the solution to that of the Kirchhoff theory, the Kirchhoff hypothesis is enforced at the nodal points in the structure. Thus, at the nodal points the normal rotations are expressed in terms of the reference surface displacements and one arrives at a conforming plate or shell element with conventional DOF as nodal connection quantities.

A limited number of applications, using this approach, are found in the literature. Wempner et al. [85] proposed a rectangular shell element on the reference surface co-ordinate based on DKT. Although the formulation was for general shells, the applications were limited to plates and cylindrical shells. Dhatt [86] has developed a number of triangular curved shell elements with 27 DOF, based on shallow-shell theory with discrete Kirchhoff constraints. Extensive numerical results are presented to show, in general, the accuracy and efficiency of the curved shell element based upon DKT. However, Dhatt [86] recognised the need to replace the shallow-shell formulation by a more accurate curved element formulation based on deep-shell theories.

Key and Beisinger [87] recognised the potential of a formulation based on DKT, and sought to develop an arbitrary thin shell element. Although they present the linear shear theory for an arbitrary shell, their 36 DOF 'KB6' quadrilateral element is embedded in the middle surface of a shell of revolution. Baltoz and co-workers have developed a 27 DOF triangular deep-shell element [88-92] for linear and geometrically non-linear analysis of general shells, based on discrete Kirchhoff theory. Extensive results, typical of pre-and-post buckling behaviour of shallow and deep shells, were also presented. Although the formulation of Boltz [88] included multilayered composite construction, no numerical results for composite shells were presented. In a recent review [92] of discrete Kirchhoff elements, it was concluded that these elements are simple, efficient and reliable from the point-of-view of researchers and engineering users for the analysis of general thin plate and shell structures.

The most recent efforts in application of DKT to the analysis of thin shells is presented by Nagtegaal and Slater [93], where a quadrilateral element, closely related to the 'semiloof' element, but using lower order interpolation functions, which they call a 'semiloof incompatible discrete Kirchhoff (SLICK)' element, is developed. Only comparisons with other higher order isoparametric thin shell elements are presented. Thus, its performance in comparison with thin shell elements cannot be assessed. In a recent work [93], a triangular cylindrical shell element based on DKT was developed. It is a 3-node, 27 DOF element using cubic polynomials for the tangential and normal displacement interpolation. The formulation can be used for modelling general anisotropic representation of multi-layered, multi directionally oriented composite construction.

Determination of the transverse shear stress variation through the thickness of a laminated plate has assumed increasing importance because such a plate is more likely to fail due to delamination caused by the scissoring effects of these stresses. Analytical solutions are few and usually restricted to problems with simple loading and boundary conditions [94,95]. Most of the FE analyses are either based on classical lamination theory (CLT) which ignores the shear deformation effect altogether, or constant shear angle theory (CST) which assumes constant shear angle through the entire thickness [76,96-99,101]. The FE analyses that are based on layerwise constant shear angle theory (LCST) are due to Mau et al. [102], Mawenya et al. [103] and Seide and Chang [104].

However only Pryor et al. [96], Spilker et al. [97,98] and Mau et al. [102] have investigated transverse shear stress variation through the thickness. The linear displacement triangular element due to Seide and Chang [104] can only compute average transverse shear stress through the thickness of a layer. The quadrilateral element due to Mau et al [102] based on assumed the stress hybrid approach has the capability of obtaining the variation of the transverse shear stress through the thickness of a thick multilayered plate, by considering stresses as unknown nodal parameters and imposing constraints on the compatibility of these stresses at each interface. However, this method appears to be limited in its applicability, as the formulation of the stiffness matrix involves too many matrix inversions at the element level. More importantly, extension by Spilker et al. [97] to a triangular element shape has produced a stiff element, and traction free edge condition is not satisfied.

While quadrilateral element shape is adequate for plates with regular boundaries, use of triangular elements is more convenient for the representation of such irregular boundaries as holes and cut-outs. Seide and Chaudhuri [51,52] have developed a highly efficient and accurate triangular plate/shell element based on LCST and assumed quadratic displacement fields. Comparisons with numerical results obtained using CST [53] suggest that LCST is close the to elasticity solution whilst CST is closer to the CLT solution.

Extension of the theories in references 22, 26 and 27, which include the linear terms in Z (in the thickness direction) in u and v (in-plane displacements) and the only constant term in w (transverse displacement), to account for higher order variations and to laminated plates, can be

found in the works of Yang, Norris and Stavsky [105], Whitney and Pagano [106], Nelson and Lorch [107], and Lo, Christtensen and Wu [108] among others. Recently, Levinson [109], Murthy [110] and Reddy [111-113] presented refined plate theories that use the idea of Basset [22] and Hildebrand, Ressiner and Thomas [26] in expanding displacement in the powers of the thickness co-ordinates. The main novelty in these publications is to expand the in-plane displacements as cubic functions of the thickness co-ordinates, treat the transverse deflection as a function of the x and y co-ordinates, and eliminate the higher order functions from the equations of the assumed displacement field, by requiring that the transverse shear stresses be zero on the bounding planes of the plate.

Murthy's [110] work differs from Levinson's [109] in two respects: first, Murthy uses average displacement through the thickness; secondly, the theory is also developed for laminated plates. The work of Reddy [111-113] differs from the other two in two respects: first, the governing equations are derived from the principle of virtual work; secondly, it also accounts for the Von Karman (non-linear) strains. Phan and Reddy [114] presented a higher order shear deformation theory based on References 111-113 to analyse laminated anisotropic composite plates for deflections, stresses, natural frequencies and buckling loads. The theory accounts for the parabolic distribution of the transverse shear stresses. The FE model is based on the cubic interpolation of transverse deflection and linear interpolation of the in-plane displacement and rotations. The theory does not account for the normal transverse

stress. A similar theory was presented by Reddy [112], containing the same number of dependent variables as in the first order shear deformation theory, which satisfies the zero tangential traction boundary condition on the surface of the plate, and produces more accurate results than does the first order shear deformation theory.

FE analyses of the large-displacement theory of solids are based on the principle of virtual work or the associated principle of stationary potential energy. Horrigmoe and Bergan [118] presented classical variational principles for non-linear problems by considering incremental deformations of a continuum. A survey of the various principles, in incremental form, is presented by Wunderlich [119]. Stricklin et al [120] presented a survey of various formulations and solution procedures for non-linear static and dynamic structural analysis. The only large-deflection analyses of laminated composite shells that can be found in the literature are the static analyses of Noor and Hartley [121], and Chang and Sawamiphakdi [122]. Noor and Hartley employed the swallow shell theory with transverse shear strains and geometric non-linearities in order to develop triangular and quadrilateral FEs. Chang and Sawamiphakdi presented a formulation of the 3-D degenerated element for geometrically non-linear bending analysis of laminated composite shells. The formulation is based on the updated Lagrangian description and does not include any numerical results for laminated shells.

The analytical approach provides reliable estimates of interlaminar stresses for understanding, and ultimately resolving, failure in composite materials. The different analytical approaches can be easily explained if the complexities presented by the free edge, holes, joints and ply discontinuities are recognised. Among the many analytical approaches suggested for this class of problem,

is the ply/sublaminate level analysis first proposed by Pagano [42,44] wherein each layer, or a sublaminate in a laminate, is treated separately, appears to be most promising.

Approximate procedures, which assume specific forms for the stress distributions near to the free edge and which utilise elastic equations of equilibrium, have also been employed with some success [116,117]. The main intention of these particular reports was to present procedures for the design of laminates with appropriate stacking sequence such that the resulting laminates are less likely to develop high interlaminar stresses and subsequent failure in the free edge region.

The objective of the present work has been stated to include FE dynamic analysis of composite plates and shells, that is to analyse the natural frequencies of free vibration of rotating composite plates and shells. The effect of rotation is highly significant since centrifugal forces act on the body which, together with the elastic restoring forces on the moving body, cause an increase in the natural frequencies of free vibration. Therefore, essentially, natural frequencies of free vibration increase with increasing rotational speed. Most of the work in the open literature, involving centrifugal stiffening, is concerned with isotropic materials only. A brief description of the literature on the subject is given in order to provide the background and impetus leading to the investigation.

Kane [120] studied the behaviour of a cantilever beam built into a rigid body that is performing a specific motion of rotation and translation. The analysis of Naidu [121] produced a method for estimating the stresses and deflections in a turbo-machinery disc. A very simple blade

impact analysis has been carried out by Cornell [122] which has been found to predict quite accurately the impact response and stresses within fan blades and similar structures.

Solids [123] concluded from his experimental measurement of strain, derived from the holographic technique, that if the vibratory behaviour is known, through a sufficiently large sample of normal modes, then the static behaviour may be calculated. Similarly, if the normal modes of a non-rotating body are known, its behaviour in a rotating system can be calculated. Thus, the centrifugal stiffening of a turbine rotor may be predicted from a knowledge of the spectrum of its normal modes. An analytical procedure was used [124] to perform a detailed analysis of high-tip-speed fibre composite compressor blades. The results indicated that the various vibration modes of these blade were highly coupled.

High performance flywheel systems differ significantly from turbine or compressor systems in two respects: the flywheel rim attachment to its hub is very flexible, for both translation and tilting, and these flexibilities depend upon the speed of rotation through centrifugal stiffening. The paper [125] describes analysis of free whirling, with suggestions for design improvement, stability analysis, response to unbalance and initial tilt, and non-linear analysis of supporting-band action.

Centrifugal stiffening, coupled with complex vibrating modes, implies a serious limit to the structural design of a gas turbine radial impeller in attempting a more favourable aerodynamic design. The paper [126] presents a rigorous FE structural method of analysis which, combined with the holographic technique, dealt with the highly stressed curved vanes and the vibration of the flexible

circular backplate so that the magnitude of the steady and vibratory stresses and of the thermal loading could be minimised. The method demonstrates a computerised procedure for the design of a modern impeller.

Kumar [127] showed that, for a rotating space boom, the difference in centrifugal stiffening for in-plane and out-of-plane vibrations is maximum for the first mode and become insignificant for higher modes. An approximate method, by Zeller [128] for including centrifugal stiffening, while allowing for a variable spin vector, was presented. The method involve the utilisation of geometric (or initial stress) stiffening matrices computed within the FE program in which the structure is modelled for until values of steady spin components and their products.

A survey of the literature on laminated composite materials leads to the following conclusions/issues:

(1) On many occasions the failure of the material is caused by interlaminar (transverse) stresses.

(2) A full 3-D FE analysis or elasticity solution is still not available for the free-edge stress problem.

(3) Much controversy exists regarding the nature and magnitude of the interlaminar stresses near the free edge.

(4) There is no work available in the open literature on centrifugal stiffening of laminated composite plates or shells.

(5) There is much scope for refinement and improvement to the existing procedures and theories applicable to the analysis of laminated composite plates and shells.

CHAPTER 3

CONSTITUTIVE EQUATIONS

3.1 Introduction

A lamina, which is a basic building block in a laminated fibre-reinforced composite, is a flat or curved assemblage of fibres in a supporting matrix. Thus, knowledge of the mechanical behaviour of a lamina is essential in order to understand the behaviour of laminated composite structures.

The stress-strain relations (generalised Hooke's law) have two commonly accepted manners of expression; compliance and stiffnesses as coefficients of stress and strain. The most attractive form of the stress-strain relations involve engineering constants, which are particularly helpful in describing composite behaviour as they are defined by the use of very obvious, and simple, tests.

An anisotropic material has properties that are different in all directions at any point in the body. There are no planes of material property symmetry and properties are a function of orientation at a point in the body. For such materials the stiffness matrix $\underline{D}$ (or compliance matrix $\underline{S}$, which is defined by the inverse of the stress-strain relation) has 36 constants, commonly known as elastic constants. However, it can be proved that these matrices are symmetric so that only 21 of the elastic constants are actually independent.

If there exists one plane of material property symmetry, the number of independent elastic constants reduces to 13. If orthogonal planes of material property symmetry for a material increase to two, symmetry will exist relative to a third mutually orthogonal direction and the material is said to be an orthotropic material. Hence, an orthotropic body has material properties that are different in three mutually perpendicular directions at a point in the body, and three mutually perpendicular planes of material symmetry. For this particular case, there are only nine independent constants in the stiffness matrix.

If, at every point in a material, there is one plane in which the mechanical properties are equal in all directions then the material is known to be transversely isotropic and the stress-strain relations have only five independent elastic constants. For the case of isotropic materials, however, there are infinite number of planes of material property symmetry, and, the material has only two independent elastic constants.

3.2 Stress-Strain Relationships for Orthotropic Materials

Let the stress and strain vectors at any point inside a continuum be defined as follow :

$$\underline{\sigma} = \{\sigma_x \ \sigma_y \ \sigma_z \ \tau_{xy} \ \tau_{yz} \ \tau_{zx}\}$$

$$\underline{\varepsilon} = \{\varepsilon_x \ \varepsilon_y \ \varepsilon_z \ \gamma_{xy} \ \gamma_{yz} \ \gamma_{zx}\}$$

For a uni- or bi- directional fibre-reinforced composite material with x', y', z' being its principal axes, then the strain-stress relation is:

$$\underline{\varepsilon}' = \underline{S}' \, \underline{\sigma}'$$

or

$$\underline{\sigma}' = \underline{D}' \, \underline{\varepsilon}'$$

where

$( )'$ refers to parameters with respect to x', y' and z' (material) axes.

$\underline{S}'$ is the compliance matrix

$\underline{D}'$ is the stiffness matrix

and, by definition:

$$\underline{D}' = \underline{S}'^{-1}$$

whereas for orthotropic materials the compliance matrix may be defined as below [55]:

$$\underline{S}' = \begin{bmatrix} 1/E_x & -\nu_{xy}/E_y & -\nu_{xz}/E_z & 0 & 0 & 0 \\ -\nu_{yx}/E_x & 1/E_y & -\nu_{yz}/E_z & 0 & 0 & 0 \\ -\nu_{zx}/E_x & -\nu_{zy}/E_y & 1/E_z & 0 & 0 & 0 \\ 0 & 0 & 0 & 1/G_{xy} & 0 & 0 \\ 0 & 0 & 0 & 0 & 1/G_{yz} & 0 \\ 0 & 0 & 0 & 0 & 0 & 1/G_{zx} \end{bmatrix}$$

such that,

E_i = Young's modulus in the i directions

G_{ij} = Shear modulus on the i-j plane

ν_{ij} = Poisson's ratio for transverse strain in the j-direction when stresses act in the i-direction

Since the above compliance matrix is symmetric, it can be shown that:

$$\nu_{ji}/E_i = \nu_{ij}/E_j$$

$$\nu_{ki}/E_i = \nu_{ik}/E_k$$

$$\nu_{kj}/E_j = \nu_{jk}/E_k$$

where,

$$i,j,k \equiv (x,y,z)$$

The local z axis will be assumed normal to the midplane of the composite lamina and in the direction of the material z' axis. For a given composite plate, x and y represent global axes (or local axes for the case of faceted shells), and it is easier to define the material axes (x' and y') with respect to x and y in terms of an angle Θ as shown in fig.3.1. For such a case the directional cosines of the material axes, with respect to the geometrical axes, are defined in terms of the following matrices:

$$\begin{bmatrix} \hat{i}' \\ \hat{j}' \\ \hat{k}' \end{bmatrix} = \underline{R}' \begin{bmatrix} \hat{i} \\ \hat{j} \\ \hat{k} \end{bmatrix}$$

where,

$$\underline{R} = \begin{bmatrix} m & n & 0 \\ -n & m & 0 \\ 0 & 0 & 1 \end{bmatrix}$$

such that

$$m = \cos\Theta$$

$$n = \sin\Theta$$

From the stress-rotation equations, it can be shown that:

$$\underline{\sigma} = \underline{R}_{\sigma}' \, \underline{\sigma}'$$

where:

$$\underline{R}_{\sigma}' = \begin{bmatrix} m^2 & n^2 & 0 & -2mn & 0 & 0 \\ n^2 & m^2 & 0 & 2mn & 0 & 0 \\ 0 & 0 & 1 & 0 & 0 & 0 \\ mn & -mn & 0 & m^2 - n^2 & 0 & 0 \\ 0 & 0 & 0 & 0 & m & n \\ 0 & 0 & 0 & 0 & -n & m \end{bmatrix}$$

It can also be shown that:

$$\underline{\sigma}' = \underline{R}_{\sigma}\ \underline{\sigma}$$

where

$$\underline{R}_{\sigma} = \underline{R}_{\sigma}'^{-1}$$

and $\underline{R}_{\sigma}$ can be obtained by putting n=-n in the above matrix.
Similarly, it can be shown that :

$$\underline{\varepsilon} = \underline{R}_{\varepsilon}'\ \underline{\varepsilon}'$$

or

$$\underline{\varepsilon}' = \underline{R}_{\varepsilon}\ \underline{\varepsilon}$$

where

$$\underline{R}_{\varepsilon}' = \begin{bmatrix} m^2 & n^2 & 0 & -mn & 0 & 0 \\ n^2 & m^2 & 0 & mn & 0 & 0 \\ 0 & 0 & 1 & 0 & 0 & 0 \\ 2mn & -2mn & 0 & m^2 - n^2 & 0 & 0 \\ 0 & 0 & 0 & 0 & m & n \\ 0 & 0 & 0 & 0 & -n & m \end{bmatrix}$$

Subsequently, $\underline{R}_{\varepsilon}$ can be obtained by putting -n instead of n in the above matrix expression, i.e.

$$\underline{R}_{\varepsilon} = (\underline{R}_{\varepsilon}')^{-1}$$

Using

$$\underline{\sigma}' = \underline{D}'\ \underline{\varepsilon}'$$

$\therefore$

$$\underline{\sigma} = \underline{R}_{\sigma}' \; \underline{\sigma}'$$

$$= \underline{R}_{\sigma}' \; \underline{D}' \; \underline{\varepsilon}'$$

$$= (\underline{R}_{\sigma}' \; \underline{D}' \; \underline{R}_{\varepsilon}) \; \underline{\varepsilon}$$

$$= \underline{D} \; \underline{\varepsilon}$$

where

$$\underline{D} = \underline{R}_{\sigma}' \; \underline{D}' \; \underline{R}_{\varepsilon}$$

Hence it can be shown that:

$$d_{11} = m^4 d_{11}' + n^4 d_{22}' + 2m^2 n^2 (d_{12}' + 2d_{44}')$$

$$d_{12} = m^2 n^2 (d_{11}' + d_{22}') + (m^4 + n^4) d_{12}' - 4m^2 n^2 d_{44}'$$

$$= d_{21}$$

$$d_{13} = m^2 d_{13}' + n^2 d_{23}'$$

$$= d_{31}$$

$$d_{14} = mn\left[m^2 d_{11}' - n^2 d_{22}' + (n^2 - m^2)(d_{12}' + 2d_{44}')\right]$$

$$= d_{41}$$

$$d_{15} = d_{51} = d_{16} = d_{61} = 0$$

$$d_{22} = n^4 d_{11}' + m^4 d_{22}' + 2m^2 n^2 (d_{12}' + 2d_{44}')$$

$$d_{23} = n^2 d_{13}' + m^2 d_{23}'$$

$$= d_{32}$$

$$d_{24} = mn\left[n^2 d'_{11} - m^2 d'_{22} + (m^2 - n^2)(d'_{12} + 2d'_{44})\right]$$

$$= d_{42}$$

$$d_{25} = d_{52} = d_{26} = d_{62} = 0$$

$$d_{33} = d'_{33}$$

$$d_{34} = mn(d'_{13} - d'_{23})$$

$$= d_{43}$$

$$d_{35} = d_{53} = d_{36} = d_{63} = 0$$

$$d_{44} = m^2 n^2 (d'_{11} + d'_{22} - 2d'_{12}) + (m^2 - n^2)^2 d'_{44}$$

$$d_{45} = d_{54} = d_{46} = d_{64} = 0$$

$$d_{55} = m^2 d'_{55} + n^2 d'_{66}$$

$$d_{56} = mn(d'_{66} - d'_{55})$$

$$= d_{65}$$

$$d_{66} = n^2 d'_{55} + m^2 d'_{66}$$

Explicitly:

$$\underline{D} = \begin{bmatrix} d_{11} & d_{12} & d_{13} & d_{14} & 0 & 0 \\ d_{21} & d_{22} & d_{23} & d_{24} & 0 & 0 \\ d_{31} & d_{32} & d_{33} & d_{34} & 0 & 0 \\ d_{41} & d_{42} & d_{43} & d_{44} & 0 & 0 \\ 0 & 0 & 0 & 0 & d_{55} & d_{56} \\ 0 & 0 & 0 & 0 & d_{65} & d_{66} \end{bmatrix}$$

Similarly, it can be shown that:

$$\underline{S} = \underline{R}_{\varepsilon}' \; \underline{S}' \; \underline{R}_{\sigma}$$

which can also be expressed explicitly as below:

$$\underline{S} = \begin{bmatrix} s_{11} & s_{12} & s_{13} & s_{14} & 0 & 0 \\ s_{21} & s_{22} & s_{23} & s_{24} & 0 & 0 \\ s_{31} & s_{32} & s_{33} & s_{34} & 0 & 0 \\ s_{41} & s_{42} & s_{43} & s_{44} & 0 & 0 \\ 0 & 0 & 0 & 0 & s_{55} & s_{56} \\ 0 & 0 & 0 & 0 & s_{65} & s_{66} \end{bmatrix}$$

Defining

$$\underline{\sigma}_s = \{\tau_{xz} \quad \tau_{yz}\}$$

$$\underline{\varepsilon}_s = \{\gamma_{xz} \quad \gamma_{yz}\}$$

then

$$\underline{\sigma}_s = \underline{D}_s \, \underline{\varepsilon}_s$$

$$= \begin{bmatrix} d_{11}^s & d_{12}^s \\ d_{21}^s & d_{22}^s \end{bmatrix} \underline{\varepsilon}_s$$

where

$$d_{11}^s = d_{66}$$

$$d_{12}^s = d_{56}$$

$$= d_{21}^s$$

$$d_{22}^s = d_{55}$$

In order to separate the transverse-stress terms from the above stiffness matrix, the expression for σ_z can be obtained as below:

$$\sigma_z = (d_{31}\varepsilon_x + d_{32}\varepsilon_y + d_{34}\gamma_{xy}) + d_{33}\varepsilon_z$$

subsequently, ε_z can be expressed as follow:

$$\varepsilon_z = (1/d_{33}) \left[\sigma_z - d_{31}\varepsilon_x - d_{32}\varepsilon_y - d_{34}\gamma_{xy}\right]$$

defining:

$$\underline{\sigma}_{xy} = \{\sigma_x \quad \sigma_y \quad \tau_{xy}\}$$

$$\underline{\varepsilon}_{xy} = \{\varepsilon_x \quad \varepsilon_y \quad \gamma_{xy}\}$$

then, by substituting the above derived expression for ε_z into the stiffness matrix, it can be shown that:

$$\underline{\sigma}_{xy} = \underline{D}_{xy}\,\underline{\varepsilon}_{xy} + \underline{\sigma}_z$$

such that

$$\underline{D}xy = \begin{bmatrix} (d_{11}-d_{13}d_{31}/d_{33}) & (d_{12}-d_{13}d_{32}/d_{33}) & (d_{14}-d_{13}d_{34}/d_{33}) \\ (d21-d23d31/d33) & (d22-d23d32/d33) & (d24-d23d34/d33) \\ (d_{41}-d_{43}d_{31}/d_{33}) & (d_{42}-d_{43}d_{32}/d_{33}) & (d_{44}-d_{43}d_{34}/d_{33}) \end{bmatrix}$$

and

$$\underline{\sigma}_z = (\sigma_z/d_{33})\ \{\ d_{31}\ d_{23}\ d_{43}\ \}$$

3.3 Stiffness Matrices of Layered Composite Materials

The laminate is presumed to consist of perfectly bonded laminae(layers), and the bonds are considered to be infintesimally thin as well as non-shear-deformable. That is, the displacements are continuous across lamina boundaries so that no lamina can slip relative to another. Thus, the laminate acts as a single layer with very special properties, but nevertheless acts as a single layer of material.

For the stress-strain relationships of composite materials with N_L number of layers, the following three stiffness matrices can be defined:

$$\underline{D}_{11} = \sum_{L=1}^{N_L} (\underline{D}^{(L)})(Z_U^{(L)} - Z_L^{(L)})$$

$$\underline{D}_{12} = (1/2) \sum_{L=1}^{N_L} (\underline{D}^{(L)})(Z_U^{2(L)} - Z_L^{2(L)})$$

$$\underline{D}_{22} = (1/3) \sum_{L=1}^{N_L} (D^{(L)})(Z_U^{3(L)} - Z_L^{3(L)})$$

such that,

$\underline{D}^{(L)}$ = stiffness matrix of the Lth layer as defined in section 3.2

$Z_L^{(L)}$ = lower surface of the Lth layer

$Z_U^{(L)}$ = upper surface of the Lth layer

where

$\underline{D}_{11}$ = Extensional Stiffness

$\underline{D}_{12}$ = Coupling Stiffness

$\underline{D}_{22}$ = Bending Stiffness

The presence of $\underline{D}_{12}$ implies coupling between bending and extension of a laminate. That is, an extensional force results in not only extensional deformation, but twisting and/or bending of the laminate. Also, such a laminate cannot be subjected to a moment without, at the same time, suffering extension of the middle surface. For laminates that are symmetric in both geometry and material properties about the middle surface, all of the terms in the coupling stiffness matrix can be shown to be zero.

CHAPTER 4

FIRST ORDER MINDLIN'S FACET SHELL ELEMENT

4.1 Introduction

Curved surfaces can be modelled approximately by facet elements, employing the assumption that the behaviour of a continuously curved surface can be adequately represented by the behaviour of a surface built up of small flat elements [50]. As the size of the subdivision decreases it would seem that convergence must occur, and indeed experience indicates such convergence. A facet shell element is essentially a combination of a plate bending element and an in-plane two-dimensional element based on plane stress theory.

Shell elements based upon Mindlin's theory are more accurate for problems in the relatively thick ranges and are simpler to employ than Kirchhoff's thin elements [56]. Another advantage is that they require C^0 continuity of the lateral deflection (w) and have independent slopes (Θ_x and Θ_y). When uniform numerical integration is used with standard Mindlin FE analysis, very disappointing results are sometimes obtained in applications in the thin range. This phenomenon, termed as shear locking is caused by imposition of the constraints by the shear strain energy terms in the total potential energy when limiting thin plate (or shell) solutions are approached, i.e., when $\gamma_{xz}=\gamma_{yz}=0$ [46].

When a reduced order of numerical integration of the stiffness terms is used on some isoparametric displacement-based Mindlin's element, improved behaviour is often obtained. A selective integration procedure, which is a reduced integration usage to evaluate the stiffness

matrix associated with the troublesome shear strain energy, may alleviate the over constraining effects of this particular portion of the stiffness matrix. Full integration is used for the remaining terms of the stiffness matrix in an attempt to retain the required accuracy of the overall stiffness matrix.

4.2 Element Description

Consider a laminated composite plate which consists of N_L layers, each layer being made of a composite material with stress-strain relationships as described earlier in chapter 3.

Consider an element described with respect to the local x-y-z system, and with each Lth layer being parallel to the x-y plane, with

$$Z = Z_L^{(L)} \qquad \text{at its lower surface}$$

$$Z = Z_U^{(L)} \qquad \text{at its upper surface}$$

$$h = Z_U^{(L)} - Z_L^{(L)} \qquad \text{its thickness}$$

The x-y plane is assumed to be the midplane, with

$$Z = -h/2 \qquad \text{at element lower surface}$$

$$Z = h/2 \qquad \text{at element upper surface}$$

where

h = Element thickness

$$= \sum_{L=1}^{N_L} h^{(L)}$$

The bending neutral plane is the plane in which there is no lateral displacement (u,v) due to bending, and only for a symmetric set of layers (with respect to the x-y plane), the neutral plane is at Z=0. Generally speaking, the neutral plane is assumed to be at $Z=Z_0$, and the value of Z_0 is determined from equilibrium conditions.

The element can be defined in terms of layers (their thicknesses and material properties) plus a set of n nodes at the bending neutral plane. Displacements and slope components at each node will define the nodal displacement vector $\underline{\delta}$, i.e.

$$\underline{\delta} = \{ u_1 \; v_1 \; w_1 \; (\Theta_x)_1 \; (\Theta_y)_1 \ldots\ldots u_n \; v_n \; w_n \; (\Theta_x)_n \; (\Theta_y)_n \}$$

where

(u_i, v_i, w_i) = displacement components at the ith node on the neutral plane in the x,y & z (local axes) directions

Θ_x = slope angle with respect to local x-axis

Θ_y = slope angle with respect to local y-axis

4.3 Displacement Components

From the basic geometrical analysis, the displacement components, at any point (x,y,z) inside the element, can be defined as follow:

$$u(x,y,z) = u_0(x,y) + (Z - Z_0)\Theta_y(x,y)$$
$$v(x,y,z) = v_0(x,y) - (Z - Z_0)\Theta_x(x,y)$$
$$w(x,y,z) = w_0(x,y)$$

where

u_0, v_0, w_0 are the displacement components at the neutral bending plane, i.e. at $Z = Z_0$

Θ_x, Θ_y are slope angles at (x,y)

Due to the consideration of transverse shear, the following interpolations will be employed:

$$u_0(x,y) = \sum_{j=1}^{n} u_j N_j(\xi,\eta)$$

$$v_0(x,y) = \sum_{j=1}^{n} v_j N_j(\xi,\eta)$$

$$w_0(x,y) = \sum_{j=1}^{n} w_j N_j(\xi,\eta)$$

$$\Theta_x(x,y) = \sum_{j=1}^{n} (\Theta_x)_j N_j(\xi,\eta)$$

$$\Theta_y(x,y) = \sum_{j=1}^{n} (\Theta_y)_j N_j(\xi,\eta)$$

where

$N_j(\xi,\eta)$ represents Lagrangian Shape Functions.

4.4 Strain-Displacement Relationships

Ignoring large deflection terms in transverse shear, the strain-displacement relationships can be summarised as follow:

$$\varepsilon_x = (\partial u/\partial x) + (1/2)\left[(\partial u/\partial x)^2 + (\partial v/\partial x)^2 + (\partial w/\partial x)^2\right]$$

$$\varepsilon_y = (\partial v/\partial y) + (1/2)\left[(\partial u/\partial y)^2 + (\partial v/\partial y)^2 + (\partial w/\partial y)^2\right]$$

$$\gamma_{xy} = (\partial u/\partial y) + (\partial v/\partial x)$$
$$+ \left[(\partial u/\partial x)(\partial u/\partial y) + (\partial v/\partial x)(\partial v/\partial y) + (\partial w/\partial x)(\partial w/\partial y)\right]$$

$$\gamma_{yz} = (\partial v/\partial z) + (\partial w/\partial y)$$

$$\gamma_{zx} = (\partial u/\partial z) + (\partial w/\partial x)$$

Thereafter, from the previous definition of displacement components, the following relationships can be derived easily:

$$\varepsilon_x = (\partial u_0/\partial x) + (Z - Z_0)(\partial \Theta_y/\partial x)$$
$$+ (1/2)\left\{\left[(\partial u_0/\partial x) + (Z - Z_0)(\partial \Theta_y/\partial x)\right]^2 + \left[(\partial v_0/\partial x) - (Z - Z_0)(\partial \Theta_x/\partial x)\right]^2 + (\partial w_0/\partial x)^2\right\}$$

$$\varepsilon_y = (\partial v_0/\partial y) - (Z - Z_0)(\partial \Theta_x/\partial y)$$
$$+ 1/2\left\{\left[(\partial u_0/\partial y) + (Z - Z_0)(\partial \Theta_y/\partial y)\right]^2 + \left[(\partial v_0/\partial y) - (Z - Z_0)(\partial \Theta_x/\partial y)\right]^2 + (\partial w_0/\partial y)^2\right\}$$

$$\gamma_{xy} = (\partial u_0/\partial y) + (\partial v_0/\partial x) + (Z - Z_0)(\partial \Theta_y/\partial y - \partial \Theta_x/\partial x)$$
$$+ \left\{\left[(\partial u_0/\partial x) + (Z - Z_0)(\partial \Theta_y/\partial x)\right]\left[(\partial u_0/\partial y) + (Z - Z_0)(\partial \Theta_y/\partial y)\right]\right.$$

CONT....

$$+ \left[(\partial v_0/\partial x) - (Z - Z_0)(\partial \Theta_x/\partial x)\right]$$

$$\left[(\partial v_0/\partial y) - (Z - Z_0)(\partial \Theta_x/\partial y)\right]$$

$$+ (\partial w_0/\partial x)(\partial w_0/\partial y)\Big]$$

$$\gamma_{yz} = -\Theta_x + (\partial w_0/\partial y)$$

$$\gamma_{zx} = \Theta_y + (\partial w_0/\partial x)$$

Neglecting terms containing $(Z-Z_0)^2$, $(\partial\Theta/\partial x)^2$ and $(\partial\Theta/\partial y)^2$ the previous equations can be approximated as follows:

$$\varepsilon_x = (\partial u_0/\partial x) + (Z - Z_0)(\partial \Theta_y/\partial x)$$

$$+ (1/2)\left[(\partial u_0/\partial x)^2 + (\partial v_0/\partial x)^2 + (\partial w_0/\partial x)^2\right]$$

$$+ (Z - Z_0)\left[(\partial u_0/\partial x)(\partial \Theta_y/\partial x) - (\partial v_0/\partial x)(\partial \Theta_x/\partial x)\right]$$

$$\varepsilon_y = (\partial v_0/\partial y) - (Z - Z_0)(\partial \Theta_x/\partial y)$$

$$+ (1/2)\left[(\partial u_0/\partial y)^2 + (\partial v_0/\partial y)^2 + (\partial w_0/\partial y)^2\right]$$

$$+ (Z - Z_0)\left[(\partial u_0/\partial y)(\partial \Theta_y/\partial y) - (\partial v_0/\partial y)(\partial \Theta_x/\partial y)\right]$$

$$\gamma_{xy} = (\partial u_0/\partial y) + (\partial v_0/\partial x) + (Z - Z_0)(\partial \Theta_y/\partial y - \partial \Theta_x/\partial x)$$

$$+ \Big[(\partial u_0/\partial x)(\partial u_0/\partial y) + (\partial v_0/\partial x)(\partial v_0/\partial y)$$

$$+ (\partial w_0/\partial x)(\partial w_0/\partial y)\Big] + (Z - Z_0)\Big[(\partial u_0/\partial x)(\partial \Theta_y/\partial y)$$

CONT....

$$+ \left(\partial u_0/\partial y\right)\left(\partial \Theta_y/\partial x\right) - \left(\partial v_0/\partial x\right)\left(\partial \Theta_x/\partial y\right)$$

$$\left. - \left(\partial v_0/\partial y\right)\left(\partial \Theta_x/\partial x\right)\right]$$

Defining

$$\underline{\varepsilon} = \{\ \varepsilon_x \quad \varepsilon_y \quad \gamma_{xy} \quad \gamma_{yz} \quad \gamma_{zx}\ \}$$

which can be partitioned as follows:

$$\underline{\varepsilon} = (\ \underline{\varepsilon}_0 + \underline{\varepsilon}_s + \underline{\varepsilon}_L\ ) + (\bar{\underline{\varepsilon}}_b + \bar{\underline{\varepsilon}}_L)$$

such that,

$$\underline{\varepsilon} = (\ \underline{\varepsilon}_0 + \underline{\varepsilon}_s + \underline{\varepsilon}_L\ ) + (Z - Z_0)\ (\hat{\underline{\varepsilon}}_b + \hat{\underline{\varepsilon}}_L)$$

where

$\underline{\varepsilon}_0 = \{\ \varepsilon_x \quad \varepsilon_y \quad \gamma_{xy} \quad 0 \quad 0\ \}_m$
is the membrane strain component due to in-plane deformation

$\underline{\varepsilon}_s = \{\ 0 \quad 0 \quad 0 \quad \gamma_{yz} \quad \gamma_{zx}\ \}_s$
is the transverse shear strain, which is taken into consideration for Mindlin thick plate elements.

$\underline{\varepsilon}_L = \{\ \varepsilon_x \quad \varepsilon_y \quad \gamma_{xy} \quad 0 \quad 0\ \}_L$
is the large deflection strain considering membrane effects only.

$\bar{\underline{\varepsilon}}_b = \{\ \varepsilon_x \quad \varepsilon_y \quad \gamma_{xy} \quad 0 \quad 0\ \}_b$
is the bending strain without transverse shear.

$\underline{\bar{\varepsilon}}_L = \{ \varepsilon_x \quad \varepsilon_y \quad \gamma_{xy} \quad 0 \quad 0 \quad \}_L$

is the large deflection strain due to membrane and bending components simultaneously.

From 2-D elasticity and plate-bending theories, it can be shown that:

$$\underline{\varepsilon}_0 = \begin{bmatrix} \partial u_0/\partial x \\ \partial v_0/\partial y \\ \partial u_0/\partial x + \partial v_0/\partial y \\ 0 \\ 0 \end{bmatrix}$$

$$\underline{\varepsilon}_s = \begin{bmatrix} 0 \\ 0 \\ 0 \\ \partial w_0/\partial y - \Theta_x \\ \partial w_0/\partial x + \Theta_y \end{bmatrix}$$

$$\underline{\varepsilon}_L = (1/2) \begin{bmatrix} (\partial u_0/\partial x)^2 + (\partial v_0/\partial x)^2 + (\partial w_0/\partial x)^2 \\ (\partial u_0/\partial y)^2 + (\partial v_0/\partial y)^2 + (\partial w_0/\partial y)^2 \\ \left[2(\partial u_0/\partial x)(\partial u_0/\partial y) + 2(\partial v_0/\partial x)(\partial v_0/\partial y) \right. \\ \left. + 2(\partial w_0/\partial x)(\partial w_0/\partial y) \right] \\ 0 \\ 0 \end{bmatrix}$$

$$\hat{\underline{\varepsilon}}_b = \begin{bmatrix} \partial\Theta_y/\partial x \\ -\partial\Theta_x/\partial y \\ \partial\Theta_y/\partial y - \partial\Theta_x/\partial x \\ 0 \\ 0 \end{bmatrix}$$

$$\hat{\underline{\varepsilon}}_L = \begin{bmatrix} (\partial u_0/\partial x)(\partial\Theta_y/\partial x) - (\partial v_0/\partial x)(\partial\Theta_x/\partial x) \\ (\partial u_0/\partial y)(\partial\Theta_y/\partial y) - (\partial v_0/\partial y)(\partial\Theta_x/\partial y) \\ \left[(\partial u_0/\partial x)(\partial\Theta_y/\partial y) + (\partial u_0/\partial y)(\partial\Theta_y/\partial x) \right. \\ \left. - (\partial v_0/\partial x)(\partial\Theta_x/\partial y) - (\partial v_0/\partial y)(\partial\Theta_x/\partial x) \right] \\ 0 \\ 0 \end{bmatrix}$$

Hence, using interpolation equations, the following $\underline{B}$ matrices can be defined for various strain vectors (excluding large deflection strains):

$$\underline{\varepsilon}_0(x,y) = \underline{B}_0(x,y)\ \underline{\delta}$$

$$\underline{\varepsilon}_s(x,y) = \underline{B}_s(x,y)\ \underline{\delta}$$

$$\underline{\varepsilon}_b(x,y) = \underline{B}_b(x,y)\ \underline{\delta}$$

where

$$\underline{B} = [\underline{b}_1 \quad \underline{b}_2 \quad \underline{b}_3 \quad \underline{b}_4 \ldots\ldots \underline{b}_i \ldots\ldots \underline{b}_n\ ]$$

Hence, it can be deduced that:

$$(\underline{b}_i)_0 = \begin{bmatrix} \partial N_i/\partial x & 0 & 0 & 0 & 0 \\ 0 & \partial N_i/\partial y & 0 & 0 & 0 \\ \partial N_i/\partial y & \partial N_i/\partial x & 0 & 0 & 0 \\ 0 & 0 & 0 & 0 & 0 \\ 0 & 0 & 0 & 0 & 0 \end{bmatrix}$$

$$(\underline{b}_i)_s = \begin{bmatrix} 0 & 0 & 0 & 0 & 0 \\ 0 & 0 & 0 & 0 & 0 \\ 0 & 0 & \partial N_i/\partial y & -N_i & 0 \\ 0 & 0 & \partial N_i/\partial x & 0 & N_i \end{bmatrix}$$

$$(\hat{\underline{b}}_i)_b = \begin{bmatrix} 0 & 0 & 0 & 0 & \partial N_i/\partial x \\ 0 & 0 & 0 & -\partial N_i/\partial y & 0 \\ 0 & 0 & 0 & -\partial N_i/\partial x & \partial N_i/\partial y \\ 0 & 0 & 0 & 0 & 0 \\ 0 & 0 & 0 & 0 & 0 \end{bmatrix}$$

In order to define interpolation equations for large deflection strains, the following rotation vectors are defined:

$$\underline{\Theta}_1 = \{\partial u_0/\partial x \quad \partial v_0/\partial x \quad \partial w_0/\partial x \quad \partial u_0/\partial y \quad \partial v_0/\partial y \quad \partial w_0/\partial y\}$$
$$\underline{\Theta}_2 = \{\partial \Theta_y/\partial x \quad -\partial \Theta_x/\partial x \quad \partial \Theta_y/\partial y \quad -\partial \Theta_x/\partial y\}$$

then, it can be deduced that:

$$\underline{\Theta}_1 = \underline{G}_1 \ \underline{\delta}$$
$$\underline{\Theta}_2 = \underline{G}_2 \ \underline{\delta}$$

With

$$\underline{G} = \begin{bmatrix} g_1 & g_2 & g_3 & g_4 & g_5 \cdots\cdots g_n \end{bmatrix}$$

then

$$(g_i)_1 = \begin{bmatrix} \partial N_i/\partial x & 0 & 0 & 0 & 0 \\ 0 & \partial N_i/\partial x & 0 & 0 & 0 \\ 0 & 0 & \partial N_i/\partial x & 0 & 0 \\ \partial N_i/\partial y & 0 & 0 & 0 & 0 \\ 0 & \partial N_i/\partial y & 0 & 0 & 0 \\ 0 & 0 & \partial N_i/\partial y & 0 & 0 \end{bmatrix}$$

$$(g_i)_2 = \begin{bmatrix} 0 & 0 & 0 & 0 & \partial N_i/\partial x \\ 0 & 0 & 0 & -\partial N_i/\partial x & 0 \\ 0 & 0 & 0 & 0 & \partial N_i/\partial y \\ 0 & 0 & 0 & -\partial N_i/\partial y & 0 \end{bmatrix}$$

It can also be shown that:

$$\underline{\varepsilon}_L = 1/2 \ \underline{A}_1 \ \underline{\Theta}_1$$

$$\hat{\underline{\varepsilon}}_L = \underline{A}_{12} \ \underline{\Theta}_2 = \underline{A}_{21} \ \underline{\Theta}_1$$

Where

$$\underline{A}_1 = \begin{bmatrix} \partial u_0/\partial x & \partial v_0/\partial x & \partial w_0/\partial x & 0 & 0 & 0 \\ 0 & 0 & 0 & \partial u_0/\partial y & \partial v_0/\partial y & \partial w_0/\partial y \\ \partial u_0/\partial y & \partial v_0/\partial y & \partial w_0/\partial y & \partial u_0/\partial x & \partial v_0/\partial x & \partial w_0/\partial x \\ 0 & 0 & 0 & 0 & 0 & 0 \\ 0 & 0 & 0 & 0 & 0 & 0 \end{bmatrix}$$

$$\underline{A}_{21} = \begin{bmatrix} \partial \Theta_y/\partial x & -\partial \Theta_x/\partial x & 0 & 0 & 0 & 0 \\ 0 & 0 & 0 & \partial \Theta_y/\partial y & -\partial \Theta_x/\partial y & 0 \\ \partial \Theta_y/\partial y & -\partial \Theta_x/\partial y & 0 & \partial \Theta_y/\partial x & -\partial \Theta_x/\partial x & 0 \\ 0 & 0 & 0 & 0 & 0 & 0 \\ 0 & 0 & 0 & 0 & 0 & 0 \end{bmatrix}$$

$$\underline{A}_{12} = \begin{bmatrix} \partial u_0/\partial x & \partial v_0/\partial x & 0 & 0 \\ 0 & 0 & \partial u_0/\partial y & \partial v_0/\partial y \\ \partial u_0/\partial y & \partial v_0/\partial y & \partial u_0/\partial x & \partial v_0/\partial x \\ 0 & 0 & 0 & 0 \\ 0 & 0 & 0 & 0 \end{bmatrix}$$

Thereafter, it can easily be shown that:

$$\begin{aligned} d\underline{\varepsilon}_L &= 1/2\ \underline{A}_1\ d\underline{\Theta}_1 + 1/2\ d\underline{A}\ \underline{\Theta}_1 \\ &\equiv 1/2\ \underline{A}_1\ d\underline{\Theta}_1 + 1/2\ \underline{A}_1\ d\underline{\Theta}_1 \\ &= \underline{A}_1\ d\underline{\Theta}_1 \end{aligned}$$

and from the definition of $\hat{\underline{\varepsilon}}_L$, it can be deduced that:

$$d\hat{\underline{\varepsilon}}_L = \underline{\underline{A}}_{12} \; d\underline{\Theta}_2 + \underline{\underline{A}}_{21} \; d\underline{\Theta}_1$$

Hence, it can be shown that:

$$d\underline{\varepsilon}_L = \underline{\underline{A}}_1 \; d\underline{\Theta}_1 = \underline{\underline{A}}_1 \; \underline{G}_1 \; d\underline{\delta}$$

$$d\hat{\underline{\varepsilon}}_L = (\underline{\underline{A}}_{12} \; \underline{G}_2 + \underline{\underline{A}}_{21} \; \underline{G}_1) \, d\underline{\delta}$$

therefore,

$$d\underline{\varepsilon}_L = \underline{B}_L \; d\underline{\delta}$$

$$d\hat{\underline{\varepsilon}}_L = \hat{\underline{B}}_L \; d\underline{\delta}$$

Where,

$$\underline{B}_L = \underline{\underline{A}}_1 \; \underline{G}_1$$

$$\hat{\underline{B}}_L = \underline{\underline{A}}_{12} \; \underline{G}_2 + \underline{\underline{A}}_{21} \; \underline{G}_1$$

Similarly, defining $\underline{\underline{A}}_1$, $\underline{\underline{A}}_{12}$, $\underline{\underline{A}}_{21}$ as before, it may be useful to define $\underline{\underline{A}}^t \underline{\sigma}$, where

$$\underline{\sigma} = \{ \; \sigma_x \quad \sigma_y \quad \tau_{xy} \quad \tau_{yz} \quad \tau_{zx} \; \}$$

$$\underline{\underline{A}}_1^t \; \underline{\sigma} = \begin{bmatrix} \sigma_x (\partial u_0/\partial x) + \tau_{xy} (\partial u_0/\partial y) \\ \sigma_x (\partial v_0/\partial x) + \tau_{xy} (\partial v_0/\partial y) \\ \sigma_x (\partial w_0/\partial x) + \tau_{xy} (\partial w_0/\partial y) \\ \tau_{xy} (\partial u_0/\partial x) + \sigma_y (\partial u_0/\partial y) \\ \tau_{xy} (\partial v_0/\partial x) + \sigma_y (\partial v_0/\partial y) \\ \tau_{xy} (\partial w_0/\partial x) + \sigma_y (\partial w_0/\partial y) \end{bmatrix} = \underline{S}_1 \; \underline{\Theta}_1$$

where

$$\underline{S}_1 = \begin{bmatrix} \sigma_x \ \underline{I}_3 & \tau_{xy} \ \underline{I}_3 \\ \tau_{xy} \ \underline{I}_3 & \sigma_y \ \underline{I}_3 \end{bmatrix}$$

and

$$\underline{I}_3 = \begin{bmatrix} 1 & 0 & 0 \\ 0 & 1 & 0 \\ 0 & 0 & 1 \end{bmatrix}$$

Hence,

$$d\underline{A}_1^t \ \underline{\sigma} = \underline{S}_1 \ d\underline{\Theta}_1$$

$$= \underline{S}_1 \ \underline{G}_1 \ d\underline{\delta}$$

Similarly,

$$\underline{A}_{21}^t \ \underline{\sigma} = \begin{bmatrix} \sigma_x(\partial\Theta_y/\partial x) + \tau_{xy}(\partial\Theta_y/\partial y) \\ \sigma_x(-\partial\Theta_x/\partial x) + \tau_{xy}(-\partial\Theta_x/\partial y) \\ 0 \\ \tau_{xy}(\partial\Theta_y/\partial x) + \sigma_y(\partial\Theta_y/\partial y) \\ \tau_{xy}(-\partial\Theta_x/\partial x) + \sigma_y(-\partial\Theta_x/\partial y) \\ 0 \end{bmatrix} = \underline{S}_{12} \ \underline{\Theta}_2$$

where

$$\underline{S}_{12} = \begin{bmatrix} \sigma_x \ \underline{I}_{3x2} & \tau_{xy} \ \underline{I}_{3x2} \\ \tau_{xy} \ \underline{I}_{3x2} & \sigma_y \ \underline{I}_{3x2} \end{bmatrix}$$

and

$$\underline{I}_{3x2} = \begin{bmatrix} 1 & 0 \\ 0 & 1 \\ 0 & 0 \end{bmatrix}$$

Therefore,

$$d\underline{A}_{21}^{t}\ \underline{\sigma} = \underline{S}_{12}\ d\underline{\Theta}_2 = \underline{S}_{12}\ \underline{G}_2\ d\underline{\delta}$$

And similarly,

$$\underline{A}_{12}^{t}\ \underline{\sigma} = \begin{bmatrix} \sigma_x(\partial u_0/\partial x) + \tau_{xy}(\partial u_0/\partial y) \\ \sigma_x(\partial v_0/\partial x) + \tau_{xy}(\partial v_0/\partial y) \\ \tau_{xy}(\partial u_0/\partial x) + \sigma_y(\partial u_0/\partial y) \\ \tau_{xy}(\partial v_0/\partial x) + \sigma_y(\partial u_0/\partial y) \end{bmatrix} = \underline{S}_{21}\ \underline{\Theta}_1$$

where

$$\underline{S}_{21} = \begin{bmatrix} \sigma_x\ \underline{I}_{2x3} & \tau_{xy}\ \underline{I}_{2x3} \\ \tau_{xy}\ \underline{I}_{2x3} & \sigma_y\ \underline{I}_{2x3} \end{bmatrix} = \underline{S}_{12}^{t}$$

and

$$\underline{I}_{2x3} = \begin{bmatrix} 1 & 0 & 0 \\ 0 & 1 & 0 \end{bmatrix} = \underline{I}_{3x2}^{t}$$

i.e.

$$d\underline{A}_{12}^{t}\ \underline{\sigma} = \underline{S}_{21}\ d\underline{\Theta}_1 = \underline{S}_{21}\ \underline{G}_1\ d\underline{\delta}$$

Finally,

$$d\underline{B}^t\underline{\sigma} = \left[d\underline{B}_L^t + (Z - Z_0)d\hat{\underline{B}}_L^t\right]\underline{\sigma}$$

$$= \left[\underline{G}_1^t\, d\underline{A}_1^t + (Z - Z_0)(\underline{G}_1^t\, d\underline{A}_{21}^t + \underline{G}_2^t\, d\underline{A}_{12}^t)\right]\underline{\sigma}$$

Subsequently, it may be shown that:

$$d\underline{B}^t\underline{\sigma} = \left[\underline{G}_1^t\, \underline{S}_1\, \underline{G}_1 + (Z - Z_0)(\underline{G}_1^t\, \underline{S}_{12}\, \underline{G}_2)\right.$$

$$\left. + (Z - Z_0)(\underline{G}_1^t\, \underline{S}_{12}\, \underline{G}_2)^t\right] d\underline{\delta}$$

4.5 Stress Components Inside the Lth Layer

From reasons of displacement continuity, the previous strain-displacement relationships are valid at any point within any layer. However, for stress components, an appropriate $\underline{D}$ matrix should be employed. For a point inside the Lth layer,

$$\underline{\sigma}^{(L)} = \underline{D}^{(L)}\, \underline{\varepsilon}$$

Assuming no thermal loading, then,

$$\underline{\sigma}^{(L)} = \underline{\sigma}_0^{(L)} + \underline{\sigma}_s^{(L)} + \underline{\sigma}_L^{(L)} + (Z - Z_0)(\hat{\underline{\sigma}}_b^{(L)} + \hat{\underline{\sigma}}_L^{(L)})$$

where for linear-elastic analysis, with small or large deformation:

$$\underline{\sigma}_0^{(L)} = \underline{D}^{(L)}\, \underline{\varepsilon}_0 \text{.....etc}$$

4.6 Element Mass Matrix and Rotating-Inertia Matrices

Consider a generalised case where the structure is moving with a constant translational acceleration $\underline{a}_0$ and rotating with respect to a fixed axis with a constant rotational speed Ω where,

$$\vec{a}_0 = (a_0)_x \hat{i} + (a_0)_y \hat{j} + (a_0)_z \hat{k}$$

$$\vec{\Omega} = \Omega_x \hat{i} + \Omega_y \hat{j} + \Omega_z \hat{k}$$

$\hat{i}$, $\hat{j}$, $\hat{k}$ are taken w.r.t. element local axes (which are fixed on the structure)

The local rigid translational acceleration at any (x,y,z) inside the element is :

$$\vec{a} = \vec{a}_0 + \vec{\Omega} \wedge (\vec{\Omega} \wedge \vec{r})$$

where

$$\vec{r} = (x - x_a)\hat{i} + (y - y_a)\hat{j} + (z - z_a)\hat{k}$$

and (x_a, y_a, z_a) is on the axis of rotation.

Defining

$$\underline{a} = \{ a_x \quad a_y \quad a_z \}$$

$$\underline{r} = \{ (x - x_a) \quad (y - y_a) \quad (z - z_a) \}$$

it can be shown that:

$$\underline{a} = \underline{a}_0 - \Omega^2 \, \bar{\underline{C}} \, \underline{r}$$

where

$$\Omega^2 = \Omega_x^2 + \Omega_y^2 + \Omega_z^2$$

$$\underline{\bar{C}} = \begin{bmatrix} 1 - l^2 & -lm & -ln \\ -ml & 1 - m^2 & -mn \\ -nl & -nm & 1 - n^2 \end{bmatrix}$$

$$l = \Omega_x/\Omega$$
$$m = \Omega_y/\Omega$$
$$n = \Omega_z/\Omega$$

This acceleration will create an inertia force which generates the stresses defining $\underline{K}_\sigma$ (for the centrifugal stiffening) for the stress analysis.

Equivalent Loading Vector

If the element is moving with an acceleration $\underline{a}$, then from D'Alembert's law ,

$$\Delta\underline{F}^{(L)} = -\rho^{(L)}\ \underline{a}\ \Delta vol$$

where $\rho^{(L)}$ is the density of the Lth layer

Defining the vector of displacement increment at any point as :

$$dg = \begin{bmatrix} du \\ dv \\ dw \end{bmatrix} = \begin{bmatrix} du_0 \\ dv_0 \\ dw_0 \end{bmatrix} + (Z - Z_0) \begin{bmatrix} d\Theta_y \\ -d\Theta_x \\ 0 \end{bmatrix}$$

then, the work done by the force $\Delta\underline{F}^{(L)}$ due to dg can be expressed as follow:

$$\Delta\left(\overset{(L)}{dW}\right) = d\underline{q}^{t}\ \Delta\underline{F}^{(L)}$$

$$= d\underline{q}^{t}\left(-\rho^{(L)}\ \underline{a}\ \Delta vol\right)$$

$$=-\rho^{(L)}\Big[(du_0 a_x + dv_0 a_y + dw_0 a_z)$$

$$+ (Z - Z_0)(d\Theta_y a_x - d\Theta_x a_y)\Big]\ \Delta vol$$

defining,

$$\underline{q}_1 = \{\ u_0 \quad v_0 \quad w_0\}$$

$$\underline{q}_2 = \{\ \Theta_x \quad \Theta_y \quad \Theta_z\}$$

where,

$$\Theta_z = 0$$

then

$$\Delta\left(\overset{(L)}{dW}\right) =-\rho^{(L)}\Big[d\underline{q}_1^{t}\underline{a} + (Z - Z_0)d\underline{q}_2^{t}\underline{a}\Big]\ \Delta vol$$

further it can be shown that:

$$d\underline{q}_1 = \underline{N}_1\ d\underline{\delta}$$

$$d\underline{q}_2 = \underline{N}_2\ d\underline{\delta}$$

where,

$$\underline{N} = \{\underline{n}_1 \quad \underline{n}_2 \quad \underline{n}_3 \ldots\ldots\ldots \underline{n}_n\ \}$$

$$(\underline{n}_i)_1 = \begin{bmatrix} N_i & 0 & 0 & 0 & 0 \\ 0 & N_i & 0 & 0 & 0 \\ 0 & 0 & N_i & 0 & 0 \end{bmatrix}$$

$$(\underline{n}_i)_2 = \begin{bmatrix} 0 & 0 & 0 & N_i & 0 \\ 0 & 0 & 0 & 0 & N_i \\ 0 & 0 & 0 & 0 & 0 \end{bmatrix}$$

Hence,

$$\Delta(dW)^{(L)} = \rho^{(L)}\, d\underline{\delta}^t \left[\underline{N}_1^t\, \underline{a} + \underline{N}_2^t\, \underline{a}\, (Z - Z_0) \right] \Delta vol$$

i.e.

$$dW^{(L)} = \rho^{(L)}\, d\underline{\delta}^t \iiint_L \left[\underline{N}_1^t\, \underline{a} + \underline{N}_2^t\, \underline{a}\, (Z - Z_0) \right] d(vol)$$

The nodal force vector per Lth layer can be obtained from:

$$dW^{(L)} = d\underline{\delta}^t\ \underline{F}^{(L)}$$

i.e.

$$\underline{F}^{(L)} = - \iint \left[\int_{Z_L}^{Z_U} \rho^{(L)} \left(\underline{N}_1^t\, \underline{a} + (Z - Z_0)\, \underline{N}_2^t\, \underline{a} \right) dz \right] dxdy$$

and for the whole element

$$\underline{F} = \sum_{L=1}^{N_L} \underline{F}^{(L)}$$

Inertial Loading Due To Structure Deformation

Consider a point (x,y,z), which after deformation will move to (x',y',z') and a relative position vector can be defined as follows

$$\underline{q} = (x' - x)\hat{i} + (y' - y)\hat{j} + (z' - z)\hat{k}$$

$$= u\hat{i} + v\hat{j} + w\hat{k}$$

Thereafter, it can be shown that:

$$\underline{a}' = \underline{a} + \ddot{\underline{q}} + 2\underline{\Omega} \wedge \dot{\underline{q}} + \underline{\Omega} \wedge (\underline{\Omega} \wedge \underline{q})$$

where,

$$\dot{\underline{q}} = \dot{u}\hat{i} + \dot{v}\hat{j} + \dot{w}\hat{k}$$

$$\ddot{\underline{q}} = \ddot{u}\hat{i} + \ddot{v}\hat{j} + \ddot{w}\hat{k}$$

and

$$\dot{\Phi} = d\Phi/dt$$

$$\ddot{\Phi} = d^2\Phi/dt^2$$

Hence, it can be shown that:

$$\underline{a}' = \underline{a} + \underline{a}_r + \underline{a}_c + \underline{a}_p$$

where

$\underline{a}_r = \ddot{\underline{q}}$ (relative acceleration)

$\underline{a}_c = 2\underline{\Omega} \wedge \dot{\underline{q}}$ (Coriolis acceleration)

$\underline{a}_p = \underline{\Omega} \wedge (\underline{\Omega} \wedge \underline{q})$ (Centripetal acceleration)

defining

$\underline{a} = \{ a_x \quad a_y \quad a_z \}$, it can be shown that:

$$\underline{a}_r = \ddot{\underline{q}}$$

$$\underline{a}_c = 2\,\Omega\;\underline{C}\;\dot{\underline{q}}$$

$$\underline{a}_p = -\Omega^2\;\underline{C}\;\underline{q}$$

where

$$\underline{g} = \{ u \quad v \quad w \}$$

$$\dot{\underline{g}} = \{ \dot{u} \quad \dot{v} \quad \dot{w} \}$$

$$\Omega = \sqrt{\Omega_x^2 + \Omega_y^2 + \Omega_z^2}$$

$$\underline{C} = \begin{bmatrix} 0 & -n & m \\ n & 0 & -l \\ -m & l & 0 \end{bmatrix}$$

$$\underline{\bar{C}} = \begin{bmatrix} 1 - l^2 & -lm & -ln \\ -ml & 1 - m^2 & -mn \\ -nl & -nm & 1 - n^2 \end{bmatrix}$$

where,

$$l = \Omega_x/\Omega$$
$$m = \Omega_y/\Omega$$
$$n = \Omega_z/\Omega$$

Equivalent Nodal Loading Vector Due To $\underline{a}_r$

From the previous analysis, it can also be deduced that:

$$\underline{F}_r^{(L)} = - \iiint \rho^{(L)} \left[\underline{N}_1^t \, \underline{a}_r + (Z - Z_0) \, \underline{N}_2^t \, \underline{a}_r \right] d(vol)$$

where,

$$\underline{a}_r = \ddot{\underline{g}} = \ddot{\underline{g}}_1 + (z - z_0)\ddot{\underline{g}}_2$$

$$= \left[\underline{N}_1 + (z - z_0)\ \underline{N}_2\right] \ddot{\underline{\delta}}$$

hence, it can be shown that:

$$\underline{F}_r^{(L)} = -\iiint \rho^{(L)} \left[\underline{N}_1^t\ \underline{N}_1 + (z - z_0)(\underline{N}_1^t\ \underline{N}_2 + \underline{N}_2^t\ \underline{N}_1) + (z - z_0)^2\ \underline{N}_2^t\ \underline{N}_2\right] d(vol)\ \ddot{\underline{\delta}}$$

Defining

$$\underline{R}_{11}^{(L)} = \int_{Z_L^{(L)}}^{Z_U^{(L)}} \rho^{(L)} \begin{bmatrix}1 & 0 & 0\\ 0 & 1 & 0\\ 0 & 0 & 1\end{bmatrix} dz = \rho^{(L)}\ h^{(L)} \begin{bmatrix}1 & 0 & 0\\ 0 & 1 & 0\\ 0 & 0 & 1\end{bmatrix}$$

$$\underline{R}_{12}^{(L)} = \int_{Z_L^{(L)}}^{Z_U^{(L)}} \rho^{(L)}(z - z_0) \begin{bmatrix}1 & 0 & 0\\ 0 & 1 & 0\\ 0 & 0 & 1\end{bmatrix} dz = \rho^{(L)}\ \Phi^{(L)} \begin{bmatrix}1 & 0 & 0\\ 0 & 1 & 0\\ 0 & 0 & 1\end{bmatrix}$$

$$\underline{R}_{22}^{(L)} = \int_{Z_L^{(L)}}^{Z_U^{(L)}} \rho^{(L)}(z - z_0)^2 \begin{bmatrix}1 & 0 & 0\\ 0 & 1 & 0\\ 0 & 0 & 1\end{bmatrix} dz = \rho^{(L)}\ \psi^{(L)} \begin{bmatrix}1 & 0 & 0\\ 0 & 1 & 0\\ 0 & 0 & 1\end{bmatrix}$$

where

$$\Phi^{(L)} = \left[(Z_U^{(L)} - z_0)^2 - (Z_L^{(L)} - z_0)^2\right](1/2)$$

$$\Psi^{(L)} = \left[(Z_U^{(L)} - Z_0)^3 - (Z_L^{(L)} - Z_0)^3 \right] (1/3)$$

thus, it can be shown that:

$$\underline{F}_r^{(L)} = - \iint_{x-y} \left[\underline{N}_1^t \underline{D}_{11}^{(L)} \underline{N}_1 + \underline{N}_1^t \underline{D}_{12}^{(L)} \underline{N}_2 + (\underline{N}_1^t \underline{D}_{12}^{(L)} \underline{N}_2)^t + \underline{N}_2^t \underline{D}_{22}^{(L)} \underline{N}_2 \right] dxdy \ \ddot{\underline{\delta}}$$

Hence,

$$\underline{F}_r = \sum_{L=1}^{N_L} \underline{F}_r^{(L)} = -\underline{M}_{(e)} \ddot{\underline{\delta}}$$

where,

$$\underline{M}_{(e)} = \underline{M}_{11} + \underline{M}_{12} + \underline{M}_{12}^t + \underline{M}_{22}$$

which is the element mass matrix, such that:

$$\underline{M}_{11} = \sum_{L=1}^{N_L} \iint \underline{N}_1^t \underline{R}_{11}^{(L)} \underline{N}_1 \ dxdy$$

$$\underline{M}_{12} = \sum_{L=1}^{N_L} \iint \underline{N}_1^t \underline{R}_{12}^{(L)} \underline{N}_2 \ dxdy$$

$$\underline{M}_{22} = \sum_{L=1}^{N_L} \iint \underline{N}_2^t \underline{R}_{22}^{(L)} \underline{N}_2 \ dxdy$$

Defining,

$$\underline{R}_{11} = \sum_{L=1}^{N_L} \underline{R}_{11}^{(L)} = \left(\sum_{L=1}^{N_L} \rho^{(L)} h^{(L)} \right) \underline{I}_3$$

$$\underline{R}_{12} = \sum_{L=1}^{N_L} \underline{R1}_2^{(L)} = \left(\sum_{L=1}^{N_L} \rho^{(L)} \Phi^{(L)} \right) \underline{I}_3$$

$$\underline{R}_{22} = \sum_{L=1}^{N_L} \underline{R}_{22}^{(L)} = \left(\sum_{L=1}^{N_L} \rho^{(L)} \Psi^{(L)} \right) \underline{I}_3$$

where,

$$\underline{I}_3 = \begin{bmatrix} 1 & 0 & 0 \\ 0 & 1 & 0 \\ 0 & 0 & 1 \end{bmatrix}$$

therefore, it can be deduced that:

$$\underline{M}_{11} = \iint_{\substack{x-y \\ \text{element}}} \underline{N}_1^t \; \underline{R}_{11} \; \underline{N}_1 \; dxdy$$

$$\underline{M}_{12} = \iint_{\substack{x-y \\ \text{element}}} \underline{N}_1^t \; \underline{R}_{12} \; \underline{N}_2 \; dxdy$$

$$\underline{M}_{22} = \iint_{\substack{x-y \\ \text{element}}} \underline{N}_2^t \; \underline{R}_{22} \; \underline{N}_2 \; dxdy$$

Equivalent Nodal Loading Vector Due To $\underline{a}_c$

From the previous analysis, it can be deduced that:

$$\underline{F}_c = - \iiint \rho^{(L)} \left[\underline{N}_1^t \; \underline{a}_c + (Z - Z_0) \; \underline{N}_2^t \; \underline{a}_c \right] d(vol)$$

where,

$$\underline{a}_c = 2 \; \Omega \; \underline{C} \; \dot{\underline{q}}$$

$$= 2 \; \Omega \; \underline{C} \left[\dot{\underline{q}}_1 + (Z - Z_0) \; \dot{\underline{q}}_2 \right]$$

$$= 2 \; \Omega \; \underline{C} \left[\underline{N}_1 + (Z - Z_0) \; \underline{N}_2 \right] \dot{\underline{\delta}}$$

$\therefore$

$$\underline{F}_c^{(L)} = -2\Omega \iint_{x-y} \int_{Z_L^{(L)}}^{Z_U^{(L)}} \rho^{(L)} \Big[\underline{N}_1^t \ \underline{C} \ \underline{N}_1 + (Z - Z_0) \ \underline{N}_1^t \ \underline{C} \ \underline{N}_2 + (Z - Z_0) \ \underline{N}_2^t \ \underline{C} \ \underline{N}_1 + (Z - Z_0)^2 \ \underline{N}_2^t \ \underline{C}_2 \ \underline{N}_2 \Big] dz dx dy \ \dot{\underline{\delta}}$$

Defining:

$$\underline{Q}_{11}^{(L)} = \int_{Z_L^{(L)}}^{Z_U^{(L)}} \rho^{(L)} \ \underline{C} \ dz = \rho^{(L)} \ h^{(L)} \ \underline{C}$$

$$\underline{Q}_{12}^{(L)} = \int_{Z_L^{(L)}}^{Z_U^{(L)}} \rho^{(L)} \ (Z - Z_0) \ \underline{C} \ dz = \rho^{(L)} \ \Phi^{(L)} \ \underline{C}$$

$$\underline{Q}_{22}^{(L)} = \int_{Z_L^{(L)}}^{Z_U^{(L)}} \rho^{(L)} \ (Z - Z_0)^2 \ \underline{C} \ dz = \rho^{(L)} \ \psi^{(L)} \ \underline{C}$$

then, it can be shown that:

$$\underline{F}_c^{(L)} = -2\Omega \iint_{x-y} \Big[\underline{N}_1^t \ \underline{Q}_{11}^{(L)} \ \underline{N}_1 + \underline{N}_1^t \ \underline{Q}_{12}^{(L)} \ \underline{N}_2 + (\underline{N}_1^t \ \underline{Q}_{12}^{(L)} \ \underline{N}_2)^t + \underline{N}_2^t \ \underline{Q}_{22}^{(L)} \ \underline{N}_2 \Big] dx dy \ \dot{\underline{\delta}}$$

hence,

$$\underline{F}_C = \sum_{L=1}^{N_L} \underline{F}_C^{(L)} = -2\ \Omega\ \underline{C}_{(e)}\ \dot{\underline{\delta}}$$

such that:

$$\underline{C}_{(e)} = \underline{C}_{11} + \underline{C}_{12} + \underline{C}_{12}^t + \underline{C}_{22}$$

and

$$\underline{C}_{11} = \iint_{\substack{x-y \\ \text{element}}} \underline{N}_1^t\ \underline{Q}_{11}\ \underline{N}_1\ dxdy$$

$$\underline{C}_{12} = \iint_{\substack{x-y \\ \text{element}}} \underline{N}_1^t\ \underline{Q}_{12}\ \underline{N}_2\ dxdy$$

$$\underline{C}_{22} = \iint_{\substack{x-y \\ \text{element}}} \underline{N}_2^t\ \underline{Q}_{22}\ \underline{N}_2\ dxdy$$

where,

$$\underline{Q}_{11} = \sum_{L=1}^{N_L} \underline{Q}_{11}^{(L)} = \left(\sum_{L=1}^{N_L} \rho^{(L)}\ h^{(L)} \right) \underline{C}$$

$$\underline{Q}_{12} = \sum_{L=1}^{N_L} \underline{Q}_{12}^{(L)} = \left(\sum_{L=1}^{N_L} \rho^{(L)}\ \Phi^{(L)} \right) \underline{C}$$

$$\underline{Q}_{22} = \sum_{L=1}^{N_L} \underline{Q}_{22}^{(L)} = \left(\sum_{L=1}^{N_L} \rho^{(L)}\ \Psi^{(L)} \right) \underline{C}$$

Equivalent Nodal Loading Vector Due To $\underline{a}_p$

Using a similar approach to that described above, it can be shown that,

$$\underline{F}_p = \Omega^2 \iint_{x-y} \left[\underline{N}_1^t \; \underline{P}_{11}^{(L)} \; \underline{N}_1 + \underline{N}_1^t \; \underline{P}_{12}^{(L)} \; \underline{N}_2 + \left(\underline{N}_1^t \; \underline{P}_{12}^{(L)} \; \underline{N}_2 \right)^t + \underline{N}_2^t \; \underline{P}_{22}^{(L)} \; \underline{N}_2 \right] dxdy \; \dot{\underline{\delta}}$$

where

$$\underline{P}_{11}^{(L)} = \int_{Z_L^{(L)}}^{Z_U^{(L)}} \rho^{(L)} \; \bar{\underline{C}} \; dz = \rho^{(L)} \; h^{(L)} \; \bar{\underline{C}}$$

$$\underline{P}_{12}^{(L)} = \int_{Z_L^{(L)}}^{Z_U^{(L)}} \rho^{(L)} \; (Z - Z_0) \; \bar{\underline{C}} \; dz = \rho^{(L)} \; \Phi^{(L)} \; \bar{\underline{C}}$$

$$\underline{P}_{22}^{(L)} = \int_{Z_L^{(L)}}^{Z_U^{(L)}} \rho^{(L)} \; (Z - Z_0)^2 \; \bar{\underline{C}} \; dz = \rho^{(L)} \; \Psi^{(L)} \; \bar{\underline{C}}$$

Hence,

$$\underline{F}_p = \sum_{L=1}^{N_L} \underline{F}_C^{(L)} = \Omega^2 \; \bar{\underline{M}}_{(e)} \delta$$

such that

$$\bar{\underline{M}}_{(e)} = \bar{\underline{M}}_{11} + \bar{\underline{M}}_{12} + \bar{\underline{M}}_{12}^t + \bar{\underline{M}}_{22}$$

where,

$$\bar{\underline{M}}_{11} = \iint_{\substack{x-y \\ \text{element}}} \underline{N}_1^t \; \underline{P}_{11} \; \underline{N}_1 \; dxdy$$

$$\bar{\underline{M}}_{12} = \iint_{\substack{x-y \\ \text{element}}} \underline{N}_1^t \quad \underline{P}_{12} \quad \underline{N}_2 \; dxdy$$

$$\bar{\underline{M}}_{22} = \iint_{\substack{x-y \\ \text{element}}} \underline{N}_1^t \quad \underline{P}_{22} \quad \underline{N}_2 \; dxdy$$

and

$$\underline{P}_{11} = \sum_{L=1}^{N_L} \underline{P}_{11}^{(L)} = \left(\sum_{L=1}^{N_L} \rho^{(L)} \; h^{(L)} \right) \bar{\underline{C}}$$

$$\underline{P}_{12} = \sum_{L=1}^{N_L} \underline{P}_{12}^{(L)} = \left(\sum_{L=1}^{N_L} \rho^{(L)} \; \Phi^{(L)} \right) \bar{\underline{C}}$$

$$\underline{P}_{22} = \sum_{L=1}^{N_L} \underline{P}_{22}^{(L)} = \left(\sum_{L=1}^{N_L} \rho^{(L)} \; \Psi^{(L)} \right) \bar{\underline{C}}$$

Therefore, due to the combined effects of $\underline{a}_r$, $\underline{a}_c$, and $\underline{a}_p$, the following expression can finally be stated.

$$\underline{F}_r + \underline{F}_c + \underline{F}_p = -\left[\underline{M}_{(e)} \; \ddot{\underline{\delta}} + 2 \; \Omega \; \underline{C}_{(e)} \; \dot{\underline{\delta}} - \Omega^2 \; \bar{\underline{M}}_{(e)} \; \underline{\delta} \right]$$

4.7 Derivation of Element Stiffness Matrix and Non-Linear Equations For Dynamic Analysis

For an n-noded finite element, from the principle of virtual work, the following is the valid relationship:

$$d\psi = dU - dW = 0$$

If the dynamic effect (as acceleration) is dealt with by D'Alembert's principle as equivalent inertial loading then dW will contain dKE.

From the basic procedure of the FEM, it can be shown, that for an element:

$$\int_{element}\int\int \underline{B}^t \ \underline{\sigma} \ d(vol) - \underline{F}_{(e)} = \underline{0}$$

and for the whole structure:

$$\sum_e \int\int_e\int \underline{B}^t \ \underline{\sigma} \ d(vol) - \underline{F} = \underline{0}$$

It can be seen to be simple and logical to beginwith elemental equations and then to assemble them in the usual way in order to derive overall structural equations.

Linearisation Of Element Equations

Considering an approximate solution in terms of $\underline{\sigma}$ and $\underline{B}$, the residual nodal force vector is defined as below:

$$\underline{R}_{(e)} = \underline{F}_{(e)} - \iiint_{element} \underline{B}^t \ \underline{\sigma} \ d(vol)$$

Let $\underline{B} + \Delta\underline{B}$, $\underline{\sigma} + \Delta\underline{\sigma}$ represent the exact solution,

Thereafter:

$$\iiint_{element} (\underline{B} + \Delta\underline{B})^t (\underline{\sigma} + \Delta\underline{\sigma}) \ d(vol) - \underline{F}_{(e)} = 0$$

Hence,

$$\iiint_{element} \Delta\underline{B}^t \ \underline{\sigma} \ d(vol) + \iiint_{element} \underline{B}^t \ \Delta\underline{\sigma} \ d(vol) \approx \underline{R}_{(e)}$$

where $\underline{B}$ is defined such that:

$$d\underline{\varepsilon} = \underline{B}\ d\underline{\delta}$$

and,

$$\underline{B} = \underline{B}_0 + \underline{B}_s + (Z - Z_0)\ \hat{\underline{B}}_b + \underline{B}_L + (Z - Z_0)\ \hat{\underline{B}}_L$$

Considering the component: $\iiint \underline{B}^t\ \Delta\underline{\sigma}\ d(vol)$

Let the incremental stress-strain relation for a linear elastic material be estimated (for the Lth layer) as follows:

$$\Delta\underline{\sigma}^{(L)} = \underline{D}^{(L)}\ \Delta\underline{\varepsilon}$$

hence,

$$\Delta\underline{\sigma}^{(L)} = \underline{D}^{(L)}\ \underline{B}\ \Delta\underline{\delta}$$

$$= \underline{D}^{(L)}\ [\underline{B}_0 + \underline{B}_s + (Z - Z_0)\ \hat{\underline{B}}_b + \underline{B}_L + (Z - Z_0)\ \hat{\underline{B}}_L]\ \Delta\underline{\delta}$$

i.e.

$$\int_{Z_L}^{Z_U} \underline{B}^{t(L)}\ \Delta\underline{\sigma}\ dz = \int_{Z_L}^{Z_U} \Big[\underline{B}_0^t + \underline{B}_s^t + (Z - Z_0)\ \hat{\underline{B}}_b^t + \underline{B}_L^t + (Z - Z_0)\ \hat{\underline{B}}_L^t\Big] \underline{D}^{(L)} \Big[\underline{B}_0 + \underline{B}_s + (Z - Z_0)\hat{\underline{B}}_b + \underline{B}_L + (Z - Z_0)\ \hat{\underline{B}}_L\Big] dz\ \Delta\underline{\delta}$$

Defining

$$\underline{D}_{11}^{(L)} = \int_{Z_L}^{Z_U} \underline{D}^{(L)}\, dz = h\, \underline{D}^{(L)}$$

$$\underline{D}_{12}^{(L)} = \int_{Z_L}^{Z_U} (Z - Z_0)\, \underline{D}^{(L)}\, dz = \Phi\, \underline{D}^{(L)}$$

$$\underline{D}_{22}^{(L)} = \int_{Z_L}^{Z_U} (Z - Z_0)^2\, \underline{D}^{(L)}\, dz = \Psi\, \underline{D}^{(L)}$$

then, it can be deduced that:

$$\int_{Z_L}^{Z_U} \underline{B}^t\, \Delta\underline{\sigma}\, dz = \Big\{ (\underline{B}_0 + \underline{B}_s + \underline{B}_L)^t\, \underline{D}_{11}^{(L)}\, (\underline{B}_0 + \underline{B}_s + \underline{B}_L)$$

$$+ (\underline{B}_0 + \underline{B}_s + \underline{B}_L)^t\, \underline{D}_{12}^{(L)}\, (\hat{\underline{B}}_b + \hat{\underline{B}}_L)$$

$$+ \Big[(\underline{B}_0 + \underline{B}_s + \underline{B}_L)^t\, \underline{D}_{12}^{(L)}\, (\hat{\underline{B}}_b + \hat{\underline{B}}_L) \Big]^t$$

$$+ (\hat{\underline{B}}_b + \hat{\underline{B}}_L)^t\, \underline{D}_{22}^{(L)}\, (\hat{\underline{B}}_b + \hat{\underline{B}}_L) \Big\}\, \Delta\underline{\delta}$$

From the physical considerations, the transverse shear strain energy is a function of the transverse shear stresses and strains only. Hence, the following relations should be true:

$$\underline{B}_s^t \; \underline{D}_{11}^{(L)} (\underline{B}_0 + \underline{B}_L) = \underline{0}$$

$$\underline{B}_s^t \; \underline{D}_{12}^{(L)} (\hat{\underline{B}}_b + \hat{\underline{B}}_L) = \underline{0}$$

$$(\hat{\underline{B}}_b + \hat{\underline{B}}_L)^t \; \underline{D}_{12}^{(L)} \underline{B}_s = \underline{0}$$

Thereafter, the above equation may be rewritten as follow:

$$\int_{(L)}^{z_U} \underline{B}^t \, \Delta\underline{\sigma} \, dz = \Big[(\underline{B}_0 + \underline{B}_L)^t \; \underline{D}_{11}^{(L)} (\underline{B}_0 + \underline{B}_L) + \underline{B}_s^t \; \underline{D}_{11}^{(L)} \underline{B}_s$$

$$z_L$$

$$+ (\underline{B}_0 + \underline{B}_L)^t \; \underline{D}_{12}^{(L)} (\hat{\underline{B}}_b + \hat{\underline{B}}_L)$$

$$+ (\hat{\underline{B}}_b + \hat{\underline{B}}_L)^t \; \underline{D}_{12}^{(L)} (\underline{B}_0 + \underline{B}_L)$$

$$+ (\hat{\underline{B}}_b + \hat{\underline{B}}_L)^t \; \underline{D}_{22}^{(L)} (\hat{\underline{B}}_b + \hat{\underline{B}}_L) \Big] \Delta\underline{\delta}$$

Defining,

$$\underline{D}_{11} = \sum_{L=1}^{N_L} \underline{D}_{11}^{(L)} = \sum_{L=1}^{N_L} (h \; \underline{D}^{(L)})$$

$$\underline{D}_{12} = \sum_{L=1}^{N_L} \underline{D}_{12}^{(L)} = \sum_{L=1}^{N_L} (\Phi \; \underline{D}^{(L)})$$

$$\underline{D}_{22} = \sum_{L=1}^{N_L} \underline{D}_{22}^{(L)} = \sum_{L=1}^{N_L} (\Psi \; \underline{D}^{(L)})$$

then it can be shown that:

$$\int_{-h/2}^{h/2} \underline{B}^t \, \Delta\underline{\sigma} \, dz = \sum_{L=1}^{N_L} \left[\int_{Z_L}^{(L)} B_-^t \, \Delta\sigma_- dz \right]^{(L)}$$

i.e.

$$\int_{-h/2}^{h/2} \underline{B}^t \, \Delta\underline{\sigma} \, dz = \Big[(\underline{B}_0 + \underline{B}_L)^t \, \underline{D}_{11} \, (\underline{B}_0 + \underline{B}_L)$$

$$+ \underline{B}_s^t \, \underline{D}_{11} \, \underline{B}_s$$

Cont....

$$+ (\underline{B}_0 + \underline{B}_L)^t \, \underline{D}_{12} \, (\hat{\underline{B}}_b + \hat{\underline{B}}_L)$$

$$+ (\hat{\underline{B}}_b + \hat{\underline{B}}_L)^t \, \underline{D}_{12} \, (\underline{B}_0 + \underline{B}_L)$$

$$+ (\hat{\underline{B}}_b + \hat{\underline{B}}_L)^t \, \underline{D}_{22} \, (\hat{\underline{B}}_b + \hat{\underline{B}}_L) \Big] \, \Delta\underline{\delta}$$

Hence, it can be shown that:

$$\iiint_{\text{element}} \underline{B}^t \, \Delta\underline{\sigma} \, d(\text{vol}) = \underline{K}_{(e)} \, \Delta\underline{\delta}$$

such that

$$\underline{K}_{(e)} = \underline{K}_{11} + \underline{K}_{12} + \underline{K}_{12}^t + \underline{K}_{22}$$

where

$$\underline{K}_{11} = \iint_{\substack{x-y \\ \text{element}}} (\underline{B}_0 + \underline{B}_L)^t \, \underline{D}_{11} \, (\underline{B}_0 + \underline{B}_L) \, dxdy$$

$$+ \iint_{\substack{x-y \\ \text{element}}} \underline{B}_s^t \, \underline{D}_{11} \, \underline{B}_s \, dxdy$$

$$\underline{K}_{12} = \iint_{\substack{x-y \\ \text{element}}} (\underline{B}_0 + \underline{B}_L)^t \quad \underline{D}_{12} \quad (\hat{\underline{B}}_b + \hat{\underline{B}}_L) \; dxdy$$

$$\underline{K}_{22} = \iint_{\substack{x-y \\ \text{element}}} (\hat{\underline{B}}_b + \hat{\underline{B}}_L)^t \quad \underline{D}_{22} \quad (\hat{\underline{B}}_b + \hat{\underline{B}}_L) \; dxdy$$

Subsequently, considering the component: $\iiint \Delta \underline{B}^t \quad \underline{\sigma}$

For the Lth layer

$$\underline{\sigma}^{(L)} = \sum_{\substack{\text{solution} \\ \text{increment}}} \Delta \underline{\sigma}^{(L)}$$

and the following expression has been derived earlier:

$$\Delta \underline{B}^t \; \underline{\sigma}^{(L)} = \Big[\underline{G}_1^t \quad \underline{S}_{11}^{(L)} \quad \underline{G}_1 + (Z - Z_0)(\underline{G}_1^t \quad \underline{S}_{12}^{(L)} \quad \underline{G}_2) + (Z - Z_0)(\underline{G}_1^t \quad \underline{S}_{12} \quad \underline{G}_2)^t \Big] \Delta \underline{\delta}$$

where,

$$\underline{S}_{11}^{(L)} = \begin{bmatrix} \sigma_x \quad \underline{I}_3 & \tau_{xy} \quad \underline{I}_3 \\ \tau_{xy} \quad \underline{I}_3 & \sigma_y \quad \underline{I}_3 \end{bmatrix}$$

$$\underline{S}_{12}^{(L)} = \begin{bmatrix} \sigma_x \quad \underline{I}_{3x2} & \tau_{xy} \quad \underline{I}_{3x2} \\ \tau_{xy} \quad \underline{I}_{3x2} & \sigma_y \quad \underline{I}_{3x2} \end{bmatrix}$$

$$\underline{I}_3 = \begin{bmatrix} 1 & 0 & 0 \\ 0 & 1 & 0 \\ 0 & 0 & 1 \end{bmatrix}$$

$$\underline{I}_{3x2} = \begin{bmatrix} 1 & 0 \\ 0 & 1 \\ 0 & 0 \end{bmatrix}$$

Defining $\Delta\underline{\sigma}_1$, $\Delta\hat{\underline{\sigma}}_2$ such that

$$\Delta\underline{\sigma} = \Delta\underline{\sigma}_1 + (Z - Z_0)\,\Delta\hat{\underline{\sigma}}_2$$

then it can be deduced that:

$$\Delta\underline{\sigma}_1^{(L)} = \underline{D}^{(L)} [\underline{B}_0 + \underline{B}_s + \underline{B}_L]$$

$$\Delta\hat{\underline{\sigma}}_2^{(L)} = \underline{D}^{(L)} [\hat{\underline{B}}_b + \hat{\underline{B}}_L]$$

and

$$\underline{\sigma}_1^{(L)} = \sum_{\text{solution increment}} \Delta\,\underline{\sigma}^{(L)}$$

$$\hat{\underline{\sigma}}_2^{(L)} = \sum_{\text{solution increment}} \Delta\,\hat{\underline{\sigma}}^{(L)}$$

For any layer let,

$$\underline{\sigma}_1^{(L)} = \left\{ \bar{\sigma}_x^{(L)} \quad \bar{\sigma}_y^{(L)} \quad \bar{\tau}_{xy}^{(L)} \quad \bar{\tau}_{yz}^{(L)} \quad \bar{\tau}_{zx}^{(L)} \right\}$$

$$\underline{\sigma}_2^{(L)} = \left\{ \hat{\sigma}_x^{(L)} \quad \hat{\sigma}_y^{(L)} \quad \hat{\tau}_{xy}^{(L)} \quad 0 \quad 0 \right\}$$

then

$$\underline{S}_{11}^{(L)} = \bar{\underline{S}}_{11}^{(L)} + (Z - Z_0)\,\hat{\underline{S}}_{11}^{(L)}$$

$$\underline{\underline{S}}_{12}^{(L)} = \bar{\underline{\underline{S}}}_{12}^{(L)} + (Z - Z_0)\ \hat{\underline{\underline{S}}}_{12}^{(L)}$$

It can therefore be shown that,

$$\begin{aligned}\Delta\underline{\underline{B}}^t\ \underline{\sigma}^{(L)} = \Big[& \underline{G}_1^t\ \bar{\underline{\underline{S}}}_{11}^{(L)}\ \underline{G}_1 + (Z - Z_0)\ \underline{G}_1^t\ \hat{\underline{\underline{S}}}_{11}^{(L)}\ \underline{G}_1 \\ & + (Z - Z_0)\ \underline{G}_1^t\ \bar{\underline{\underline{S}}}_{12}^{(L)}\ \underline{G}_2 \\ & + (Z - Z_0)^2\ \underline{G}_1^t\ \hat{\underline{\underline{S}}}_{12}^{(L)}\ \underline{G}_2 \\ & + (Z - Z_0)\ (\underline{G}_1^t\ \bar{\underline{\underline{S}}}_{12}^{(L)}\ \underline{G}_2)^t \\ & + (Z - Z_0)^2\ (\underline{G}_1^t\ \hat{\underline{\underline{S}}}_{12}^{(L)}\ \underline{G}_2)^t \Big]\ \Delta\underline{\delta}\end{aligned}$$

Hence, it can be shown that:

$$\int_{\text{element}}\int\int \Delta\underline{\underline{B}}^t\ \underline{\sigma}^{(L)}\ d(\text{vol}) = \underline{\underline{K}}_{\sigma(e)}\Delta\underline{\delta}$$

where,

$$\underline{\underline{K}}_{\sigma(e)} = \bar{\underline{\underline{K}}}_{11} + \hat{\underline{\underline{K}}}_{11} + (\bar{\underline{\underline{K}}}_{12} + \hat{\underline{\underline{K}}}_{12}) + (\bar{\underline{\underline{K}}}_{12} + \hat{\underline{\underline{K}}}_{12})^t$$

such that:

$$\bar{\underline{\underline{K}}}_{11} = \iint_{\substack{x-y\\ \text{element}}} \underline{G}_1^t\ \bar{\underline{\underline{S}}}_{11}\ \underline{G}_1\ dxdy$$

$$\hat{\underline{\underline{K}}}_{11} = \iint_{\substack{x-y\\ \text{element}}} \underline{G}_1^t\ \hat{\underline{\underline{S}}}_{11}\ \underline{G}_1\ dxdy$$

$$\bar{\underline{K}}_{12} = \iint_{\substack{x-y \\ \text{element}}} \underline{G}_1^t \quad \bar{\underline{S}}_{12} \; \underline{G}_2 \; dxdy$$

$$\hat{\underline{K}}_{12} = \iint_{\substack{x-y \\ \text{element}}} \underline{G}_1^t \quad \hat{\underline{S}}_{12} \; \underline{G}_2 \; dxdy$$

where

$$\bar{\underline{S}}_{11} = \sum_{L=1}^{N_L} \int_{Z_L^{(L)}}^{Z_U^{(L)}} \bar{\underline{S}}_{11}^{(L)} \, dz = \sum_{L=1}^{N_L} h^{(L)} \; \bar{\underline{S}}_{11}^{(L)}$$

$$\hat{\underline{S}}_{11} = \sum_{L=1}^{N_L} \int_{Z_L^{(L)}}^{Z_U^{(L)}} (Z - Z_0) \; \hat{\underline{S}}_{11}^{(L)} \, dz = \sum_{L=1}^{N_L} \Phi^{(L)} \; \hat{\underline{S}}_{11}^{(L)}$$

$$\bar{\underline{S}}_{12} = \sum_{L=1}^{N_L} \int_{Z_L^{(L)}}^{Z_U^{(L)}} (Z - Z_0)^2 \; \bar{\underline{S}}_{12}^{(L)} \, dz = \sum_{L=1}^{N_L} \Phi^{(L)} \; \bar{\underline{S}}_{12}^{(L)}$$

$$\hat{\underline{S}}_{12} = \sum_{L=1}^{N_L} \int_{Z_L^{(L)}}^{Z_U^{(L)}} (Z - Z_0)^2 \; \hat{\underline{S}}_{12}^{(L)} \, dz = \sum_{L=1}^{N_L} \Psi^{(L)} \; \bar{\underline{S}}_{12}^{(L)}$$

Final Equation

It can therefore be shown that for an element:

$$(\underline{K} + \underline{K}_\sigma)_e \quad \Delta\underline{\delta} \approx \underline{R}_{(e)}$$

and the above equation can be assembled in the usual way, obtaining:

$$(\underline{K} + \underline{K}_{\sigma}) \ \Delta\underline{\delta} = \underline{R}$$

which can be solved by means of an iterative algorithm.

For dynamic analysis, $\underline{\delta}(t)$ will be measured from the static equilibrium, and from the above equations, it can be shown, for such a case, that:

$$(\underline{K} + \underline{K}_{\sigma})_e \ \underline{\delta}(t) = -\left[\underline{M}_{(e)} \ \underline{\ddot{\delta}} + 2\Omega \ \underline{C}_{(e)} \ \underline{\dot{\delta}} - \Omega^2 \ \underline{\bar{M}}_{(e)} \ \underline{\delta} \right] + \underline{F}\ (t)$$

The above matrix equation can be assembled for all the elements, and rearranged as follow:

$$\underline{M} \ \underline{\ddot{\delta}} + 2\Omega \ \underline{C} \ \underline{\dot{\delta}} + (\underline{K} + \underline{K}_{\sigma} - \Omega^2 \ \underline{\bar{M}}) \ \underline{\delta} = \underline{F}(t)$$

which, represents the dynamic equations with the centrifugal stiffening and rotating inertia effects.

CHAPTER 5

FIRST ORDER CURVED SHELL ELEMENT

5.1 Introduction

In the idealization of a curved shell by finite elements (FEs) the geometrical simplification, which involves the replacement of the curved shell with an assembly of flat elements, is frequently used. With this simplification a large number of elements must inevitably be used, and any advantage that can be gained by use of more sophisticated elements (which in smaller numbers can yield improved accuracy), is lost.

A large number of curved shell FEs has appeared in the literature. The difficulty has been to assess the validity of various combinations of these proposals and to identify and possibly correct, their shortcomings.

Ahmad et al [50] presented an extensive paper discussing the representation of thick and thin shell structures by curved FEs. These authors presented a new process using curved, thick shell FEs which overcame problems arising in previous approximations to the geometry of a structure and resulting from the non-consideration of transverse shear deformation. Several illustrated examples, ranging from thin to thick shell applications, were given to assess the possible accuracy attainable, and to illustrate the versatility of the the new formulation. Curved elements are generally found to be more economical with an adequate representation of a complex problem by very few elements holding the promise of cheap and simple design modification, and representing an essential step in computer-aided design.

Ahmad's curved shell element is simple and efficient for thick shells, and can also be employed for thin shells if a selective integration scheme is employed [59]. Unfortunately, the work published in relation to this element has been, so far, limited to static analysis of isotropic materials only.

In this chapter, an attempt is made to extend the basic concept of Ahmad's element so as to deal with static as well as dynamic analysis of composite layered plates and shells, with a varying number of layers and varying thickness. Since the formulation carried out in this work is aimed at the study of rotating components manufactured from composite materials, the derivations will also include the effect of centrifugal stiffening.

5.2 Geometrical Description

If the element has a total thickness h(x,y), a midsurface will be assumed to divide the thickness into two halves. The element is considered to consist of N_L layers each with thickness $h^{(L)}$ and each made from a composite material of known properties.

Elemental total thickness at any point (x,y) is such that:

$$h(x,y) = \sum_{L=1}^{N_L} h^{(L)}$$

Three different systems of axes can be defined as below:

(i) A system for principal axes of the material (for individual layers). It is preferred to denote this system by (x'', y'', Z''). Coordinates of this system in any event not required in this work.

(ii) A local system for the element which will be denoted by (x', y', z'), where z' is in the normal direction to the midsurface. Usually z'' is in the same direction as z' and for every Lth layer, an angle Θ_L is required which is measured from the x' axis to the x'' (or from the y' axis to the y'') where:

$$C^{(L)} = \text{Cos}\ \Theta^{(L)}$$

$$S^{(L)} = \text{Sin}\ \Theta^{(L)}$$

and from the basic stress-strain relationship;

$$\underline{\sigma} = \underline{D}^{(L)}\ \underline{\varepsilon}$$

Where $\underline{\sigma}$ and $\underline{\varepsilon}$ are measured with respect to element local axes and may be denoted in this section as σ' and ε'.

(iii) Structural global axes (x,y,z).

Geometrical Definition of n-noded Element

The element is defined in terms of:

(i) Midsurface curved element, which is defined (isoparametrically) in terms of n-nodes $[(x_i, y_i, z_i),\ i=1,2.....n]$, where x_i, y_i, z_i are measured with respect to the structural global axes.

(ii) Thickness distribution, i.e., for every node on the Lth layer:

$$Z' = Z_U^{(L)} \qquad \text{at its upper surface}$$

$$Z' = Z_L^{(L)} \qquad \text{at its lower surface}$$

Hence,

$$h^{(L)} = Z_U^{(L)} - Z_L^{(L)} \qquad \text{is its thickness}$$

For the purpose of analysis, the following three geometrical parameters will be defined for each layer, at any (x,y) on the midsurface:

$$h^{(L)} = \int_{Z_L^{(L)}}^{Z_U^{(L)}} dz' = Z_U^{(L)} - Z_L^{(L)}$$

$$\Phi^{(L)} = \int_{Z_L^{(L)}}^{Z_U^{(L)}} (Z' - Z_0') \, dz'$$

$$= (1/2)\left[(Z_U^{(L)} - Z_0')^2 - (Z_L^{(L)} - Z_0')^2\right]$$

$$\Psi^{(L)} = \int_{Z_L^{(L)}}^{Z_U^{(L)}} (Z' - Z_0')^2 \, dz'$$

$$= (1/3)\left[(Z_U^{(L)} - Z_0')^3 - (Z_L^{(L)} - Z_0')^3\right]$$

(iii) The neutral surface for bending is the surface at which the bending stresses are zero. Note that (x',y',z') represents an orthogonal curvilinear system, and, the neutral surface will generally be defined such that:

$$z' = z'_0$$

For a symmetric construction of layers:

$$z'_0 = 0$$

Direction Cosines of Local Axes

The midsurface element can be transformed into a uniform ξ,η intrinsic element, and at any (ξ,η) the corresponding global coordinates can be obtained by means of an isoparametric transformation as below:

$$x(\xi,\eta) = \sum_{i=1}^{n} x_i N_i(\xi,\eta)$$

$$y(\xi,\eta) = \sum_{i=1}^{n} y_i N_i(\xi,\eta)$$

$$z(\xi,\eta) = \sum_{i=1}^{n} z_i N_i(\xi,\eta)$$

Consider three points $a'(\xi,\eta)$, $b'(\xi+\Delta\xi,\eta)$, $c'(\xi,\eta+\Delta\eta)$ which have corresponding position as a,b,c in the x-y-z space, as shown in the figure 5.1. Therefore, it can be deduced that:

$$\vec{ab} = \left[(\Delta x/\Delta\xi)\ \hat{i} + (\Delta y/\Delta\xi)\ \hat{j} + (\Delta z/\Delta\xi)\ \hat{k} \right] \Delta\xi$$

$$\vec{ac} = \left[(\Delta x/\Delta\eta)\ \hat{i} + (\Delta y/\Delta\eta)\ \hat{j} + (\Delta z/\Delta\eta)\ \hat{k} \right] \Delta\eta$$

Taking the limits $\Delta\xi \to 0$, $\Delta\eta \to 0$, two tangential vectors to the midsurface can be defined as follow:

$$\vec{V}_\xi = (\partial x/\partial\xi)\ \hat{i} + (\partial y/\partial\xi)\ \hat{j} + (\partial z/\partial\xi)\ \hat{k}$$

$$\vec{V}_\eta = (\partial x/\partial\eta)\ \hat{i} + (\partial y/\partial\eta)\ \hat{j} + (\partial z/\partial\eta)\ \hat{k}$$

Hence, a vector in the normal direction to the surface (the z' direction) can be defined as follow:

$$\vec{V}_{z'} = \vec{V}_\xi \wedge \vec{V}_\eta$$

$$= \begin{bmatrix} i & j & k \\ \partial x/\partial\xi & \partial y/\partial\xi & \partial z/\partial\xi \\ \partial x/\partial\eta & \partial y/\partial\eta & \partial z/\partial\eta \end{bmatrix}$$

$$= J_x\hat{i} + J_y\hat{j} + J_z\hat{k}$$

where,

$$J_x = \begin{bmatrix} \partial y/\partial\xi & \partial z/\partial\xi \\ \partial y/\partial\eta & \partial z/\partial\eta \end{bmatrix}$$

$$J_y = \begin{bmatrix} \partial z/\partial\xi & \partial x/\partial\xi \\ \partial z/\partial\eta & \partial x/\partial\eta \end{bmatrix}$$

$$J_z = \begin{bmatrix} \partial x/\partial\xi & \partial y/\partial\xi \\ \partial x/\eta & \partial y/\partial\eta \end{bmatrix}$$

Defining,

$$J = \sqrt{(J_x)^2 + (J_y)^2 + (J_z)^2}$$

it can be shown that :

$$\hat{k}' = \bar{V}_{z'} / |\bar{V}_{z'}|$$

$$= l_3\hat{i} + m_3\hat{j} + n_3\hat{k}$$

where,

$\hat{k}'$ is a unit vector in the z' direction

and

$$l_3 = J_x/J$$

$$m_3 = J_y/J$$

$$n_3 = J_z/J$$

Also, from the definition of $\overrightarrow{ab}$, $\overrightarrow{ac}$

$$\overrightarrow{ab} \wedge \overrightarrow{ac} = \Delta A \ \hat{k}'$$

where ΔA is the elemental area abdc. For $\Delta\xi \to 0$, $\Delta\eta \to 0$, it can be proved that:

$$dA = J \, d\xi \, d\eta$$

An intrinsic axis ζ can be assumed orthogonal to the ξ and η axes and its projection in the x-y-z space will be such that:

$$\zeta = 0 \quad \text{at } z' = -h/2$$
$$\zeta = 1 \quad \text{at } z' = h/2$$

and it can be shown that:

$$z' = h(\zeta - 0.5)$$

Hence, at any (ξ, η, ζ);

(i) (x,y,z) on the $z'=0$ surface can be obtained from the previous equation (isoparametric transformation) and denoted by (x_0,y_0,z_0)

(ii) $z' = h(\zeta - 0.5)$

Let

$$\underline{r} = (x - x_0)\hat{i} + (y - y_0)\hat{j} + (z - z_0)\hat{k}$$

then it can be deduced that:

$$\underline{r} = z' \hat{k}'$$

$$= z'(l_3\hat{i} + m_3\hat{j} + n_3\hat{k})$$

Comparing the above two equations, it can be shown that:

$$x(\xi,\eta,\zeta) = x_0(\xi,\eta) + l_3 z'$$

$$y(\xi,\eta,\zeta) = y_0(\xi,\eta) + m_3 z'$$

$$z(\xi,\eta,\zeta) = z_0(\xi,\eta) + n_3 z'$$

i.e.

$$x(\xi,\eta,\zeta) = \left[\sum_{i=1}^{n} x_i N_i(\xi,\eta) \right] + l_3 h\ (\zeta - 0.5)$$

$$y(\xi,\eta,\zeta) = \left[\sum_{i=1}^{n} y_i N_i(\xi,\eta) \right] + m_3 h\ (\zeta - 0.5)$$

$$z(\xi,\eta,\zeta) = \left[\sum_{i=1}^{n} z_i N_i(\xi,\eta) \right] + n_3 h\ (\zeta - 0.5)$$

A three dimensional Jacobian matrix can be defined as below:

$$\underline{J}\left[\frac{x,y,z}{\xi,\eta,\zeta}\right]=\begin{bmatrix}\partial x/\partial\xi & \partial y/\partial\xi & \partial z/\partial\xi\\ \partial x/\partial\eta & \partial y/\partial\eta & \partial z/\partial\eta\\ \partial x/\partial\zeta & \partial y/\partial\zeta & \partial z/\partial\zeta\end{bmatrix}$$

Thereafter, it can be proved that;

$$\underline{J}\left[\frac{x,y,z}{\xi,\eta,\zeta}\right]=\begin{bmatrix}\partial x_0/\partial\xi & \partial y_0/\partial\xi & \partial z_0/\partial\xi\\ \partial x_0/\partial\eta & \partial y_0/\partial\eta & \partial z_0/\partial\eta\\ l_3h & m_3h & n_3h\end{bmatrix}$$

and

$$|\underline{J}| = l_3h\,J_x + m_3hJ_y + n_3hJ_z$$
$$= (h/J)\left|\left[J_x^2 + J_y^2 + J_z^2\right]\right| = hJ$$

i.e.;

$$d(vol) \equiv dx\,dy\,dz$$
$$\equiv |\underline{J}|\,d\xi\,d\eta\,d\zeta$$
$$= hJd\xi\,d\eta\,d\zeta$$
$$= J\,d\xi\,d\eta\,dz'$$

The disadvantage of using the projection of ξ-η as the local axes is that this will limit the freedom of selection of local axes for each element. Compatibility requires that on the boundaries between elements local axes should be identical. Hence the following criterion can be adopted:

(i) If $|\hat{j}\wedge\hat{k}'|\neq 0$

local x' axis will be selected orthogonal to both local z' and global y, i.e.;

$$\hat{i}' = \hat{j} \wedge \hat{k}' / | \hat{j} \wedge \hat{k}' |$$

$$\hat{j}' = \hat{k}' \wedge \hat{i}'$$

(ii) Otherwise

$$\hat{i}' = \hat{j} \wedge \hat{k}' / | \hat{j} \wedge \hat{k}' |$$

$$\hat{j}' = \hat{k}' \wedge \hat{i}'$$

Explicitly,

$$\hat{j} \wedge \hat{k}' = \begin{bmatrix} i & j & k \\ 0 & 1 & 0 \\ l_3 & m_3 & n_3 \end{bmatrix}$$

$$= n_3\hat{i} - l_3\hat{k}$$

Defining

$$\hat{i}' = l_1\hat{i} + m_1\hat{j} + n_1\hat{k}$$

then

(a) if $\sqrt{l_3^2 + n_3^2} > 0$

$$l_1 = n_3 / \sqrt{l_3^2 + n_3^2}$$

$$m_1 = 0$$

$$n_1 = -l_3 / \sqrt{l_3^2 + n_3^2}$$

(b) if $\sqrt{l_3^2 + n_3^2} = 0$

then,

$$l_3 = 0, \quad m_3 = 1.0, \quad n_3 = 0$$

and

$$\hat{k}' = \hat{j}$$

$$\hat{i}' = \hat{i} \wedge \hat{k}' = \hat{i} \wedge \hat{j} = \hat{k}$$

while

$$l_1 = 0, \quad m_1 = 0, \quad n_1 = 1.0$$

(c) $\hat{j}' = \hat{i}' \wedge \hat{j}'$

$$= \hat{l}_2 i + m_2 \hat{j} + n_2 \hat{k}$$

i.e.;

$$l_2 = m_3 n_1 - m_1 n_3$$

$$m_2 = n_3 l_1 - n_1 l_3$$

$$n_2 = l_3 m_1 - l_1 m_3$$

the relation between local and global components can be expressed as follow:

$$\begin{bmatrix} \Delta x' \\ \Delta y' \\ \Delta z' \end{bmatrix} = \underline{R} \begin{bmatrix} \Delta x \\ \Delta y \\ \Delta z \end{bmatrix}$$

or

$$\begin{bmatrix} \Delta x \\ \Delta y \\ \Delta z \end{bmatrix} = \underline{R}^t \begin{bmatrix} \Delta x' \\ \Delta y' \\ \Delta z' \end{bmatrix}$$

where

$$\underline{R} = \begin{bmatrix} l_1 & m_1 & n_1 \\ l_2 & m_2 & n_2 \\ l_3 & m_3 & n_3 \end{bmatrix}$$

and

$$\underline{\bar{R}}^1 = \underline{R}^t$$

5.3 Displacement Components

As this element is considered as a generalisation of Ahmad's element, nodal values (at the ith node) are selected in the manner suggested by Ahmad et al [58], i.e

u_i, v_i, w_i	Global displacement components on the neutral bending surface
α_i	Rotation angle with respect to local y′-axis
β_i	Rotation angle with respect to local x′-axis

The displacement and rotation components at any (ξ,η) on the midsurface will be defined in terms of Lagrangian 2D Shape functions as follow:

$$u_0(\xi,\eta) = \sum_{i=1}^{n} u_i N_i(\xi,\eta)$$

$$v_0(\xi,\eta) = \sum_{i=1}^{n} v_i N_i(\xi,\eta)$$

$$w_0(\xi,\eta) = \sum_{i=1}^{n} w_i N_i(\xi,\eta)$$

$$\alpha(\xi,\eta) = \sum_{i=1}^{n} \alpha_i N_i(\xi,\eta)$$

$$\beta(\xi,\eta) = \sum_{i=1}^{n} \beta_i N_i(\xi,\eta)$$

and the nodal displacement vector for an n-noded element is:

$$\underline{\delta} = \{ u_1 \quad v_1 \quad w_1 \quad \alpha_1 \quad \beta_1 \ldots u_n \quad v_n \quad w_n \quad \alpha_n \quad \beta_n \}$$

The vector of global displacement components at (x,y,z) can be defined as follow:

$$\bar{q}(x,y,z) = u(x,y,z)\hat{i} + v(x,y,z)\hat{j} + w(x,y,z)\hat{k}$$

Defining (x_0,y_0,z_0) as the normal projection of (x,y,z) on the bending neutral surface with respect to the z' axis, it can be shown that;

$$\bar{r} = (x - x_0)\hat{i} + (y - y_0)\hat{j} + (z - z_0)\hat{k}$$

$$= (z' - z'_0)\hat{k}'$$

where z'_0 is the value of z' at the neutral surface,

Hence,

$$\bar{r} = l_3(z' - z'_0)\hat{i} + m_3(z' - z'_0)\hat{j} + n_3(z' - z'_0)\hat{k}$$

Defining also

$$\bar{q}_0 = u_0\hat{i} + v_0\hat{j} + w_0\hat{k}$$

= the displacement vector for (x_0,y_0,z_0)

$$\bar{\Theta} = \alpha\hat{j}' + \beta\hat{i}'$$

= the rotation vector at (x_0,y_0,z_0) or at (x,y,z)

then, it can be shown, for small α and β, that:

$$\underline{q} = \underline{q}_0 + \underline{\Theta} \wedge \underline{r}$$

$$= \underline{q}_0 + (z' - z'_0)\ \underline{\phi}$$

where

$$\underline{\phi} = \underline{\Theta} \wedge \underline{r}$$

$$= (l_1\alpha - l_2\beta)\,\hat{i} + (m_1\alpha - m_2\beta)\,\hat{j} + (n_1\alpha - n_2\beta)\,\hat{k}$$

or

$$\mathfrak{q} = \mathfrak{q}_0 + (z' - z'_0)\ \underline{\phi}$$

where

$$\mathfrak{q} = \begin{bmatrix} u \\ v \\ w \end{bmatrix}$$

$$\mathfrak{q}_0 = \begin{bmatrix} u_0 \\ v_0 \\ w_0 \end{bmatrix}$$

$$\underline{\phi} = \begin{bmatrix} l_1\alpha - l_2\beta \\ m_1\alpha - m_2\beta \\ n_1\alpha - n_2\beta \end{bmatrix}$$

5.4 Strain-Displacement Relationships

Because of compatibility and continuity of deformation, the element in a laminated composite structure has no effect on the strain-displacement relationships. Hence, from the previous analysis, the following can be deduced:

$$\underline{\varepsilon} = \{ \varepsilon_x \quad \varepsilon_y \quad \gamma_{xy} \quad \gamma_{yz} \quad \gamma_{zx} \}$$

and by proper partitioning:

$$\underline{\varepsilon}' = \underline{\varepsilon}_0' + \underline{\varepsilon}_s' + \underline{\varepsilon}_b' + \underline{\varepsilon}_L'$$

where,

$$\underline{\varepsilon}_0 = \begin{bmatrix} \partial u_0'/\partial x' \\ \partial v_0'/\partial y' \\ \partial u_0'/\partial y' + \partial v_0'/\partial x' \\ 0 \\ 0 \end{bmatrix}$$

$$\underline{\varepsilon}_s' = \begin{bmatrix} 0 \\ 0 \\ 0 \\ -\beta + \partial w_0'/\partial y' \\ \alpha + \partial w_0'/\partial x' \end{bmatrix}$$

$$\underline{\varepsilon}_b' = (z' - z_0') \begin{bmatrix} \partial\alpha/\partial x' \\ -\partial\beta/\partial y' \\ \partial\alpha/\partial y' - \partial\beta/\partial x' \\ 0 \\ 0 \end{bmatrix}$$

$$\underline{\varepsilon}_L' = (1/2) \begin{bmatrix} \left[(\partial u_0'/\partial x')^2 + (\partial v_0'/\partial x')^2 + (\partial w_0'/\partial x')^2\right] \\ \left[(\partial u_0'/\partial y')^2 + (\partial v_0'/\partial y')^2 + (\partial w_0'/\partial y')^2\right] \\ 2\left[(\partial u_0'/\partial x')(\partial u_0'/\partial y') + (\partial v_0'/\partial x')(\partial v_0'/\partial y') + (\partial w_0/\partial x)(\partial w_0/\partial y)\right] \\ 0 \\ 0 \end{bmatrix}$$

The various $\underline{B}$ matrices (excluding large deformation) can be defined such that:

$$\underline{\varepsilon}_0' = \underline{B}_0 \ \underline{\delta}$$

$$\underline{\varepsilon}_s' = \underline{B}_s \ \underline{\delta}$$

$$\underline{\varepsilon}_b' = (z - z_0)\ \hat{\underline{B}}_b \ \underline{\delta}$$

Each $\underline{B}$ matrix will be defined in terms of nodal submatrices, i.e.

$$\underline{B} = [\ \underline{b}_1 \ \ \underline{b}_2 \ \ \underline{b}_3 \cdots\cdots \underline{b}_i \cdots\cdots\cdots \underline{b}_n\ ]$$

such that,

$\underline{B}$ is a 5x5n matrix

$\underline{b}_i$ is a 5x5 matrix

And,

$$(\underline{b}_i)_0 = \begin{bmatrix} l_1 C_{1,i} & m_1 C_{1,i} & n_1 C_{1,i} & 0 & 0 \\ l_2 C_{2,i} & m_2 C_{2,i} & n_2 C_{2,i} & 0 & 0 \\ l_1C_{2,i}+l_2C_{1,i} & m_1C_{2,i}+m_2C_{2,i} & n_1C_{2,i}+n_1C_{1,i} & 0 & 0 \\ 0 & 0 & 0 & 0 & 0 \\ 0 & 0 & 0 & 0 & 0 \end{bmatrix}$$

$$(\underline{b}_i)_s = \begin{bmatrix} 0 & 0 & 0 & 0 & 0 \\ 0 & 0 & 0 & 0 & 0 \\ 0 & 0 & 0 & 0 & 0 \\ l_3 C_{2,i} & m_3 C_{2,i} & n_3 C_{2,i} & 0 & -N_i \\ l_3 C_{1,i} & m_3 C_{1,i} & n_3 C_{1,i} & N_i & 0 \end{bmatrix}$$

$$(\hat{b}_i)_b = \begin{bmatrix} 0 & 0 & 0 & C_{1,i} & 0 \\ 0 & 0 & 0 & 0 & -C_{2,i} \\ 0 & 0 & 0 & C_{2,i} & -C_{1,i} \\ 0 & 0 & 0 & 0 & 0 \\ 0 & 0 & 0 & 0 & 0 \end{bmatrix}$$

Whereas

$$C_{s,i} = A_{s1}\partial N_i/\partial\xi + A_{s2}\partial N_i/\partial\eta$$

such that,

$$A_{11} = \alpha_{22}/\alpha$$

$$A_{22} = \alpha_{11}/\alpha$$

$$A_{12} = -\alpha_{12}/\alpha$$

$$A_{21} = -\alpha_{21}/\alpha$$

where

$$\alpha_{st} = J_{s1}l_t + J_{s2}m_t + J_{s3}n_t$$

$$\alpha = \alpha_{11}\alpha_{22} - \alpha_{12}\alpha_{21}$$

and

$$s = 1,2$$

$$t = 1,2$$

$$i = 1,2.....n$$

$$\underline{J}_{3x3} = \underline{J}\left[\frac{x,y,z}{\xi,\eta,\zeta}\right] \text{ as defined earlier.}$$

In order to define the interpolation equations for large deformation strains, the following rotation vectors are defined:

$$\underline{\Theta}_x = \{\ \partial u_0'/\partial x' \quad \partial v_0'/\partial x' \quad \partial w_0'/\partial x'\ \}$$

$$\underline{\Theta}_y = \{\ \partial u_0'/\partial y' \quad \partial v_0'/\partial y' \quad \partial w_0'/\partial y'\ \}$$

then, it can be deduced that:

$$\underline{\Theta}_x = \underline{G}_x \quad \underline{\delta}$$

$$\underline{\Theta}_y = \underline{G}_y \quad \underline{\delta}$$

with

$$\underline{G} = [\ g_1 \quad g_2 \quad g_3 \ldots\ldots\ldots g_n\ ]$$

and

$$(\ g_i)_x = \left[\ C_{1,i}\ \underline{R} \qquad \underline{0}_{3x2}\right]$$

$$(\ g_i)_y = \left[\ C_{2,i}\ \underline{R} \qquad \underline{0}_{3x2}\right]$$

where $\underline{0}_{mxn}$ is a null matrix of order mxn

Hence, it can be shown that:

$$d\underline{\varepsilon}'_L = \underline{B}_L\ d\underline{\delta}$$

where

$$\underline{B}_L = \underline{A}\ \underline{G}$$

with

$$\underline{G} = \begin{bmatrix} \underline{G}_x \\ \\ \underline{G}_y \end{bmatrix}$$

$$\underline{A} = \begin{bmatrix} \Theta_x^t & \underline{0}_{3x2} \\ \\ \underline{0}_{3x2} & \Theta_y^t \\ \\ \Theta_y^t & \Theta_x^t \end{bmatrix}$$

An interesting result can also be deduced from the large deflection analysis

$$d\underline{B}_L^t\ \underline{\sigma}'\ =\ \underline{G}^t\ \underline{S}\ \ \underline{G}\ \ d\underline{\delta}$$

such that

$$\underline{\sigma}' = \{\ \sigma_x'\ \ \sigma_y'\ \ \tau_{xy}'\ \ \tau_{yz}'\ \ \tau_{zx}'\ \}$$

$$\underline{S} = \begin{bmatrix} \underline{\sigma}_x' \ \underline{I}_3 & \underline{\tau}_{xy}' \ \underline{I}_3 \\ \underline{\tau}_{xy}' \ \underline{I}_3 & \underline{\sigma}_y' \ \underline{I}_3 \end{bmatrix}$$

$$\underline{I}_3 = \begin{bmatrix} 1 & 0 & 0 \\ 0 & 1 & 0 \\ 0 & 0 & 1 \end{bmatrix}$$

5.5 Derivation Of Element Stiffness Matrix

From the analysis in the previous chapter, it can be deduced that the linearised equation of equilibrium for an element is:

$$\iiint_{\text{element}} \Delta\underline{B}^t \ \underline{\sigma}' \ d(\text{vol}) + \iiint_{\text{element}} \underline{B}^t \ \Delta\underline{\sigma}' \ d(\text{vol}) \approx \underline{R}_{(e)}$$

where

$$\underline{R}_{(e)} = \underline{F}_{(e)} - \iiint_{\text{element}} \underline{B}^t \ \underline{\sigma}' d(\text{vol})$$

and

$$d\underline{\varepsilon}' = \underline{B} \ d\underline{\delta}$$

and from previous analysis:

$$\underline{B} = \underline{B}_0 + \underline{B}_s + \underline{B}_L + (z' - z_0') \ \hat{\underline{B}}_b$$

Considering the component: $\iiint \underline{B}^t \ \Delta\underline{\sigma}' \ d(vol)$

The incremental stress-strain relation for the Lth layer can be deduced from equation (4) as follows:

$$\Delta\underline{\sigma}^{(L)} = \underline{D}^{(L)} \ \Delta\underline{\varepsilon}',$$

Hence,

$$\Delta\underline{\sigma}^{(L)} = \underline{D}^{(L)} \ [\underline{B}_0 + \underline{B}_s + \underline{B}_L + (z' - z_0') \ \hat{\underline{B}}_b \ ] \ \Delta\underline{\delta}$$

whereas,

$$\underline{B}^t \Delta\underline{\sigma}^{(L)}$$

$$= \left[\underline{B}_0 + \underline{B}_s + B_L + (z' - z_0')\hat{\underline{B}}_b\right]^t D^{(L)} \left[\underline{B}_0 + \underline{B}_s + \underline{B}_L + (z' - z_0') \ \hat{\underline{B}}_b\right] \ \Delta\underline{\delta}$$

and from the nature of $\underline{\varepsilon}_s$, $\underline{\sigma}_s$ it can be shown that

$$\underline{B}_s \ \underline{D}^{(L)} \ [\underline{B}_0 + \underline{B}_L + (z' - z_0') \ \hat{\underline{B}}_b] = \underline{0} \qquad \text{etc} \quad \text{etc}$$

Therefore,

$$\underline{B}^t \ \Delta\underline{\sigma}^{(L)} = \Big[(\underline{B}_0 + \underline{B}_L)^t \ \underline{D}^{(L)} \ (\underline{B}_0 + \underline{B}_L) + \underline{B}_s^t \ \underline{D}^{(L)} \ \underline{B}_s$$

$$+ (z' - z_0') \ \hat{\underline{B}}_b^t \ \underline{D}^{(L)} \ (\underline{B}_0 + \underline{B}_L)$$

$$+ (z' - z_0') (\underline{B}_0 + \underline{B}_L)^t \ \underline{D}^{(L)} \ \hat{\underline{B}}_b$$

$$+ (z' - z_0')^2 \ \hat{\underline{B}}_b^t \ D^{(L)} \ \hat{\underline{B}}_b \Big] \ \Delta\underline{\delta}$$

Defining:

$$\underline{D}_{11}^{(L)} = \int_{Z_L^{(L)}}^{Z_U^{(L)}} \underline{D}^{(L)} \, dz' = h^{(L)} \, \underline{D}^{(L)}$$

$$\underline{D}_{12}^{(L)} = \int_{Z_L^{(L)}}^{Z_U^{(L)}} (z' - z_0') \, \underline{D}^{(L)} \, dz' = \Phi^{(L)} \, \underline{D}^{(L)}$$

$$\underline{D}_{22}^{(L)} = \int_{Z_L^{(L)}}^{Z_U^{(L)}} (z' - z_0')^2 \, \underline{D}^{(L)} \, dz' = \Psi^{(L)} \, \underline{D}^{(L)}$$

Then, it can be shown that:

$$\int_{ZL^{(L)}}^{Z_U^{(L)}} \underline{B}^t \, \Delta\underline{\sigma} \, dz' = \Big\{ (\underline{B}_0 + \underline{B}_L)^t \, \underline{D}_{11}^{(L)} \, (\underline{B}_0 + \underline{B}_L)$$

$$+ \underline{B}_s^t \, \underline{D}_{11}^{(L)} \, \underline{B}_s + (\underline{B}_0 + \underline{B}_L)^t \, \underline{D}_{12}^{(L)} \, \hat{\underline{B}}_b$$

$$+ \left[(\underline{B}_0 + \underline{B}_L)^t \, \underline{D}_{12}^{(L)} \, \hat{\underline{B}}_b \right]^t$$

$$+ \hat{\underline{B}}_b^t \, \underline{D}_{22}^{(L)} \, \hat{\underline{B}}_b \Big\} \, \Delta\underline{\delta}$$

Furthermore, the following matrices can be defined for the whole element,

$$\underline{D}_{11} = \int_{-h/2}^{h/2} \underline{D}^{(L)}\, dz = \sum_{L=1}^{N_L} \underline{D}_{11}^{(L)} = \sum_{L=1}^{N_L} (h \quad \underline{D}^{(L)})$$

$$\underline{D}_{12} = \int_{-h/2}^{h/2} (z' - z_0')\, \underline{D}^{(L)}\, dz = \sum_{L=1}^{N_L} \underline{D}_{12}^{(L)} = \sum_{L=1}^{N_L} (\Phi \quad \underline{D}^{(L)})$$

$$\underline{D}_{22} = \int_{-h/2}^{h/2} (z' - z_0')^2\, \underline{D}^{(L)}\, dz = \sum_{L=1}^{N_L} \underline{D}_{22}^{(L)} = \sum_{L=1}^{N_L} (\Psi \quad \underline{D}^{(L)})$$

Hence, it can be deduced that:

$$\int_{-h/2}^{h/2} \underline{B}^t\, \Delta\sigma\, dz = \Big[(\underline{B}_0 + \underline{B}_L)^t\, \underline{D}_{11}\, (\underline{B}_0 + \underline{B}_L) + \underline{B}_s^t\, \underline{D}_{11}\, \underline{B}_s + (\underline{B}_0 + \underline{B}_L)^t\, \underline{D}_{12}\, \hat{\underline{B}}_b + \Big[(\underline{B}_0 + \underline{B}_L)^t\, \underline{D}_{12}\, \hat{\underline{B}}_b \Big]^t + \hat{\underline{B}}_b^t\, \underline{D}_{22}\, \hat{\underline{B}}_b \Big]\, \Delta\underline{\delta}$$

Finally, it can be shown that:

$$\iiint_{\text{element}} \underline{B}^t\, \Delta\underline{\sigma}\, d(\text{vol}) = \underline{K}_{(e)}\, \Delta\underline{\delta}$$

such that:

$$\underline{K}_{(e)} = \underline{K}_{11} + \underline{K}_{12} + \underline{K}_{12}^t + \underline{K}_{22}$$

where

$$\underline{K}_{11} = \iint_{\xi\eta} (\underline{B}_0 + \underline{B}_L)^t \; \underline{D}_{11} (\underline{B}_0 + \underline{B}_L) \; J \; d\xi \, d\eta$$

$$+ \iint_{\xi\eta} \underline{B}_s^t \; \underline{D}_{11} \; \underline{B}_s \; J \; d\xi \, d\eta$$

$$\underline{K}_{12} = \iint_{\xi\eta} (\underline{B}_0^t + \underline{B}_L)^t \; \underline{D}_{12} \; \hat{\underline{B}}_b \; J \; d\xi \, d\eta$$

$$\underline{K}_{22} = \iint_{\xi\eta} \hat{\underline{B}}_b^t \; \underline{D}_{22} \; \hat{\underline{B}}_b \; J \; d\xi \, d\eta$$

Subsequently, considering the component: $\iiint \Delta \underline{B}^t \; \underline{\sigma} \; d(\text{vol})$

For the Lth layer

$$\Delta \underline{\sigma}^{(L)} = \sum_{\text{sol.inc.}} \left[\Delta \underline{\sigma}_1^{(L)} + (Z' - Z_0') \; \hat{\Delta \underline{\sigma}}_2^{(L)} \right]$$

where,

$$\Delta \underline{\sigma}_1^{(L)} = \underline{D}^{(L)} \; (\underline{B}_0 + \underline{B}_s + \underline{B}_L) \; \Delta \underline{\delta}$$

$$\hat{\Delta \underline{\sigma}}_2^{(L)} = \underline{D}^{(L)} \; \hat{\underline{B}}_b \; \Delta \underline{\delta}$$

Defining

$$\underline{S}^{(L)} = \begin{bmatrix} \sigma_x^{(L)} \; \underline{I}_3 & \tau_{xy}^{(L)} \; \underline{I}_3 \\ \tau_{xy}^{(L)} \; \underline{I}_3 & \sigma_y^{(L)} \; \underline{I}_3 \end{bmatrix}$$

then

$$\underline{S}^{(L)}_{(z')} = \underline{S}^{(L)}_1 + (z' - z'_0)\ \underline{S}^{(L)}_2$$

where

$\underline{S}^{(L)}_1$ is based upon $\underline{\sigma}^{(L)}_1$

$\underline{S}^{(L)}_2$ is based upon $\hat{\underline{\sigma}}^{(L)}_2$

from the previous analysis, it can be deduced that:

$$\Delta\underline{B}^t\ \underline{\sigma}^{(L)} = \underline{G}^t\ \underline{S}^{(L)}\ \underline{G}\ \Delta\underline{\delta}$$

$$= \left[\underline{G}^t\ \underline{S}^{(L)}_1\ \underline{G} + (z' - z'_0)\ \underline{G}^t\ \underline{S}^{(L)}_2\ \underline{G}\right]\Delta\underline{\delta}$$

therefore,

$$\int_{z_L}^{z_U(L)} \Delta B^t\ \sigma^{(L)}\ dz'$$

$$= \underline{G}^t \left\{ \int_{z_L}^{z_U(L)} \left[\underline{S}^{(L)}_1 + (z' - z'_0)\ \underline{S}^{(L)}_2 \right] dz' \right\}\ \underline{G}\ \Delta\underline{\delta}$$

Defining

$$\underline{D}^{(L)}_s = \int_{z_L}^{z_U(L)} \left[\underline{S}^{(L)}_1 + (z' - z'_0)\ \underline{S}^{(L)}_2 \right] dz$$

$$= h^{(L)} \underline{S}_1^{(L)} + \Phi^{(L)} \underline{S}_2^{(L)}$$

$$\underline{D}_s = \sum_{L=1}^{N_L} \int_{Z_L^{(L)}}^{Z_U^{(L)}} \underline{D}_s^{(L)} = \sum_{L=1}^{N_L} \left[h^{(L)} \underline{S}_1^{(L)} + \Phi^{(L)} \underline{S}_2^{(L)} \right]$$

then it can be shown that:

$$\int_{Z_L^{(L)}}^{Z_U^{(L)}} \Delta \underline{B}^t \, \underline{\sigma}^{(L)} \, dz' = \underline{G}^t \, \underline{D}_s^{(L)} \, \underline{G} \, \Delta \underline{\delta}$$

and

$$\int_{-h/2}^{h/2} \Delta \underline{B}^t \, \underline{\sigma} \, dz' = \underline{G}^t \, \underline{D}_s \, \underline{G} \, \Delta \underline{\delta}$$

and it can, therefore, be shown that:

$$\iiint_{\text{element}} \Delta \underline{B}^t \, \underline{\sigma} \, d(\text{vol}) = \left[\iint_{\xi \eta} \underline{G}^t \, \underline{D}_s \, \underline{G} \, J \, d\xi \, d\eta \right] \Delta \underline{\delta}$$

i.e.;

$$\iiint_{\text{element}} \Delta \underline{B}^t \, \underline{\sigma} \, d(\text{vol}) = \underline{K}_{\sigma(e)} \, \Delta \underline{\delta}$$

Where,

$$\underline{K}_{\sigma(e)} = \iint_{\xi \eta} \underline{G}^t \, \underline{D}_s \, \underline{G} \, J \, d\xi \, d\eta$$

Final equation

It can therefore, be shown that for an element:

$$(\underline{K} + \underline{K}_{\sigma})_{(e)} \quad \Delta\underline{\delta} \approx \underline{R}_{(e)}$$

which can be assembled in the usual way, leading to :

$$(\underline{K} + \underline{K}_{\sigma}) \Delta\underline{\delta} = \underline{R}$$

where

$$\underline{R} = \underline{F} - \sum_{e=1}^{ne} \iiint_{e} \underline{B}^{t} \quad \underline{\sigma}' \; d(vol)$$

5.6 Derivation of Element Mass and Rotating Inertia Matrices

Following the procedure explained in an earlier chapter, if a curved-shell element is rotating with a constant rotational speed Ω then the acceleration at any point (x,y,z) is:

$$\underline{a}' = \underline{a} + \underline{a}_r + \underline{a}_c + \underline{a}_p$$

where $\underline{a}$ is the rigid body acceleration

$$= \underline{a}_0 + \underline{\Omega} \wedge (\underline{\Omega} \wedge \underline{r})$$

$\underline{a}_r$ is the relative acceleration

$$= \ddot{\underline{q}}$$

$\underline{a}_c$ is the Coriolis acceleration

$$= 2 \underline{\Omega} \wedge \dot{\underline{q}}$$

$\vec{a}_p$ is the centripetal acceleration

$$= \vec{\Omega} \wedge (\vec{\Omega} \wedge \vec{q})$$

Defining the components of $\vec{\Omega}$ with respect to the global axes, such that

$$\vec{\Omega} = \vec{\Omega}_x \hat{i} + \vec{\Omega}_y \hat{j} + \vec{\Omega}_z \hat{k}$$

and

$$l = \Omega_x / \Omega$$

$$m = \Omega_y / \Omega$$

$$n = \Omega_z / \Omega$$

then , it can be deduced that:

$$\underline{a}_r = \ddot{\underline{q}}_0 + (z' - z'_0) \ddot{\underline{\phi}}$$

$$\underline{a}_c = 2 \Omega \underline{C} \dot{\underline{q}}$$

$$= 2 \Omega \underline{C} \left[\underline{q}_0 + (z' - z_0) \dot{\underline{\phi}} \right]$$

$$\underline{a}_p = -\Omega^2 \underline{\bar{C}} \underline{q}$$

$$= -\Omega^2 \underline{\bar{C}} \left[\underline{q}_0 + (z' - z'_0) \underline{\phi} \right]$$

where

$$\underline{C} = \begin{bmatrix} 0 & -n & m \\ n & 0 & -l \\ -m & l & 0 \end{bmatrix}$$

and

$$\underline{\bar{C}} = \begin{bmatrix} 1.0 - l^2 & -lm & ln \\ -ml & 1.0 - m^2 & -mn \\ -nl & -nm & 1.0 - n^2 \end{bmatrix}$$

Usually $\bar{r}$ is measured relative to a point on the axis of rotation, as explained earlier.
From the definition of $\underline{q}_0$ and $\underline{\phi}$ it can be deduced that:

$$\underline{q}_0 = \begin{bmatrix} u_0 \\ v_0 \\ w_0 \end{bmatrix} = \underline{N}_1 \ \underline{\delta}$$

$$\underline{\phi} = \begin{bmatrix} l_1 \alpha - l_2 \beta \\ m_1 \alpha - m_2 \beta \\ n_1 \alpha - n_2 \beta \end{bmatrix} = \underline{N}_2 \ \underline{\delta}$$

with

$$\underline{N} = [\ \underline{n}_1 \quad \underline{n}_2 \quad \underline{n}_3 \ldots\ldots\ldots\ldots \underline{n}_n\ ]$$

$$(\underline{n}_i)_1 = \begin{bmatrix} N_i & 0 & 0 & 0 & 0 \\ 0 & N_i & 0 & 0 & 0 \\ 0 & 0 & N_i & 0 & 0 \end{bmatrix}$$

$$(\underline{n}_i)_2 = \begin{bmatrix} 0 & 0 & 0 & l_1 N_i & -l_2 N_i \\ 0 & 0 & 0 & m_1 N_i & -m_2 N_i \\ 0 & 0 & 0 & n_1 N_i & -n_2 N_i \end{bmatrix}$$

with

$$\underline{a} = \begin{bmatrix} a_x \\ a_y \\ a_z \end{bmatrix}$$

then

$$\Delta\left(d\overset{(L)}{W}\right) = -\rho^{(L)}\, d\underline{g}^t\, \underline{a}$$

$$= -\rho^{(L)}\, d\underline{\delta}^t \left[\underline{N}_1^t\ \underline{a} + (Z' - Z_0')\ \underline{N}_2^t\ \underline{a} \right]$$

Hence, the equivalent nodal force for inertial loading (by means of $\underline{a}$) can be defined as follow:

$$\underline{F} = -\int_{\xi}\int_{\eta}\left[\sum_{L=1}^{N_L} \int_{Z_L^{(L)}}^{Z_U^{(L)}} \rho^{(L)} \left[\underline{N}_1^t\ \underline{a} + (Z' - Z_0')\ \underline{N}_2^t\ \underline{a} \right] dz'\, J\, d\xi\, d\eta \right]$$

If $\underline{a}$ represents rigid body acceleration only, and defining

$$\rho_1 = \sum_{L=1}^{N_L} \rho^{(L)}\ h^{(L)}$$

$$\rho_2 = \sum_{L=1}^{N_L} \rho^{(L)}\ \Phi^{(L)}$$

then it can be deduced that

$$\underline{F} = -\int_{\xi}\int_{\eta}\left[\rho_1\ \underline{N}_1^t\ \underline{a} + \rho_2\ \underline{N}_2^t\ \underline{a} \right] J\, d\xi\, d\eta$$

Equivalent Nodal Force Vector due to $\underline{a}_r$

From the previous analysis, it can be deduced that:

$$\underline{F}_r = -\iiint \rho \left[\underline{N}_1^t \, \underline{a}_r + (z' - z_0') \, \underline{N}_2^t \, \underline{a}_r \right] d(vol)$$

$$= -\iiint \rho \left\{ \underline{N}_1^t \left[\ddot{\underline{q}}_0 + (z' - z_0') \, \ddot{\underline{\phi}} \right] \right.$$

$$\left. + (z' - z_0') \, \underline{N}_2^t \left[\ddot{\underline{q}}_0 + (z' - z_0') \, \ddot{\underline{\phi}} \right] \right\} d(vol)$$

From an earlier definition, it was shown that:

$$\ddot{\underline{q}}_0 = \underline{N}_1 \, \ddot{\underline{\delta}}$$

$$\ddot{\underline{\phi}} = \underline{N}_2 \, \ddot{\underline{\delta}}$$

Defining $\underline{R}_{11}^{(L)}$, $\underline{R}_{12}^{(L)}$ and $\underline{R}_{22}^{(L)}$ as given earlier, it can be shown that:

$$\underline{F}_r = -\underline{M}_{(e)} \, \ddot{\underline{\delta}}$$

such that

$$\underline{M}_{(e)} = \underline{M}_{11} + \underline{M}_{12} + \underline{M}_{21}^t + \underline{M}_{22}$$

whereas

$$\underline{M}_{11} = \iint_{\xi\,\eta} \underline{N}_1^t \, \underline{R}_{11} \, \underline{N}_1 \, J \, d\xi \, d\eta$$

$$\underline{M}_{12} = \iint_{\xi\,\eta} \underline{N}_1^t \, \underline{R}_{12} \, \underline{N}_2 \, J \, d\xi \, d\eta$$

$$\underline{M}_{22} = \iint_{\xi\eta} \underline{N}_2^t \quad \underline{R}_{22} \quad \underline{N}_2 \; J \; d\xi \, d\eta$$

and

$$\underline{R}_{11} = \sum_{L=1}^{N_L} \underline{R}_{11}^{(L)} = \left(\sum_{L=1}^{N_L} \rho^{(L)} \; h^{(L)} \right) \underline{I}_3$$

$$\underline{R}_{12} = \sum_{L=1}^{N_L} \underline{R}_{12}^{(L)} = \left(\sum_{L=1}^{N_L} \rho^{(L)} \; \Phi^{(L)} \right) \underline{I}_3$$

$$\underline{R}_{22} = \sum_{L=1}^{N_L} \underline{R}_{22}^{(L)} = \left(\sum_{L=1}^{N_L} \rho^{(L)} \; \psi^{(L)} \right) \underline{I}_3$$

Equivalent Nodal Force Vector due to $\underline{a}_c$

Using an analysis similar to that given in an earlier section, it can be proved that;

$$\underline{F}_c = -2 \; \Omega \underline{C}_{(e)} \; \dot{\delta}$$

where

$$\underline{C}_{(e)} = \underline{C}_{11}^{+} \quad \underline{C}_{12}^{+} \quad \underline{C}_{12}^{t+} \quad \underline{C}_{22}$$

such that

$$\underline{C}_{11} = \iint_{\xi\eta} \underline{N}_1^t \quad \underline{Q}_{11} \quad \underline{N}_1 \; J \; d\xi \, d\eta$$

$$\underline{C}_{12} = \iint_{\xi\eta} \underline{N}_1^t \quad \underline{Q}_{12} \quad \underline{N}_2 \; J \; d\xi \, d\eta$$

$$\underline{C}_{22} = \iint_{\xi\eta} \underline{N}_2^t \quad \underline{Q}_{22} \quad \underline{N}_2 \; J \; d\xi \, d\eta$$

and $\underline{Q}_{11}$, $\underline{Q}_{12}$, $\underline{Q}_{22}$ are as defined earlier.

Equivalent Nodal Force Vector due to $\underline{a}_p$

Using an approach as described earlier, it can be shown that:

$$\underline{F}_p = \Omega^2 \quad \bar{\underline{M}}_{(e)} \quad \underline{\delta}$$

such that

$$\bar{\underline{M}}_{(e)} = \quad \bar{\underline{M}}_{11} + \quad \bar{\underline{M}}_{12} + \quad \bar{\underline{M}}_{12}^t + \quad \bar{\underline{M}}_{22}$$

Whereas,

$$\bar{\underline{M}}_{11} = \int_{\xi}\int_{\eta} \underline{N}_1^t \quad \underline{P}_{11} \quad \underline{N}_1 \; J \; d\xi \, d\eta$$

$$\bar{\underline{M}}_{12} = \int_{\xi}\int_{\eta} \underline{N}_1^t \quad \underline{P}_{12} \quad \underline{N}_2 \; J \; d\xi \, d\eta$$

$$\bar{\underline{M}}_{22} = \int_{\xi}\int_{\eta} \underline{N}_2^t \quad \underline{P}_{22} \quad \underline{N}_2 \; J \; d\xi \, d\eta$$

The final Dynamic Equation can be achieved by the assembly of the element matrices as below:

$$\underline{M} \; \ddot{\underline{\delta}} + 2 \; \Omega \; \underline{C} \; \dot{\underline{\delta}} + (\; \underline{K} + \underline{K}_\sigma - \Omega^2 \; \bar{\underline{M}} \;) \; \underline{\delta} = \underline{F}(t)$$

Missing pages are unavailable

CHAPTER 6

HIGHER-ORDER ELEMENTS FORMULATION

6.1 Introduction

The development and application of classical plate theory (CPT) is one of the achievements of modern engineering. It is being continuously updated to deal with new problems and design information. In spite of its successes, however, the inherent limitations of CPT necessitates the development of more refined, and higher-order, theories of plate behaviour. More sophisticated plate models find application to problems where CPT is simply inadequate for describing the behaviour. Some typical examples of modern trends include plate cutouts, contact problems, and laminated composite plates, particularly for thick laminates.

For laminated composite systems the components of the stress and strain acting in the plane (transverse to the plane) of the laminate strongly influence the materials behaviour. This influence is due to the high ratio of the in-plane modulus to the transverse shear modulus. Shear deformation effects are more pronounced in composite laminates subjected to transverse loads than in isotropic plates under similar loading. However in classical laminate theory (CLPT) also, which is an extension of CPT to laminated plates, the transverse stress components are ignored.

Plate theories can be developed by expanding the displacements in a power series of the coordinate normal to the middle plane. In principle, theories developed by this process can be made as accurate as desired simply by

including a sufficiently large number of terms. In practice, however, a point of diminishing returns is reached wherein the complexity of the resulting analysis becomes too great. The high order theories are cumbersome and computationally more demanding, because, with each additional power of the thickness coordinate, an additional dependent unknown is introduced into the theory.

6.2 Displacement Functions

For a laminate of thickness h, which has 'N_L' number of layers, it is obvious from the boundary conditions that the transverse shear stresses are zero at the upper and lower surfaces of the laminate i.e;

$$\left.\begin{aligned} \tau_{xy} &= 0 \\ \tau_{yz} &= 0 \end{aligned}\right] \quad \text{at} \quad Z = -h/2, \quad +h/2$$

Therefore, the transverse shear strains will vanish at the same extreme surfaces i.e;

$$\left.\begin{aligned} \gamma_{xz} &= 0 \\ \gamma_{yz} &= 0 \end{aligned}\right] \quad \text{at} \quad Z = -h/2, \; +h/2$$

If the transverse shear strains are approximated as quadratic functions in Z, then for a symmetric laminate, these strains can be calculated at any point through the thickness in terms of their values at the mid-plane. It follows, therefore, that:

$$\gamma_{xz} = \Phi_x(x,y)\,(1-4Z^2/h^2)$$

$$\gamma_{yz} = \Phi y(x,y)\,(1-4Z^2/h^2)$$

where

$$\left.\begin{aligned} \Phi_x &= \gamma_{xz} \\ \Phi_y &= \gamma_{yz} \end{aligned}\right] \quad \text{at} \quad Z = 0$$

For most of the highest refined elements dealing with isotropic materials, displacement in the thickness direction (w) is considered as a function of 4th degree in the coordinate normal to the middle plane (Z). For symmetric laminated plates a practical assumption is to consider w(x,y,z) as an even function in Z , i.e.

$$w(x,y,z) \approx w_0(x,y) + (2Z/h)^2 \; w_1(x,y) + (2Z/h)^4 \; w_2(x,y) + \text{negligible terms}$$

Where w_1 and w_2 are the corresponding higher-order terms in the Taylor's series expansion, and are defined at the reference plane.

From the definition of transverse strain:

$$\gamma_{xz} = \partial w/\partial x + \partial u/\partial z$$

Hence,

$$\Phi_x(1 - 4Z^2/h^2) = \partial w/\partial x + \partial u/\partial z$$

therefore, from the comparison:

$$\partial u/\partial z = -\partial w_0/\partial x - (2Z/h)^2 \partial w_1/\partial x - (2Z/h)^4 \partial w_2/\partial x + \Phi_x(1-4Z^2/h^2)$$

The above equation can be integrated with respect to Z, and an expression for the displacement in the x-direction, can be derived as a function of 5th degree in Z (coordinate normal to the middle plane)as follow:

$$u(x,y,z) = u_0(x,y) + \Phi_x(Z - 4Z^3/3h^2)$$

$$- Z\left[\partial w_0/\partial x + (1/3)(2Z/h)^2 \partial w_1/\partial x\right.$$

$$\left. + (1/5)(2Z/h)^4(\partial w2/\partial x)\right]$$

Similarly, the following expression can be derived for the displacement in the Y-direction as a function of 5th degree in Z as under:

$$v(x,y,z) = v_0(x,y) + \Phi_y(Z - 4Z^3/3h^2)$$

$$- Z\left[\partial w_0/\partial y + (1/3)(2Z/h)^2 \partial w_1/\partial y\right.$$

$$\left. + (1/5)(2Z/h)^4 \partial w2/\partial y)\right]$$

For dynamic analysis, besides x and y, the variables in the above equations are also a function of time (t) i.e;

$$u(x,y,z,t)= u_0(x,y,t) + \Phi_x(x,y,t)(Z - 4Z^3/3h^2)$$

$$- Z\left[\partial w_0/\partial x + (1/3)(2Z/h)^2 \partial w_1/\partial x\right.$$

$$\left. + (1/5)(2Z/h)^4(\partial w2/\partial x)\right]$$

$$v(x,y,z,t) = v_0(x,y,t) + \Phi_y(x,y,t)(Z - 4Z^3/3h^2)$$

$$- Z\left[\partial w_0/\partial y + (1/3)(2Z/h)^2 \partial w_1/\partial y\right.$$

$$\left. + (1/5)(2Z/h)^4(\partial w2/\partial y)\right]$$

$$w(x,y,z,t) = w_0(x,y,t) + (2Z/h)^2 w_1(x,y,t)$$

$$+ (2Z/h)^4 w2(x,y,t)$$

6.3 Nodal Parameters and Interpolated Displacement Components

In engineering cases, such as plates (or shells) in bending, the interpolation problem reduces to that of expressing the field function, at any point inside a finite element, in terms of its values and values of some of its derivatives. Hence such cases require that the field function should satisfy higher continuity conditions than the C^0 continuity. Hermite's interpolation formula provides an expression for a single variable polynomial in terms of its values and the values of its first-order derivative at some given points.

It was decided therefore, in the present work to employ both Lagrangian and Hermitian interpolations. Considering a two-dimensional element in the neutral plane (Z=0) with:

n_L = Number of Lagrangian nodes
n_H = Number of Hermitian nodes

The nodal displacement vector of the element (at time t) will be defined as follow:

$$\underline{\delta}(t) = \{ \underline{\delta}_m(t) \quad \underline{\delta}_b(t) \quad \underline{\delta}_s(t) \}$$

and

$$\underline{\delta}_b(t) = \{ \overset{(0)}{\underline{\delta}_b}(t) \quad \overset{(1)}{\underline{\delta}_b}(t) \quad \overset{(2)}{\underline{\delta}_b}(t) \}$$

where

$$\underline{\delta}_m = \{ (u_0)_1 \quad (v_0)_1 \quad (u_0)_2 \quad (v_0)_2 \cdots\cdots (u_0)_{n_L} \quad (v_0)_{n_L} \}$$

$$\underline{\delta}_s = \{ (\Phi_x)_1 \quad (\Phi_y)_1 \quad (\Phi_x)_2 \quad (\Phi_y)_2 \cdots\cdots (\Phi_x)_{n_L} \quad (\Phi_y)_{nL} \}$$

$$\underline{\delta}_b = \{ (w_i)_1 \quad (\partial w_i/\partial x)_1 \quad (\partial w_i/\partial y)_1 \quad (w_i)_2 \quad (\partial w_i/\partial x)_2$$

$$(\partial w_i/\partial y)_2 \cdots\cdots (w_i)_{n_H} \quad (\partial w_i/\partial x)_{n_H} \quad (\partial w_i/\partial y)_{n_H} \}$$

(i)

where

$i=0,1,2$

Let

N_i = Lagrangian Shape Function, where $i=1,2,\ldots n_L$

H_i = Hermitian Shape Function, where $i=1,2,..3n_H$

then, it can be shown that:

$$u_0(x,y,t) = \sum_{i=1}^{n_L} N_i(x,y) \; [u_0(t)]_i$$

$$v_0(x,y,t) = \sum_{i=1}^{n_L} N_i(x,y) \; [v_0(t)]_i$$

$$\Phi_x(x,y,t) = \sum_{i=1}^{n_L} N_i(x,y) \quad [\Phi_x(t)]_i$$

$$\Phi_y(x,y,t) = \sum_{i=1}^{n_L} N_i(x,y) \quad [\Phi y(t)]_i$$

$$w_j(x,y,t) = \sum_{i=1}^{n_H} \Big[H_{3i-2}[w_j(t)]_i + H_{3i-1}[\partial w_j/\partial x]_i + H_{3i}[\partial w_j/\partial y]_i \Big]$$

where

$$j = 0,1,2$$

6.4 Strain Components

In order to simplify the analysis, in-plane and out-of-plane strains are grouped separately and, therefore, the following vectors can therefore subsequently be defined as follow:

$$\underline{\varepsilon}_{xy} = \begin{bmatrix} \varepsilon_x \\ \varepsilon_y \\ \gamma_{xy} \end{bmatrix}$$

$$\underline{\varepsilon}_s = \begin{bmatrix} \gamma_{xz} \\ \gamma_{yz} \end{bmatrix}$$

Similarly, by definition, the strains can be expanded as follows:

$$\varepsilon_x = \partial u/\partial x$$

$$= \partial u_0/\partial x + (Z - 4Z^3/3h^2)\partial \Phi_x/\partial x - Z\left[\partial^2 w_0/\partial x^2 + (1/3)(2Z/h)^2 \partial^2 w_1/\partial x^2 + (1/5)(2Z/h)^4 \partial^2 w_2/\partial x^2\right]$$

$$\varepsilon_y = \partial v/\partial y$$

$$= \partial v_0/\partial y + (Z - 4Z^3/3h^2)\partial \Phi_y/\partial y - Z\left[\partial^2 w_0/\partial y^2 + (1/3)(2Z/h)^2 \partial^2 w_1/\partial y^2 + (1/5)(2Z/h)^4 \partial^2 w_2/\partial y^2\right]$$

$$\gamma_{xy} = \partial u/\partial y + \partial v/\partial x$$

$$= (\partial u_0/\partial y + \partial v_0/\partial x) + (Z - 4Z^3/3h^2)(\partial \Phi_x/\partial x + \partial \Phi_y/\partial y) - 2Z\left[\partial^2 w_0/\partial x \partial y + (1/3)(2Z/h)^2 \partial^2 w_1/\partial x \partial y + (1/5)(2Z/h)^4 \partial^2 w_2/\partial x \partial y\right]$$

$$\gamma_{xz} = \Phi_x(1 - 4Z^2/h^2)$$

$$\gamma_{yz} = \Phi_y(1 - 4Z^2/h^2)$$

For further simplification, and ease of operation, the following strain vectors can be defined:

$$\underline{\varepsilon}_m = \begin{bmatrix} \partial u_0/\partial x \\ \partial v_0/\partial y \\ \partial u_0/\partial y + \partial v_0/\partial x \end{bmatrix}$$

$$\underline{\hat{\varepsilon}}_s = \begin{bmatrix} \Phi_x \\ \\ \Phi_y \end{bmatrix}$$

$$\underline{\varepsilon}_t = \begin{bmatrix} \partial\Phi_x/\partial x \\ \\ \partial\Phi_y/\partial y \\ \\ \partial\Phi_x/\partial y + \partial\Phi_y/\partial x \end{bmatrix}$$

$$\underline{\varepsilon}_b^{(i)} = \begin{bmatrix} \partial^2 w_i/\partial x^2 \\ \\ \partial^2 w_i/\partial y^2 \\ \\ 2\partial^2 w_i/\partial x \partial y \end{bmatrix} \quad \text{where} \quad i=0,1,2$$

then it can be deduced that:

$$\underline{\varepsilon}_{xy} = \underline{\varepsilon}_m + (Z - 4Z^3/3h^2)\ \underline{\varepsilon}_t - Z\ \underline{\varepsilon}_b^{(0)}$$

$$- (Z/3)(2Z/h)^2\ \underline{\varepsilon}_b^{(1)} - (Z/5)(2Z/h)^4\ \underline{\varepsilon}_b^{(2)}$$

$$\underline{\varepsilon}_s = (1 - 4Z^2/h^2)\ \underline{\hat{\varepsilon}}_s$$

Further, it can be shown that,

$$\underline{\varepsilon}_m = \underline{B}_m\ \underline{\delta}_m$$

$$\underline{\hat{\varepsilon}}_s = \underline{B}_s\ \underline{\delta}_s$$

$$\underline{\varepsilon}_t = \underline{B}_m\ \underline{\delta}_s$$

$$\underline{\varepsilon}_b^{(i)} = \underline{B}_b^{(i)}\ \underline{\delta}_b$$

where

$$\underline{B}_{Lagrangian} = [\underline{b}_1 \quad \underline{b}_2 \ldots\ldots\ldots \underline{b}_{n_L}]$$

$$\underline{B}_b = [\underline{b}_1 \quad \underline{b}_2 \ldots\ldots\ldots \underline{b}_{3n_H}]$$

$$(\underline{b}_i)_m = \begin{bmatrix} \partial N_i/\partial x & 0 \\ 0 & \partial N_i/\partial y \\ \partial N_i/\partial y & \partial N_i/\partial x \end{bmatrix}$$

$$(\underline{b}_i)_s = \begin{bmatrix} N_i & 0 \\ 0 & N_i \end{bmatrix}$$

$$(\underline{b}_i)_b = \begin{bmatrix} \partial^2 H_i/\partial x^2 \\ \partial^2 H_i/\partial y^2 \\ 2\partial^2 H_i/\partial x \partial y \end{bmatrix}$$

The effect of transverse normal stress and strain σ_z, ε_z is ignored simply because their strain energy contribution is negligible.

6.5 Stress Components For the Lth Layer

As for in the case of strains, in-plane and out-of-plane stresses are grouped separatly and, the following vectors may be written:

$$\underline{\sigma}_{xy} = \begin{bmatrix} \sigma_x \\ \sigma_y \\ \tau_{xy} \end{bmatrix}$$

$$\underline{\sigma}_s = \begin{bmatrix} \tau_{xz} \\ \\ \tau_{yz} \end{bmatrix}$$

Then, the stress-strain relationships for each layer can be expressed as below:

$$\underline{\sigma}_{xy} = \underline{D}^{(L)}_{xy}\ \underline{\varepsilon}_{xy}$$

$$\underline{\sigma}_s = \underline{D}^{(L)}_{s}\ \underline{\varepsilon}_s$$

where, $\underline{D}^{(L)}_{xy}$ and $\underline{D}^{(L)}_{s}$ are as defined in Chapter 3.

6.6 Derivation of Element Stiffness Matrix

By definition, the strain energy per unit volume, for the Lth layer, can be expressed as follow:

$$\bar{U}^{(L)} = (1/2)\ \underline{\varepsilon}^{t}_{xy}\ \underline{D}^{(L)}_{xy}\ \underline{\varepsilon}_{xy} + (1/2)\ \underline{\varepsilon}^{t}_{s}\ \underline{D}^{(L)}_{s}\ \underline{\varepsilon}_s$$

$$= \bar{U}^{(L)}_m + \bar{U}^{(L)}_b + \bar{U}^{(L)}_t + \bar{U}^{(L)}_s + \bar{U}^{(L)}_{mb} + \bar{U}^{(L)}_{mt} + \bar{U}^{(L)}_{bt}$$

Where

$$\bar{U}^{(L)}_m = (1/2)\ \underline{\varepsilon}^{t}_{m}\ \underline{D}^{(L)}_{xy}\ \underline{\varepsilon}_m$$

$$\bar{U}_b^{(L)} = (1/2)\left[Z \underline{\varepsilon}_b^{(0)} + (4Z^3/3h^2)\, \underline{\varepsilon}_b^{(1)} + (16Z^5/5h^4)\, \underline{\varepsilon}_b^{(2)} \right]^t$$

$$\underline{D}_{xy}^{(L)} \left[Z \underline{\varepsilon}_b^{(0)} + (4Z^3/3h^2)\, \underline{\varepsilon}_b^{(1)} + (16Z^5/5h^4)\, \underline{\varepsilon}_b^{(2)} \right]$$

$$\bar{U}_t^{(L)} = (1/2)\left(Z - 4Z^3/3h^2 \right)^2 \underline{\varepsilon}_t^t \; \underline{D}_{xy}^{(L)} \; \underline{\varepsilon}_t$$

$$\bar{U}_s^{(L)} = (1/2)\, \underline{\varepsilon}_s^t \; \underline{D}_s^{(L)} \; \underline{\varepsilon}_s$$

$$= (1/2)\left(1 - 4Z^2/h^2 \right)^2 \hat{\underline{\varepsilon}}_s^t \; \underline{D}s^{(L)} \; \hat{\underline{\varepsilon}}_s$$

$$\bar{U}_{mb}^{(L)} = -\underline{\varepsilon}_m^t \; \underline{D}_{xy}^{(L)} \left[Z \underline{\varepsilon}_b^{(0)} + (4Z^3/3h^2)\, \underline{\varepsilon}_b^{(1)} + (16Z^5/5h^4)\, \underline{\varepsilon}_b^{(2)} \right]$$

$$\bar{U}_{mt}^{(L)} = (Z - 4Z^3/3h^2)\, \underline{\varepsilon}_m^t \; \underline{D}_{xy}^{(L)} \; \underline{\varepsilon}_t$$

$$\bar{U}_{bt}^{(L)} = -\left[Z\underline{\varepsilon}_b^{(0)} + (4Z^3/3h^2)\, \underline{\varepsilon}_b^{(1)} + (16Z^5/5h^4)\, \underline{\varepsilon}_b^{(2)} \right] \underline{D}_{xy}^{(L)} (Z - 4Z^3/3h^2) \; \underline{\varepsilon}_t$$

From the symmetry of the laminate, it can easily be seen that:

$$\int_{-h/2}^{h/2} Z^{2n-1}\, \underline{D}_{xy}^{(L)}\, dZ = \underline{0}$$

Subsequently, integrating the above stated strain energy expressions with respect to Z, the corresponding expressions for the laminate strain energy per unit area may be deduced as under:

$$\text{(i)} \quad U_m' = \int_{-h/2}^{h/2} \bar{U}_m^{(L)}\, dz = 1/2\ \underline{\varepsilon}_m^t \quad \hat{\underline{D}}_m \quad \underline{\varepsilon}_m$$

where,

$$\hat{\underline{D}}_m = \underline{D}^{(0)}$$

and

$$\underline{D}^{(n)} = \int_{-h/2}^{h/2} z^n \quad \underline{D}_{xy}^{(L)}\, dz$$

$$= \sum_{L=1}^{N_L} \int_{Z_L^{(L)}}^{Z_U^{(L)}} z^n \quad \underline{D}_{xy}^{(L)}\, dz$$

$$= \sum_{L=1}^{N_L} \left\{ \left[\left(\quad Z_U^{(L)} \quad \right) \right]^{n+1} - \left[\left(\quad Z_L^{(L)} \quad \right) \right]^{n+1} \right\} \underline{D}_{xy} \,/(n+1)$$

$$\text{(ii)} \quad U_b' = \int_{-h/2}^{h/2} \bar{U}_b^{(L)}\, dZ$$

$$= (1/2)\ \underline{\varepsilon}_b^{(0)t} \quad \underline{D}^{(2)} \quad \underline{\varepsilon}_b^{(0)} + (1/2)\ \underline{\varepsilon}_b^{(1)t} \quad (16/9h^4)\ \underline{D}^{(6)} \quad \underline{\varepsilon}_b^{(1)}$$

$$+ (1/2)\ \underline{\varepsilon}_b^{(2)t} \quad (256/25h^8)\ \underline{D}^{(10)} \quad \underline{\varepsilon}_b^{(2)}$$

CONT....

$$+ \underline{\varepsilon}_b^{(0)t} (4/3h^2) \underline{D}^{(4)} \underline{\varepsilon}_b^{(1)} + \underline{\varepsilon}_b^{(0)t} (16/5h^4) \underline{D}^{(6)} \underline{\varepsilon}_b^{(2)}$$

$$+ \underline{\varepsilon}_b^{(1)t} (64/15h^6) \underline{D}^{(8)} \underline{\varepsilon}_b^{(2)}$$

or

$$U_b' = (1/2) \sum_{i=0}^{2} \sum_{j=0}^{2} \underline{\varepsilon}_b^{(i)t} \hat{\underline{D}}_{i,j} \underline{\varepsilon}_b^{(j)}$$

where

$$\hat{D}_{0,0} = D^{(2)}$$

$$\hat{D}_{1,1} = (16/9h^4) \underline{D}^{(6)}$$

$$\hat{D}_{2,2} = (256/25h^8) \underline{D}^{(10)}$$

$$\hat{D}_{0,1} = (4/3h^2) \underline{D}^{(4)} = \hat{D}_{1,0}$$

$$\hat{D}_{0,2} = (16/5h^4) \underline{D}^{(6)} = \hat{D}_{2,0}$$

$$\hat{D}_{1,2} = (64/15h^6) \underline{D}^{(8)} = \hat{D}_{2,1}$$

(iii) $$U_t' = \int_{-h/2}^{h/2} \bar{U}_s^{(L)} dZ$$

$$= (1/2) \hat{\underline{\varepsilon}}_s^t \hat{\underline{D}}_t \hat{\underline{\varepsilon}}_s$$

where,

$$\hat{\underline{D}}_t = \int_{-h/2}^{h/2} (Z - 4Z^3/3h^2)^2 \quad \overset{(L)}{\underline{D}}_{xy} \quad dZ$$

$$= \overset{(2)}{\underline{D}} - (8/3h^2) \overset{(4)}{\underline{D}} + (16/9h^4) \overset{(6)}{\underline{D}}$$

$$= \hat{\underline{D}}_{0,0} - 2\hat{\underline{D}}_{0,1} + \hat{\underline{D}}_{1,1}$$

(iv) $U_s' = (1/2) \hat{\underline{\varepsilon}}_s^t \quad \hat{\underline{D}}_s \quad \hat{\underline{\varepsilon}}_s$

where,

$$\hat{\underline{D}}_s = \int_{-h/2}^{h/2} (1 - 4Z^2/h^2)^2 \quad \overset{(L)}{\underline{D}}_s \quad dz$$

$$= \sum_{L=1}^{N_L} \left\{ \left[\overset{(L)}{Z_U} - (8/3h^2) \left(\overset{(L)}{Z_U} \right)^3 + (16/5h^4) \left(\overset{(L)}{Z_U} \right)^5 \right] \right.$$

$$\left. - \left[\overset{(L)}{ZL} - (8/3h^2) \left(\overset{(L)}{ZL} \right)^3 + (16/5h^4) \left(\overset{(L)}{ZL} \right)^5 \right] \right\} \overset{(L)}{\underline{D}}_s$$

(v) $U_{mb}' = \int_{-h/2}^{h/2} \bar{U}_{mb}^{(L)} \, dZ = 0$

(vi) $U_{mt}' = \int_{-h/2}^{h/2} \bar{U}_{mt}^{(L)} \, dZ = 0$

$$\text{(vii)}\quad U'_{bt} = \int_{-h/2}^{h/2} \bar{U}_{bt}^{(L)}\, dZ$$

$$= \sum_{i=0}^{2} \underline{\varepsilon}_b^{(i)}\ \underline{D}_{bt}^{(i)}\ \underline{\varepsilon}_t$$

where

$$\underline{D}_{bt}^{(0)} = \int_{-h/2}^{h/2} (Z^2 - 4Z^4/3h^2)\ \underline{D}_{xy}^{(L)}\, dZ$$

$$= \underline{D}^{(2)} - (4/3h^2)\ \underline{D}^{(4)}$$

$$= \hat{\underline{D}}_{0,0} - \hat{\underline{D}}_{0,1}$$

$$\underline{D}_{bt}^{(1)} = \int_{-h/2}^{h/2} \left[4Z^4/3h^2 - 16Z^6/9h^4\right]\ \underline{D}_{xy}^{(L)}\, dZ$$

$$= \hat{\underline{D}}_{0,1} - \hat{\underline{D}}_{1,1}$$

$$\underline{D}_{bt}^{(2)} = \int_{-h/2}^{h/2} (16Z^6/5h^4 - 64Z^8/15h^6)\ \underline{D}_{xy}^{(L)}\, dZ$$

$$= \hat{\underline{D}}_{0,2} - \hat{\underline{D}}_{1,2}$$

The above strain energy expressions can be shown in terms of nodal displacements as below:

$$\text{(i)}\qquad U'_m = (1/2)\ \underline{\delta}_m^t\ \underline{B}_m^t\ \hat{\underline{D}}_m\ \underline{B}_m\ \underline{\delta}_m$$

(ii) $$U_b' = (1/2) \sum_{i=0}^{2} \sum_{j=0}^{2} \underline{\delta}_b^{(i)t} \; \underline{B}_b^t \; \underline{\hat{D}}_{i,j} \; \underline{B}_b \; \underline{\delta}_b^{(j)}$$

(iii) $$U_t' = (1/2) \; \underline{\delta}_s^t \; \underline{B}_m^t \; \underline{\hat{D}}_t \; \underline{B}_m \; \underline{\delta}_s$$

(iv) $$U_s' = (1/2) \; \underline{\delta}_s^t \; \underline{B}_s^t \; \underline{\hat{D}}_s \; \underline{B}_s \; \underline{\delta}_s$$

(v) $$U_{mb}' = 0$$

(vi) $$U_{mt}' = 0$$

(vii) $$U_{bt}' = -\sum_{i=0}^{2} \underline{\delta}_b^{(i)} \; \underline{B}_b^t \; \underline{D}_{bt}^{(i)} \; \underline{B}_m \; \underline{\delta}_s$$

By integrating the above expressions, with respect to x and y, the total strain energy of the system may be derived as below:

$$U = \int\int U' \, dxdy$$

$$= U_m + U_b + U_t + U_s + U_{bt}$$

where,

(i) $$Um = (1/2) \; \underline{\delta}_m^t \; \underline{K}_m \; \underline{\delta}_m$$

(ii) $$U_b = (1/2) \sum_{i=0}^{2} \sum_{j=0}^{2} \underline{\delta}_b^{(i)t} \; \underline{K}_b^{(i,j)} \; \underline{\delta}_b^{(j)}$$

(iii) $$U_t = (1/2) \; \underline{\delta}_s^t \; \underline{K}_t \; \underline{\delta}_s$$

(iv) $$U_s = (1/2) \; \underline{\delta}_s^t \; \underline{K}_s \; \underline{\delta}_s$$

$$(v) \qquad U_{bt} = \sum_{i=0}^{2} \underline{\delta}_b^{(i)t} \; \underline{K}_{bt} \; \underline{\delta}_s^{(i)}$$

The individual stiffness matrices used in the above strain energy expressions are defined as below:

$$\underline{K}_m = \iint \underline{B}_m^t \; \hat{\underline{D}}_m \; \underline{B}_m \; dxdy$$

$$\underline{K}_b^{(i,j)} = \iint \underline{B}_b^t \; \hat{\underline{D}}_{i,j} \; \underline{B}_b \; dxdy$$

$$\underline{K}_t = \iint \underline{B}_m^t \; \hat{\underline{D}}_t \; \underline{B}_m \; dxdy$$

$$\underline{K}_s = \iint \underline{B}_s^t \; \hat{\underline{D}}_s \; \underline{B}_s \; dxdy$$

$$\underline{K}_{bt}^{(i)} = \iint \underline{B}_b \; \underline{D}_{bt}^{(i)} \; \underline{B}_m \; dxdy$$

while the various $\underline{D}$ matrices used in the above defined stiffness matrices can be represented as follows:

$$\hat{\underline{D}}_m = \underline{D}^{(0)}$$

$$\hat{\underline{D}}_{0,0} = \underline{D}^{(2)}$$

$$\hat{\underline{D}}_{1,1} = (16/9h^4) \; \underline{D}^{(6)}$$

$$\hat{\underline{D}}_{2,2} = (256/25h^8) \; \underline{D}^{(10)}$$

$$\hat{\underline{D}}_{0,1} = (4/3h^2) \; \underline{D}^{(4)} = \hat{\underline{D}}_{1,0}$$

$$\underline{\hat{D}}_{0,2} = (16/5h^4)\ \underline{D}^{(6)} = \underline{\hat{D}}_{2,0}$$

$$\underline{\hat{D}}_{1,2} = (64/15h^6)\ \underline{D}^{(8)} = \underline{\hat{D}}_{2,1}$$

$$\underline{\hat{D}}_t = \underline{\hat{D}}_{0,0} - 2\underline{\hat{D}}_{0,1} + \underline{\hat{D}}_{1,1}$$

$$\underline{\hat{D}}_{bt}^{(i)} = \underline{\hat{D}}_{0,i} - \underline{\hat{D}}_{1,i}$$

$$\underline{D}^{(n)} = \int_{-h/2}^{h/2} z^n\ \underline{D}_{xy}^{(L)}\ dx$$

$$\underline{\hat{D}}_s = \int_{-h/2}^{h/2} (1 - 4z^2/h^2)^2\ \underline{D}_s^{(L)}$$

Hence, the various stiffness matrices can be assembled together, as below:

$$K\ \delta = \begin{bmatrix} K & 0 & 0 & 0 & 0 \\ -m & - & - & - & - \\ & (0,0) & (0,1) & (0,2) & (0) \\ 0 & K & K & K & -K \\ - & -b & -b & -b & -bt \\ & (1,0) & (1,1) & (1,2) & (1) \\ 0 & K & K & K & -K \\ - & -b & -b & -b & -bt \\ & (2,0) & (2,1) & (2,2) & (2) \\ 0 & K & K & K & -K \\ - & -b & -b & -b & -bt \\ & (0)t & (1)t & (2)t & \\ 0 & -K & -K & -K & K + K \\ & -bt & -bt & -bt & -t \quad -s \end{bmatrix} \begin{bmatrix} \delta \\ -m \\ (0) \\ \delta \\ -b \\ (1) \\ \delta \\ -b \\ (2) \\ \delta \\ -b \\ \delta \\ -s \end{bmatrix}$$

6.7 Derivation of Element Mass Matrix

Velocity components can easily be deduced by differentiating the previousely derived displacement components, as follows:

$$\dot{u}(x,y,z,t) = \dot{u}_0 + \dot{\Phi}_x\left(Z - 4Z^3/3h^2\right) - \left[Z\partial\dot{w}_0/\partial x + (4Z^3/3h^2)\partial\dot{w}_1/\partial x + (16Z^5/5h^4)\partial\dot{w}_2/\partial x\right]$$

$$\dot{v}(x,y,z,t) = \dot{v}_0 + \dot{\Phi}_y(Z - 4Z^3/3h^2) - \left[Z\partial\dot{w}_0/\partial y + (4Z^3/3h^2)\partial\dot{w}_1/\partial y + (16Z^5/5h^4)\partial\dot{w}_2/\partial y\right]$$

$$\dot{w}(x,y,z,t) = \dot{w}_0 + (4Z^2/h^2)\ \dot{w}_1 + (16Z^4/h^4)\ \dot{w}_2$$

Using interpolation equations, relationships between velocity components and shape functions may be shown as below:

$$\begin{bmatrix} \dot{u}_0 \\ \dot{v}_0 \end{bmatrix} = \underline{N}\ \underline{\dot{\delta}}_m$$

$$\begin{bmatrix} \dot{\Phi}_x \\ \dot{\Phi}_y \end{bmatrix} = \underline{N}\ \dot{\underline{\delta}}_m$$

$$\left.\begin{aligned} \begin{bmatrix} \dot{w} \\ (i) \end{bmatrix} &= \underline{H}\ \dot{\underline{\delta}}^{(i)} \\ \begin{bmatrix} \partial \dot{w}_i/\partial x \\ \\ \partial \dot{w}_i/\partial y \end{bmatrix} &= \underline{H}'\ \dot{\underline{\delta}}_b^{(i)} \end{aligned}\right\} \text{where } i = 0,1,2$$

Where

$$\underline{N} = \begin{bmatrix} N_1 & 0 & N_2 & 0 \ldots\ldots\ldots N_{n_L} & 0 \\ \\ 0 & N_1 & 0 & N_2 \ldots\ldots\ldots 0 & N_{n_L} \end{bmatrix}$$

$$\underline{H} = \begin{bmatrix} H_1 & H_2 & H_3 \ldots\ldots\ldots\ldots\ldots H_{3n_H} \end{bmatrix}$$

$$\underline{H}' = \begin{bmatrix} \partial H_1/\partial x & \partial H_2/\partial x & \ldots\ldots\ldots \partial H_{3n_H}/\partial x \\ \\ \partial H_1/\partial y & \partial H_2/\partial y & \ldots\ldots\ldots \partial H_{3n_H}/\partial Y \end{bmatrix}$$

By definition, the kinetic energy per unit volume for the Lth layer can be expressed as below:

$$\overset{-(L)}{KE} = (1/2)\ \rho^{(L)} \left[\dot{u}^2 + \dot{v}^2 + \dot{w}^2 \right]$$

$$= (1/2)\ \rho^{(L)} \left\{ \left[\dot{u}_0 + \dot{\Phi}_x (Z - 4Z^3/3h^2) \right. \right.$$

CONT....

$$- \left[z\,(\partial \dot{w}_0/\partial x) + (4z^3/3h^2)\,(\partial \dot{w}_1/\partial x) + (16z^5/5h^4)\,(\partial \dot{w}_2/\partial x) \right] \Bigg]^2$$

$$+ \left[\dot{v}_0 + \dot{\Theta}_y (z - 4z^3/3h^2) \right.$$

$$- \left[z\,(\partial \dot{w}_0/\partial x) + (4z^3/3h^2)\,(\partial \dot{w}_1/\partial x) + (16z^5/5h^4)\,(\partial \dot{w}_2/\partial x) \right] \Bigg]^2$$

$$+ \left[\dot{w}_0 + (4z^2/h^2)\dot{w}_1 + (16z^4/h^4)\dot{w}_2 \right]^2 \Bigg\}$$

For simplicity, and ease of operation, the following vectors may be defined:

$$\underline{\dot{u}}_0 = \begin{bmatrix} \dot{u}_0 \\ \\ \dot{v}_0 \end{bmatrix} = \underline{N}\ \underline{\dot{\delta}}_m$$

$$\underline{\dot{\Phi}} = \begin{bmatrix} \dot{\Phi}_x \\ \\ \dot{\Phi}_y \end{bmatrix} = \underline{N}\ \underline{\dot{\delta}}_m$$

$$\underline{\dot{w}}_i = [\ \dot{w}_i\ ] = \underline{H}\ \underline{\dot{\delta}}_b^{(i)}$$

$$\underline{\dot{w}}_i' = \begin{bmatrix} \partial \dot{w}_i/\partial x \\ \\ \partial \dot{w}_i/\partial y \end{bmatrix} = \underline{H}' \ \underline{\dot{\delta}}_b^{(i)}$$

Similarly, the kinetic energy of each Lth layer can be partioned, as shown below:

$$\bar{KE}^{(L)} = \bar{KE}^{(L)}_{u,v} + \bar{KE}^{(L)}_{w}$$

Where

$$\bar{KE}^{(L)}_{u,v} = (1/2)\ \rho^{(L)}\ (\dot{u}^2 + \dot{v}^2)$$

$$= \bar{KE}^{(L)}_{m} + \bar{KE}^{(L)}_{s} + \bar{KE}^{(L)}_{b} + \bar{KE}^{(L)}_{ms} + \bar{KE}^{(L)}_{mb} + \bar{KE}^{(L)}_{bs}$$

$$\bar{KE}^{(L)}_{w} = (1/2)\ \rho^{(L)}\ \dot{w}^2$$

Hence, it can be shown that,

$$\text{(i)} \quad \bar{KE}^{(L)}_{m} = (1/2)\ \rho^{(L)}\ \underline{\dot{u}}_0^t\ \underline{\dot{u}}_0$$

$$\text{(ii)} \quad \bar{KE}^{(L)}_{s} = (1/2)\ \rho^{(L)}\ (Z - 4Z^3/3h^2)^2\ \underline{\dot{\Phi}}^t\ \underline{\dot{\Phi}}$$

$$\text{(iii)} \quad \bar{KE}^{(L)}_{b} = (1/2)\rho^{(L)} \left[Z\underline{\dot{w}}_0'' + (4Z^3/3h^2)\underline{\dot{w}}_1'' + (16Z^5/5h^4)\underline{\dot{w}}_2'' \right]^t$$

$$\left[Z\underline{\dot{w}}_0'' + (4Z^3/3h^2)\underline{\dot{w}}_1'' + (16Z^5/5h^4)\underline{\dot{w}}_2'' \right]$$

$$\text{(iv)}\quad \bar{KE}^{(L)}_{ms} = (1/2)\,\rho^{(L)}\,(Z - 4Z^3/3h^2)\,(\dot{\underline{u}}_0^{t}\,\dot{\underline{\Phi}} + \dot{\underline{\Phi}}^{t}\,\dot{\underline{u}}_0)$$

$$\text{(v)}\quad \bar{KE}^{(L)}_{mb} = -\rho^{(L)}\,\dot{\underline{u}}_0^{t}\left[\ddot{Z\underline{w}}_0' + (4Z^3/3h^2)\ddot{\underline{w}}_1' + (16Z^5/5h^4)\ddot{\underline{w}}_2'\right]$$

$$\text{(vi)}\quad \bar{KE}^{(L)}_{bs} = -\rho^{(L)}\,(Z - 4Z^3/3h^2)\left[Z\,\ddot{\underline{w}}_0' + (4Z^3/3h^2)\dot{\underline{w}}_1' + (16Z^5/5h^4)\ddot{\underline{w}}_2'\right]^{t}\dot{\underline{\Phi}}$$

$$\text{(vii)}\quad \bar{KE}^{(L)}_{w} = (1/2)\,\rho^{(L)}\left[\dot{\underline{w}}_0 + (4Z^2/h^2)\dot{\underline{w}}_1 + (16Z^4/h^4)\dot{\underline{w}}_2\right]^{t}$$

$$\left[\dot{\underline{w}}_0 + (4Z^2/h^2)\dot{\underline{w}}_1 + (16Z^4/h^4)\dot{\underline{w}}_2\right]$$

By integrating the above kinetic energy expressions with respect to Z, the kinetic energy per unit area for the laminate can be expressed as follows:

$$\dot{KE} = \int_{-h/2}^{h/2} \bar{KE}^{(L)}\,dZ$$

$$= \dot{KE}_m + \dot{KE}_s + \dot{KE}_b + \dot{KE}_{ms} + \dot{KE}_{mb} + \dot{KE}_{bs} + \dot{KE}_w$$

and by definition:

$$\hat{\rho}^{(n)} = \int_{-h/2}^{h/2} Z^n\,\rho^{(L)}\,dz$$

$$= \sum_{L=1}^{N_L} \int_{Z_L^{(L)}}^{Z_U^{(L)}} Z^n \; \rho^{(L)} \, dZ$$

$$= \sum_{L=1}^{N_L} \left\{ \left[Z_U^{(L)} \right]^{n+1} - \left[Z_L^{(L)} \right]^{n+1} \right\} \rho^{(L)} / (n+1)$$

For symmetric composites

$$\hat{\rho}^{(2n+1)} = 0$$

If all layers have the same density ρ then,

$$\hat{\rho}^{n} = \left[(h/2)^{n+1} - (h/2)^{n+1} \right] \rho / (n+1)$$

$$= 0 \qquad \text{for odd } n$$

$$= h^{n+1} \; \rho \; / \; Z^n \; (n+1) \qquad \text{for even } n$$

Hence, the kinetic energy per unit area for the laminate, can be expressed in terms of density, nodal velocity vectors and shape functions as shown below:

(i) $K\dot{E}'_m = (1/2) \; \hat{\rho}^{(0)} \; \underline{\dot{\delta}}_m^t \; \underline{N}^t \; \underline{N} \; \underline{\dot{\delta}}_m$

(ii) $K\dot{E}'_s = (1/2) \; \hat{\rho}_s \; \underline{\dot{\delta}}_s^t \; \underline{N}^t \; \underline{N} \; \underline{\dot{\delta}}_s$

(iii) $K\dot{E}'_b = (1/2) \sum_{i=0}^{2} \sum_{j=0}^{2} \rho^{(i,j)} \; \underline{\dot{\delta}}_b^{(i)} \; \underline{H}'^t \; \underline{H}' \; \underline{\dot{\delta}}_b^{(j)}$

(iv) $K\dot{E}'_{ms} = 0$

(v) $\dot{KE}'_{mb} = 0$

(vi) $\dot{KE}'_{bs} = \sum_{i=0}^{2} \rho_{bs}^{(i)} \, \underline{\delta}_b^{(i)} \, \underline{H}'^{t} \, \underline{N} \, \dot{\underline{\delta}}_s$

(vii) $\dot{KE}'_{w} = (1/2) \sum_{i=0}^{2} \sum_{j=0}^{2} \rho_w^{(i,j)} \, \underline{\delta}_b^{(i)} \, \underline{H}^{t} \, \underline{H} \, \underline{\delta}_b^{(j)}$

Where,

$$\rho_b^{(0,0)} = \hat{\rho}^{(2)}$$

$$\rho_b^{(1,1)} = (16/9h^4) \, \hat{\rho}^{(6)}$$

$$\rho_b^{(2,2)} = (256/25h^8) \, \hat{\rho}^{(10)}$$

$$\rho_b^{(0,1)} = (4/3h^2) \, \hat{\rho}^{(4)} \qquad = \rho_b^{(1,0)}$$

$$\rho_b^{(0,2)} = (16/5h^4) \, \hat{\rho}^{(6)} \qquad = \rho_b^{(2,0)}$$

$$\rho_b^{(1,2)} = (64/15h^6) \, \hat{\rho}^{(8)} \qquad = \rho_b^{(2,1)}$$

$$\hat{\rho}_s = \rho_b^{(0,0)} - 2 \, \rho_b^{(0,1)} + \rho_b^{(1,1)}$$

$$\rho_{bs}^{(i)} = \rho_b^{(0,i)} - \rho_b^{(1,i)}$$

$$\rho_w^{(0,0)} = \hat{\rho}^{(0)}$$

$$\rho_w^{(1,1)} = (16/h^4) \, \hat{\rho}^{(4)}$$

$$\rho_w^{(2,2)} = (256/h^8)\ \hat{\rho}^{(8)}$$

$$\rho_w^{(0,1)} = (4/h^2)\ \hat{\rho}^{(2)} \qquad = \rho_w^{(1,0)}$$

$$\rho_w^{(0,2)} = (16/h^4)\ \hat{\rho}^{(4)} \qquad = \rho_w^{(2,0)}$$

$$\rho_w^{(1,2)} = (64/h^6)\ \hat{\rho}^{(6)} \qquad = \rho_w^{(2,1)}$$

By integrating the above kinetic energy expressions, with respect to x and y, the total kinetic energy expression for the plate may be derived as follows:

$$KE = \iint K\dot{E}\ dxdy = (1/2)\ \underline{\dot{\delta}}^t\ \underline{M}\ \underline{\dot{\delta}}$$

$$= KE_m + KE_s + KE_b + KE_{bs} + KE_w$$

Where,

$$KE_m = (1/2)\ \underline{\dot{\delta}}_m^t\ \underline{M}_m\ \underline{\dot{\delta}}_m$$

$$KE_s = (1/2)\ \underline{\dot{\delta}}_s^t\ \underline{M}_s\ \underline{\dot{\delta}}_s$$

$$KE_b = (1/2) \sum_{i=0}^{2} \sum_{j=0}^{2} \underline{\dot{\delta}}_b^{(i)t}\ \underline{M}_b^{(i,j)}\ \underline{\dot{\delta}}_b^{(j)}$$

$$KE_{bs} = (-1/2) \sum_{i=0}^{2} \underline{\dot{\delta}}_b^{(i)t}\ \underline{M}_{bs}^{(i)}\ \underline{\dot{\delta}}_s$$

$$KE_w = (1/2) \sum_{i=0}^{2} \sum_{j=0}^{2} \underline{\dot{\delta}}_b^{(i)t}\ \underline{M}_w^{(i,j)}\ \underline{\dot{\delta}}_b^{(j)}$$

Similarly the mass matrices used in the above derived kinetic energy expressions can be defined in terms of the density and shape functions as shown below:

$$\underline{M}_m = \iint \hat{\rho}^{(0)} \; \underline{N}^t \; \underline{N} \; dxdy$$

$$\underline{M}_s = \iint \hat{\rho}_s \; \underline{N}^t \; \underline{N} \; dxdy$$

$$\underline{M}_b^{(i,j)} = \iint \rho_b^{(i,j)} \; \underline{H}'^t \; \underline{H}' \; dxdy$$

$$\underline{M}_{bs}^{(i)} = \iint \rho_{bs}^{(i)} \; \underline{H}'^t \; \underline{N} \; dxdy$$

$$\underline{M}_w^{(i,j)} = \iint \rho_w^{(i,j)} \; \underline{H}^t \; \underline{H}$$

Hence, the various mass matrices may be assembled as shown below:

$$\underline{M}\,\dot{\underline{\delta}} = \begin{bmatrix} M & 0 & 0 & 0 & 0 \\ -m & - & - & - & - \\ & (0,0) & (0,1) & (0,2) & (0) \\ 0 & M & M & M & -M \\ - & -bw & -bw & -bw & -bs \\ & (1,0) & (1,1) & (1,2) & (1) \\ 0 & M & M & M & -M \\ - & -bw & -bw & -bw & -bs \\ & (2,0) & (2,1) & (2,2) & (2) \\ 0 & M & M & M & -M \\ - & -bw & -bw & -bw & -bs \\ & (0)t & (1)t & (2)t & \\ 0 & -M & -M & -M & M \\ - & -bs & -bs & -bs & -s \end{bmatrix} \begin{bmatrix} \dot{\delta} \\ -m \\ \\ .(0) \\ \delta \\ -b \\ \\ .(1) \\ \delta \\ -b \\ \\ .(2) \\ \delta \\ -b \\ \\ . \\ \delta \\ -s \end{bmatrix}$$

where

$$\underline{M}_{bw}^{(i,j)} = \underline{M}_{b}^{(i,j)} + \underline{M}_{w}^{(i,j)}$$

and

$$\underline{M}_{bw}^{(i,j)} = \underline{M}_{bw}^{(j,i)}$$

6.8 Simplified Element

In order to test the preceeding developed theory, it would appear to be appropriate to employ initially a rather simplified element which has displacement in the thickness direction (w) expressed as a function of the coordinates x and y (x,y and t for dynamic analysis) only. It may also be assumed that the higher order terms in the Taylor's series expansion for the element are negligible (w_1 and w_2 are zeros) i.e

$$w(x,y,z,t) = w_0(x,y,t)$$

From the previous analysis, expressions for the displacements in the x and y directions can easily be deduced as below:

$$u(x,y,z,t) = u_0(x,y,t) - Z\,\partial w_0/\partial x + (Z - 4Z^3/3h^2)\,\Phi_x(x,y,t)$$

$$v(x,y,z,t) = v_0(x,y,t) - Z\,\partial w_0/\partial y + (Z - 4Z^3/3h^2)\,\Phi_y(x,y,t)$$

Therefore the nodal displacement vector of the element (at time t) can be defined as follows:

$$\underline{\delta}(t) = \{\ \underline{\delta}_m(t) \quad \underline{\delta}_b(t) \quad \underline{\delta}_s(t)\ \}$$

Hence, using the previous notation for $\underline{D}$ and ρ, the stiffness and mass matrices for the simplified element may be shown as reduced shapes of the previousely derived expressions as below:

$$K = \begin{bmatrix} K & 0 & 0 \\ -m & - & - \\ & & \\ & (0,0) & (0) \\ 0 & K & -K \\ - & -b & -bt \\ & & \\ & (0)t & \\ 0 & -K & K + K \\ - & -bt & -t \quad -s \end{bmatrix}$$

$$M = \begin{bmatrix} M & 0 & 0 \\ -m & - & - \\ & & \\ & (0,0) & (0) \\ 0 & M & -M \\ - & -bw & -bs \\ & & \\ & (0)t & \\ 0 & -M & M \\ - & -bs & -s \end{bmatrix}$$

CHAPTER 7

HIGH ORDER LARGE DEFORMATION ANALYSIS

7.1 Large Deformation Analysis Ignoring In-Plane Effects

7.1.1 Displacement Components

From the previous analysis of high order elements, displacement components can be simplified as follows:

$$u(x,y,z) = u_0(x,y) + (h/2)(\zeta - \zeta^3/3)\Phi_x$$

$$- \sum_{i=0}^{2} \left[\zeta^{2i+1}/(2i+1)\right](h/2)\partial w_i/\partial x$$

$$v(x,y,z) = v_0(x,y) + (h/2)(\zeta - \zeta^3/3)\Phi_y$$

$$- \sum_{i=0}^{2} \left[\zeta^{2i+1}/(2i+1)\right](h/2)\partial w_i/\partial y$$

$$w(x,y,z) = \sum_{i=0}^{2} \zeta^{2i} w_i(x,y)$$

where

$$\zeta = 2Z/h$$

The nodal displacement vector is as defined earlier, i.e.

$$\underline{\delta} = \{ \underline{\delta}_m \quad \underline{\delta}_b^{(0)} \quad \underline{\delta}_b^{(1)} \quad \underline{\delta}_b^{(2)} \quad \underline{\delta}_s \}$$

such that

$$\underline{\delta}_m = \{ (u_0)_1 \ (v_0)_1 \ (u_0)_2 \ (v_0)_2 \ldots\ldots (u_0)_{n_L} (v_0)_{n_L} \}$$

$$\underline{\delta}_s = \{ (\Phi_x)_1 \ (\Phi_y)_1 \ (\Phi_x)_2 \ (\Phi_y)_2 \cdots \ (\Phi_x)_{n_L} (\Phi_y)_{n_L} \}$$

$$\underline{\delta}_b^{(i)} = \{ (w_i)_1 \ (\partial w_i/\partial x)_1 \ (\partial w_i/\partial y)_1 \cdots (\partial w_i/\partial x)_{n_H} (\partial w_i/\partial y)_{n_H} \}$$

where

$$i = 0,1,2$$

7.1.2 Strain Components

Using Green's large strain matrix, and ignoring large deformation terms in transverse shear then the various strains may be defined as below:

$$\varepsilon_x = (\partial u/\partial x) + (1/2)\left[(\partial u/\partial x)^2 + (\partial v/\partial x)^2 + (\partial w/\partial x)^2\right]$$

$$\varepsilon_y = (\partial v/\partial y) + (1/2)\left[(\partial u/\partial y)^2 + (\partial v/\partial y)^2 + (\partial w/\partial y)^2\right]$$

$$\gamma_{xy} = (\partial u/\partial y) + (\partial v/\partial x)$$

$$+\left[(\partial u/\partial x)(\partial u/\partial y) + (\partial v/\partial x)(\partial v/\partial y) + (\partial w/\partial x)(\partial w/\partial y)\right]$$

$$\gamma_{yz} = \Phi_x(1 - \zeta^2) = (\partial u/\partial z) + (\partial w/\partial x)$$

$$\gamma_{yz} = \Phi_y(1 - \zeta^2) = (\partial v/\partial z) + (\partial w/\partial y)$$

At this point it will be assumed that large deformation is due to $w_0(x,y)$ only, i.e.,

$$\varepsilon_x \approx (\partial u/\partial x) + (1/2)(\partial w_0/\partial x)^2$$

$$\varepsilon_y \approx (\partial v/\partial y) + (1/2)(\partial w_0/\partial y)^2$$

$$\gamma_{xy} \approx (\partial u/\partial y) + (\partial v/\partial x) + (\partial w_0/\partial x)(\partial w_0/\partial y)$$

Notice that, $\underline{\varepsilon}_{xy}$ can be redefined such that:

$$\underline{\varepsilon}_{xy} = \underline{\varepsilon}_0 + \underline{\varepsilon}_L$$

where,

$$\underline{\varepsilon}_0 = \begin{bmatrix} \partial u/\partial x \\ \partial v/\partial y \\ \partial u/\partial y + \partial v/\partial x \end{bmatrix}$$

$$\underline{\varepsilon}_L = (1/2) \begin{bmatrix} (\partial w_0/\partial x)^2 \\ (\partial w0/\partial y)^2 \\ 2(\partial w_0/\partial x)(\partial w_0/\partial y) \end{bmatrix}$$

$$= (1/2)\ \underline{A}_w\ \underline{\Theta}_w$$

and,

$$\underline{A}_w = \begin{bmatrix} \partial w_0/\partial x & 0 \\ 0 & \partial w_0/\partial y \\ \partial w_0/\partial y & \partial w_0/\partial x \end{bmatrix}$$

$$\underline{\Theta}_w = \begin{bmatrix} \partial w_0/\partial x \\ \partial w_0/\partial y \end{bmatrix}$$

For infinitesimal dw_0,

$$d\underline{\varepsilon}_L = \begin{bmatrix} (\partial w_0/\partial x)\left[\partial\,(dw_0)/\partial x\right] \\ \partial w_0/\partial y\left[\partial\,(dw_0)/\partial y\right] \\ \partial w_0/\partial x\left[\partial\,(dw_0)/\partial y\right] + \partial w_0/\partial y\left[\partial\,(dw_0)/\partial x\right] \end{bmatrix}$$

$$= \underline{A}_w \; d\underline{\Theta}_w$$

where,

$$d\underline{\Theta}_w = \begin{bmatrix} \partial\,(dw_0)/\partial x \\ \\ \partial\,(dw_0)/\partial y \end{bmatrix}$$

From the above, the following relationships can also be derived:

$$\underline{A}_w{}^t \underline{\sigma}_{xy} = \begin{bmatrix} (\partial w_0/\partial x)\sigma_x + (\partial w_0/\partial y)\tau_{xy} \\ \\ (\partial w_0/\partial y)\sigma_y + (\partial w_0/\partial x)\tau_{xy} \end{bmatrix}$$

$$= \underline{S}_{xy} \; \underline{\Theta}_w$$

such that,

$$\underline{S}_{xy} = \begin{bmatrix} \sigma_x & \tau_{xy} \\ \\ \tau_{xy} & \sigma_y \end{bmatrix}$$

Similarly, it can be shown that:

$$d\underline{A}_w^t \; \underline{\sigma}_{xy} = \underline{S}_{xy} \; d\underline{\Theta}_w$$

7.1.3 Strains in Terms of Nodal Displacements

From previous analysis, it can be shown that:

$$\underline{\varepsilon}_0 = \underline{\varepsilon}_m + (Z - 4Z^3/3h^2)\ \underline{\varepsilon}_t - Z\ \underline{\varepsilon}_b^{(0)}$$

$$- (4Z^3/3h^2)\ \underline{\varepsilon}_b^{(1)} - (16Z^5/5h^4)\ \underline{\varepsilon}_b^{(2)}$$

$$\underline{\varepsilon}_s = (1 - 4Z^2/h^2)\ \hat{\underline{\varepsilon}}_s$$

where,

$\underline{\varepsilon}_m$, $\underline{\varepsilon}_t$.... are as defined earlier

$$\underline{\varepsilon}_0 = \underline{B}_m\ \underline{\delta}_m + (Z - 4Z^3/3h^2)\ \underline{B}_m\ \underline{\delta}_s$$

$$- \sum_{i=1}^{2} \left[h/2(i+1) \right] \zeta^{(i+1)}\ \underline{B}_b\ \underline{\delta}_b^{(i)}$$

$$\underline{\varepsilon}_s = (1 - \zeta^2)\ \underline{B}_s\ \underline{\delta}_s$$

It can also be deduced that:

$$\underline{\Theta}_w = \underline{G}_w\ \underline{\delta}_b^{(0)}$$

where,

$$\underline{G}_w = \begin{bmatrix} \partial H_1/\partial x & \partial H_2/\partial x \ldots\ldots \partial (H)_{3n_H}/\partial x \\ \\ \partial H_1/\partial y & \partial H_2/\partial y \ldots\ldots \partial (H)_{3n_H}/\partial y \end{bmatrix} \equiv \underline{H}'$$

i.e.

$$d\underline{\varepsilon}_L = \underline{A}_w \, \underline{G}_w \, d\underline{\delta}_b^{(0)}$$

$$= \underline{B}_w \, d\underline{\delta}_b^{(0)}$$

such that

$$\underline{B}_w = \underline{A}_w \, \underline{G}_w$$

and

$$\underline{\varepsilon}_L = (1/2) \, \underline{B}_w \, \underline{\delta}_b^{(0)}$$

7.1.4 Linearised Equations of Equilibrium

Using first order elasticity considerations, the principle of virtual work reduces to the following expression:

$$\iiint d\underline{\varepsilon}^t \underline{\sigma} \; d(\text{vol}) - dW = 0$$

For incremental strain and incremental work done:

$$d\underline{\varepsilon} = \underline{B} \, d\underline{\delta}$$

$$dW = d\underline{\delta}^t \, \underline{F}$$

And, it can be shown that:

$$\iiint \underline{B}^t \, \underline{\sigma} \; d(\text{vol}) - \underline{F} = 0$$

where,

$$\underline{B} = \underline{B}_0 + \underline{B}_L$$

Initially, supposing that $\underline{B} \approx \underline{B}_0$

$$\iiint \underline{B}_0^t \, \underline{\sigma}_0 \, d(vol) - \underline{F} = \underline{0}$$

Thereafter, a small deflection solution is obtained, from which $\underline{B}_L$ and $\underline{B}$ can be defined, but,

$$\iiint \underline{B}^t \, \underline{\sigma} \, d(vol) - \underline{F} \neq \underline{0}$$

$$(\underline{\sigma} \equiv \underline{\sigma}_0)$$

For a more accurate solution $\Delta\underline{B}$ and $\Delta\underline{\sigma}$ are used such that:

$$\iiint (\underline{B} + \Delta\underline{B})^t \, (\underline{\sigma} + \Delta\underline{\sigma}) \, d(vol) - \underline{F} = \underline{0}$$

$$\iiint \underline{B}^t \, \Delta\underline{\sigma} \, d(vol) + \iiint \Delta\underline{B}^t \, \underline{\sigma} \, d(vol) \approx \underline{R}$$

where,

$$\underline{R} = \underline{F} - \iiint \underline{B}^t \, \underline{\sigma} \, d(vol)$$

Considering the components: $\iiint \Delta\underline{B}^t \, \underline{\sigma} \, d(vol)$

$$\Delta\underline{B} = \Delta\underline{B}_L = \Delta (\underline{A}_w \, \underline{G}_w)$$

$$= \Delta\underline{A}_w \quad \underline{G}_w$$

Therefore,

$$\Delta\underline{B}^t = \underline{G}_w^t \quad \Delta\underline{A}_w^t$$

and,

$$\Delta\underline{B}^t\ \underline{\sigma} = \underline{G}_w^t\ (\Delta\underline{A}_w^t\ \underline{\sigma}\ )$$

$$= \underline{G}_w^t\ \ \underline{S}_{xy}\ \Delta\underline{\Theta}_w$$

i.e.

$$\Delta\underline{B}^t\ \underline{\sigma} = (\underline{G}_w^t\ \underline{S}_{xy}\ \underline{G}_b)\ \ \Delta\underline{\delta}_b^{(0)}$$

Hence,

$$\iiint_e \Delta\underline{B}^t\ \underline{\sigma} = \left[\ \iiint\ (\ \underline{G}_w^t\ \ \underline{S}_{xy}\ \underline{G}_w)\,d(vol)\right]\ \Delta\delta^{(0)}$$

$$= \underline{K}_\sigma\ \Delta\underline{\delta}_b^{(0)}$$

where,

$$\underline{K}_\sigma = \iiint\ \ \underline{G}_w^t\ \underline{S}_{xy}\ \underline{G}_w\ d(vol)$$

$$= \iint_{\substack{x-y\\ \text{element}}}\ \underline{G}_w^t\ \hat{\underline{S}}_{xy}\ \underline{G}_w\ dxdy$$

and

$$\hat{\underline{S}}_{xy} = \int_{-h/2}^{h/2}\ \underline{S}_{xy}\ dz$$

$$= \sum_{L=1}^{N_L}\ \int_{Z_L^{(L)}}^{Z_U^{(L)}}\ \underline{S}_{xy}^{(L)}\ dz$$

If $\underline{S}_{xy}$ is measured in terms of $\underline{\sigma}_L^{(L)}$, and $\underline{\sigma}_U^{(L)}$ (lower and upper stresses), then, within the order of approximation we may write,

$$\underline{S}_{xy}^{(L)} = \begin{bmatrix} \bar{\sigma}_x & \bar{\tau}_{xy} \\ \bar{\tau}_{xy} & \bar{\sigma}_y \end{bmatrix}$$

where,

$$\underline{\bar{\sigma}} = (1/2)\left[\underline{\sigma}_L^{(L)} + \underline{\sigma}_U^{(L)} \right]$$

and

$$\underline{\hat{S}}_{xy} = \sum_{L=1}^{N_L} t^{(L)} \underline{\bar{S}}_{xy}^{(L)}$$

such that

$$t^{(L)} = Z_U^{(L)} - Z_L^{(L)}$$

Subsequently considering the component: $\iiint \underline{B}^t \, \Delta\underline{\sigma} \; d(\text{vol})$

Considering large strain, then the following strain vector may be defined:

$$\underline{\varepsilon}_{xy} = \left[\underline{B}_m \, \underline{\delta}_m + \underline{B}_w \, \underline{\delta}_b^{(0)} \right] + (Z - 4Z^3/3h^2) \, \underline{B}_m \, \underline{\delta}_s$$

$$- \sum_{i=0}^{2} \left[h/2(i+1) \right] \zeta^{(i+1)} \underline{B}_b \, \underline{\delta}_b^{(i)}$$

Using analysis similar to that employed in the previous chapter, it can be shown that:

$$\iiint \underline{B}^t \, \Delta\underline{\sigma} \, d(vol) = \underline{K}_L \, \Delta\underline{\delta}$$

and using definitions contained in the earlier chapter together with the following definitions:

$$\underline{K}_{mw} = \iint \underline{B}_m^t \; \hat{\underline{D}}_m \; \underline{B}_w \; dxdy$$

$$\underline{K}_w = \iint \underline{B}_w^t \; \hat{\underline{D}}_m \; \underline{B}_w \; dxdy$$

It can be shown that:

$$\underline{K}_L\underline{\delta} = \begin{bmatrix} K_{-m} & K_{-mw} & 0_{-} & 0_{-} & 0_{-} \\ K_{-mw}^{t} & \begin{pmatrix} (0,0) \\ K \\ -b \end{pmatrix} + K_{-w} + K_{-\sigma} & \begin{matrix} (0,1) \\ K \\ -b \end{matrix} & \begin{matrix} (0,2) \\ K \\ -b \end{matrix} & \begin{matrix} (0) \\ -K \\ -bt \end{matrix} \\ 0_{-} & \begin{matrix} (1,0) \\ K \\ -b \end{matrix} & \begin{matrix} (1,1) \\ K \\ -b \end{matrix} & \begin{matrix} (1,2) \\ K \\ -b \end{matrix} & \begin{matrix} (1) \\ -K \\ -bt \end{matrix} \\ 0_{-} & \begin{matrix} (2,0) \\ K \\ -b \end{matrix} & \begin{matrix} (2,1) \\ K \\ -b \end{matrix} & \begin{matrix} (2,2) \\ K \\ -b \end{matrix} & \begin{matrix} (2) \\ -K \\ -bt \end{matrix} \\ 0_{-} & \begin{matrix} (0)t \\ -K \\ -bt \end{matrix} & \begin{matrix} (1)t \\ -K \\ -bt \end{matrix} & \begin{matrix} (2)t \\ -K \\ -bt \end{matrix} & K_{-t} + K_{-s} \end{bmatrix} \begin{bmatrix} \delta_{-m} \\ (0) \\ \delta_{-b} \\ (1) \\ \delta_{-b} \\ (2) \\ \delta_{-b} \\ \delta_{-s} \end{bmatrix}$$

For a simplified element with $w(x,y,z) = w_0(x,y)$, it can be deduced that:

$$\iiint \Delta\underline{B}^{t}\ \underline{\sigma}\ d(vol) + \iiint \underline{B}^{t}\ \Delta\underline{\sigma}\ d(vol) = \underline{K}\ \ \Delta\underline{\delta}$$

$$\underset{-}{K}\ \Delta\underline{\delta} = \begin{bmatrix} K & & K & 0 \\ -m & & -mw & - \\ & & & \\ t & \begin{pmatrix}(0,0) & & \end{pmatrix} & (0) \\ K & \begin{pmatrix}K + & K + & K\end{pmatrix} & -K \\ -mw & \begin{pmatrix}-b & -w & -\sigma\end{pmatrix} & -bt \\ & & & \\ & & (0)t & \\ 0 & & K & (K + K) \\ - & & -bt & -t\ \ -s \end{bmatrix} \begin{bmatrix} \delta \\ -m \\ \\ (0) \\ \delta \\ -b \\ \\ \delta \\ -s \end{bmatrix}$$

7.2 Large Deformation Analysis Considering In-Plane Effects

7.2.1 Displacement and Strain Components

As discussed earlier, the displacement components may be represented as below:

$$u(x,y,z) = u_0(x,y) + (h/2)\left[(\zeta - \zeta^3/3)\Phi_x - \sum_{i=0}^{2} \zeta^{2i+1} \frac{\partial w_i/\partial x}{(2i+1)}\right]$$

$$v(x,y,z) = v_0(x,y) + (h/2)\left[(\zeta - \zeta^3/3)\Phi_y - \sum_{i=0}^{2} \zeta^{2i+1} \frac{\partial w_i/\partial y}{(2i+1)}\right]$$

$$w(x,y,z) = \sum_{i=0}^{2} \zeta^{2i}\ w_i(x,y)$$

Whereas,

$$\zeta = 2Z/h$$

Therefore, the strain components may be defined such that,

$$\underline{\varepsilon}_{xy} = \underline{\varepsilon}_0 + \underline{\varepsilon}_L$$

$$\underline{\varepsilon}_L = \underline{\varepsilon}_{uv} + \underline{\varepsilon}_w$$

where

$$\underline{\varepsilon}_{uv} = (1/2)\begin{bmatrix} (\partial u/\partial x)^2 + (\partial v/\partial x)^2 \\ (\partial u/\partial y)^2 + (\partial v/\partial y)^2 \\ 2(\partial u/\partial x)(\partial u/\partial y) + 2(\partial v/\partial x)(\partial v/\partial y) \end{bmatrix}$$

$$\underline{\varepsilon}_w = (1/2)\begin{bmatrix} (\partial w/\partial x)^2 \\ (\partial w/\partial y)^2 \\ 2(\partial w/\partial x)(\partial w/\partial y) \end{bmatrix}$$

From the displacement equations, it can be shown that:

$$2\underline{\varepsilon}_{uv} = \begin{bmatrix} (\partial u_0/\partial x)^2 + (\partial v_0/\partial x)^2 \\ (\partial u_0/\partial y)^2 + (\partial v_0/\partial y)^2 \\ 2(\partial u_0/\partial x)(\partial u_0/\partial y) + 2(\partial v_0/\partial x)(\partial v_0/\partial y) \end{bmatrix}$$

CONT....

$$+(h/2)^2(\zeta-\zeta^3/3)^2\left[\begin{array}{c}(\partial\Phi_x/\partial x)^2+(\partial\Phi_y/\partial x)^2\\(\partial\Phi_x/\partial y)^2+(\partial\Phi_y/\partial y)^2\\\left[2\left[(\partial\Phi_x/\partial x)(\partial\Phi_x/\partial y)+(\partial\Phi_y/\partial x)(\partial\Phi_y/\partial y)\right]\right]\end{array}\right]$$

$$+\sum_{i=0}^{2}\sum_{j=0}^{2}\frac{(h/2)^{2(i+j+1)}\zeta^{2(i+j+1)}}{(2i+1)(2j+1)}\left[\begin{array}{c}\left[(\partial^2w_i/\partial x^2)\quad(\partial^2w_j/\partial x^2)\right]\\+\left[(\partial^2w_i/\partial x\partial y)\quad(\partial^2w_j/\partial x\partial y)\right]\\\left[(\partial^2w_i/\partial x\partial y)\quad(\partial^2w_j/\partial y\partial x)\right]\\+\left[(\partial^2w_i/\partial y^2)\quad(\partial^2w_j/\partial y^2)\right]\\\left[2(\partial^2w_i/\partial x^2)\quad(\partial^2w_j/\partial y\partial x)\right]\\+\left[2(\partial^2w_i/\partial x\partial y)\quad(\partial^2w_j/\partial y^2)\right]\end{array}\right]$$

$$+h(\zeta-\zeta^3/3)\left[\begin{array}{c}(\partial u_0/\partial x)(\partial\Phi_x/\partial x)+(\partial v_0/\partial x)(\partial\Phi_y/\partial x)\\(\partial u_0/\partial y)(\partial\Phi_x/\partial y)+(\partial v_0/\partial y)(\partial\Phi_y/\partial y)\\\left[(\partial u_0/\partial x)(\partial\Phi_x/\partial y)+(\partial u_0/\partial y)(\partial\Phi_x/\partial x)\right.\\\left.+(\partial v_0/\partial x)(\partial\Phi_y/\partial y)+(\partial v_0/\partial y)(\partial\Phi_y/\partial x)\right]\end{array}\right]$$

CONT....

$$-2\sum_{i=0}^{2} h\zeta^{2i+1} \begin{bmatrix} (\partial u_0/\partial x)(\partial^2 w_i/\partial x^2) + (\partial v_0/\partial x)(\partial^2 w_i/\partial x\partial y) \\ (\partial u_0/\partial y)(\partial^2 w_i/\partial y\partial x) + (\partial v_0/\partial y)(\partial^2 w_i/\partial x\partial y) \\ \dfrac{\left[(\partial u_0/\partial x)(\partial^2 w_i/\partial y\partial x) + (\partial u_0/\partial y)(\partial^2 w_i/\partial x^2)\right.}{2(2i+1)} \\ \left.+(\partial v_0/\partial x)(\partial^2 w_i/\partial y^2) + (\partial v_0/\partial y)(\partial^2 w_i/\partial x\partial y)\right] \end{bmatrix}$$

$$-2\sum_{i=0}^{2} h^2(\zeta-\zeta^3)\zeta^{2i+1} \begin{bmatrix} (\partial \Phi_x/\partial x)(\partial^2 w_i/\partial x^2)+(\partial \Phi_y/\partial x)(\partial^2 w_i/\partial x\partial y) \\ (\partial \Phi_x/\partial y)(\partial^2 w_i/\partial y\partial x)+(\partial \Phi_y/\partial y)(\partial^2 w_i/\partial y^2) \\ \dfrac{\left[(\partial \Phi_x/\partial x)(\partial^2 w_i/\partial y\partial x)+(\partial \Phi_x/\partial y)(\partial^2 w_i/\partial x\partial y)\right.}{4(2i+1)} \\ \left.+(\partial \Phi_y/\partial x)(\partial^2 w_i/\partial y^2)+(\partial \Phi_y/\partial y)(\partial^2 w_i/\partial x\partial y)\right] \end{bmatrix}$$

$$2\varepsilon_{-w} = \sum_{i=0}^{2}\sum_{j=0}^{2} \zeta^{2(i+j)} \begin{bmatrix} (\partial w_i/\partial x)(\partial w_j/\partial y) \\ (\partial w_i/\partial y)(\partial w_j/\partial y) \\ (\partial w_i/\partial x)(\partial w_j/\partial y)+(\partial w_i/\partial y)(\partial w_j/\partial x) \end{bmatrix}$$

Defining the following matrices and vectors:

$$\underline{\Theta}_m = \{\partial u_0/\partial x \quad \partial v_0/\partial x \quad \partial u_0/\partial y \quad \partial v_0/\partial y\}$$

$$\underline{\Theta}_s = \{\partial \Phi_x/\partial x \quad \partial \Phi_y/\partial x \quad \partial \Phi_x/\partial y \quad \partial \Phi_y/\partial y\}$$

$$\underline{\Theta}_b^{(i)} = \{ \partial^2 w_i/\partial x^2 \quad \partial^2 w_i/\partial x\partial y \quad \partial^2 w_i/\partial y\partial x \quad \partial^2 w_i/\partial y^2 \}$$

$$\underline{\Theta}_w^{(i)} = \{\partial w_i/\partial x \quad \partial w_i/\partial y\}$$

and

$$\underline{A}_m = \begin{bmatrix} \partial u_0/\partial x & \partial v_0/\partial x & 0 & 0 \\ 0 & 0 & \partial u_0/\partial y & \partial v_0/\partial y \\ \partial u_0/\partial y & \partial v_0/\partial y & \partial u_0/\partial x & \partial v_0/\partial x \end{bmatrix}$$

$$\underline{A}_s = \begin{bmatrix} \partial \Phi_x/\partial x & \partial \Phi_y/\partial x & 0 & 0 \\ 0 & 0 & \partial \Phi_x/\partial y & \partial \Phi_y/\partial y \\ \partial \Phi_x/\partial y & \partial \Phi_y/\partial y & \partial \Phi_x/\partial x & \partial \Phi_y/\partial x \end{bmatrix}$$

$$\underline{A}_b^{(i)} = \begin{bmatrix} \partial^2 w_i/\partial x^2 & \partial^2 w_i/\partial x\partial y & 0 & 0 \\ 0 & 0 & \partial^2 w_i/\partial y\partial x & \partial^2 w_i/\partial y^2 \\ \partial^2 w_i/\partial y\partial x & \partial^2 w_i/\partial y^2 & \partial^2 w_i/\partial x^2 & \partial^2 w_i/\partial x\partial y \end{bmatrix}$$

$$\underline{A}_w^{(i)} = \begin{bmatrix} \partial w_i/\partial x & 0 \\ 0 & \partial w_i/\partial y \\ \partial w_i/\partial y & \partial w_i/\partial x \end{bmatrix}$$

It can be shown that:

$$2\underline{\varepsilon}_L = \underline{A}_m\ \underline{\Theta}_m + (Z - 4Z^3/3h^2)^2 \underline{A}_s\ \underline{\Theta}_s$$

$$+ \sum_{I=0}^{2}\sum_{J=0}^{2}\left[\frac{Z^{2(i+j+1)}\ \underline{A}_b^{(i)}\ \underline{\Theta}_b^{(j)}}{(2i+1)(2j+1)(h/2)^{2(i+j)}}\right]$$

$$+ \sum_{i=0}^{2}\sum_{j=0}^{2}(2Z/h)^{2(i+j)}\ \underline{A}_w^{(i)}\ \underline{\Theta}_w^{(j)}$$

$$+ (Z - 4Z^3/3h^2)(\underline{A}_m\ \underline{\Theta}_s + \underline{A}_s\ \underline{\Theta}_m)$$

$$- \sum_{i=0}^{2} Z^{2i+1}\left[\underline{A}_b^{(i)}\ \underline{\Theta}_m + \underline{A}_m\ \underline{\Theta}_b^{(i)}\right]/(2i+1)(h/2)^{2i}$$

$$- \sum_{i=0}^{2}(Z^2 - 4Z^4/3h^2)(2Z/h)^{2i}\left[\underline{A}_b^{(i)}\ \underline{\Theta}_s + \underline{A}_s\ \underline{\Theta}_b^{(i)}\right]/(2i+1)$$

It can also be shown that:

$$d\underline{\varepsilon}_L = \underline{A}_m\ d\underline{\Theta}_m + (Z - 4Z^3/3h^2)^2\ \underline{A}_s\ d\underline{\Theta}_s$$

$$+ \sum_{i=0}^{2}\sum_{j=0}^{2} Z^{2(i+j+1)}\ \underline{A}_b^{(i)}\ d\underline{\Theta}_b^{(j)} / \left[(2i+1)(2j+1)(h/2)^{2(i+j)}\right]$$

$$+ \sum_{i=0}^{2}\sum_{j=0}^{2}(2Z/h)^{2(i+j)}\ \underline{A}_w^{(i)}\ d\underline{\Theta}_w^{(j)}$$

CONT....

$$+ \ (Z - 4Z^3/3h^2)\,(\underline{A}_m \ d\underline{\Theta}_s + \underline{A}_s \ d\underline{\Theta}_m)$$

$$- \sum_{i=0}^{2} Z^{2i+1}\left[\ \overset{(i)}{\underline{A}_b} \ d\underline{\Theta}_m + \underline{A}_m \ \overset{(i)}{d\underline{\Theta}_b} \ \right] / \ (2i+1)\,(h/2)^{2i}$$

$$- \sum_{i=0}^{2} (Z^2 - 4Z^4/3h^2)\,(2Z/h)^{2i} \left[\ \overset{(i)}{\underline{A}_b} \ d\underline{\Theta}_s + \underline{A}_s \ \overset{(i)}{d\underline{\Theta}_b} \ \right]/(2i+1)$$

Using interpolation equations, itcan be shown that:

$$d\underline{\Theta}_m = \underline{G}_m \quad d\underline{\delta}_m$$

$$d\underline{\Theta}_s = \underline{G}_m \quad d\underline{\delta}_s$$

$$\overset{(i)}{d\underline{\Theta}_b} = \underline{G}_b \quad \overset{(i)}{d\underline{\delta}_b}$$

$$\overset{(i)}{d\underline{\Theta}_w} = \underline{G}_w \quad \overset{(i)}{d\underline{\delta}_b}$$

whereas

$$\underline{G}_m = \begin{bmatrix} .. & \partial N_i/\partial x & 0 & .. \\ .. & 0 & \partial N_i/\partial x & .. \\ .. & \partial N_i/\partial y & 0 & .. \\ .. & 0 & \partial N_i/\partial y & .. \end{bmatrix}$$

where

$$i = 1,2,.....n_L$$

$$\underline{G}_b = \begin{bmatrix} .. & \partial^2 H_i/\partial x^2 & .. \\ .. & \partial^2 H_i/\partial x \partial y & .. \\ .. & \partial^2 H_i/\partial y \partial x & .. \\ .. & \partial^2 H_i/\partial y^2 & .. \end{bmatrix}$$

and

$$\underline{G}_w = \begin{bmatrix} .. & \partial H_i/\partial x & .. \\ .. & \partial H_i/\partial y & .. \end{bmatrix} = \underline{H}'$$

where,

$$i = 1,2.....3n_H$$

Hence, it can be shown that:

$$d\underline{\varepsilon}_L = \hat{\underline{B}} \; d\underline{\delta}$$

$$= \hat{\underline{B}}_m \; d\underline{\delta}_m + (Z - 4Z^3/3h^2)^2 \; \hat{\underline{B}}_s \; d\underline{\delta}_s$$

$$+ \sum_{i=0}^{2} \sum_{j=0}^{2} \left[\frac{Z^{2(i+j+1)} \; \hat{\underline{B}}_b^{(i)} \; d\underline{\delta}_b^{(j)}}{(2i+1)(2j+1)(h/2)^{2(i+j)}} \right]$$

$$+ \sum_{i=0}^{2} \sum_{j=0}^{2} (2Z/h)^{2(i+j)} \; \hat{\underline{B}}_w^{(i)} \; d\underline{\delta}_b^{(j)}$$

$$+ (Z - 4Z^3/3h^2)(\hat{\underline{B}}_{ms} \; d\underline{\delta}_s + \hat{\underline{B}}_{sm} \; d\underline{\delta}_m)$$

CONT....

$$- \sum_{i=0}^{2} z^{2i+1} \left[\hat{\underline{B}}_{bm}^{(i)} \, d\underline{\delta}_m + \hat{\underline{B}}_{mb} \, d\underline{\delta}_b^{(i)} \right] \left[1/(2i+1)\,(h/2)^{2i} \right]$$

$$- \sum_{i=0}^{2} (z^2 - 4z^4/3h^2)\,(2z/h)^{2i} \left[\hat{\underline{B}}_{bs}^{(i)} \, d\underline{\delta}_s + \hat{\underline{B}}_{sb} \, d\underline{\delta}_b^{(i)} \right] / (2i+1)$$

where

$$\hat{\underline{B}}_m = \underline{A}_m \, \underline{G}_m = \hat{\underline{B}}_{ms}$$

$$\hat{\underline{B}}_s = \underline{A}_s \, \underline{G}_m = \hat{\underline{B}}_{sm}$$

$$\hat{\underline{B}}_b^{(i)} = \underline{A}_b^{(i)} \, \underline{G}_b$$

$$\hat{\underline{B}}_w^{(i)} = \underline{A}_w^{(i)} \, \underline{G}_w$$

$$\hat{\underline{B}}_{bm}^{(i)} = \underline{A}_b^{(i)} \, \underline{G}_m = \hat{\underline{B}}_{bs}^{(i)}$$

$$\hat{\underline{B}}_{mb} = \underline{A}_m \, \underline{G}_b$$

$$\hat{\underline{B}}_{sb} = \underline{A}_s \, \underline{G}_b$$

Note also that:

$$d\underline{A}_m^t \, \underline{\sigma}_{xy} = \underline{S} \, d\underline{\Theta}_m = \underline{S} \, \underline{G}_m \, d\underline{\delta}_m$$

$$d\underline{A}_s^t \, \underline{\sigma}_{xy} = \underline{S} \, d\underline{\Theta}_s = \underline{S} \, \underline{G}_m \, d\underline{\delta}_s$$

$$d\underline{A}_b^{(i)t} \, \underline{\sigma}_{xy} = \underline{S} \, d\underline{\Theta}_b^{(i)} = \underline{S} \, \underline{G}_b \, d\underline{\delta}_b^{(i)}$$

$$d\underline{A}_w^{(i)t} \, \underline{\sigma}_{xy} = \underline{S}_w \, d\underline{\Theta}_b^{(i)} = \underline{S}_w \, \underline{G}_w \, d\underline{\delta}_b^{(i)}$$

where

$$\underline{\sigma}_{xy} = \{ \sigma_x \quad \sigma_y \quad \tau_{xy} \}$$

$$\underline{S} = \begin{bmatrix} \sigma_x & 0 & \tau_{xy} & 0 \\ 0 & \sigma_x & 0 & \tau_{xy} \\ \tau_{xy} & 0 & \sigma_y & 0 \\ 0 & \tau_{xy} & 0 & \sigma_y \end{bmatrix}$$

$$\underline{S}_w = \begin{bmatrix} \sigma_x & \tau_{xy} \\ \tau_{xy} & \sigma_y \end{bmatrix}$$

7.2.3 Linearised Equations of Equilibrium

From the principle of virtual work the following relationship can be established:

$$\Sigma \iiint_e d\underline{\varepsilon}^t \underline{\sigma} \; d(\text{vol}) = d\underline{\delta}^t \underline{F}$$

where

$$\underline{\sigma} = \underline{D} \; \underline{\varepsilon}$$

$$\underline{\varepsilon} = \underline{\varepsilon}_0 + \underline{\varepsilon}_L$$

$$\underline{\varepsilon}_0 = \underline{B}_0 \; \underline{\delta}$$

$$\underline{\varepsilon}_L = (1/2) \; \hat{\underline{B}} \; \underline{\delta}$$

$$d\underline{\varepsilon} = d\underline{\varepsilon}_0 + d\underline{\varepsilon}_L$$

$$= (\underline{B}_0 + \hat{\underline{B}})\ \underline{\delta}$$

$$= \underline{B}\ \underline{\delta}$$

and

$$\underline{B} = \underline{B}_0 + \hat{\underline{B}}$$

For the exact solution:

$$d\underline{\delta}^t \left[\Sigma \iiint_e \underline{B}^t\ \underline{\sigma}\ d(\text{vol}) \right] = d\underline{\delta}^t\ \underline{F}$$

If

$$\underline{B} = \underline{B}_1$$
$$\underline{\sigma} = \underline{\sigma}_1$$

represents an approximate solution, then let the exact solution be expressed as follows:

$$\underline{\sigma} \equiv \underline{\sigma}_1 + \Delta\underline{\sigma}$$

$$\underline{B} \equiv \underline{B}_1 + \Delta\underline{B} = \underline{B}_1 + \Delta\hat{\underline{B}}$$

then

$$d\underline{\delta}^t \left[\Sigma \iiint_e (\underline{B} + \Delta\hat{\underline{B}})^t (\underline{\sigma} + \Delta\underline{\sigma})\, d(\text{vol}) \right] = d\underline{\delta}^t \underline{F}$$

where,

$$(\underline{\sigma},\ \underline{B}) \equiv (\underline{\sigma}_1,\ \underline{B}_1)$$

i.e;

$$d\underline{\delta}^t \left[\Sigma \iiint_e (\underline{B}^t\ \Delta\underline{\sigma} + \Delta\hat{\underline{B}}^t\ \underline{\sigma})\ d(\text{vol}) \right] \approx d\underline{\delta}^t \underline{R}$$

where,

$$\underline{R} = \underline{F} - \Sigma \iiint_{e} \underline{B}^{t}\, \underline{\sigma}\, d(vol)$$

And $d\underline{\delta}$ represents a vector of virtual nodal displacement with $\Delta\underline{\delta}$ representing the required correction, to obtain

$$\Delta\underline{\varepsilon} = \underline{B}\ \Delta\underline{\delta}$$
$$\Delta\underline{\sigma} = \underline{D}\ \Delta\underline{\varepsilon}$$

Considering the component: $d\underline{\delta}^{t} \left[\iiint \Delta\hat{\underline{B}}^{t}\, \underline{\sigma}\, d(vol) \right]$

From the previous analysis, it can be shown that:

$$d\underline{\delta}^{t}\underline{K}_{\sigma}\ \Delta\delta = d\underline{\delta}^{t} \left[\iiint_{e} \Delta\hat{\underline{B}}^{t}\, \underline{\sigma}\, d(vol) \right]$$

$$= d\underline{\delta}_{m}^{t}\ \overset{\sigma}{\underline{K}}_{m}\ \Delta\underline{\delta}_{m} + d\underline{\delta}_{s}^{t}\ \overset{\sigma}{\underline{K}}_{s}\ \Delta\underline{\delta}_{s}$$

$$+ \sum_{i=0}^{2}\sum_{j=0}^{2} d\underline{\delta}_{b}^{(i)}\ \underline{K}_{b}^{\sigma(i,j)}\ \Delta\underline{\delta}_{b}^{(i)}$$

$$+ d\underline{\delta}_{m}^{t}\ \overset{\sigma}{\underline{K}}_{ms}\ \Delta\underline{\delta}_{s} + d\underline{\delta}_{s}^{t}\ \overset{\sigma}{\underline{K}}_{sm}\ \Delta\underline{\delta}_{m}$$

$$- \sum_{i=0}^{2} \left[d\underline{\delta}_{b}^{(i)t}\ \underline{K}_{bm}^{\sigma(i)}\ \Delta\underline{\delta}_{m} + d\underline{\delta}_{m}^{t}\ \underline{K}_{mb}^{\sigma(i)}\ \Delta\underline{\delta}_{b}^{(i)} \right]$$

$$- \sum_{i=0}^{2} \left[d\underline{\delta}_{b}^{(i)t}\ \underline{K}_{bs}^{\sigma(i)}\ \Delta\underline{\delta}_{s} + d\underline{\delta}_{s}^{t}\ \underline{K}_{sb}^{\sigma(i)}\ \Delta\underline{\delta}_{b}^{(i)} \right]$$

CONT....

$$+ \sum_{i=0}^{2} \sum_{j=0}^{2} d\underline{\delta}_b^{(i)} \; \underline{K}_w^{\sigma(i,j)} \; \Delta\underline{\delta}_b^{(j)}$$

where

$$\underline{K}_m^{\sigma} = \iint \underline{G}_m^t \; \underline{S}_m \; \underline{G}_m \; dxdy$$

$$\underline{K}_s^{\sigma} = \iint \underline{G}_m^t \; \underline{S}_s \; \underline{G}_m \; dxdy$$

$$\underline{K}_b^{\sigma(i,j)} = \iint \underline{G}_b^t \; \underline{S}_b^{(i,j)} \; \underline{G}_b \; dxdy$$

$$\underline{K}_w^{\sigma(i,j)} = \iint \underline{G}_w^t \; \underline{S}_w^{(i,j)} \; \underline{G}_w \; dxdy$$

$$\underline{K}_{ms}^{\sigma} = \iint \underline{G}_m^t \; \underline{S}_{ms} \; \underline{G}_m \; dxdy$$

$$= \underline{K}_{ms}^{\sigma t}$$

$$\underline{K}_{bm}^{\sigma(i)} = \iint \underline{G}_b^t \; \underline{S}_{bm}^{(i)} \; \underline{G}_m \; dxdy$$

$$= \underline{K}_{mb}^{\sigma(i)t}$$

$$\underline{K}_{bs}^{\sigma(i)} = \iint \underline{G}_b^t \; \underline{S}_{bs}^{(i)} \; \underline{G}_m \; dxdy$$

$$= \underline{K}_{sb}^{\sigma(i)t}$$

and:

$$\underline{S}_m = \int_{-h/2}^{h/2} \underline{S}\, dz$$

$$\underline{S}_s = \int_{-h/2}^{h/2} (Z - 4Z^3/3h^2)^2\, \underline{S}\, dz$$

$$\underline{S}_b^{(i,j)} = \int_{-h/2}^{h/2} \left[\frac{Z^{2(i+j+1)} \;/\; (h/2)^{2(i+j)}}{(2i+1)\;\;(2j+1)} \right] \underline{S}\, dz$$

$$\underline{S}_w^{(i,j)} = \int_{-h/2}^{h/2} (2Z/h)^{2(i+j)} \underline{S}_w\, dz$$

$$\underline{S}_{ms} = \int_{-h/2}^{h/2} (Z - 4Z^3/3h^2)\, \underline{S}\, dz$$

$$\underline{S}_{bm}^{(i)} = \int_{-h/2}^{h/2} Z^{2i+1} \left[/\,(2i+1)\,(h/2)^{2i} \right] \underline{S}\, dz$$

$$\underline{S}_{bs}^{(i)} = \int_{-h/2}^{h/2} (Z^2 - 4Z^4/3h^2)\,(2Z/h)^{2i} \left[/\,(2i+1) \right] \underline{S}\, dz$$

If the element is made up of a number of thin layers, then the trapezoidal rule of integration can be employed as follows:

$$\underline{S}_m = \sum_{L=1}^{N_L} \hat{\underline{S}}^{(L)}$$

$$\underline{S}_s = \sum_{L=1}^{N_L} \left[Z^{(L)} - 4Z^{(L)3}/3h^2 \right]^2 \hat{\underline{S}}^{(L)}$$

$$\underline{S}_b^{(i,j)} = \sum_{L=1}^{N_L} \left\{ Z^{(L)2(i+j+1)} \left[1/(2i+1)(2j+1)(h/2)^{2(i+j)} \right] \hat{S}^{(L)} \right\}$$

$$\underline{S}_w^{(i,j)} = (2Z^{(L)}/h)^{2(i+j)} \underline{S}_w^{\hat{}(L)}$$

$$\underline{S}_{ms} = \left[Z^{(L)} - 4Z^{(L)3}/3h^2 \right] \hat{\underline{S}}^{(L)}$$

$$\underline{S}_{bm}^{(i)} = Z^{(L)2i+1} \left[1/(2i+1)(h/2)^{2i} \right] \hat{\underline{S}}^{(L)}$$

$$\underline{S}_{bs}^{(i)} = \left[(Z^{(L)2} - 4Z^{(L)4}/3h^2)(2Z^{(L)}/h)^{2i}/(2i+1) \right] \hat{\underline{S}}^{(L)}$$

where

$$Z^{(L)} = (1/2)\left[Z_L^{(L)} + Z_U^{(L)} \right]$$

$$\hat{S}^{(L)} = (1/2)\left[Z_U^{(L)} - Z_L^{(L)} \right]\left[S_U^{(L)} + S_L^{(L)} \right]$$

$()_U^{(L)}$ for upper surface of Lth layer

$()_L^{(L)}$ for lower surface of Lyth layer

Similarly,

$$\hat{\underline{S}}_w^{(L)} = (1/2)\left[ZU^{(L)} - Z_L^{(L)} \right] \left[\underline{S}_{wU}^{(L)} + \underline{S}_{wL}^{(L)} \right]$$

Subsequently Considering component: $d\underline{\delta}^t \left[\iiint \underline{B}^t \, \Delta\underline{\sigma} \; d(vol) \right]$

For simplification of large deformation analysis, the above term is usually approximated as below:

$$d\underline{\delta}^t \left[\iiint \underline{B}^t \, \Delta\underline{\sigma} \; d(vol) \right] \approx d\delta^t \left[\iiint \underline{B}_0 \, \underline{D} \, \underline{B}_0 \; d(vol) \right] \Delta\underline{\delta}$$

$$= d\underline{\delta}^t \, \underline{K} \, \Delta\underline{\delta}$$

and $\underline{K} \, \Delta\underline{\delta}$ is as expressed in the earlier chapter

Linearised Equations of Equilibrium

From previous analysis:

$$d\underline{\delta}^t (\underline{K} + \underline{K}_\sigma) \, \Delta\underline{\delta} = d\underline{\delta}^t \, \underline{R}$$

i.e.

$$(\underline{K} + \underline{K}_\sigma) \, \Delta\underline{\delta} = \underline{R}$$

For a pre-stressed structure $\underline{K}_\sigma$ represents stiffening due to pre-stressing

7.3 Equivalent Nodal Loading Due to Inertial Force

Let

$$\underline{a} = \{\underline{a}_x \quad \underline{a}_y \quad \underline{a}_z\}$$

represent the vector of acceleration at (x,y,z) with respect to local axes. At the Lth layer:

$$\Delta\underline{F}^{(L)} = -\rho^{(L)} \underline{a}\, d(vol)$$

$$\Delta(dW^{(L)}) = d\underline{q}^t \Delta\underline{F}^{(L)}$$

where,

$$d\underline{q} = \{u \quad v \quad w\}$$

From the previous analysis it can be shown that:

$$d\underline{q} = \{d\underline{q}_{uv} \quad d\underline{q}_w\}$$

$$d\underline{q}_{uv} = d\underline{q}_m + d\underline{q}_s (Z - 4Z^3/3h^2)$$

$$-\sum_{i=0}^{2} Z^{2i+1} \left[1/(2i+1)(h/2)^{2i}\right] \begin{bmatrix} \partial w_i/\partial x \\ \\ \partial w_i/\partial y \end{bmatrix}$$

$$d\underline{q}_w = \underline{w}_0 + (4Z^2/h^2)\underline{w}_1 + (16Z^4/h^4)\underline{w}_2$$

where

$$d\underline{q}_m = \begin{bmatrix} \dot{du}_0 \\ \\ \dot{dv}_0 \end{bmatrix} = \underline{N}\, d\underline{\delta}_m$$

$$d\underline{q}_s = \begin{bmatrix} d\Phi_x \\ \\ d\Phi_y \end{bmatrix} = \underline{\underline{N}}\ d\underline{\delta}_s$$

$$\underline{\underline{H}}',\ \underline{\delta}_b^{(i)} = \begin{bmatrix} \partial \dot{w}_i/\partial x \\ \\ \partial \dot{w}_i/\partial y \end{bmatrix}$$

$$w_i = \underline{\underline{H}}\ \underline{\delta}_b^{(i)} = \underline{w}_i$$

Hence, it can be shown that:

$$d\underline{q}_{uv} = \underline{\underline{N}}\ d\underline{\delta}_m + (Z - 4Z^3/3h^2)\ \underline{\underline{N}}\ d\underline{\delta}_s$$

$$- \sum_{i=0}^{2} z^{2i+1}\left[1/(2i+1)(h/2)^{2i}\right]\ \underline{\underline{H}}'\ d\underline{\delta}_b^{(i)}$$

$$d\underline{q}_w = \sum_{i=0}^{2} z^{2i}\left[1/(h/2)^{2i}\right]\ \underline{\underline{H}}'\ d\underline{\delta}_b^{(i)}$$

and, similarly:

$$\Delta(\ dW^{(L)}\ ) = \Delta(\ dW_{uv}^{(L)}) + \Delta(\ dW_w^{(L)}\ )$$

where,

$$\Delta(\ dW_{uv}^{(L)}) = d\underline{q}_{uv}^t\ \ \Delta\underline{F}_{x-y}^{(L)}$$

$$\Delta(\ dW_w^{(L)}\ ) = d\underline{q}_w^t\ \ \Delta\underline{F}_z^{(L)}$$

and

$$\Delta\underline{F}_{xy}^{(L)} = -\rho\ \ \underline{a}_{xy}^{(L)}\ \ d(vol)$$

$$\Delta \underline{F}_z^{(L)} = -\rho^{(L)} \underline{a}_z \, d(vol)$$

$$\underline{a}_{xy} = \begin{bmatrix} a_x \\ \\ a_y \end{bmatrix}$$

$$\underline{a}_z = [\, a_z \,]$$

The work done per unit volume for the Lth layer is:

$$d\bar{W}^{(L)} = d\bar{W}_{uv}^{(L)} + d\bar{W}_w^{(L)}$$

where

$$d\bar{W}_{uv}^{(L)} = -d\underline{q}_{uv}^t \, \rho^{(L)} \, \underline{a}_{xy}$$

$$d\bar{W}_w^{(L)} = -dq^t \, \rho_w^{(L)} \, \underline{a}_z$$

Hence, it can be shown that:

$$d\bar{W}^{(L)} = \left\{ \left[d\underline{\delta}_m^t \, \underline{N}^t + (Z - 4Z^3/3h^2) \, d\underline{\delta}_s^t \, \underline{N}^t \right] \underline{a}_{xy} \right.$$

$$- \sum_{i=0}^{2} Z^{2i+1} \left[1/(2i+1)(h/2)^{2i+1} \right] d\underline{\delta}_b^{(i)t} \, \underline{H}^{',t} \, \underline{a}_{xy}$$

$$\left. + \sum_{i=0}^{2} (2Z/h)^{2i} \, d\underline{\delta}_b^{(i)t} \, \underline{H}^{',t} \underline{a}_w \right\} (-\rho^{(L)})$$

Integrating with respect to Z, thereafter it can be shown that:

$$dW' = \int_{-h/2}^{h/2} d\bar{W}^{(L)}\, dZ$$

$$= d\underline{\delta}_m^t \; \underline{F}_m' + d\underline{\delta}_s^t \; \underline{F}_s' + \sum_{i=0}^{2} d\underline{\delta}_b^{(i)} \left(\underline{F}_b^{',(i)} + \underline{F}_w^{',(i)} \right)$$

where

$$\underline{F}_m' = \underline{N}^t \int_{-h/2}^{h/2} (-\rho^{(L)}) \; \underline{a}_{xy} \; dZ$$

$$= \underline{N}^t \; \hat{\underline{a}}_m$$

$$\underline{F}_s' = \underline{N}^t \; \hat{\underline{a}}_s$$

$$\underline{F}_b^{',(i)} = \underline{H}'^t \; \hat{\underline{a}}_b^{(i)}$$

$$\underline{F}_w^{',(i)} = \underline{H}^t \; \hat{\underline{a}}_w^{(i)}$$

$$\hat{\underline{a}}_m = \int_{-h/2}^{h/2} \rho^{(L)} \; (-\underline{a}_{xy}) \; dZ$$

$$\hat{\underline{a}}_s = \int_{-h/2}^{h/2} (Z - 4Z^3/3h^2) \; \rho^{(L)} \; (-\underline{a}_{xy}) \; dZ$$

$$\underline{\hat{a}}_b^{(i)} = \int_{-h/2}^{h/2} z^{2i+1} \left[1/(2i+1)(h/2)^{2i}\right] \rho^{(L)} \underline{a}_{xy}\, dz$$

$$\underline{\hat{a}}_w^{(i)} = -\int_{-h/2}^{h/2} (2Z/h)^{2i} \rho^{(i)} \underline{a}_z\, dZ$$

For centrifugal acceleration $\underline{a}_{xy}$, $\underline{a}_w$ or $\underline{a}_x$, $\underline{a}_y$ and $\underline{a}_z$ are functions of (x,y,z). For the special case of (a_x, a_y, a_z) being independent of Z and considering symmetric composite plates, then:

$$\underline{\hat{a}}_m = -\underline{a}_{xy} \int_{-h/2}^{h/2} \rho^{(L)}\, dZ$$

$$\underline{\hat{a}}_s = 0$$

$$\underline{a}_b^{(i)} = 0$$

$$\underline{\hat{a}}_w^{(i)} = -\underline{a}_w \int_{-h/2}^{h/2} (2Z/h)^{2i} \rho^{(i)}\, dZ$$

Finally, integrating with respect to x and y it can be deduced that:

$$dW = \iint dW'\, dxdy = d\underline{\delta}^t \underline{F}$$

$$= d\underline{\delta}_m^t \underline{F}_m + d\underline{\delta}_s^t \underline{F}_s + \sum_{i=0}^{2} d\underline{\delta}_b^{(i)} \left(\underline{F}_b^{(i)} + \underline{F}_w^{(i)} \right)$$

where

$$\underline{F}_m = \iint N^t \quad \hat{\underline{a}}_m \quad dxdy$$

$$\underline{F}_s = \iint \underline{N}^t \quad \hat{\underline{a}}_s \quad dxdy$$

$$\overset{(i)}{\underline{F}_b} = \iint \underline{H}'^t \overset{(i)}{\underline{a}_b} dxdy$$

$$\overset{(i)}{\underline{F}_w} = \iint \underline{H}^t \quad \overset{(i)}{\underline{a}_w} \quad dxdy$$

For a simplified element (i.e., i = 0 only):

$$\hat{\underline{a}}_b^{(0)} = \int_{-h/2}^{h/2} Z \quad \rho \quad \overset{(L)}{\underline{a}_{xy}} \quad dz$$

$$\underline{a}_w^{(0)} = -\int_{-h/2}^{h/2} \underline{a}_z \quad \rho \quad \overset{(i)}{} \quad dz$$

and

$$dW = d\underline{\delta}_m^t \underline{F}_m + d\underline{\delta}_s^t \underline{F}_s + d\underline{\delta}_b \left(\overset{(0)}{\underline{F}_b} + \overset{(0)}{\underline{F}_w} \right)$$

$$= d\delta^t \quad F$$

$$\overset{(0)}{\underline{F}_b} = \iint \underline{H}'^t \quad \overset{(0)}{\underline{a}_b} \quad dxdy$$

$$\overset{(0)}{\underline{F}_w} = \iint \overset{(0)}{\underline{a}_w} \quad \underline{H}^t \; dx \; dy$$

CHAPTER 8

FINITE-ELEMENT PROGRAMMING

8.1 Introduction

A finite element package, which is capable of static and dynamic stress analysis of laminated composite plates and shells, or of any other similar structure, was designed on the basis of the theory described in the previous chapters. It is difficult to explain the different parts and segments of the package in this limited context, and only a brief review of the package structure will, therefore, be given in this chapter.

8.2 Package Structure

Modular design is a feature of large general-purpose programs. A module is a set of statements that comprises one logical subset of the program. For the FE programming, each module corresponds to one of the basic steps of the FE solution in the package.

Modules of a program must share a data base, which is a collection of files or records. Ideally, the program has little waste space, it can be accessed quickly either sequentially or directly, and is flexible to allow for growth and change. Data transmitted between modules should be minimal. A module may contain a number of subroutines or functions.

A modular design approach has been adopted for the present package. The package consists of several modules which are stored as separate computer files. Any program required for a particular task will be linked from one or

more of these files according to the task specified. Such an approach facilitates the development and expansion of the package.

The package structure can be seen in Figs.8.1 and 8.2, whereas the following are the various modules of the package:

- Module Static-Master
- Module Static-Front
- Module Dynamic-Band
- Module Dynamic-Front
- Module Facet-Ut
- Module Facet-Vt
- Module Ahmad-Ut
- Module Ahmad-Vt
- Module Facet-Vt
- Module Common-Ut
- Module Common-Vt
- Module Common-Her
- Module Material-Ut
- Module Common-Vt
- Module Common-Her

Listing of module segments can be seen in Appendices A-1 through A-11.

8.3 Program Data

Information, sufficient for the specification and solution of a particular problem, is correctly defined and transmitted to the various programming modules. The input data is for reading the necessary geometric, material and loading information in order to establish FE arrays. These arrays store the number of elements and their type, the number of nodes and their co-ordinates together with

topology arrays, material properties, boundary restraint code, prescribed nodal forces and displacements etc.

The data required for analysis to be carried out by the package, are described in the Data subroutine in terms of simple segments with self explanatory titles. The package contains a number of subroutines for the interpretation and error-diagnosis of such data segments. If the package detects illogical input data parameters, descriptive messages will be printed as a warning and the program will be terminated.

8.4 Static Analysis

The package is capable of carrying out static analysis for plates and shells. For a problem involving plates or faceted shells, first order and higher order analyses are possible, whilst only first order analysis is available for curved shells. Following the previously described modular programming approach, the analysis programs are composed of different files each of which has a specified task. The line diagrams for the static analysis are shown in Fig.8.3 and 8.4 using ordinary and frontal solvers, respectively.

8.4.1 Element Stiffness Matrix Generator (ESMG)

The element stiffness matrix for an element can generally be defined as follow:

$$\underline{K}_{(e)} = \iiint \underline{B}^{t}\ \underline{D}\ \ \underline{B}\ \ \mathrm{dvol}$$

The stiffness matrices, based upon the theories developed in earlier Chapters, are generated in different files. Block diagrams for the ESMG using first order facet shell elements, first order curved shell elements and the higher-order facet shell elements are shown in Figs.8.7

through 8.9 respectively.

A rotation matrix is employed in the construction of the ESMG which is composed of the segments described below. The contribution made by each of these segments to the relevant ESMG can be seen in Figs. 8.7 to 8.9

ESMGM and ESMGIN

These components of the ESMG are designed to generate element stiffness matrices due to in-plane effects only.

ESMGB

This segment covers the effect of bending in the generation of the element stiffness matrices.

ESMGS

This component of the ESMG is employed for the addition of any stiffness generated by shear effects in the structure.

ESMGMB and ESMGINB

This part of the ESMG generates the element stiffness matrices due to the effects of coupling between extension and bending/twisting.

ESMGT

This component covers the contribution made to the ESMG by the effect of coupling between shear and extension.

ESMGBT

This segment is employed for the generation of the contribution to the stiffness matrix made by the effects of coupling between shear and bending.

The development of the above stiffness matrices requires various D-matrices, B-matrices and matrix algebra together with a subroutine (PZ) for dealing with structures of variable thickness.

The various D-matrices used generally represent the variation in the material property with the thickness of the structure being analysed. For a lamina this variation may be included in its stiffness matrix, whereas for a laminated composite structure, it may be included in the extensional stiffness, bending stiffness and coupling stiffness matrices, as defined earlier in Chapter 3. The different D-matrices used for the higher order elements are as defined earlier in Chapter 6.

The following are various types of B-matrices used for the definition of the derivatives of the shape functions in the package.

B-MATRIXM

This subroutine defines the strain-displacement relationship considering in-plane effects only.

B-MATRIXB

This subroutine is designed for the definition strain-displacement relationship considering bending effects only.

B-MATRIXS

This subroutine defines the relationship between shear strain and displacement.

The B-matrix generators require a Jacobian matrix, intrinsic derivatives, cartesian derivatives and shape functions for their formulation.

Matrix manipulation subroutines are defined for matrix initiation, product, transpose, summation etc.

8.4.2 Assembly and Solution

The following basic procedures are available for the assembly and solution of the load-deflection equations:

(i) Banded Solver

Using banded matrices, the following separate subroutines are designed for the assembly and solution of equations:

Assembler

In this subroutine equations for the whole structure are obtained by assembling all element

equations in order to formulate the stiffness matrix $\underline{K}$ (in a banded form) and the nodal loading vector $\underline{F}$.

Reducer

In this subroutine a reduced system of equations is obtained by applying the boundary conditions. Hence, rows and columns in $\underline{K}$ and $\underline{F}$, corresponding to restrained DOF are eliminated in order to formulate the reduced stiffness matrix $\underline{K}_R$ (in the banded form) and the reduced loading vector $\underline{F}_R$ for the structure.

Solver

In this subroutine the reduced system of equations are solved, with the aid of Gauss elimination or Choleski-factorisation methods, for the unknown displacements.

(ii) Frontal Solver

The frontal solver is very efficient for a complex structure and may result in a considerable saving in both the computer core storage and CPU time expended. A frontal solver based upon the Gauss-elimination method is adopted in this work and is composed of the following main sections:

Initiator

This subroutine initiates a number of vectors and matrices required for the frontal operation and also estimates the maximum front width.

Eliminator

Through this subroutine, each element stiffness matrix is assembled, reduced, and eliminated (whenever applicable) in a step-by-step procedure. As soon as an equation is eliminated it will immediately be stored in the back-up storage, keeping only a small matrix(the front) in the direct access store.

Solver

In this section the FE equations are solved using Gaussion backward substitution to obtain the nodal displacements. The eliminated equations are recalled, one-by-one, in reverse order to the direct access store which leads to the final solution.

8.4.3 Nodal Displacements and Reactions

After calculating the reduced displacements, a subroutine is employed to calculate and list the total nodal displacements $\underline{\delta}$ for the structure. Another subroutine is used to calculate the nodal reactions according to the following equations:

$$\underline{R} = \underline{F} - \underline{K}\,\underline{\delta}$$

8.4.4 Stress and Strain

Subroutines are available for the calculation of the stress and strain distributions at different nodal locations.

8.5 Dynamic Analysis

The package is capable of carrying out natural frequency analyses with or without centrifugal stiffening. Using different types of dynamic solver, for different plate and shell structures, the analysis can be achieved in a manner similar to that explained earlier, for the static analysis. There are also many files for this objective and the program relevant to a specified job can be linked with those files. The relevant module, for the dynamic analysis, can be seen in Appendices A-3 and A-4, and the line diagrams for the same are shown in Figs.8.5 and 8.6, respectively. Dynamic analysis using first order facet and curved shell, and higher order facet shell, elements are available in the package.

8.5.1 Element Matrix Generator

Both the element stiffness and mass matrices are required for any FE dynamic analysis. Subroutines for the ESMG are the same as those used for static analysis.

The mass matrix for an FE analysis is defined below:

$$\underline{M}_{(e)} = \iiint_{e} \underline{N}^{t} \, \underline{D} \, \underline{N} \; d(vol)$$

The mass matrices, based upon the theories developed in earlier Chapters, are generated in different files. Subroutines have been designed for the generation of the mass matrices for every type of element, in a way similar to that explained earlier for the ESMG. The block diagrams for the element mass matrix generator (EMMG), using various elements, can be seen in Fig.8.10 through 8.12.

Construction of the EMMG requires the employment of the rotation matrix and may consist of components similar to those defined earlier for the ESMG, with contributions from in-plane bending, shear and coupling effects etc.

The formulation of the above mass matrices makes use of various N-matrices, D-matrices and matrix algebra together with the subroutine PZ.

The N-matrices generally contain different shape functions designed for use with the different components of the EMMG. These matrices require a Jacobian matrix, intrinsic derivatives, cartesian derivatives and shape functions for their formulation.

The D-matrix generators define the variation in material properties in terms of density, and are also designed to be used for the various parts of the EMMG.

8.5.2 Natural Frequency Analysis

Subroutines for the assembly and reduction of banded stiffness and mass matrices are available as are eigenvalue solvers which employ subspace iteration with symmetric banded matrices.

The most efficient eigenvalue solver is the frontal solver with subspace iteration. Files for this type of solver have also been implemented for all of the types of element available in this package.

8.6 Non-Linear Stiffness Analysis

The residual nodal force vector produced by geometrical effects is equal to the product of the stiffness matrix due to centrifugal stiffening and the

incremental displacement vector, that is

$$\Delta \underline{F} = \underline{K}_{\sigma(e)} \Delta \underline{\delta} = \iiint \Delta \underline{B}^{t} \underline{\sigma} \, d(vol)$$

The centrifugal stiffness matrices, based upon the theory discussed in earlier Chapters, are generated in a manner similar to that employed for the formulation of the ESMG and EMMG matrices. The block diagrams of the element centrifugal stiffness matrix generators are shown in Fig.8.13 through 8.15.

The construction of the centrifugal stiffness matrix also employs a rotation matrix and may consist of components similar to those defined earlier for the ESMG and EMMG.

These stiffness matrices require various stress-matrices, G-matrices and matrix algebra together with the subroutine PZ for their construction.

The different stress matrices employed in this section, include stress matrices generated as a result of in-plane bending, shear and the coupling effects. The construction of these matrices requires a Jacobian matrix, intrinsic derivatives, cartesian derivatives and shape functions etc.

The G-matrices define the various shape function derivatives, and are designed to be employed with the various components of the stiffness matrix.

CHAPTER 9

RESULTS AND DISCUSSIONS

9.1 Introduction

An important step to be taken before the present programming package is used for the analysis of practical engineering structures, is to verify the reliability and assess the accuracy of the package. Naturally during the compilation of the present work a great number of individual verifications have been carried out throughout, and at all of the various stages of its development.

A direct approach for the validation of the completed FE package is to compare its results with those obtained from other reliable packages, which have the same facilities and for the same boundary and loading conditions. As there was no package available at Cranfied which can achieve stress analysis including centrifugal stiffening, this approach was obviously not possible.

Verification of the present work can also be achieved by comparing the results obtained from the developed package with available or experimental published results but, unfortunately, results of natural frequencies of free vibration of rotating plates and shells are rare. Many researchers publish results for tests, but most of these do not include the details of the geometry of the blade analysed, effectively preventing other workers from using their results for verification. The number of useful tests available in the literature are therefore also very limited.

Validations can also be achieved by comparing the results of a developed package with those from a known analytical solution. Analytical techniques are available but these are cumbersome and limited to calculation of the fundamental frequency only.

Hence, it was decided to partly verify the package by using it for problems of less complexity, but for which there are known analytical solutions; plus a comparison of the package results to some limited experimental results. Some of these experimental results were carried out within the framework of the present investigation and some were kindly supplied by Rolls Royce Ltd.

Simple validation cases have been dealt with in section 9.2 for the deflection and natural frequency analysis applicable to thick structures. Whilst validation of thin structures including centrifugal stiffening effects, have been covered in the real engineering cases described sections 9.2 and 9.3.

9.2 Simple Validation Cases

During these analyses isotropic material properties were transformed into orthotropic material properties. For different runs, the structures were considered to be made of various symmetric layers, inclined at different angles to the material axis. Results were obtained thereafter, employing first order elements and higher order element analysis, respectively. Provided the total dimensions of the structures were constant, variations in the number of layers or the inclination angles, did not effect the results.

9.2.1 Disc Cases

For this case study, a disc was used with the following properties;

Modulus of Elasticity	= 10000	Kg/cm^2
Possion's ratio	= 0.3	
Density	= 10	Kg/cm^3
Radius	= 10	cm

From reasons of symmetry, analysis of only one quarter of the disc was necessary. The disc was discretised into 25 3-noded triangular elements, as shown in Fig.9.1. The following two different cases were studied:

Clamped Disc Under Distributed Loading

A clamped disc under distributed loading was modelled for the purpose of analysis by the developed package. Subsequently the package was run for a wide range of thickness. An analytical solution [131] was used for comparison with the results. The results obtained are plotted in Fig.9.2.

Simply Supported Disc Under Distributed Loading

Similarly, a simply supported disc under distributed loading was also used for the purpose of validating the developed package. Again the package was run many times for the various thickness values. The results obtained are compared with those from an analytical solution [131] and are shown in Fig.9.3

It can be seen from the above figures that the results obtained with the aid of the present package, employing first order shell element analysis, converges to the closed-form solution with increase in thickness. It is also clear that, whilst using uniform quadrature, the first order shell element analysis leads to great inaccuracy in the thin range of the structure. However, it is later shown that the application of reduced and/or selective integration can improve the results in that range.

It can also be seen that the newly developed theory for the higher order element analysis correlates well with the analytical solution over a wide range of thickness.

9.2.2 Rectangular Plate Case

The rectangular plate used for the purpose of this analysis has the following properties:

Modulus of elasticity	=	1000	Kg/cm^2
Poission's ratio	=	0.3	
Density	=	10	Kg/cm^3
length	=	10	cm

One quarter of the plate is discretised into 25 4-noded quadrilateral elements as shown in Fig.9.4. The package was run for a wide range of the thickness. The results obtained are compared with those from an analytical solution [130] and are plotted in Fig.9.5.

It can be seen from Fig.9.5 that the package results obtained from the first order shell element analysis again converges to the analytical solution with increase in thickness. It is also later shown that the application of

selective and/or reduced integration improves the results in the thin range. The results obtained from the higher order element analysis are closer to the analytical solution for both the thick and the thin range of the structure.

9.2.3 Cantilever Plate

For this analysis, a cantilever plate as shown in Fig.9.6, was employed with the following properties:

Youngs Modules	=	193.9	Gpa
Density	=	7700	Kg/m^3
Poission ratio	=	0.3	
Length (l)	=	0.7	m
Width (b)	=	0.6	m
Thickness(h)	=	0.025	m

The plate was discretised into 84 3-noded triangular elements as shown in Fig.9.7. For the purpose of comparison, an analytical solution [129], was employed for the calculation of the first and second bending natural frequencies.

The results obtained are shown in Table.9.1A. It can be seen that the results obtained from the developed package are very close to those derived from the analytical solution. The first bending frequency, as determined by the package, is identical to the closed-form value when the first order and higher order elements are employed. However, the second bending frequency calculated with the aid of higher order elements is closer to the analytical solution than that obtained from the other elements.

9.3 Case Study Of Isotropic Compressor Blade

9.3.1 Case Definition

It is, perhaps, appropriate to validate the present programming package, in the first instance, using a model based upon isotropic material properties instead of the non-isotropic properties for which it was developed. This can be achieved by supplying the isotropic properties of the model in place of the orthotropic properties earlier used for the simple validation cases. For this purpose a current Rolls Royce compressor blade was used. This steel blade is manufactured from nominally isotropic material for which properties were provided as shown below;

$E = 193.9\ GPa = 28.1x10^6\ lbf/in^2$

$\gamma = 0.3$

$\rho = 7700\ Kg/m^3 = 0.278\ lb/in^3$

Rolls-Royce also provided some experimental vibration data for this blade, as shown in Figs.9.9 to 9.11.

Data received included co-ordinates in x and y for 55 points at a fixed z value, in a sequence starting from the leading edge eight different blade heights(z values) were used.

The above co-ordinates have been used for the definition of the blade midsurface by averaging values of the x and y co-ordinates for the upper and lower surfaces of each section. The co-ordinates supplied have also been used to determine the thickness at various points on the

mid-surface of the sections. However, the assemblage of the mid-surfraces of the various sections describes the mid-surface of the complete blade. Two hundred and ten 3-noded triangular elements were incorporated into analysis, as shown in Figs.9.12 and 9.13.

9.3.2 Package Results

The results were obtained for the analysis of the blade using first order and higher order elements, employing full and selective integration. The derived results, can be seen in Table 9.1 through 9.3. Fig.9.14 represents results obtained for the variation of frequency with speed showing natural frequencies of blade.

9.3.3 Discussion Of Results

The following observations can be made from the results obtained:

(i) The results obtained with the help of the developed package are quite close to the experimental values and are probably within an acceptable accuracy range. In particular, the results obtained with the aid of the higher order elements are quite close to the experimental values.

(ii) Although selective integration improved the results obtained from first order facet and curved shell element analysis, its effect on the results obtained from higher order element analysis was negligible.

(iii) As expected, the effect of centrifugal stiffening on the first bending mode natural frequency is significant, whilst its effect on the higher frequencies is

small. By comparing the results plotted in Fig.9.14 with those of Figs. 9.9 to 9.11, it would appear that the present package does deal adequately with centrifugal stiffening effects.

9.4 Case Study Of Composite Compressor Blade

9.4.1 Case Definition

For the engineering case study of a structure made of layered composite materials, a Rolls Royce RB162 Stage 6 blade has been analysed. The blade is made of symmetric composite material which is transversely isotropic in nature and has the following properties:

E_{xx} = 43.0 GPa

E_{yy} = 17.2 GPa

G_{xy} = 5.9 GPa

γ = 0.25

ρ = 1.99 Mg/m^3

The blade is manufactured from 20 layers of the same material, with each layer having a constant thickness of 0.14mm. Fibres in 16 of layers lie along the radial direction, while in two layers (2 and 19) the fibre orientation was $+45^{o}$ and in two others (3 and 18) it was -45^{o}. Dimensions of the layers are variable, hence the blade may be defined as having variable thickness. The blade has been discretised into 32, 8-noded, elements. Topology arrays of these elements have been defined, together with the co-ordinates at the mid-surface. Thickness of the blade at these nodes has also been provided.

From the thickness values, the total number of layers were determined at various nodes. The exact size (1:1) of the different layers has also been provided, as shown in Figs.9.15 and 9.16, which helped to determine the contribution of the various layers at a particular node.

From the data provided, it is simple to determine the co-ordinates of an additional node at the centre of each element, by taking simple averages of the co-ordinates at the corner nodes of the elements. In this way a 9-noded element could be defined. Similarly, 4-noded and 3-noded elements were also generated, by considering corner nodes only. The various meshes generated for this analysis can be seen in Figs.9.17 through 9.24.

9.4.3 Package Results

Results were obtained for the analysis of the composite blade using first order and higher order elements and employing full, selective and/or reduced integration, respectively. These results are shown in Tables 9.4 through 9.25. Fig.9.26 represents the variation of the natural frequencies with rotating speed.

9.4.2 Experimental Work

Holography is a non-contacting method capable of measuring both dynamic and static displacement, and offering an accurate plot of the nodal pattern and vibration amplitude over the whole surface of the vibrating object with an accuracy of less than the wave length of the laser light.

Many different holographic techniques are available for a wide range of applications. The technique of dynamic

time-averaged interferometric holography was employed for the present investigation. This allows for the production of a pictorial representation of any specific mode of vibration for the whole surface of a vibrating component. The modal pattern at a particular natural frequency can be studied using only one holographic exposure which provides information about the amplitude of vibration and the location of the vibratory nodes.

The apparatus set up can be seen in Fig.9.25, it was then found that to produce the brightest hologram, the light intensities of object and reference beam had to be equal, this was achieved using a variable density filter/beam splitter. Since the HE-NE laser had a power output of only 15mw it was necessary to paint the object matt white so as to produce maximum reflection of the object wave front.

Piezo-electric crystals were used to excite the blade because contact between the whole crystal face and the blade could be obtained and because the piezo-electric crystals had very low mass. This meant that the energy losses were very small since spurious noise was eliminated. Since the mass of the crystal was negligible, compared with the mass of the blade, the resonant frequencies could be accurately tuned.

Before a mode shape could be produced, the natural frequency for that mode shape had to be found. This was achieved by monitoring the change across the signal crystal and comparing it with the change in voltage across a crystal cemented on to the blade to pick-up its frequency response. Both signals were displayed on an oscilloscope simultaneously, it would then be seen when for a particular frequency a maximum peak-to-peak voltage across the pick-up crystal was produced. This particular frequency was

accurately monitored using a frequency counter connected through the oscilloscope to the signal generator.

To produce the time-averaged hologram, the blade was vibrated at a natural frequency while recording a transmission hologram. The compressor blade demonstrated in Fig.9.8, has been analysed using the previous technique. The various holograms can be seen in Figs.9.27 through 29 which were measured as 874(1F), 1935(1T) and 3855(2F) Hz, respectively.

9.4.4 Discussion Of Results

Although the experimental results were static only (that is, non-rotating only), convergence of the analytical results to these static values may provide an indication of the accuracy of the analytical results. Of course, the validity of the centrifugal stiffening analysis has already been shown for the Rolls-Royce steel blade.

From the results obtained by the package, the following observations can be made:

(i) Results obtained indicate that the natural frequencies increases with operating speed and (obviously) are maximum at the maximum operating speed. Increase in the natural frequencies, due to the centrifugal stiffening, can be as high as 45% of the calculated stationary values.

(ii) While employing a very crude mesh of 4-noded quadrilateral elements with first order facet and curved shell element analysis, acceptable results were obtained to within 23% of the accuracy range. Employing the reduced and selective integration procedures the results were improved to within 8% of the accuracy range.

(iii) With full integration, and when employing 8-noded quadrilateral elements, the first order element analysis results were, as expected, more accurate than those obtained by employing 4-noded elements. The results obtained were within 13% of accuracy range, but were improved by making use of selective and reduced integrations.

(iv) The analysis which employed 9-noded quadrilateral elements with first order elements produced quite satisfactory result. The results obtained from analysis which employed reduced integration compared very favourably with the experimental results.

(v) Using 3-noded triangular elements and full integration, the higher order facet shell element analysis gave very encouraging results. The results were within 11% of the experimental values, while results obtained from first order shell element analysis were also within an acceptable range. Although the reduced and the selective integration procedures improved results when using first order element analysis, these could not significantly effect the results which arose from the higher order elements.

CHAPTER 10

CONCLUSIONS

A finite element package based upon original derivations, which is capable of static and dynamic stress analysis of laminated composite plates and shells, or similar structures, has been designed and proved to be accurate and reliable.

A newly developed theory for higher order element analysis has proved to perform very well for a wide range of structural thicknesses, i.e., from very thin to moderately thick.

Although theories derived for the first order shell elements performed well within the thick range of the structure, the introduction of reduced and selective integration procedures were necessary if accurate results were to be obtained for the thin range.

Analysis of the non-linear effects, in the form of centrifugal stiffening has been included. It has been shown that can be a large error in estimating the fundamental frequency if the centrifugal stiffening effect is ignored.

The package has also proved to be fully capable of accurate static and dynamic stress analysis of plates and shells made of isotropic materials, by simply supplying isotropic material properties in terms of orthotropic properties.

RECOMMENDATIONS FOR THE FUTURE WORK

During the development of the present package, only simple higher order elements have been programmed. It is possible that the introduction of the some complex higher order elements may further improve the package results. A proper validation of centrifugal stiffening effects should be carried out.

REFERENCES

1. Z.Hashin "Theory of fibre reinforced materials" NASA Rep. CR-1974 (72)

2. G.P.Sendeckj "Elastic behaviour of composites" J. Composite Materials-2 (1974)

3. L.J.Walpole "Elastic behaviour of composite materials: Theoretical Fundamentals" Advances in Appl. Mech.-21 (1981)

4. C.W.Bert "Experimental characterization of composites" J. Composite Materials-8 (1975)

5. S.K.Datta, H.M.Ledbetter & R.D.Kriz "Calculated elastic constants of composite containing anisotropic fibres" Int. J. Solids Structures-2 (1984)

6. G.Lubin "Hand-book of fibreglass and advanced plastic composites" 1st edn. Van Nostrand-Reinhold (1969)

7. J.V.Noyes "Composites in the construction of Lear Fan 2100 aircraft" J.Composite Materials-14 (1983)

8. S.W.Tsai & H.T.Hahn "Introduction to composite materials" Technomic Westport CT (1980)

9. B.W.Cole & R.B.Pipes "Filamentary composite laminates subjected to biaxial stress field" AFB, AFFDL-TR-73-115 (1973)

10. Leonard R. "Composite FEM analysis for layered systems"J. Herrmann, M. Engg. Mechanics-110 (1984)
ASCE, Kenneth
R.Welch &
Chang K.Lim

11. Gent,A.N. & "Compression, bending and shear of bonded Meinecke,E.A. rubber blocks" Polymer Engg. and Science-10 (1970)

12. Gent,A.N., "Interfacial stresses for bonded rubber blocks Henry,R.L. & in compression and shear" J. Appl. Mech. ASME- Roxbury,M.L. 41 (1974)

13. Lindley,P.B. "Some numerical stiffnesses of soft elastic & Teo,S.C. blocks bonded to rigid and plates" Plastic and Rubber, Material application (1978)

14. Rejcha,C. "Design of elastometer bearing" PCI J.-9 (1964)

15. Herrmann,L.R. "Numerical analysis of reinforced soil & Al-Yassin,Z systems" Proce. of Sympo. on Earth Reinforcement, ASCE (1978)

16. Pagano,N.J. "Stress fields in composite laminates" Int. J. Solid and Structures-14 (1978)

17. Herrmann,L.R. "Elasticity equations for incompressible and nearly incompressible materials by a variational theorem" AIAAJ-3 (1965)

18. Herrmann,L.R. "Finite element modelling of composite edge effects" Presented at ASCE 7th conference on Electronic Computations at St.Louis Mo (1979)

19. Wang,A.S.D. & Crossman,F.W. "Calculation of edge effects in multilayered laminates by sub-structuring" J. Composite Materials-12 (1978)

20. Herrmann,L.R. "Mixed finite elements for coupled-stress analysis" Proce. Int. Sympo. on hybrid and mixed FE analysis (1981)

21. Herrmann,L.R. & Schamber, R.A. "Finite element analysis of layered systems with edge effects" Numerical Methods for coupled problems, Pineridge Press (1981)

22. A.B.Basset "On the extension and flexure of cylindrical and spherical thin elastic shells" Phil Trans. Roy. Soc. (London). ser.A..181 (6) (1890)

23. E.Reissner "On the theory of bending of elestic plates" J. Math. Phys.-23 (1944)

24. E.Reissner "The effect of transverse shear deformation on the bending of elastic plates" J.Appl.Mech.-12 (1945)

25. E.Reissner "On bending of elastic plates" Q. Appl.Math.-5 (1947)

26. F.B.Hildebrand,E.Reissner & G.B.Thomas — "Notes on the foundations of the theory of small displacement of orthotropic shells" NACA Technical Note 1833 (1947)

27. R.D.Mindlin — "Influence of rotatory inertia and shear on flexural motion of isotropic, elastic plates" J. Appl. Mech.-18 (1951)

28. J.N.Reddy — "Energy and variational methods in Applied Mechanics" Wily, N.Y. (1984)

29. J.M.Whitney & A.W.Leissa — "Analysis of heterogeneous anisotropic plates" J. Appl. Mech. (1969)

30. R.Byron Pipes & N.J.Pagano — "Interlaminar stresses in composite laminates under uniform axial extension" J. Composite Materials-4 (1970)

31. Peter W. Hsu & Carl T. Herakovich — "Edge effects in angle-ply composite laminates" J. Composite Materials-11 (1977)

32. S.S.Wang & R.J.Stango — "Optimally discretized finite elements for boundary layer stresses in composite laminates" 23rd structures, structural dynamics and materials coference,part-1 (1982)

33. J.D.Whitcomb, I.S.Raju & J.G.Goree — "Reliability of finite element method for calculating free edge stresses in composite laminates" Computers and Structures-4 (1982)

34. A.S.D.Wang & Frank W. Crossman — "Some new results on edge effects in symmetric composite laminates" J. Composite Materials-11 (1977)

35. T.C.T.Ting & P.H.Hoang — "Singularities at the tip of a crack normal to the interface of an anisotropic layered composite" Int. J. Solid Structures-20 (1984)

36. R.I.Zwiers, T.C.T.Ting & R.L.Spilker — "On the logarithmic singularity of free edge stress in laminated composites under uniform extension" J. Appl. Mech.-49 (1982)

37. Lawrence W.Rehfield, Erian A.Armanios & Rao Valisetty — "Simplified sublaminate analysis of composite and application" Computers and Structures-20 (1985)

38. R.B.Pipes & N.J.Pagano — "Interlaminar stresses in composite laminates under uniform axial extension" J. Composite Materials-4 (1970)

39. A.S.D.Wang & F.W.Crossman — "Some new results on edge effects in symmetric composite laminate" J. Composite Materials-11 (1977)

40. I.S.Raju & J.H.Crews Jr. — "Interlaminar stress singularities at a straight free edge in composite laminates" Computers and Structures-14 (1981)

41. S.Tang & A.Levy — "A boundary layer theory part-2: Extension of laminated finite strip" J. Composite Materials -9 (1975)

42. N.J.Pagano "Stress field in composite laminates" Int. J. Solid Structures-14 (1978)

43. J.T.S.Wang & J.N.Dixon "Interlaminar stresses in symmetric composite laminates" J. Composite Materials-12 (1978)

44. N.J.Pagano & S.R.Soni "Global local laminate variational model" Int. J. Solid Structures-19 (1983)

45. C.W.Pryor Jr. & R.M.Barker "A finite element analysis including transverse shear effects for applications to laminated plates" AIAAJ (1971)

46. O.C.Zienkiewicz,R.L.Taylor & J.M.Toot "Reduced integration techniques in general analysis of plates and shells" Int. J. Num. Methd. in Engg., Vol.3 (1971)

47. N.J.Pagano "Exact solution for composite laminates in cylindrical bending" J. Composite Materials-3 (1969)

48. J.Ergatoudis, B.M.Iron & O. C.Zienkiewicz "Curved isoparametric quadrilateral elements for finite element analysis" Int. J. Solids Structures-4 (1968)

49. Richard M.Barker,Fu Tien Lin & Jon R. Dana "3-dimensional finite element analysis of laminated composites" Computers and Structures-2 (1972)

50. S.Ahmad, B.M. Iron & O.C. Zienkiewicz "Analysis of thick and thin shells structures by curved finite element" Int. J. Numerical Methods in Engg.-2 (1970)

51. R.A.Chaudhuri "Static analysis of fibre reinforced laminated plates and shells with shear deformation using quadratic triangular elements" Ph.D. dissertation USC Los Angles CA (1983)

52. P.Seide & R.A.Chaudhuri "Triangular finite element for analysis of thick laminated shells" Int. J. Numerical Methods in Engg.

53. R.A.Chaudhuri "An equilibrium method for prediction of transverse shear stresses in a thich laminated plate" Computers and Structures-23 (1986)

54. R.D.Henshell & K.G.Shaw "Crack tip finite elements are necessory" Int. J. Numerical Methods in Engg.-9 (1975)

55. Robert M.J. "Mechamics of composite materials" McGRAW-HILL KOGAKUSHA LTD (1975)

56. R.Jones, R. Callinan,K.K. Teh & K.C. Brown "Analysis of multilayer laminates using three-dimensional super element" Short communication John Wiley & Sons Ltd. (1983)

57. R.W.Clough "The FEM in plane stress analysis" Proceeeding of ASCE (1960)

58. S.T.Mau, P. Tong & T.H.H. Pian — "Finite element solutions for laminated thick plates" J. Composite Materials-6 (1972)

59. R.D.Cook — "Two hybrid elements for analysis of thick, thin and sandwich plates" Int. J. Numerical Methods in Engg.-5 (1972)

60. S.T.Mau & T.H.H.Pian — "Linear dynamic analyses of laminated plates and shells by the hybrid stress finite element method" MIT ASRL TR 172-2 (1973)

61. R.L.Spilker & N.I.Munir — "The hybrid stress model for thin plates" Int. J. Numerical Methods in Engg.-15 (1980)

62. R.L.Spilker & N.I.Munir — "A hybrid stress quadratic serendipity displacement Mindlin plate bending element" Computers and Structures-12 (1980)

63. R.L.Spilker & N.I.Munir — "A serendipity cubic displacement hybrid stress element for thin and moderatly thick plates" Int. J. Numerical Methods in Engg.-15 (1980)

64. R.L.Spilker — "Hybrid stress eight node elements for thin and thick multilayer laminated plates" Int. J. Numerical Methods in Engg.-18 (1982)

65. R.L.Spilker — "An invariant eight node hybrid stress element for thin and thick multilayer laminated plates" Int. J. Numerical Methods in Engg.-20 (1984)

66. I.S.Raju, J. D.Whitcomb & J.G.Goree "A new look at numerical analyses of free-edge stresses in composite laminates" NASA TP 1751 (1980)

67. R.L.Spilker & S.C.Chou "Edge effects in symmetric composite laminates: Importance of satisfying the traction-free-edge condition" J. Composite Materials-14 (1980)

68. S.S.Wang & F.K.Yuan "A singular hybrid finite element analysis of boundary-layer stresses in composite laminates" Int. J. solid Structures-9 (1983)

69. S.S.Wang & I.Choi "Boundary layer effect in composite laminates. Part-1: Free edge stress singularities,Part-2: Free edge stress solutions and basic considerations" J. Appl. Mech.-30 (1982)

70. E.Altus, A. Rotem & M. Shmueli "Free edge effect in angle-ply laminates. A new three-dimensional finite difference solution" J. Composite Materials-14 (1980)

71. S.R.Soni & N.J.Pagano "Elastic response of composite laminates" Mech. Compos. Mater.-1 (1983)

72. N.J.Salamon "An assessment of the interlaminar stress problem in laminated composite" J. Composite Materials-14 (1980)

73. W.C.Chao & J.N.Reddy — "Analysis of laminated composite shells using a degenerated 3-dimensional element" Int. J. Numerical Methods in Engg.-20 (1984)

74. J.M.Whitney & C.T.Sun — "A refined theory for laminated anisotropic cylindrical shells" J. Appl. Mech. (1974)

75. T.J.R.Hughes, T.E.Tezduyar — "Finite elements based upon Mindlin plate theory with particular reference to the 4-node bilinear isoparametric element" J. Appl. Mech. -48 (1981)

76. J.N.Reddy — "A penalty plate-bending element for the analysis of laminated anisotropic composite plates" Int. J. Numerical Methods in Engg.-15 (1980)

77. K.J.Bathe & S.Bolourchi — "A geometric and material non-linear plate and shell element" Computers and Structures-11 (1980)

78. L.W.Rehfield & R.R.Valisetty — "A simple refined theory for bending and stretching of homogeneous plates" AIAAJ

79. R.R.Valisetty & L.W.Rehfield — "A theory for structural analysis of composite laminates" Presented at 24th AIAA conference Nevada (1983)

80. R.R.Valisetty — "Bending of beams, plates and laminates: Refined theories and comparative study" Ph.D. thesis GIT (1983)

31. B.M.Iron & K.J.Draper — "Inadequacy of nodal connections in a stiffness solution for plate bending" AIAAJ-3 (1965)

32. R.J.Melosh — "A flat triangular shell element stiffness matrix" AFFDL-TR-66-80, 503-515 (1966)

33. S.Utku — "Stiffness matrices for thin triangular elements of non zero Gaussian curvature" AIAAJ -9 (1967)

34. S.W.Kay & Z. E.Beisinger — "The analysis of thin shells with transverse shear strains by the finite element method" Proce. 2nd Conf. Matrix Meth. Struct. Mech. Wright-Patterson AFB, Ohio (1968)

35. G.A.Wempner, J.T.Oden & D.A.Kross — "Finite element analysis of thin shells" Proce. ASCE J. Engg. Mech. Div; No.EM6 (1968)

36. G.S.Dhatt — "Numerical results of thin shells by curved triangular elements based DK hypothesis" Proce Sympo. Appl. FEM civil Engg. Vanderbilt Univ. (1969)

37. S.W.Key & Z. E.Beisinger — "The analysis of thin shells by the finite element method" IUTAM Sympo.,Liege Univ. (1970)

38. J.L.Boltoz & G.S.Dhatt — "Buckling of deep shells" 2nd Int. Confe. on Structural Mech. in Reactor Tech. Berlin (1977)

89. J.L.Boltoz et al. "Finite element large deflection analysis of shallow shells" Int. J. Numerical Methods in Engg.-10 (1976)

90. J.L.Boltoz & G.S.Dhatt "Linear and nonlinear finite element analysis of deep shells; influnce of shell theories" CANCAM 77 Vancouver (1977)

91. J.L.Boltoz & G.S.Dhatt "An evaluation of two simple and effective triangular and quadrilateral plate bending elements" Proce. New and future development in commercial FEM Los Angeles (1981)

92. J.C.Nagtegaal & J.G.Slater "A simple non-compatible thin shell element based on discrete Kirchhoff theory" Nonlinear FE analysis of plates and shells, AMD-48 (1981)

93. S.Sridhara Murthy & Richard H. Gallagher "Anisotropic cylindrical shell element based on discrete Kirchhoff theory" Int. J. Numerical Methods in Engg.-19 (1983)

94. N.J.Pagano "Exact solution for composite laminates in cylindrical bending" J. Composite Materials-3 (1969)

95. N.J.Pagano "Exact solution for rectangular bidirectional composites and sandwich plates" J. Composite Materials-4 (1970)

96. C.W.Pryor Jr. & R.M.Barker "A finite element analysis including transverse shear effects for application to laminated plates" AIAAJ-9 (1971)

97. R.L.Spilker, O. Orringer, E.A. Witmer, S.Verbiese, S.E. French & A.Harris "Use of hybrid stress finite element model for the static and dynamic analysis of multilayer composite plates and shells" Dept. AMMRC CTR 79-29 ASRL TR 181-2 MIT (1976)

98. R.L.Spilker, S.C.Chou & O.Orringer "Alternate hybrid stress element for analysis of multilayer composite plates" J. Composite Materials-11 (1977)

99. S.C.Panda & R.Natarajan "Finite element analysis of laminated composite plates" Int. J. Numerical Methods in Engg.-14 (1979)

100. M.J.Turner, R.W.Clough H.C.Martin & L.J.Topp "Stiffness and Deflection analysis of complex structures" J.Aero, vol.23, No.9, (1956)

101. G.R.Bhashyam & R.H.Gallagher "A triangular shear-flexible finite element for moderately thick laminated plates" Comput. Meth. Appl. Mech. Engg.-40 (1983)

102. S.T.Mau, P. Tong & T.H. H.Pian "Finite element solutions for laminated thick platees" J. Composite Materials-6 (1972)

103. A.S.Mawenya & J.D.Davis — "Finite element bending analysis of multilayer plates" Int. J. Numerical Methods in Engg.-8 (1974)

104. P.Seide & P.H.H.Chang — "Finite element analysis of laminated plates and shells" NASA-CR-157106 157107 (1978)

105. P.C.Yang, C. H.Norris & Y.Stavsky — "Elastic wave propagation in heterogeneous plates" Int. J. Solids Structures-2 (1966)

106. J.M.Whitney & N.J.Pagano — "Shear deformation in heterogeneous anisotropic plates" J. Appl. Mech.-37 (1970)

107. R.B.Nelson & D.R.Lorch — "A refined theory for laminated orthotropic plates" J. Appl. Mech.-41 (1974)

108. K.H.Lo, R.M. Christensen & E.W.Wu — "A higher order theory of plate deformation, Part-2: laminated plates" J. Appl. Mech.-44 (1977)

109. M.Levinson — "An accurate, simple theory of the statics and dynamics of elastic plates" Mech. Res.Commun-7 (1980)

110. M.V.V.Murthy — "An improved transverse shear deformation theory for laminated anisotropic plates" NASA Tech. paper 1903 (1981)

111. J.N.Reddy "An accurate prediction of natural frequencies of laminated plates by a higher-order theory" Adv. Aerospace Struct. Mater. Dynam. AD-106 (1983)

112. J.N.Reddy "A simple higher-order theory for laminated composite plates" J. Appl. Mech.-51 (1984)

113. J.N.Reddy "A refined nonlinear theory of plates with transverse shear deformation" J. Solids and Structures-20 (1984)

114. N.D.Phan & J.N.Reddy "Analysis of laminated composite plates using a higher-order shear deformation theory" Int. J. Numerical Methods in Engg.-21 (1985)

115. G.Horrigmoe & P.G.Bergon "Incremental variational principles and finite element models for nonlinear problems" Comput. Meth. Appl. Mech. Engg.-7 (1976)

116. W.Wunderlich "Incremental formulations for geometrically nonlinear problems" Formulations and Algorithm in FE analysis

117. A. Strcklin, W.E. Haisley & W.A.Von Risemann "Evaluation of solution procedures for materials and/or geometrically nonlinear structure analysis" AIAAJ-11 (1971)

118. A.K.Noor & S.J.Hartley "Nonlinear shell analysis via mixed isoparametric elements" Computers and Structures-7 (1977)

119. T.Y.Chang & Sawamiphakdi "Large deformation analysis of laminated shells by finite element method" Computers and Structures-13 (1981)

120. Kane, T.R.; Ryan, R.R. & Baberjee,A.K. "Dynamics of a cantilever beam attached to a moving base" J Guid Control Dyn Vol-10, No.2 (1987)

121. Naidu,A.C.B.; Srinath,H. "Flexure of orthotropic rotating disks" Int. J. Mech. Sci. Vol-21 (1979)

122. Cornell,R.W. "Elementary three-dimensional interactive rotor blade impact nalysis" ASME, Vol-98, No.4 1976)

123. Sollid, J.E.; Stetson,K.A. "Strains from holographic data" Experimental Mechanics, Vol-18 (1978)

124. Chamis, C.C.; Lynch, J.E. "High - tip - speed fibre composite compressor blades - vibration and strength analysis"AIAA (1974)

125. Bert, C.W. "Rotor dynamics: Dynamics of rim-type flywheel supported by flexible band" Proc of Mech and Magn Energy Storage, USA (1979)

126. Kuo, P.S.; Collinge,K.S. "Structural analysis of a gas turbine impeller using finite element and holographic techniques" Propul and Energy panel meet, Cleveland, (1978)

127. Kumar, R. "Vibrations of space booms under centrifugal force field" CASI Transaction, Vol-7 (1974)

128. Zeller,T.A.; Buttrill,C.S. "Dynamic analysis of an unrestrained, rotating structure through non-linear simulation" AIAA, (1988)

129. William,T.T. "Theory of vibration with application" 2nd edn. George Allen & Unmin London

130. S.Y.Long,C. A.Brebbia & J.C.F.Telles "Boundary Element bending analysis of moderately thick plates." Engineering Analysis, June 1988, Vol.5, No.2

131. S.Timoshenko & S.W.Krieger "Theory of plates and shells" McGraw Hill second edition. 1970

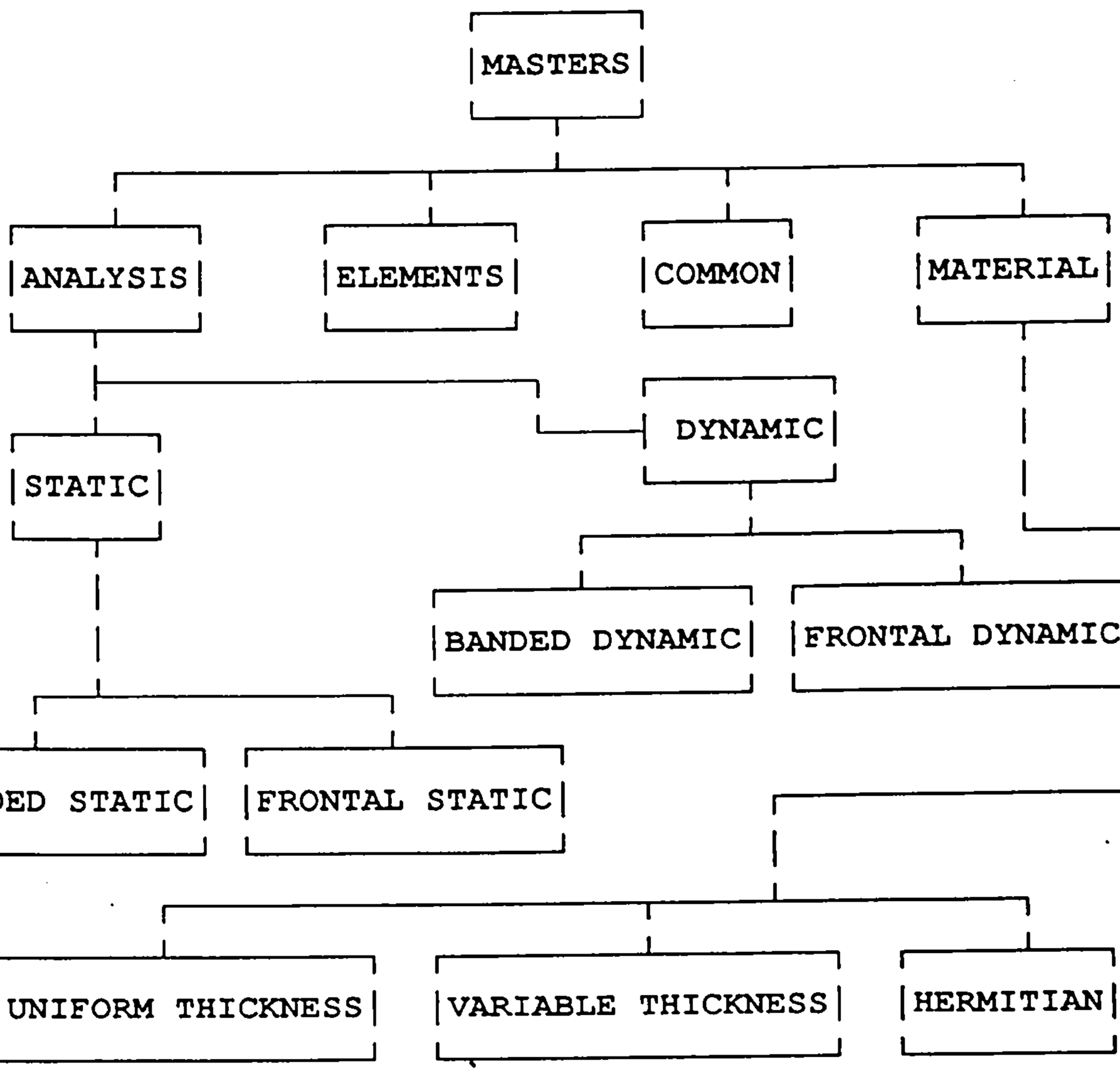

FIG.8.1 LINE DIAGRAM OF THE PACKAGE STRUCTURE

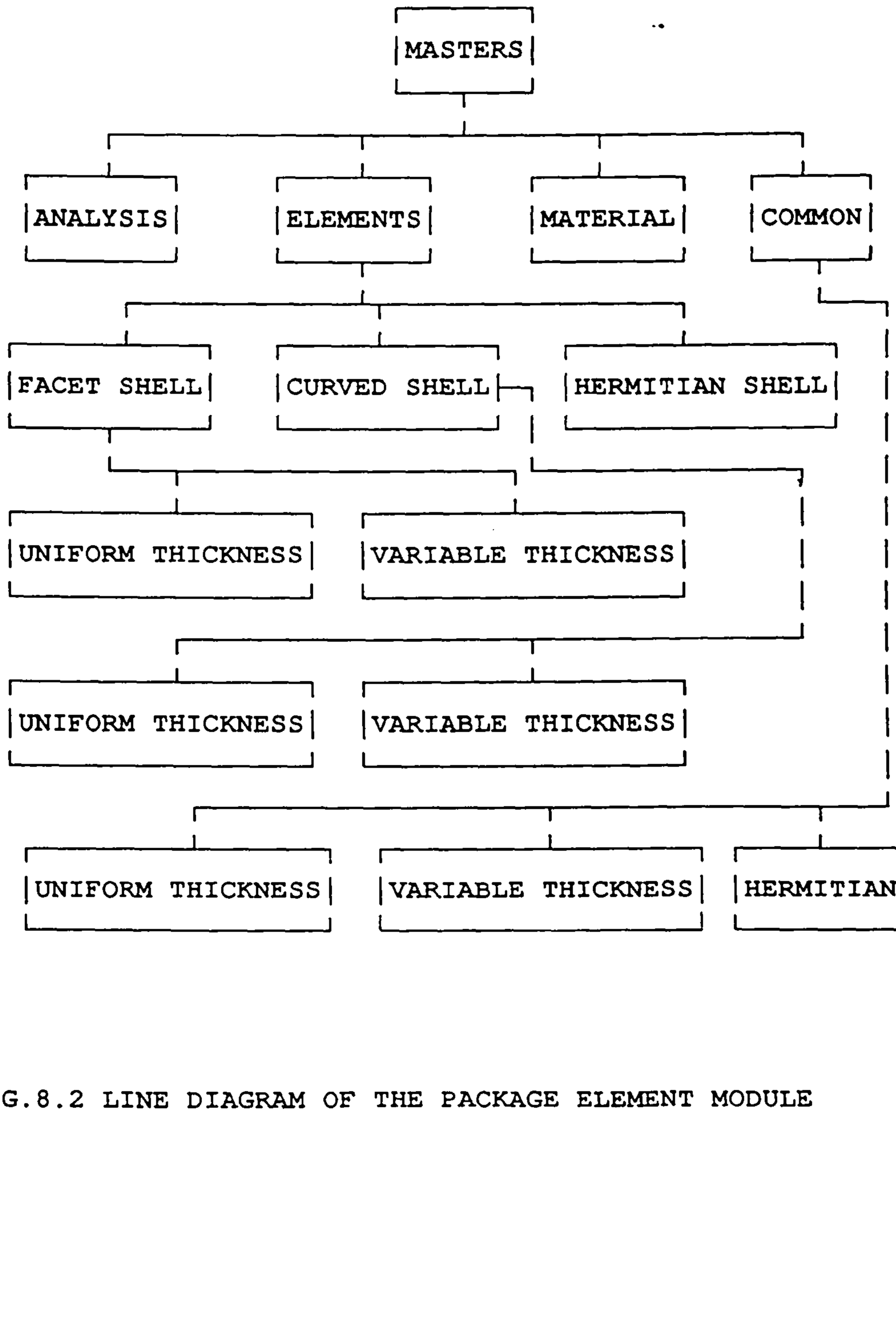

FIG.8.2 LINE DIAGRAM OF THE PACKAGE ELEMENT MODULE

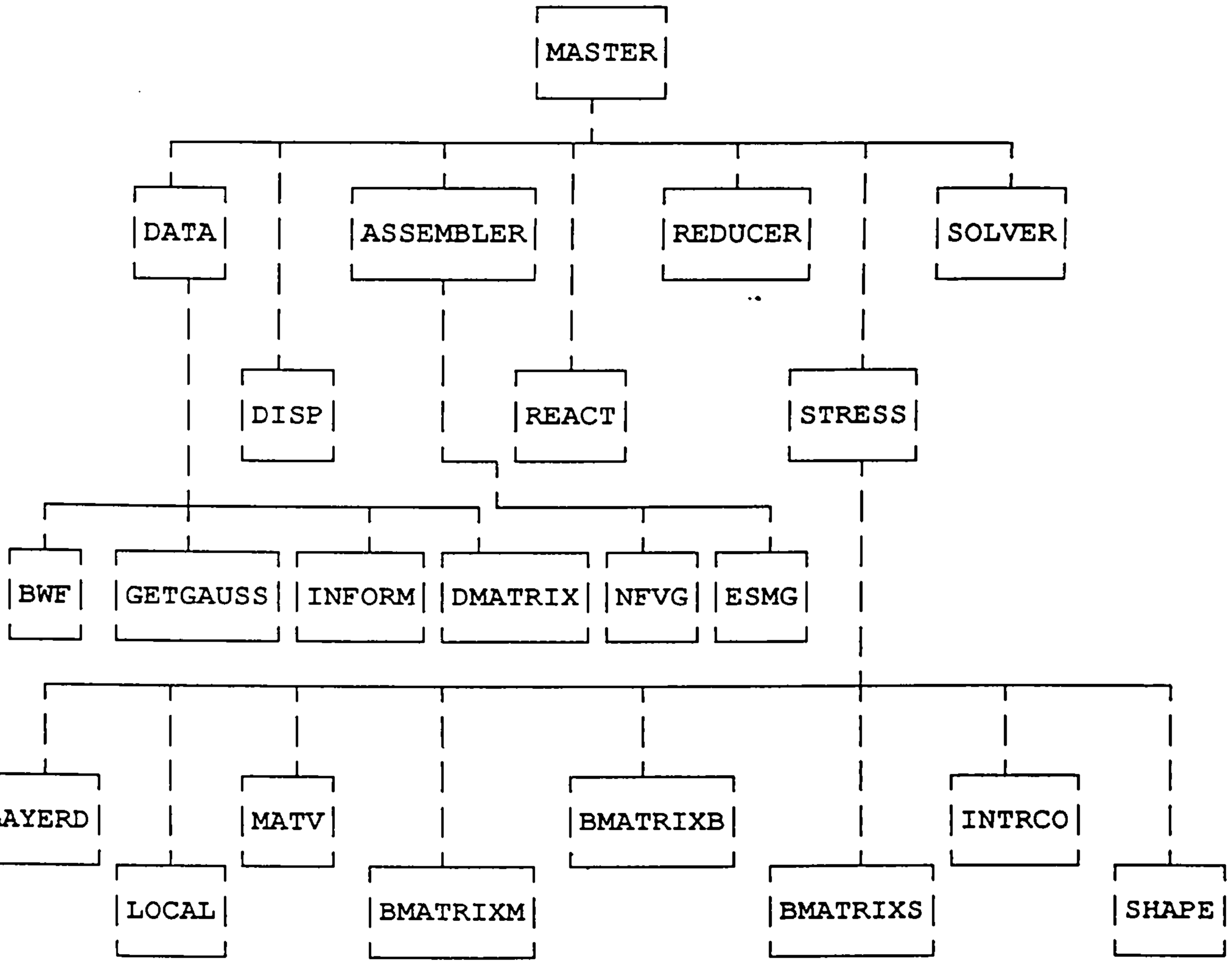

FIG.8.3 LINE DIAGRAM FOR STATIC ANALYSIS USING AN ORDINARY SOLVER.

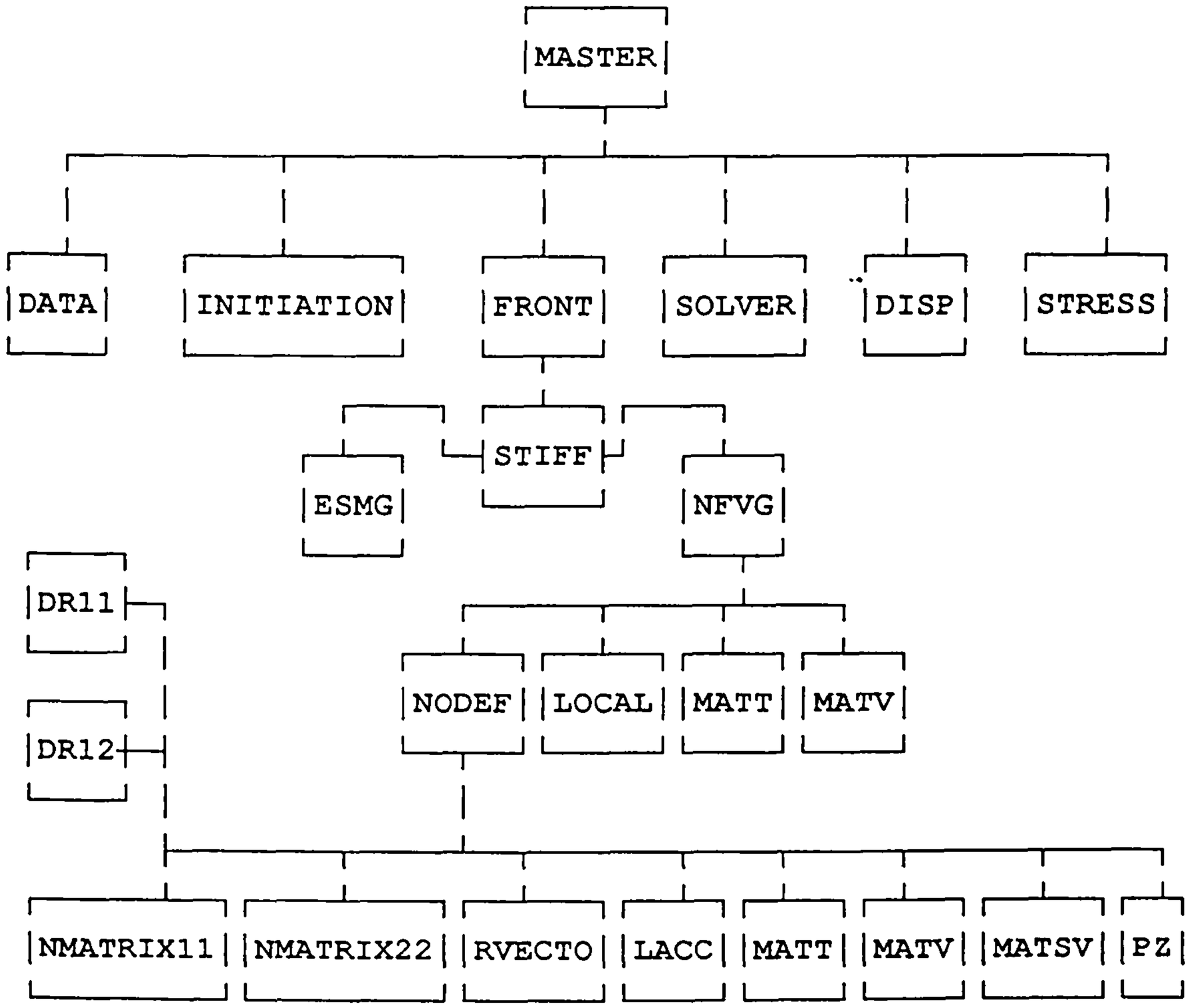

FIG.8.4 LINE DIGRAM FOR STATIC ANALYSIS USING A FRONTAL SOLVER.

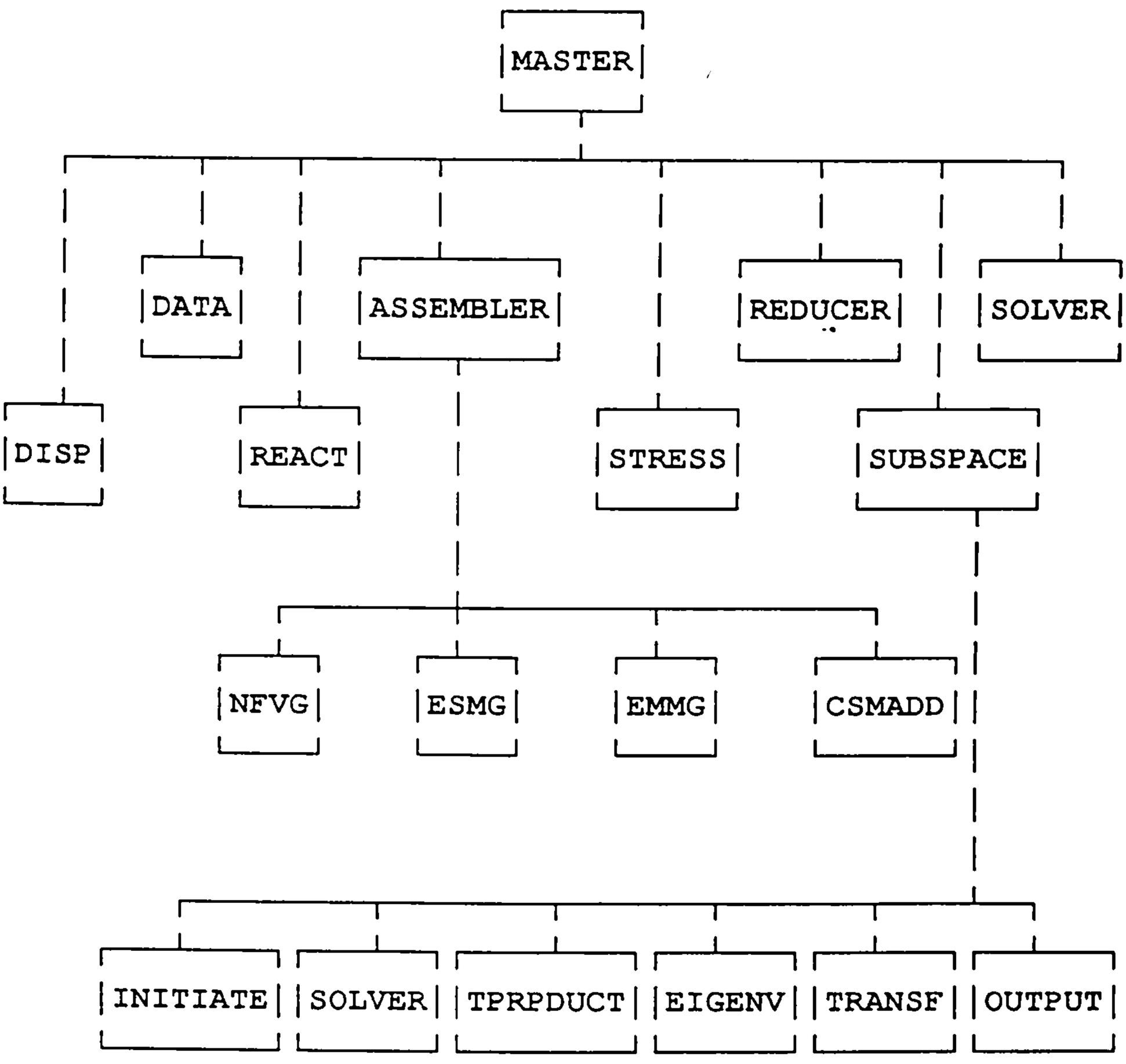

FIG.8.5 LINE DIAGRAM FOR DYNAMIC ANALYSIS USING AN ORDINARY SOLVER.

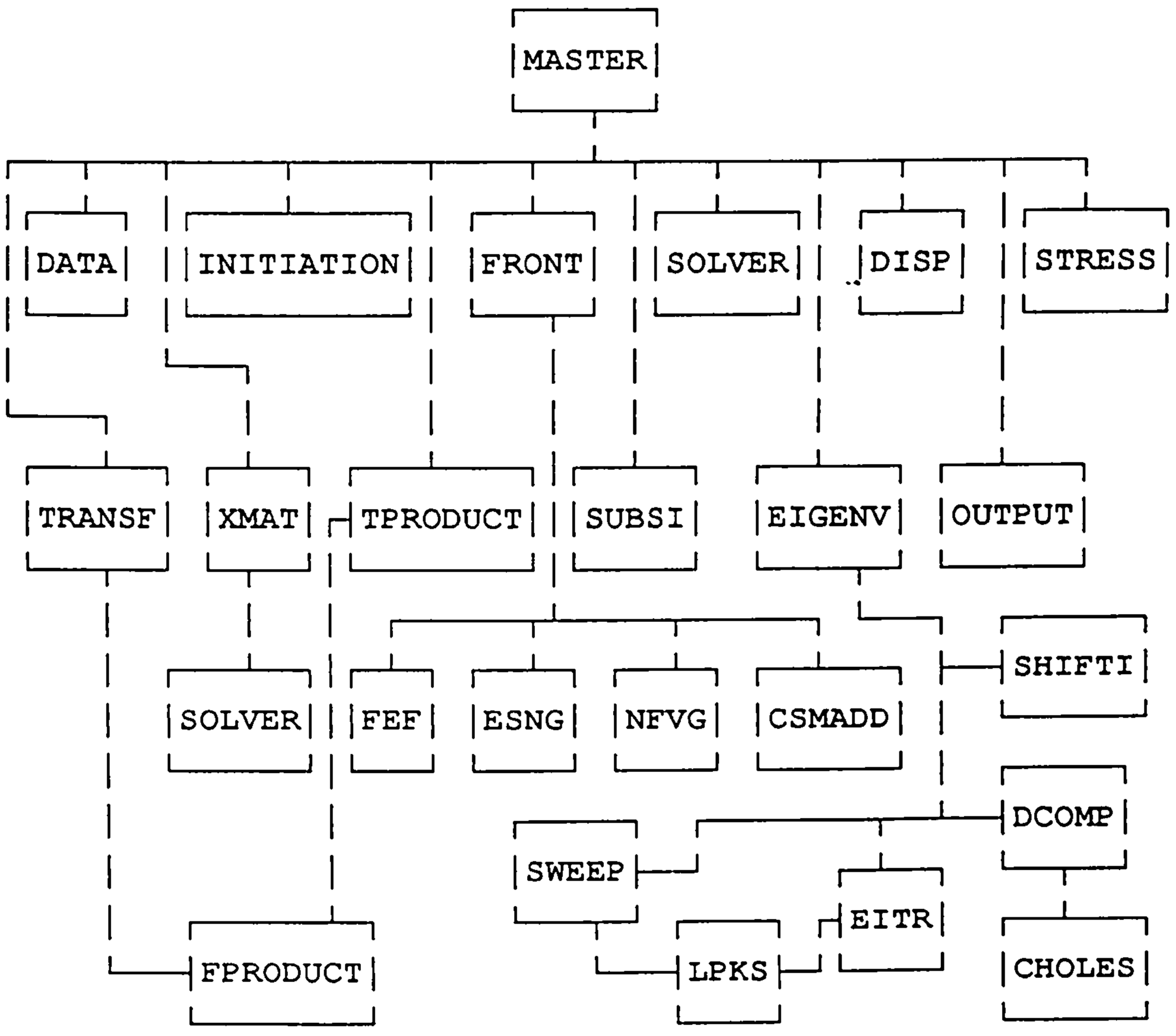

FIG.8.6 LINE DIAGRAM FOR DYNAMIC ANALYSIS USING A FRONTAL SOLVER.

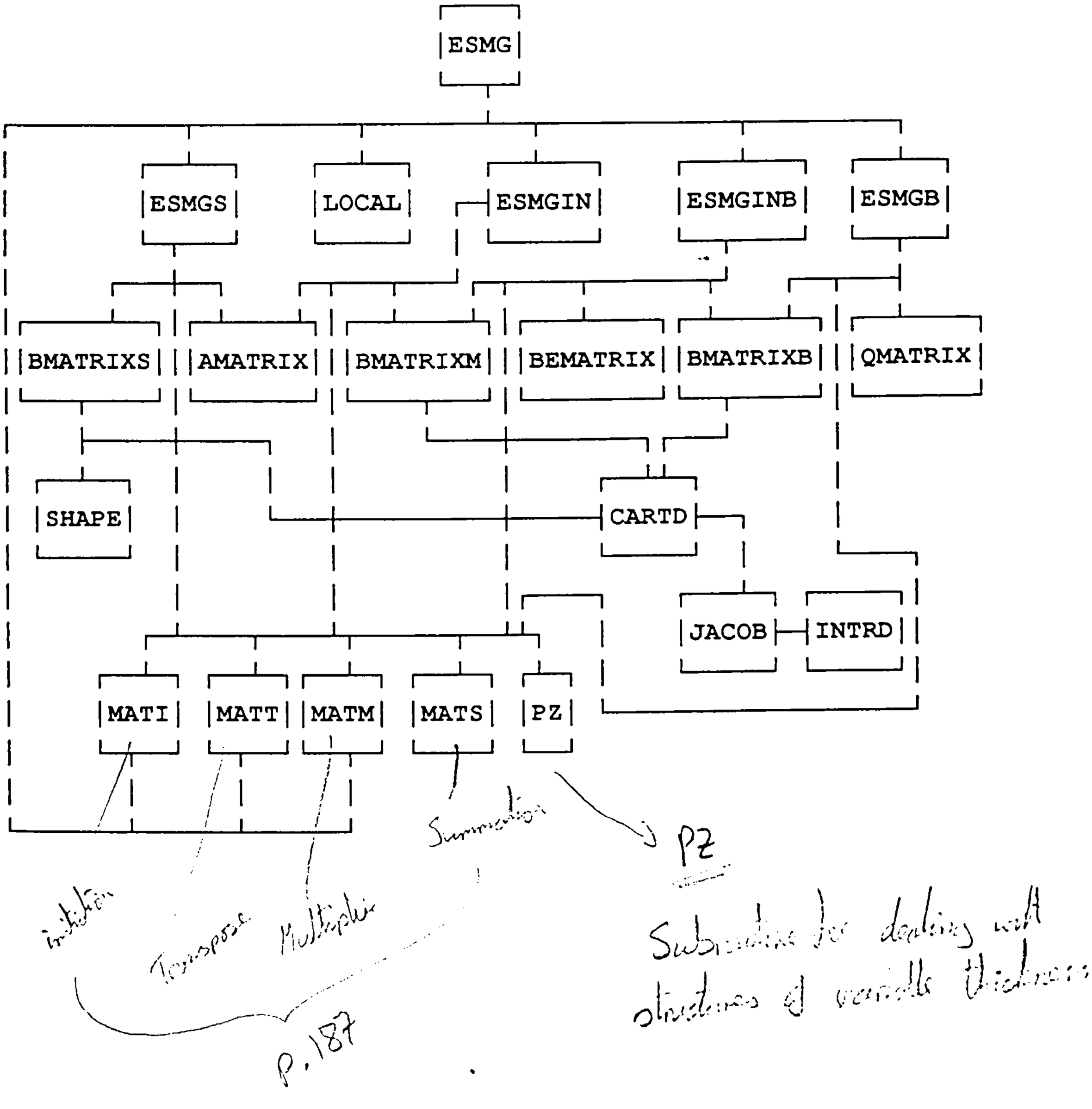

FIG 8.7 LINE DIAGRAM OF ELEMENT STIFFNESS MATRIX GENERATOR USING FIRST ORDER FACET SHELL ELEMENTS.

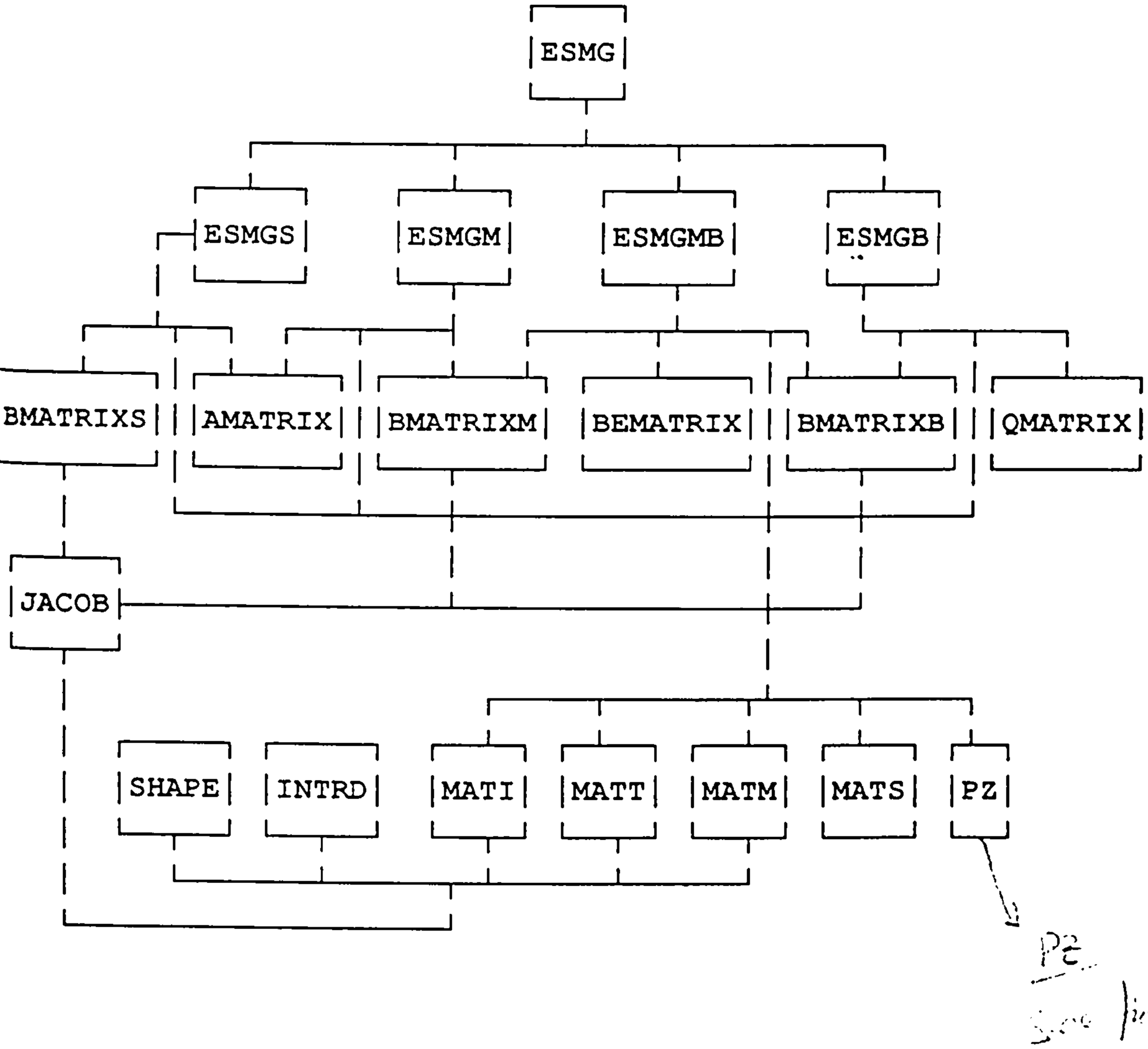

FIG.8.8 LINE DIAGRAM OF ELEMENT STIFFNESS MATRIX GENERATOR USING FIRST ORDER CURVED SHELL ELEMENTS.

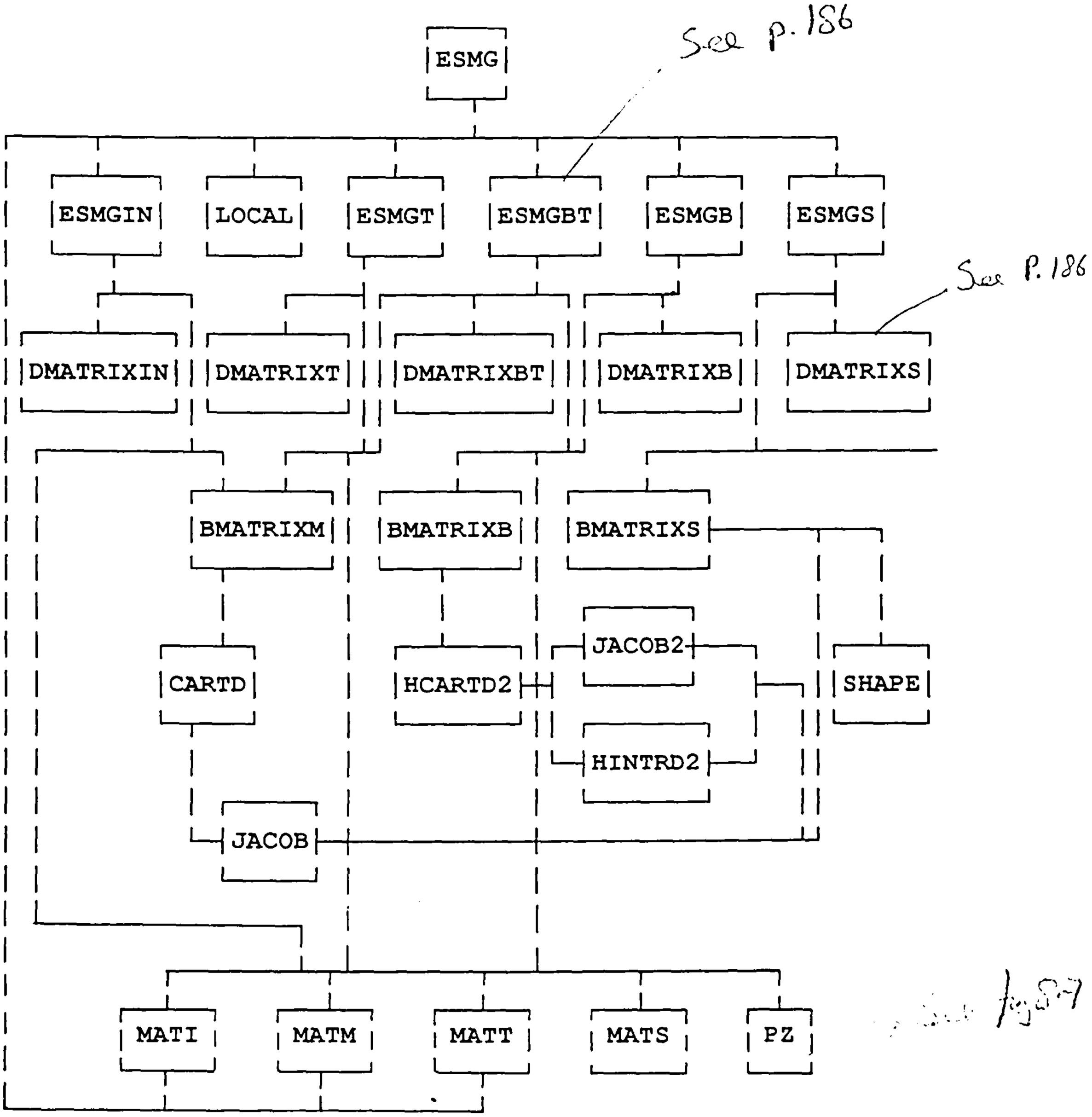

FIG.8.9 LINE DIAGRAM FOR ELEMENT STIFFNESS MATRIX GENERATOR USING HIGH ORDER FACET SHELL ELEMENTS.

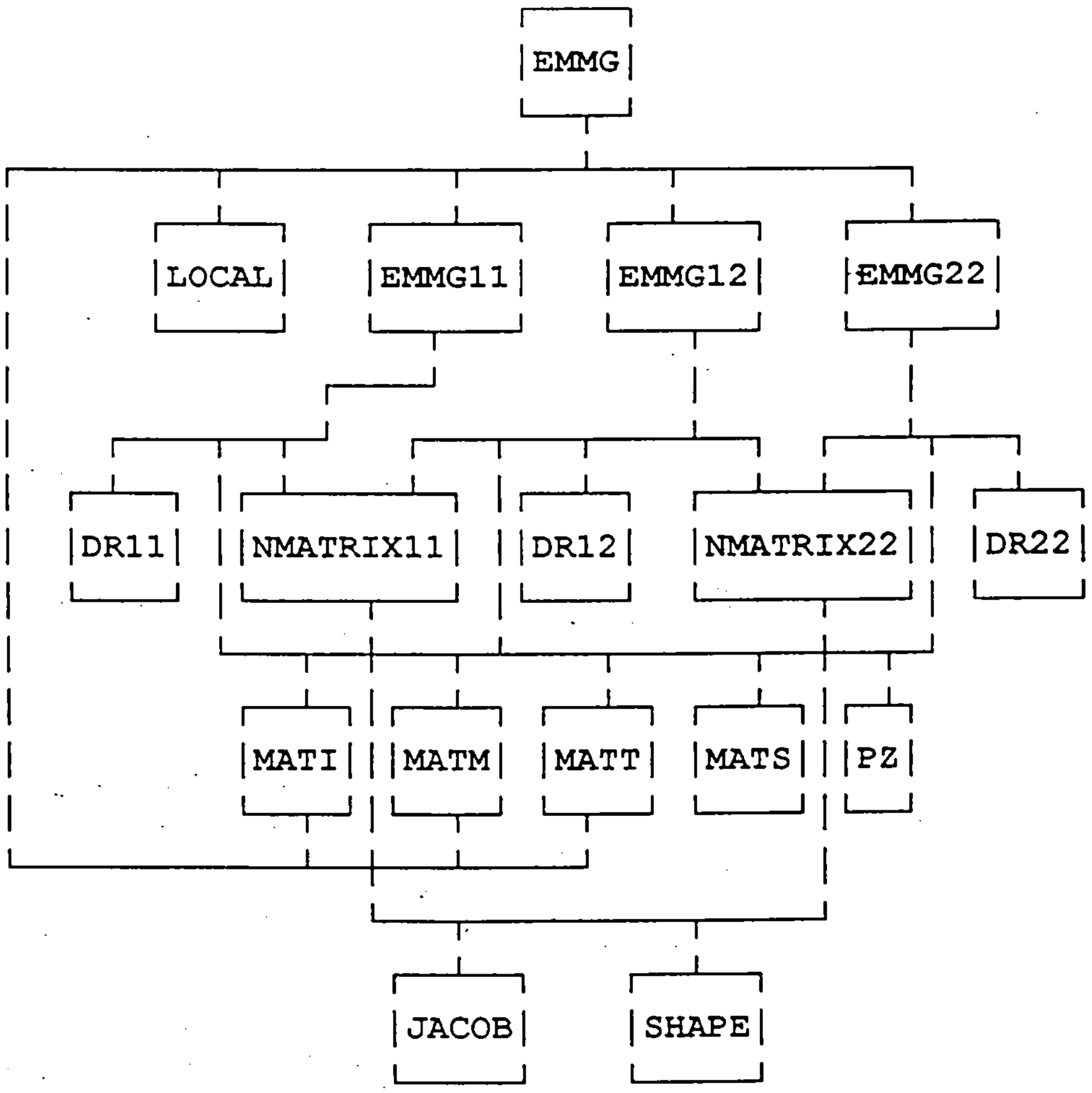

FIG.8.10 LINE DIAGRAM OF ELEMENT MASS MATRIX GENERATOR USING FIRST ORDER FACET SHELL ELEMENTS.

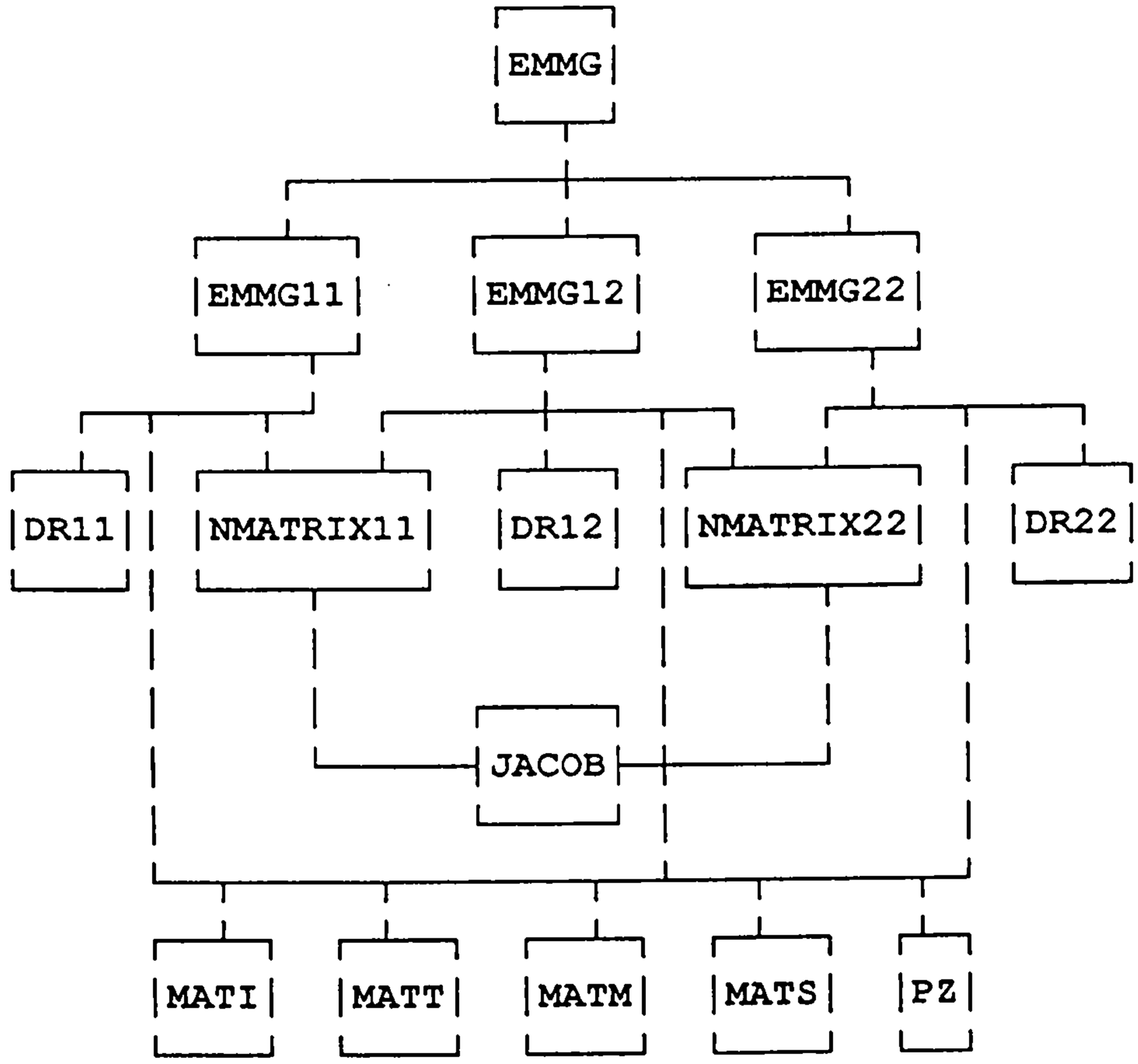

FIG.8.11 LINE DIAGRAM OF ELEMENT MASS MATRIX GENERATOR USING FIRST ORDER CURVED SHELL ELEMENTS.

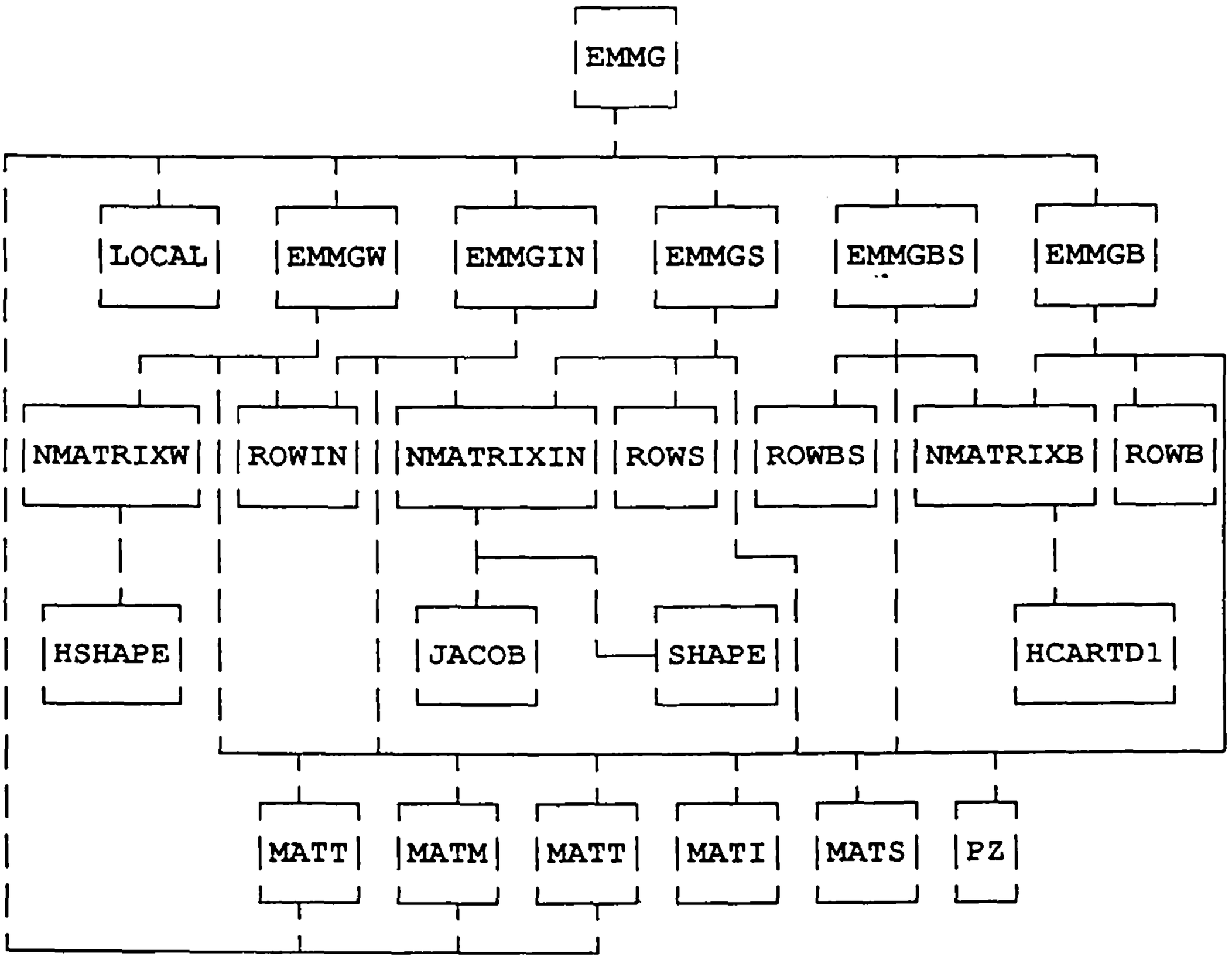

FIG.8.12 LINE DIAGRAM OF ELEMENT MASS MATRIX GENERATOR USING HIGH ORDER FACET SHELL ELEMENTS.

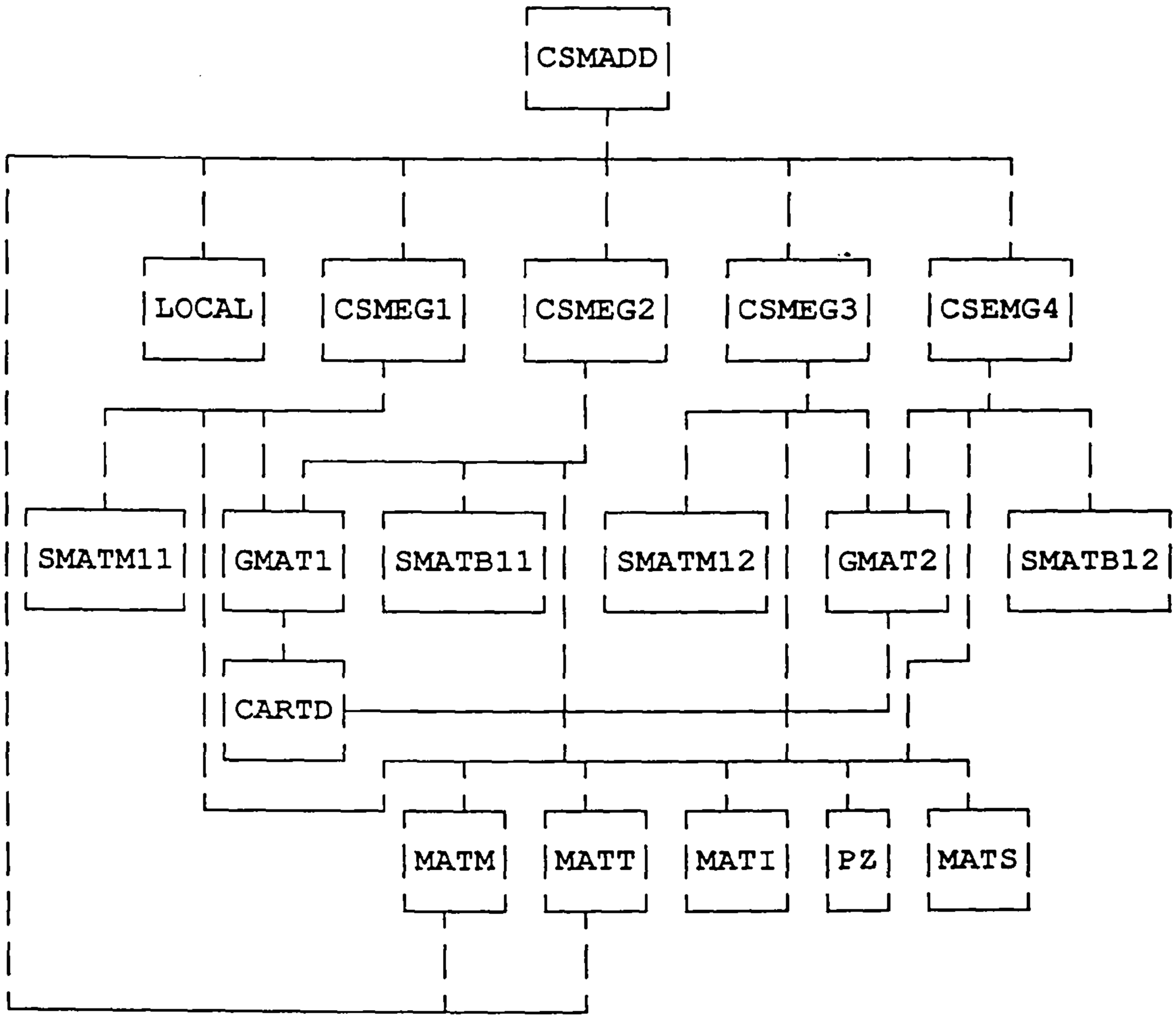

FIG.8.13 LINE DIAGRAM OF ELEMENT CENTRIFUGAL STIFFNESS MATRIX GENERATOR USING FIRST ORDER FACET SHELL ELEMENT.

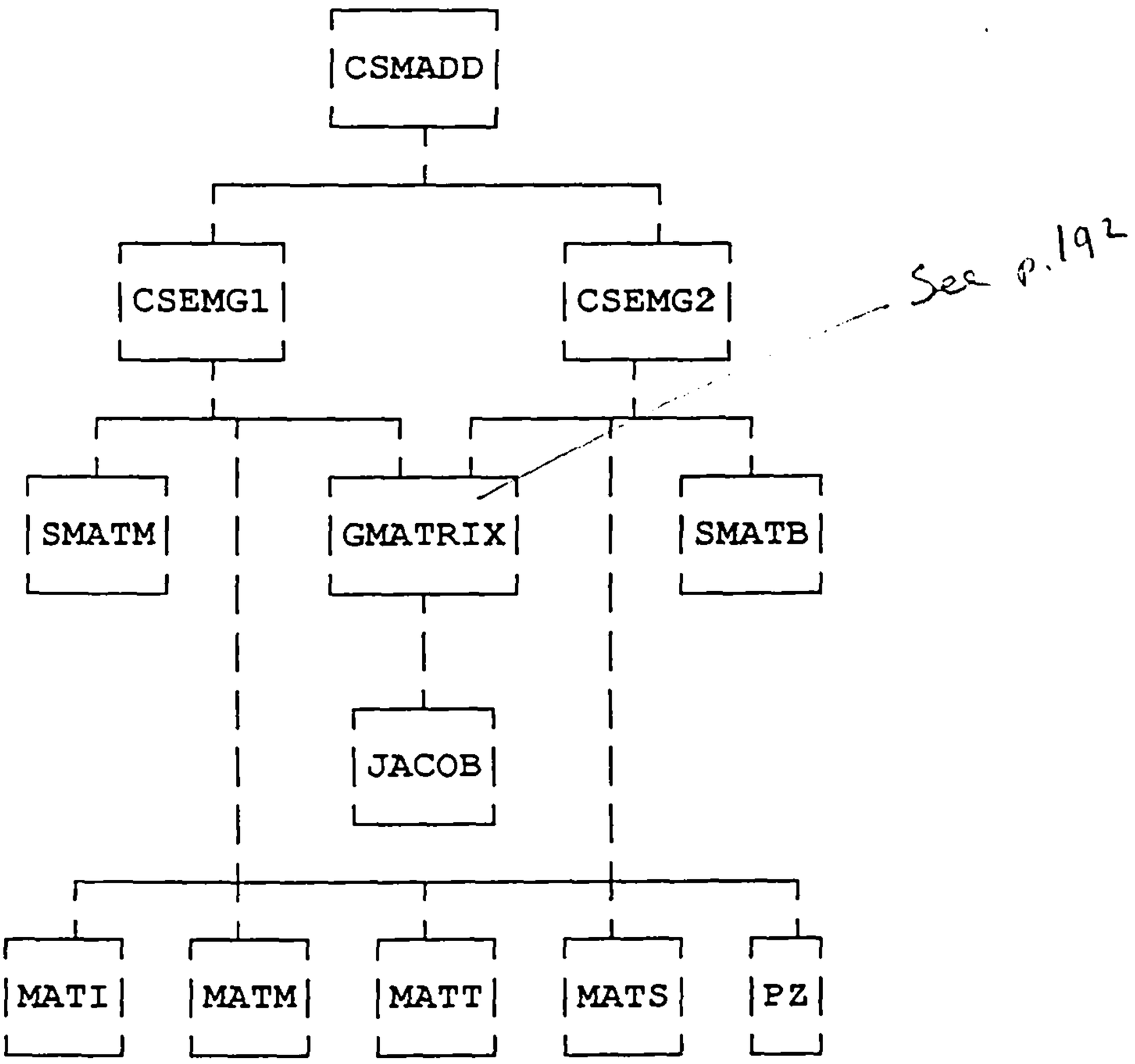

FIG.8.14 LINE DIAGRAM OF ELEMENT CENTRIFUGAL STIFFENING GENERATOR USING FIRST ORDER CURVED SHELL ELEMENTS.

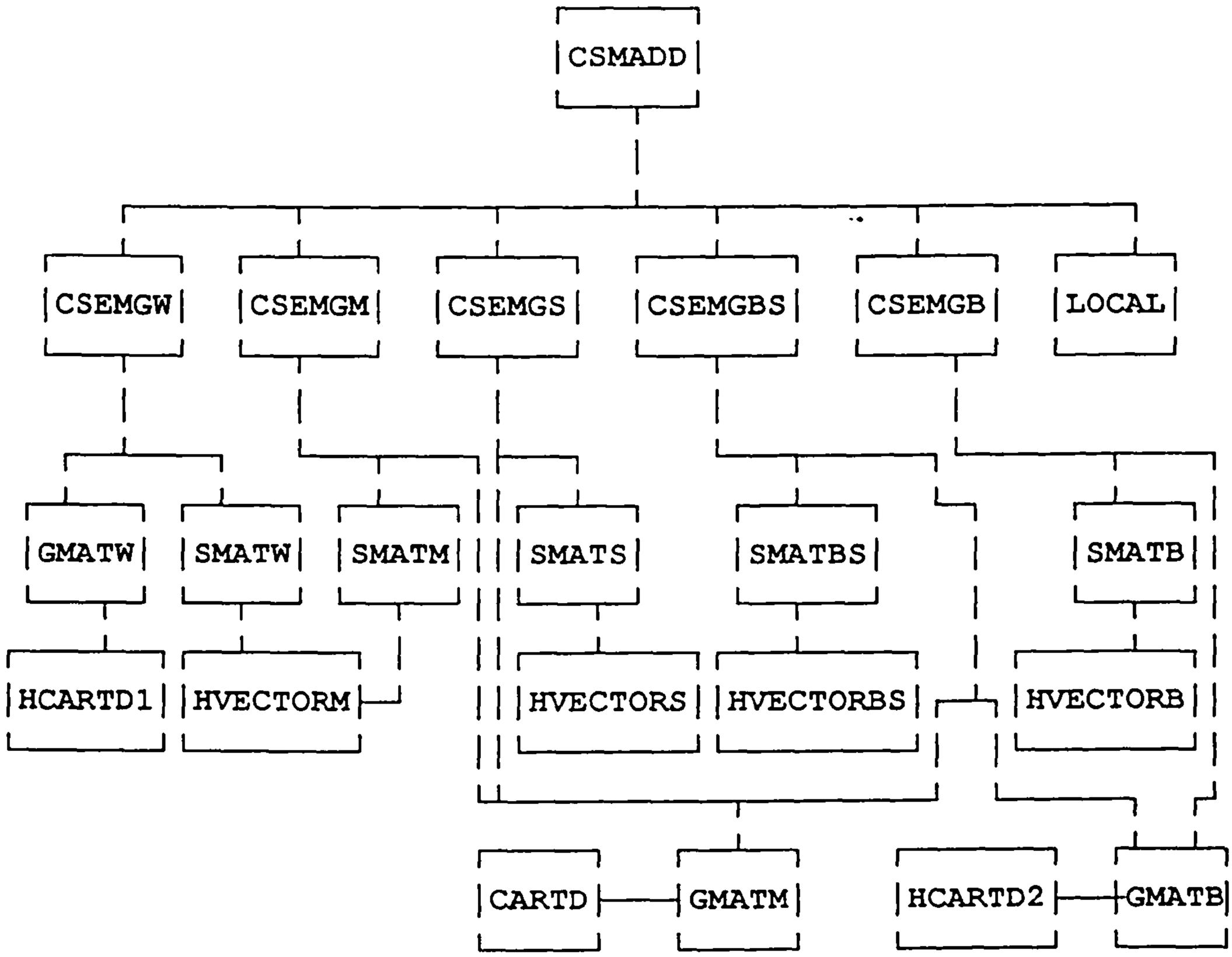

FIG.8.15 LINE DIAGRAM OF ELEMENT CENTRIFUGAL STIFFNESS MATRIX USING HIGHER ORDER FACET SHELL ELEMENTS.

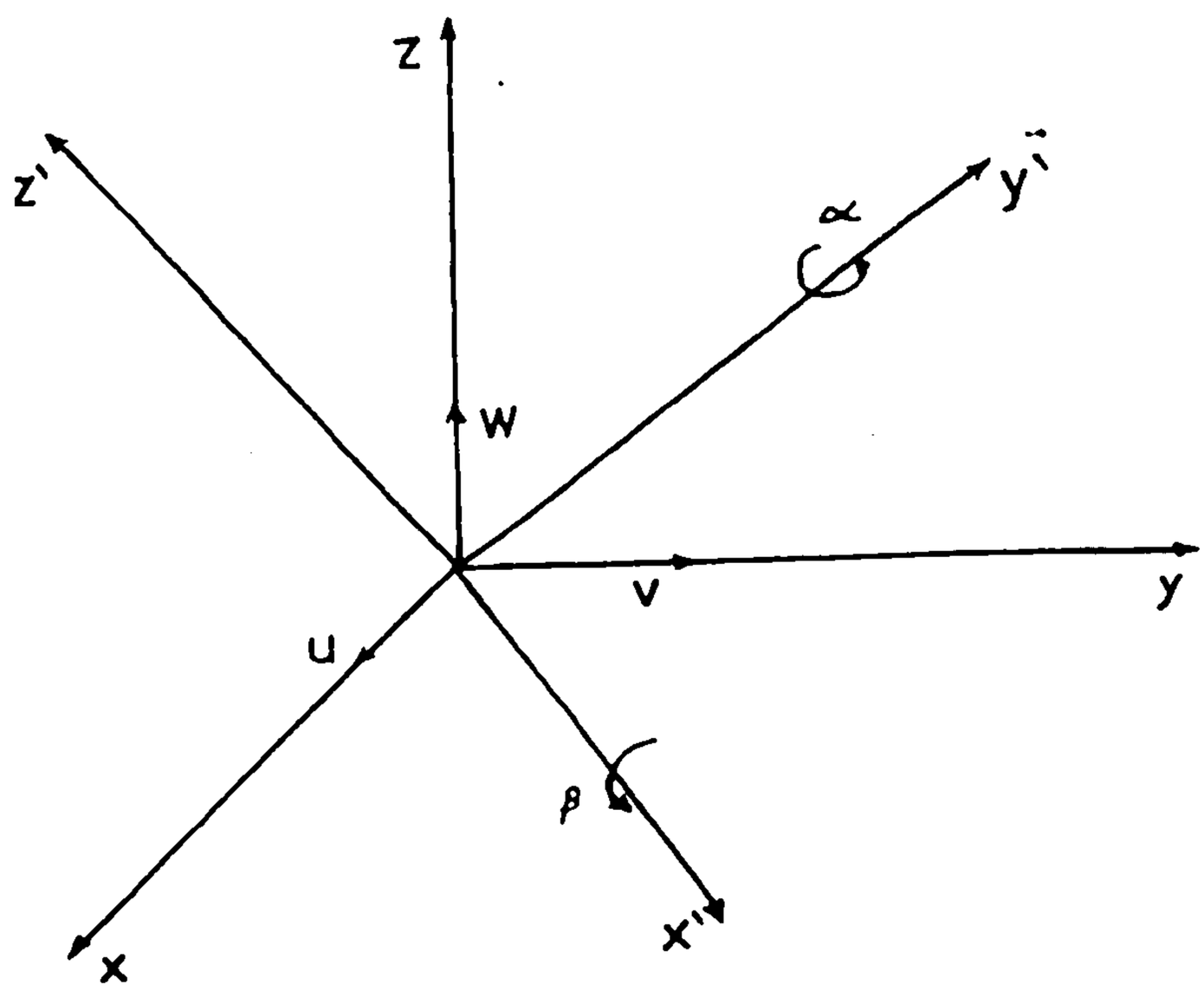

Figure 8.16 Local and Global Axis

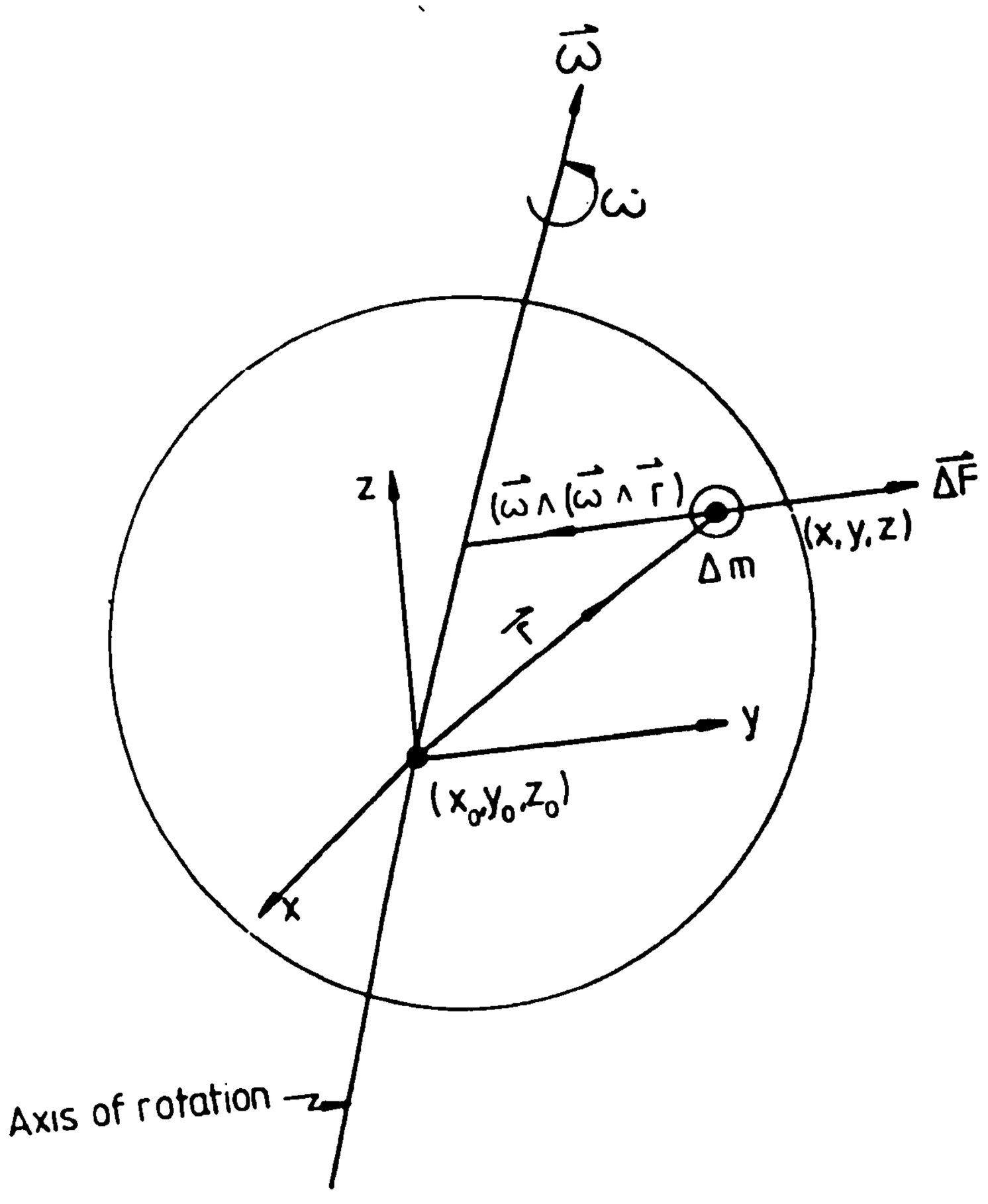

FIGURE 8.17 FORCE DUE TO ROTATIONAL INERTIA.

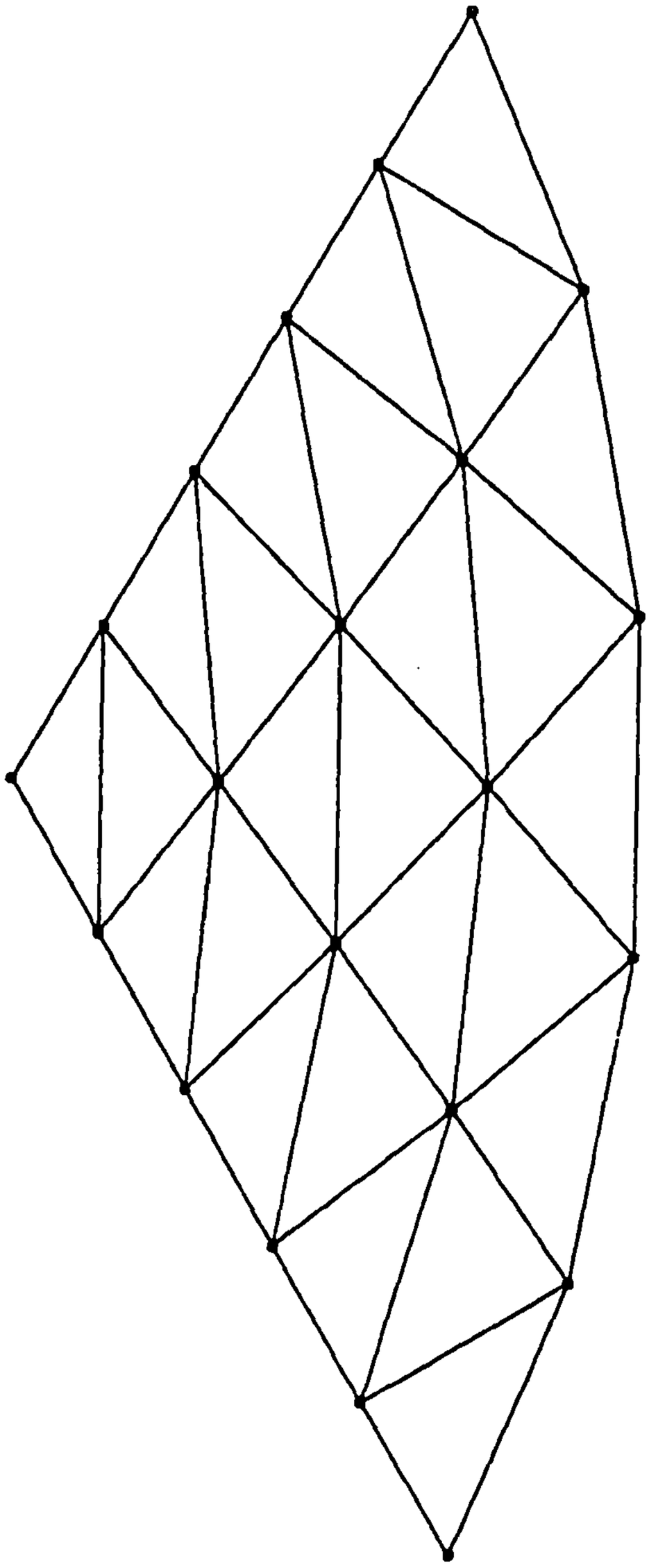

ABES Package
Run on 12-SEP-1989 14:37:59

Z
Y
X

Fig.9.1 3-D Mesh Generation, Using 3-Noded Triangular Element, For The Disc Analysis.

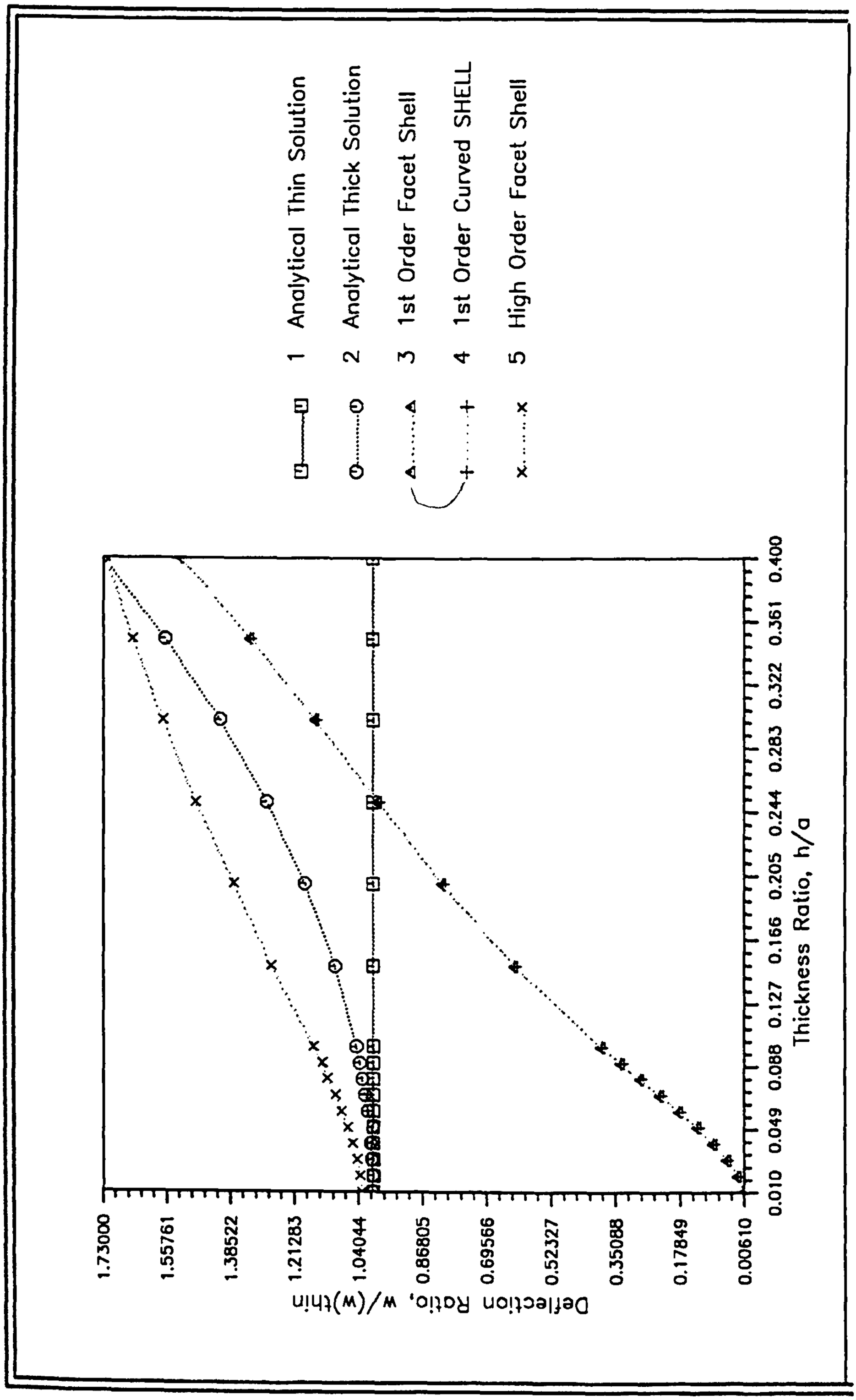

Fig.9.2 Deflection Analysis For A Clamped Disc Under Uniformly Distributed Loading.

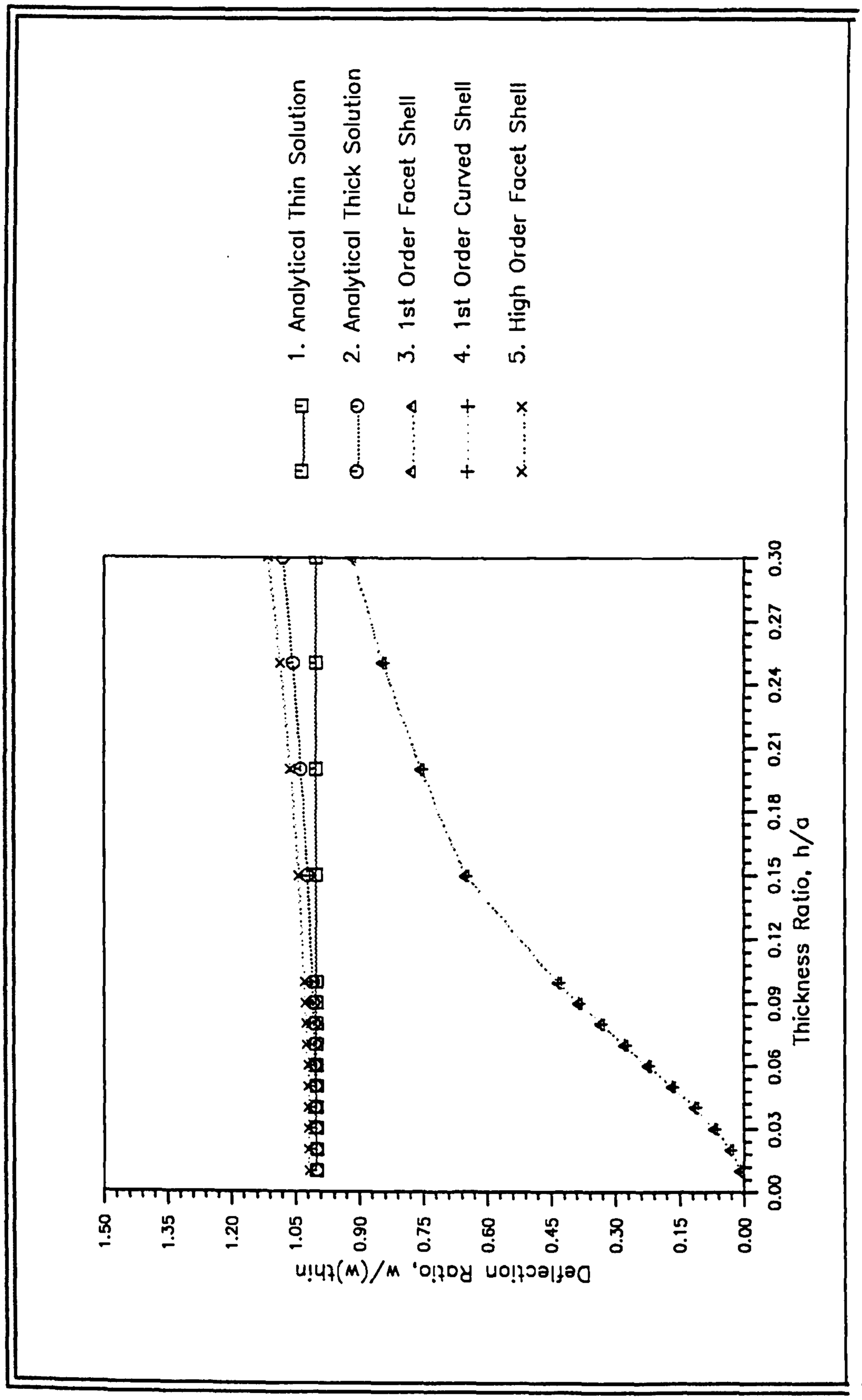

Fig.9.3 Deflection Analysis For A Simply Supported Disc Under Uniformly Distributed Loading

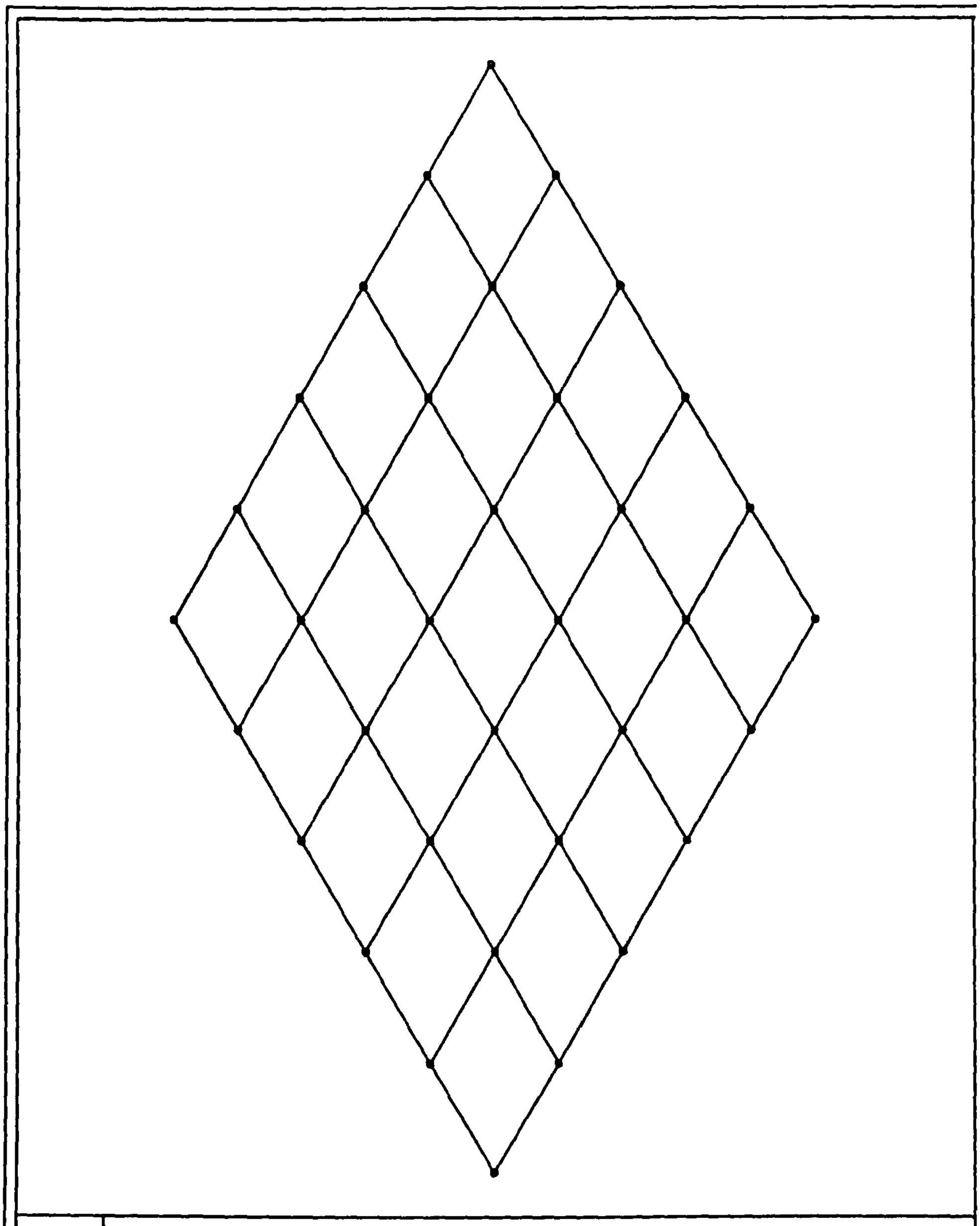

Fig.9.4 3-D Mesh Generation, Using 4-Noded Quadrilateral Element, For The Rectangular Plate Analysis.

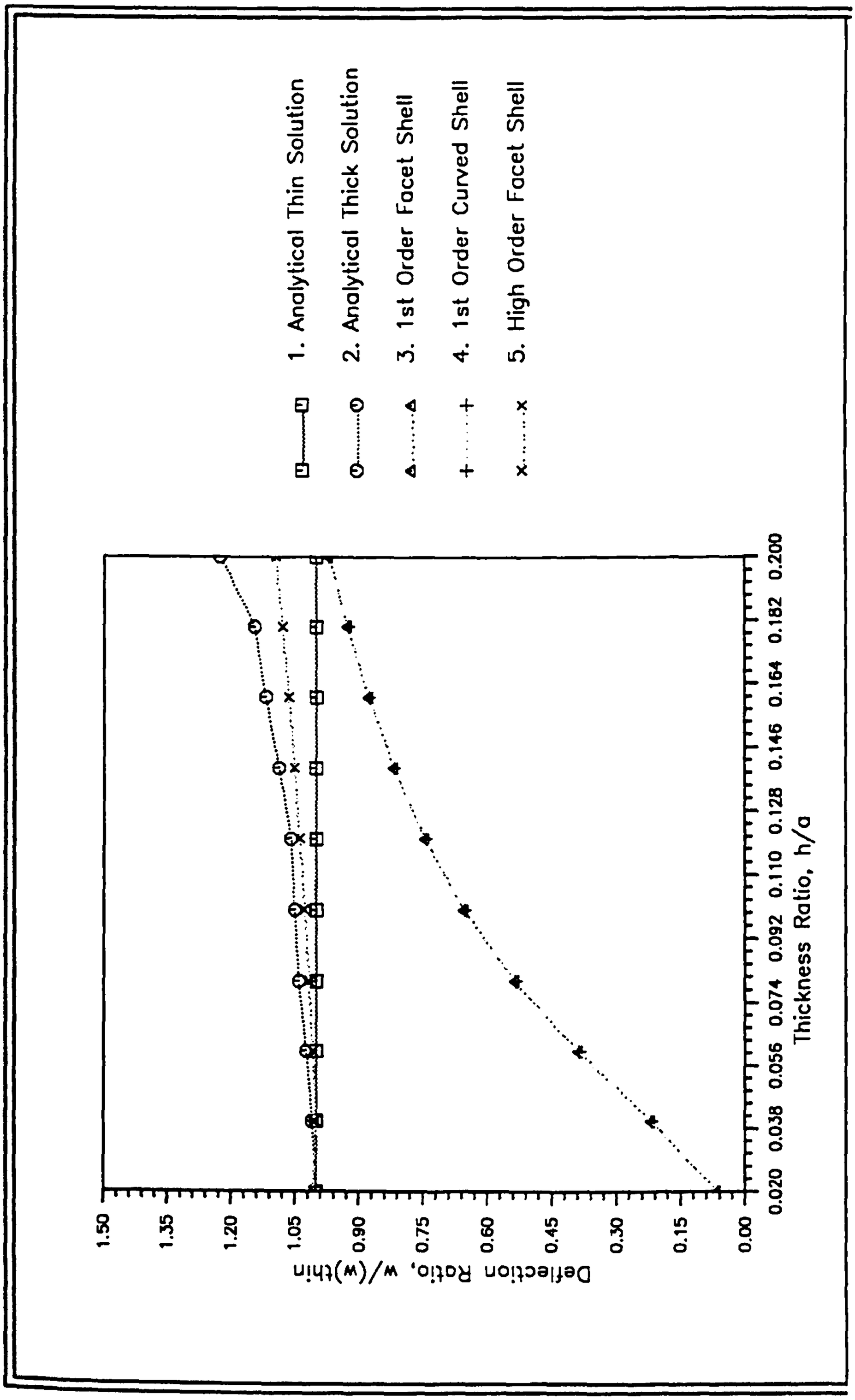

Fig.9.5 Deflection Analysis Of Simply Supported Rectangular Plate Under Uniformly Distributed Loading.

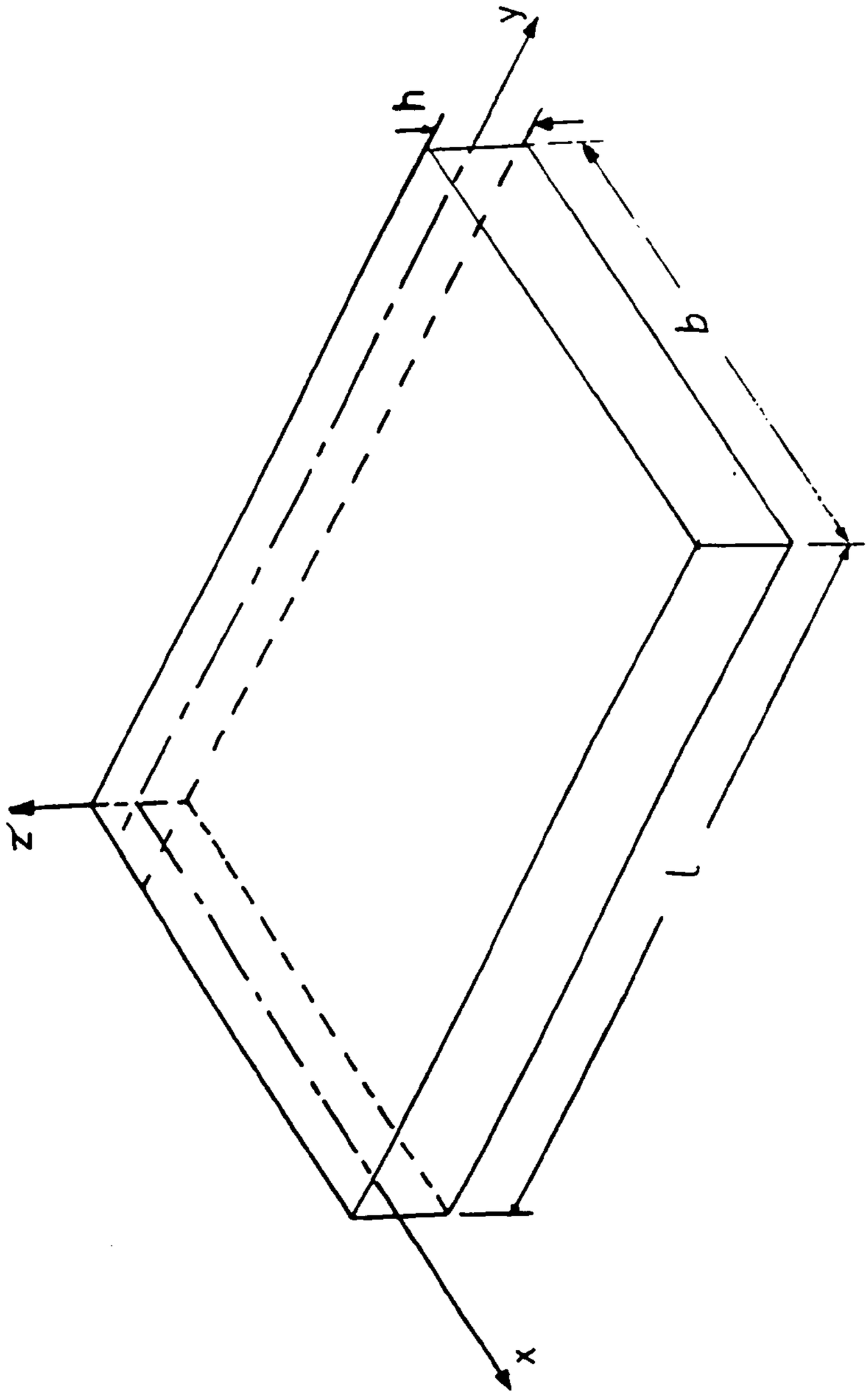

Fig.9.6 Cantilever Plate Used For Package Verification.

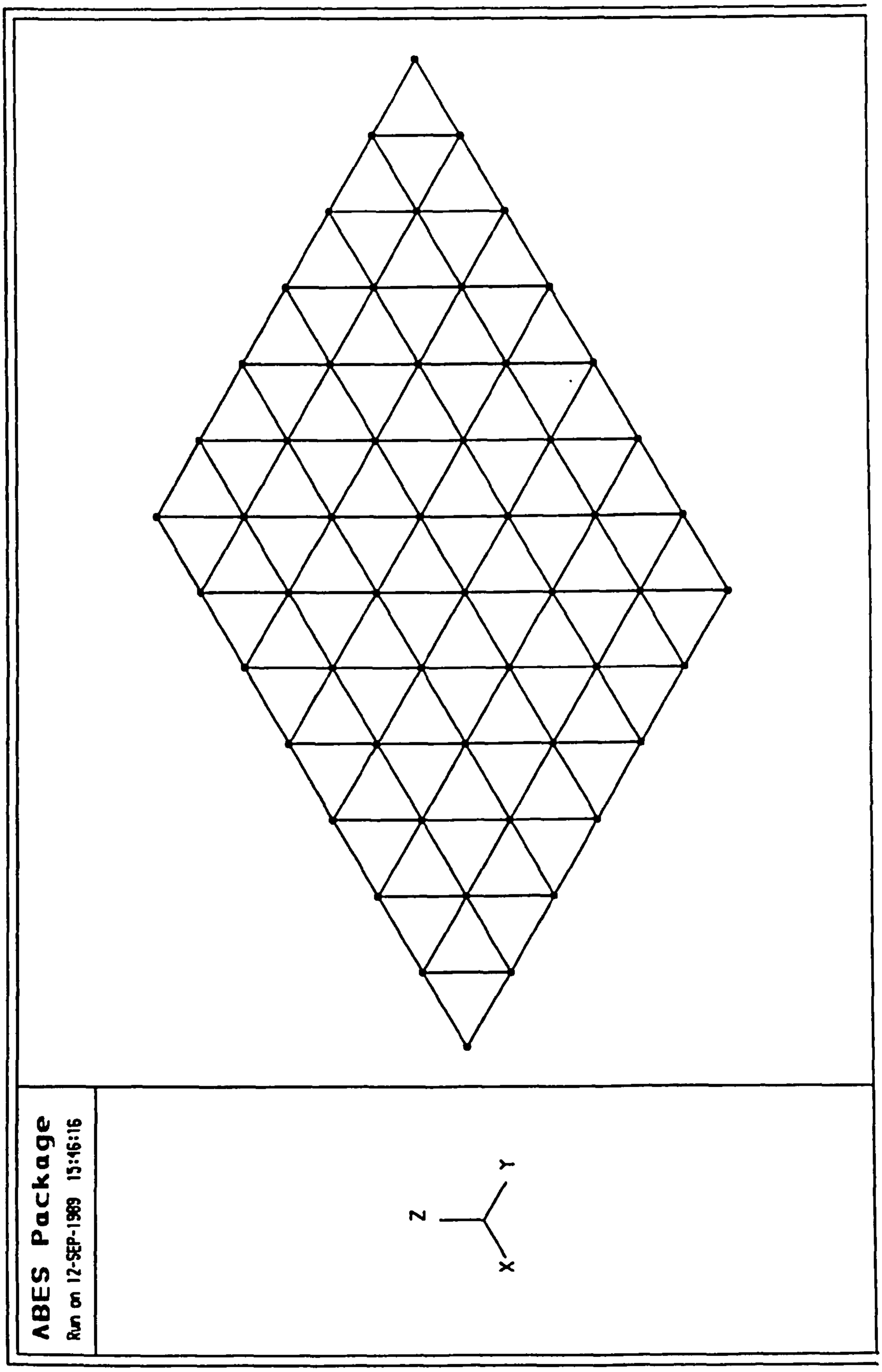

Fig.9.7 3-D Mesh Generated, Using 3-Noded Triangular Elements, For The Analysis Of Cantilever Plate.

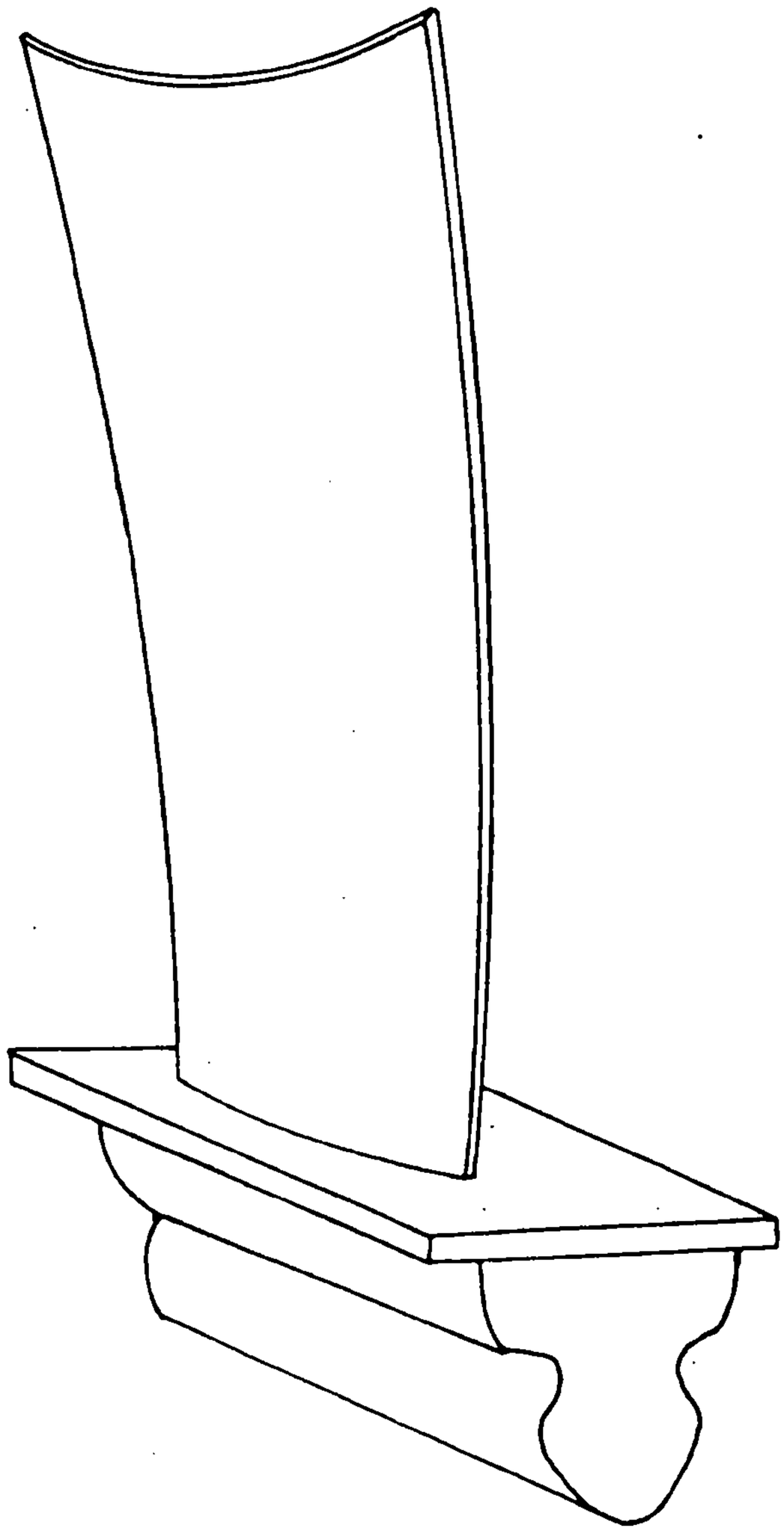

Fig.9.8 A typical turbomachine blade.

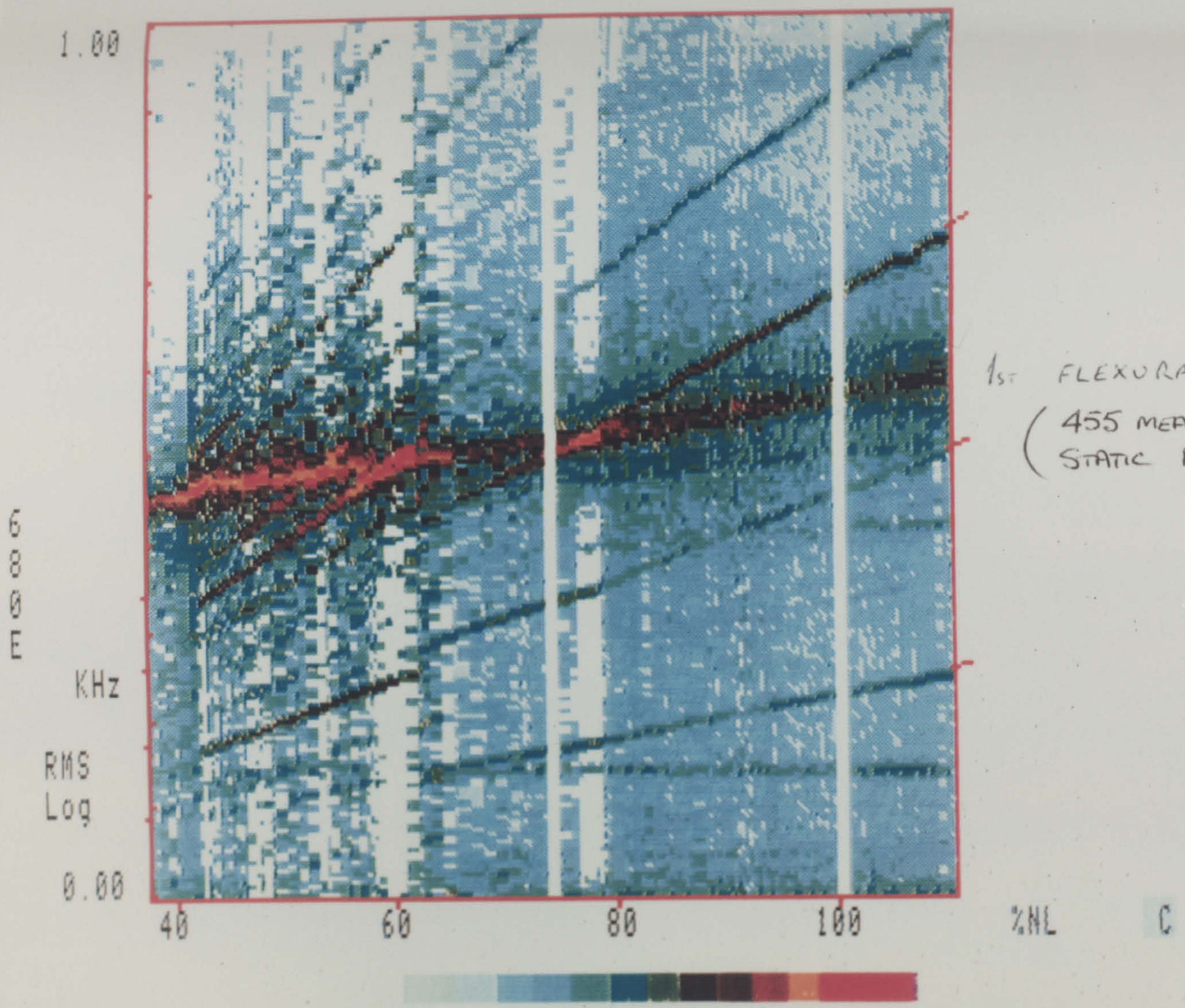

1ST FLEXURAL (1F)
(455 MEASURED STATIC FREQ.)

Fig.9.9 Frequency vs Speed Plot Showing Natural Frequencies of RR Isotropic Blade(0 to 1 KHZ)

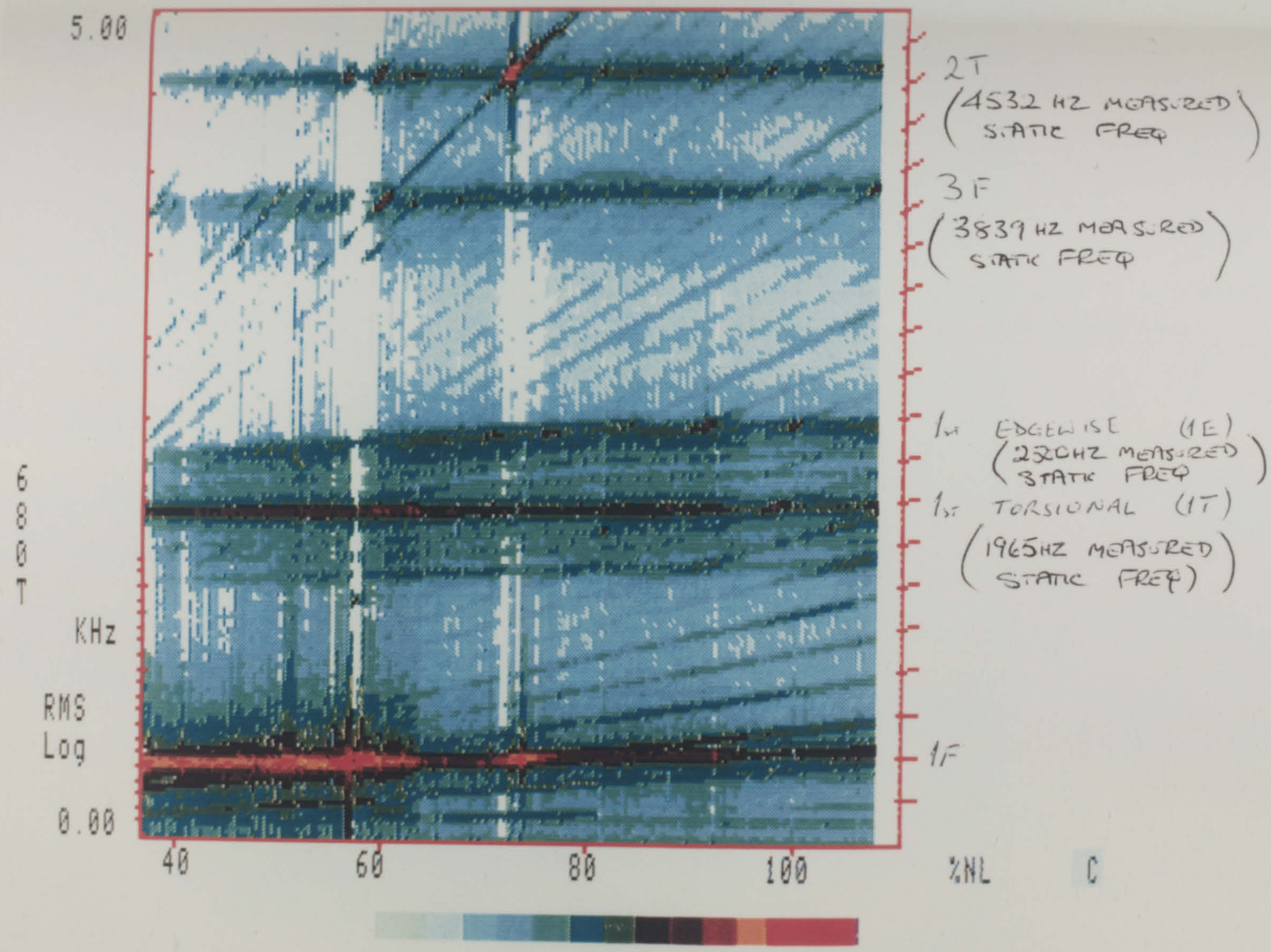

Fig.9.10 Frequency vs Speed Plot Showing Natural Frequencies of RR Isotropic Blade(0 to 5 KHZ)

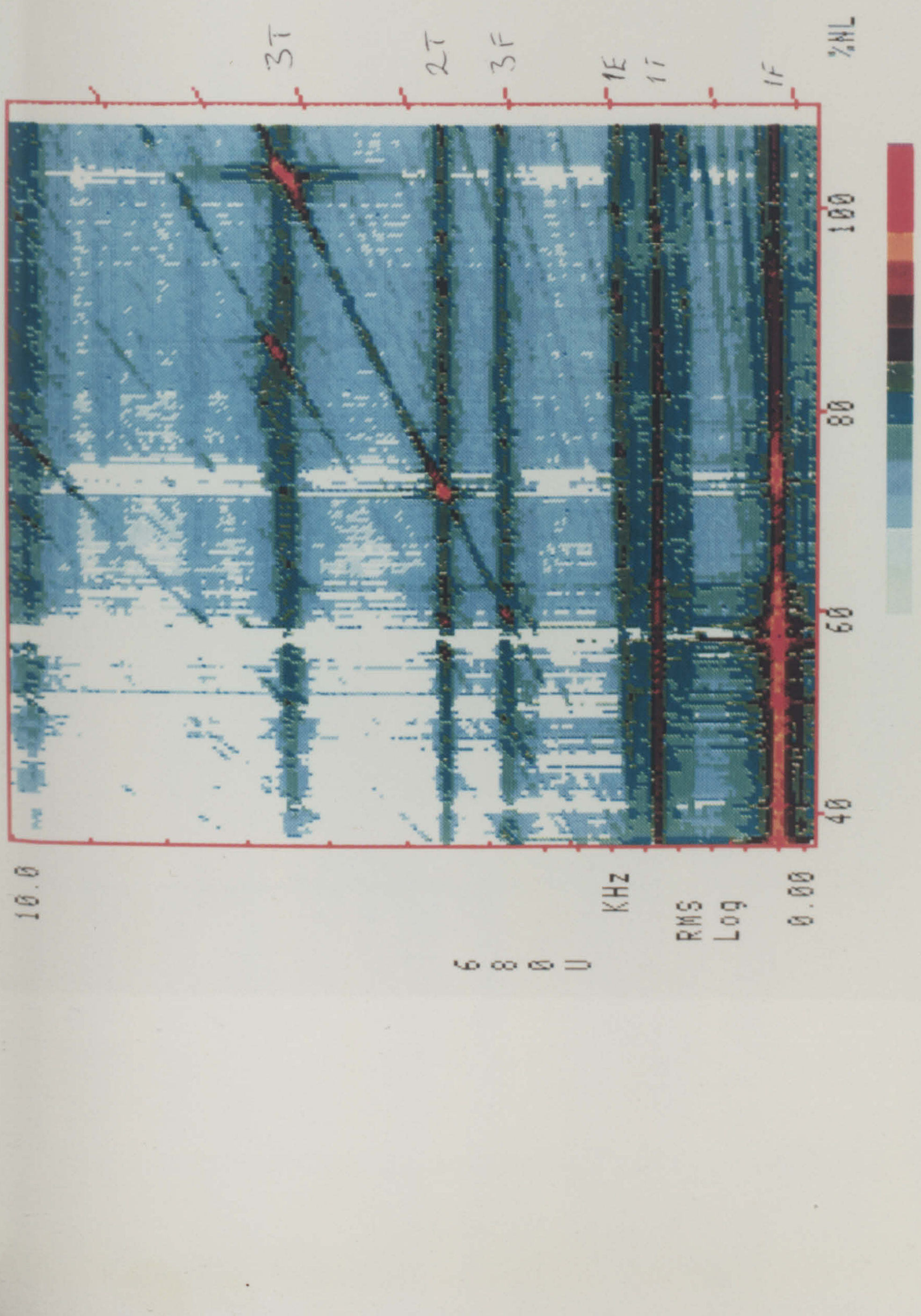

Frequency vs Speed Plot Showing Natural
Frequencies of RR Isotropic Blade(0 to 10 KHZ)

Fig.9.11

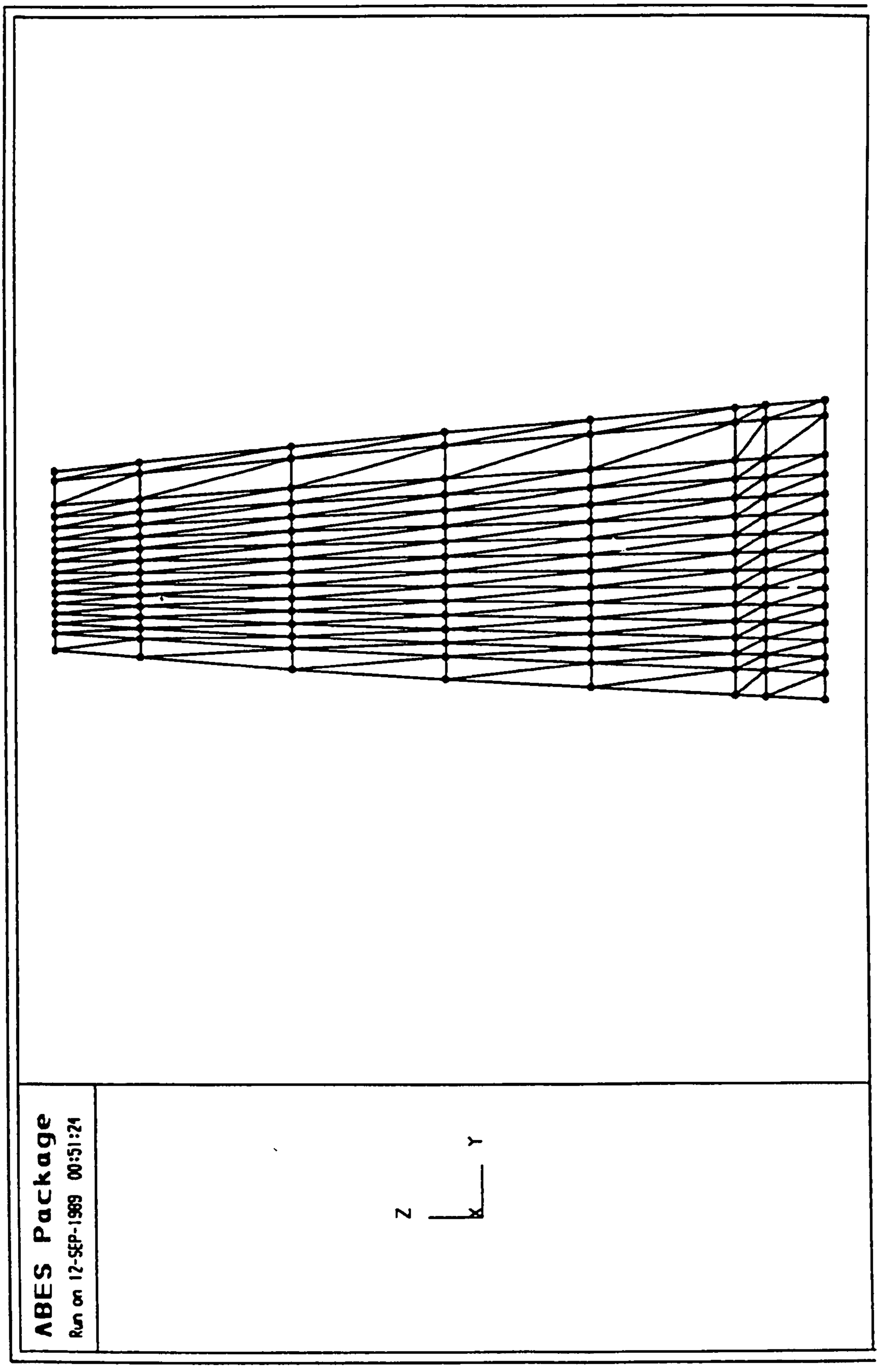

Fig.9.12 2-D Mesh Generated, Using 3-Noded Triangular Elements, For The Analysis Of RR Isotropic Blade.

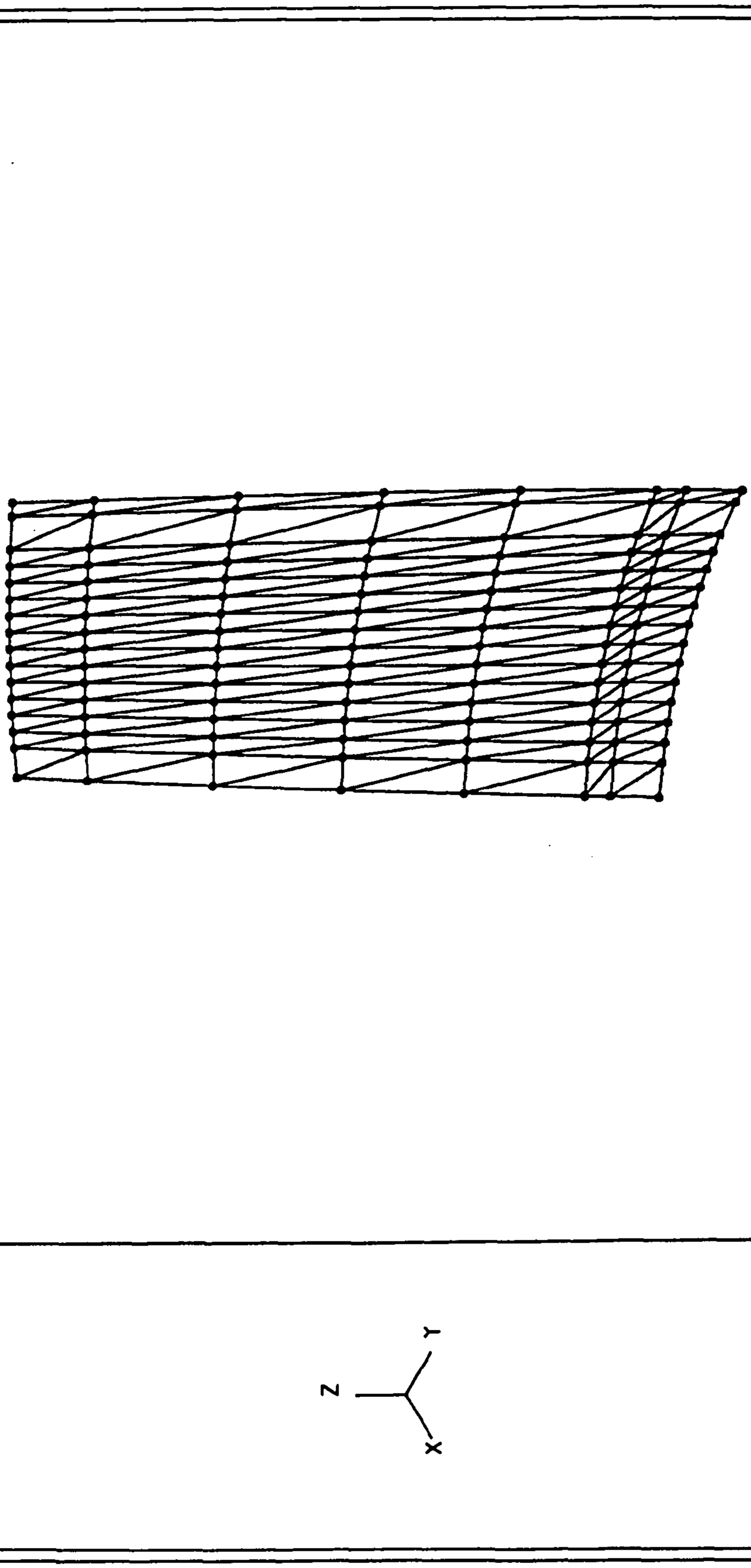

Fig.9.13 3-D Mesh Generated, Using 3-Noded Triangular Elements, For The Analysis of RR Isotropic Blade.

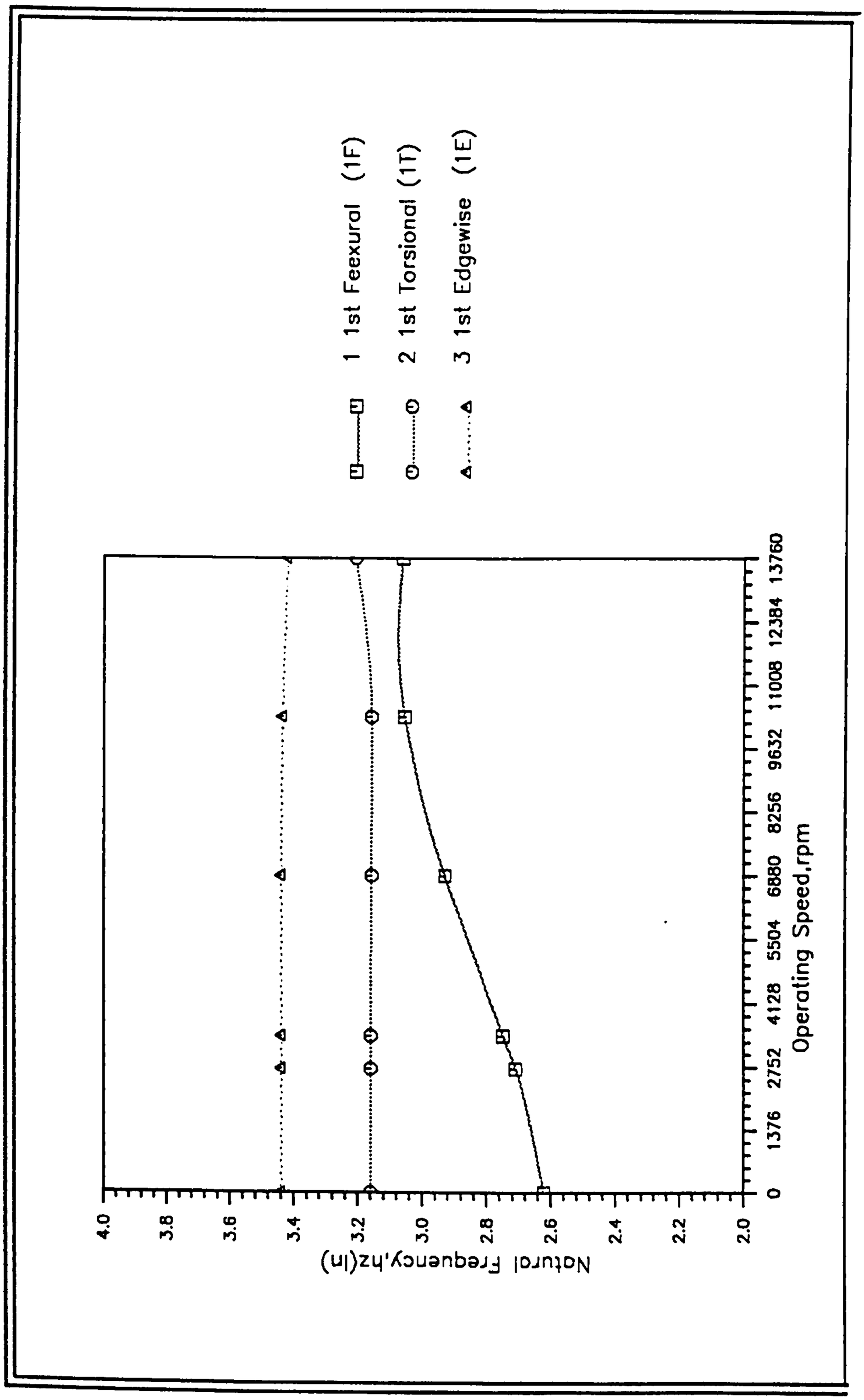

Fig.9.14 Plot Showing Natural Frequency Of Isotropic Blade At Various Speeds.

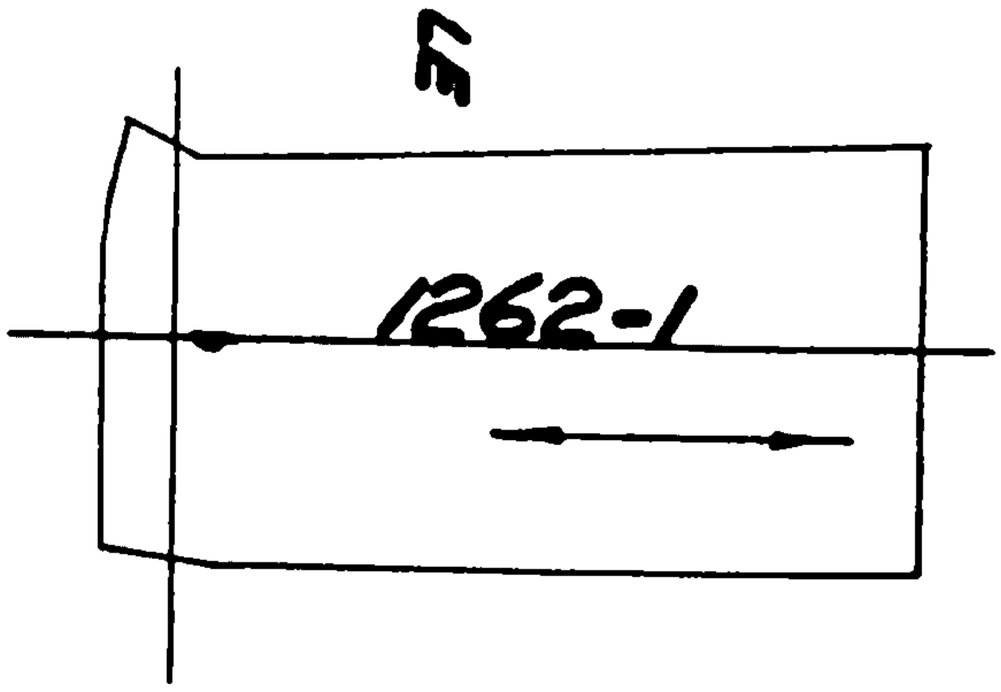

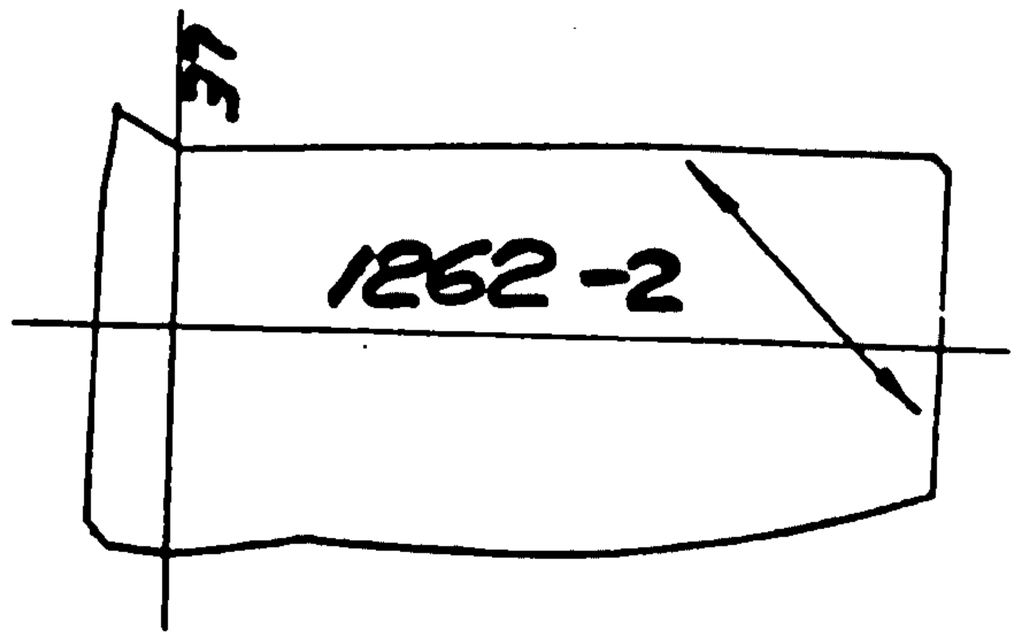

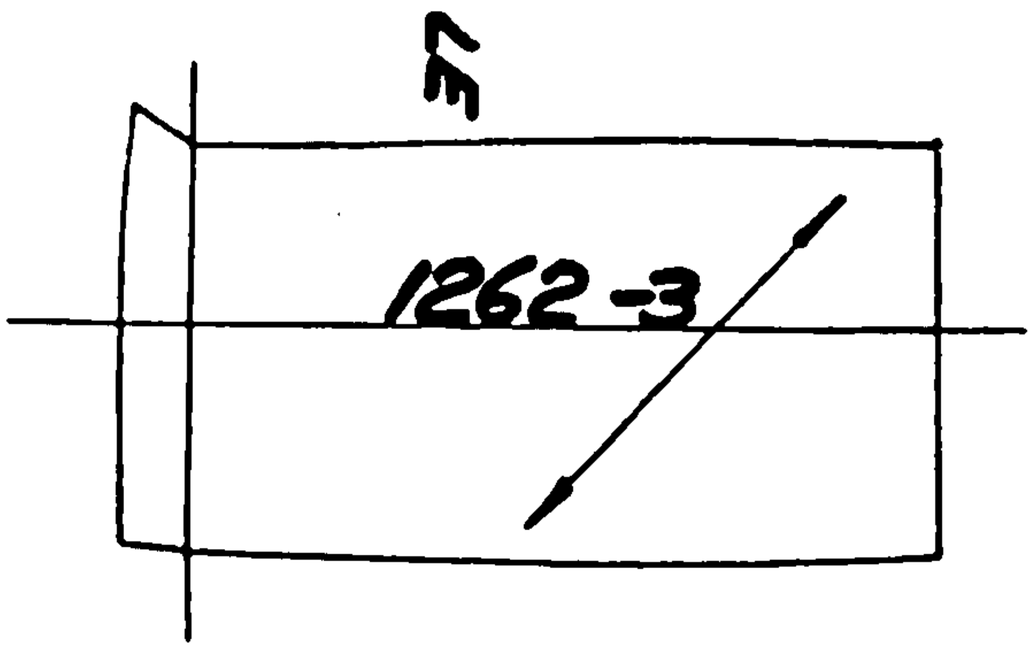

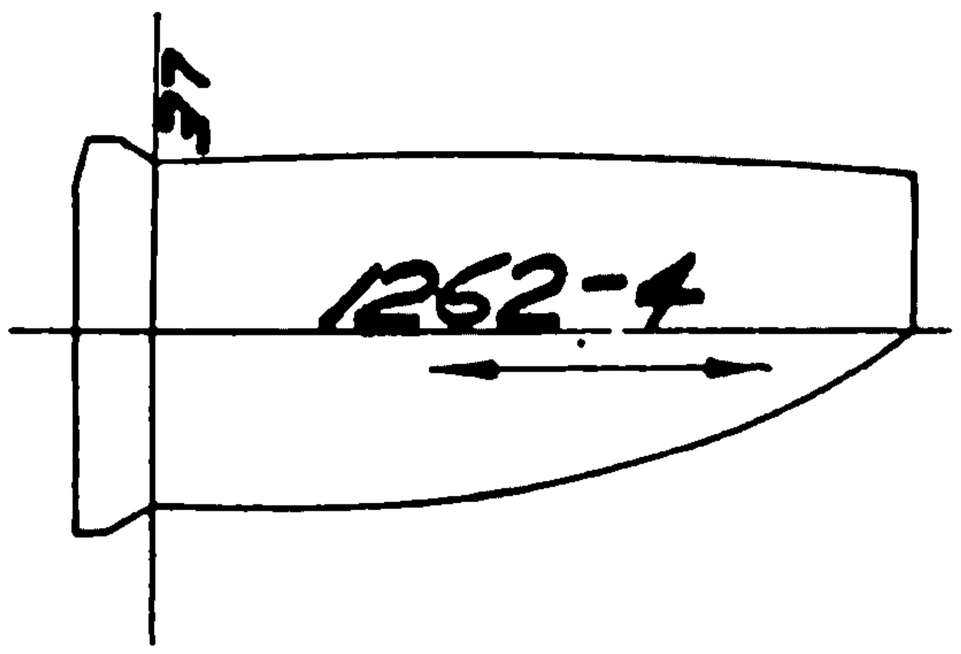

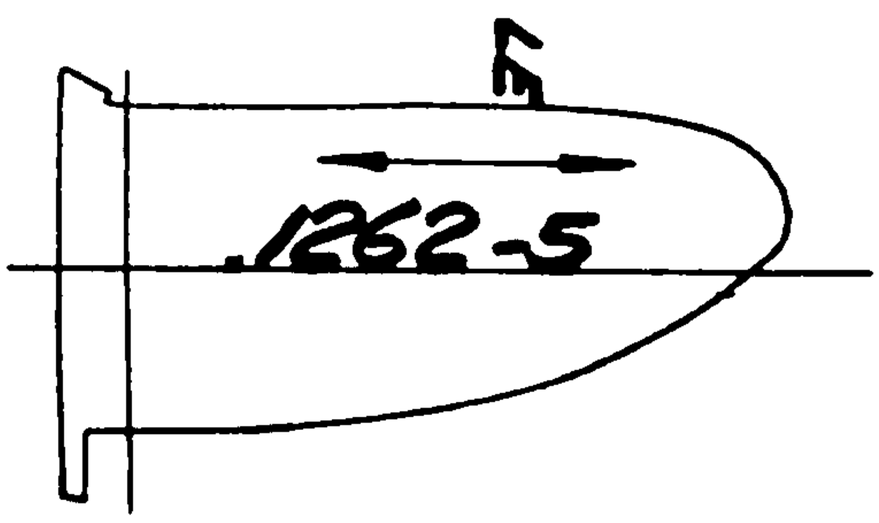

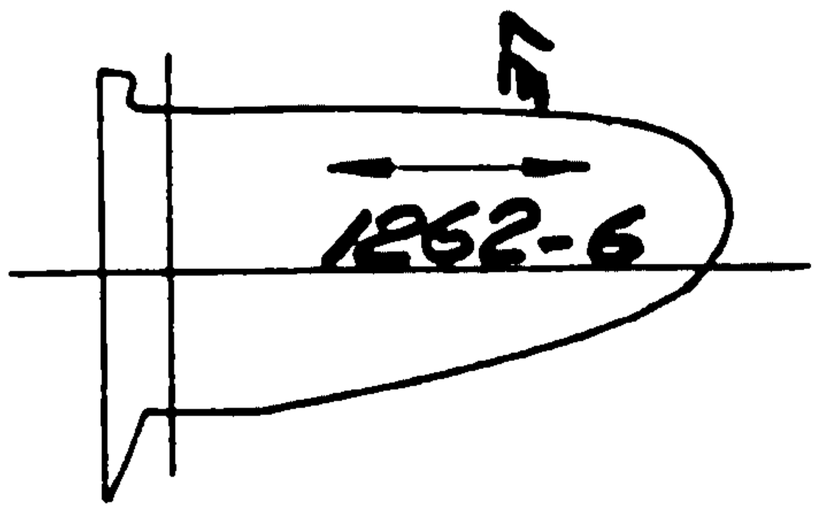

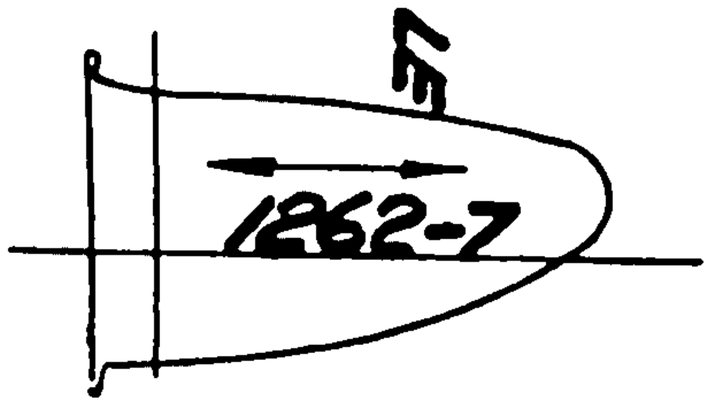

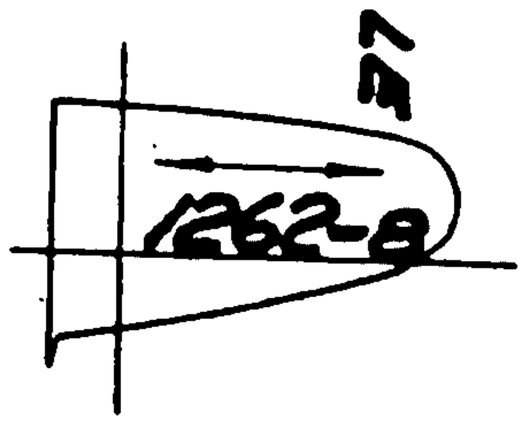

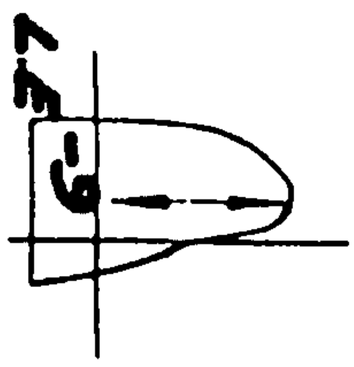

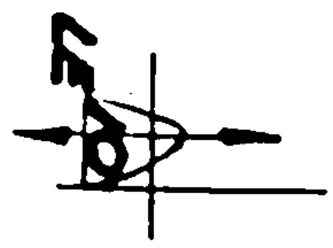

Fig.9.15 Exact Dimensions Of Different Layers (1 To 10) Of RR RB162, Stage 6 Compressor Blade.

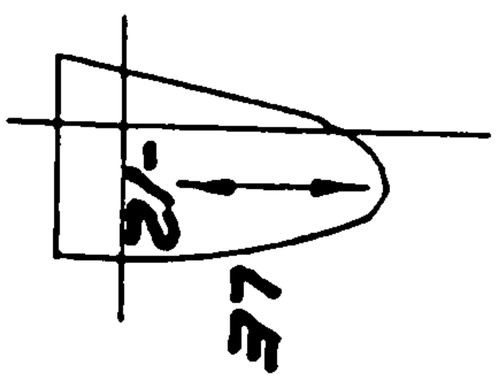
27-2
37

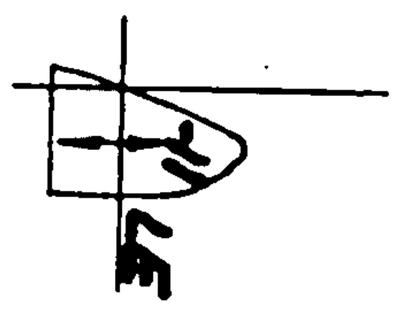
37

1262-14

1262-13

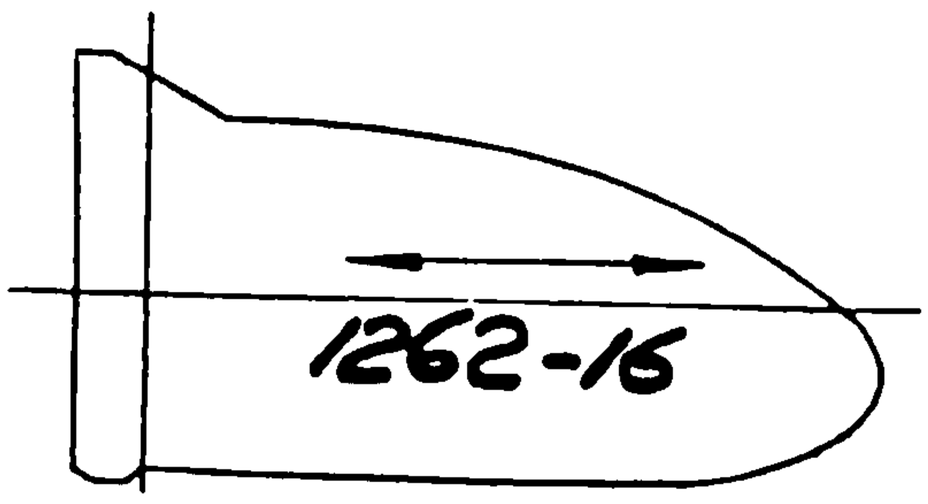
1262-16

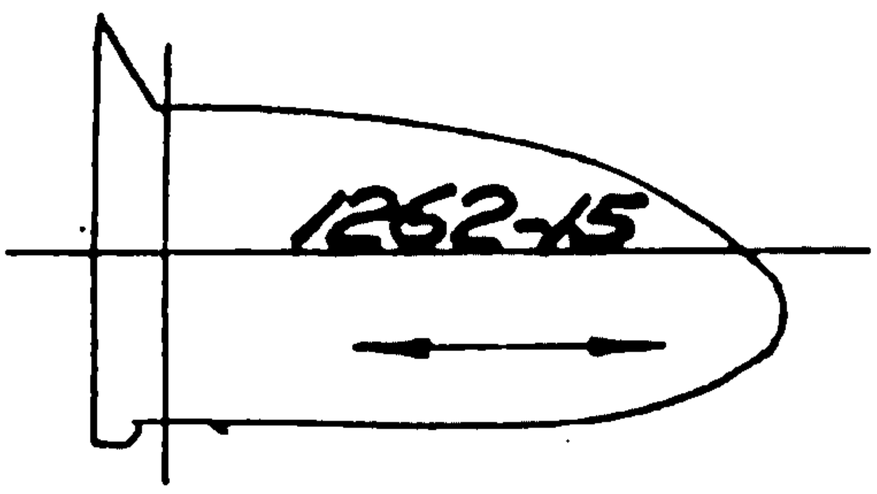
1262-15

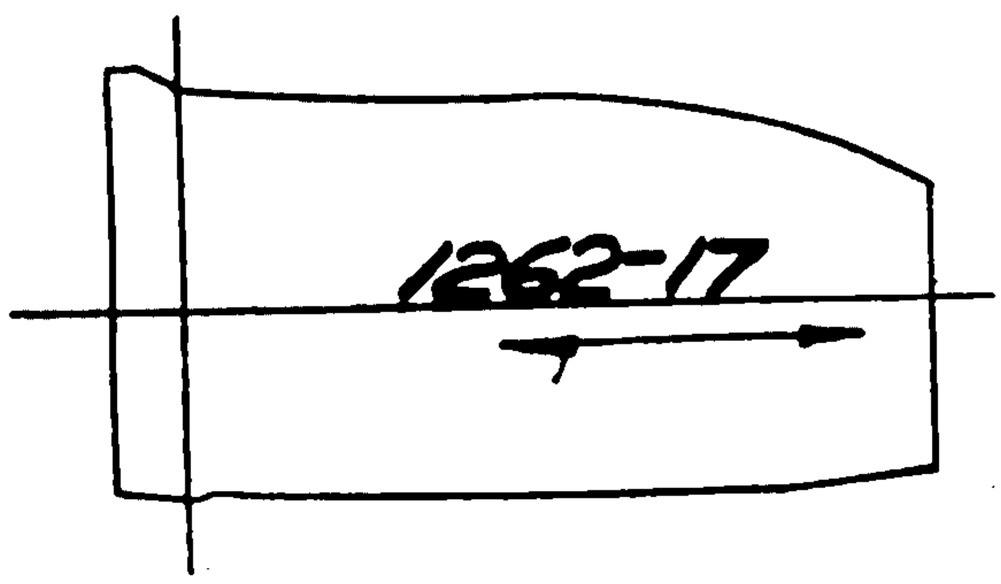
1262-17

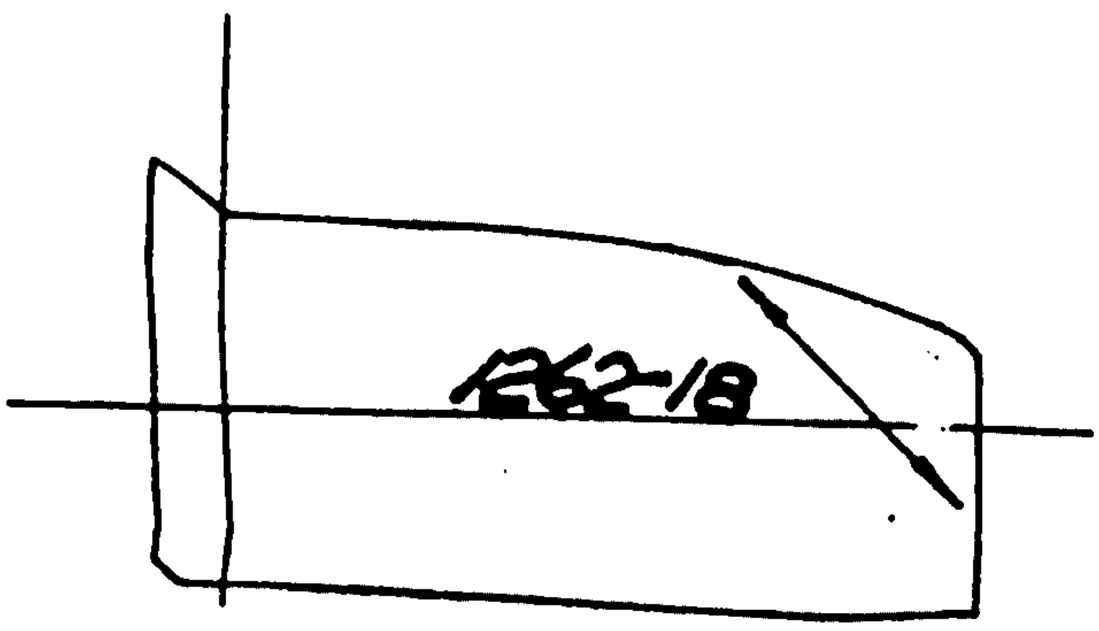
1262-18

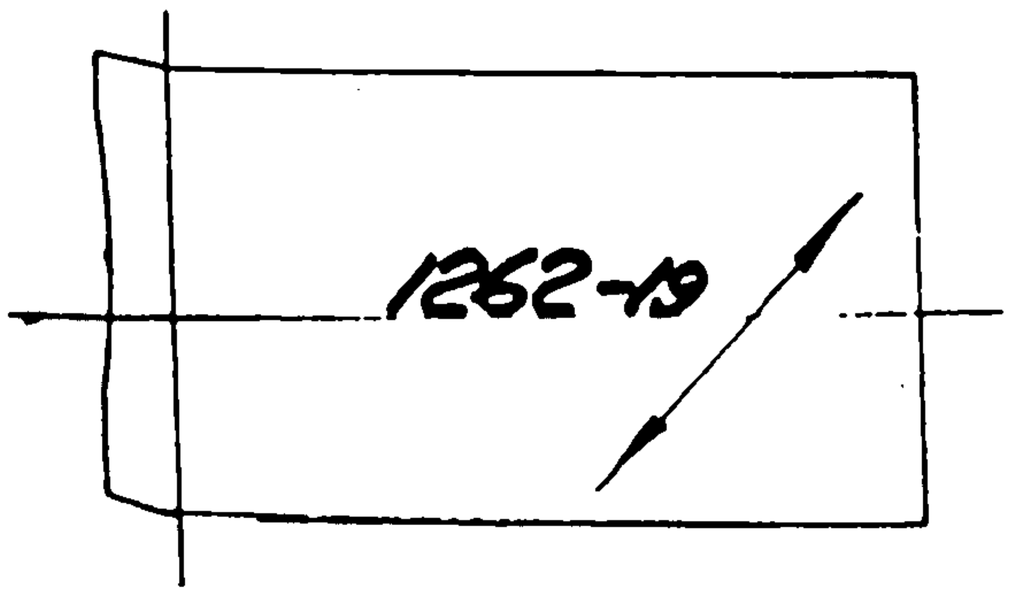
1262-19

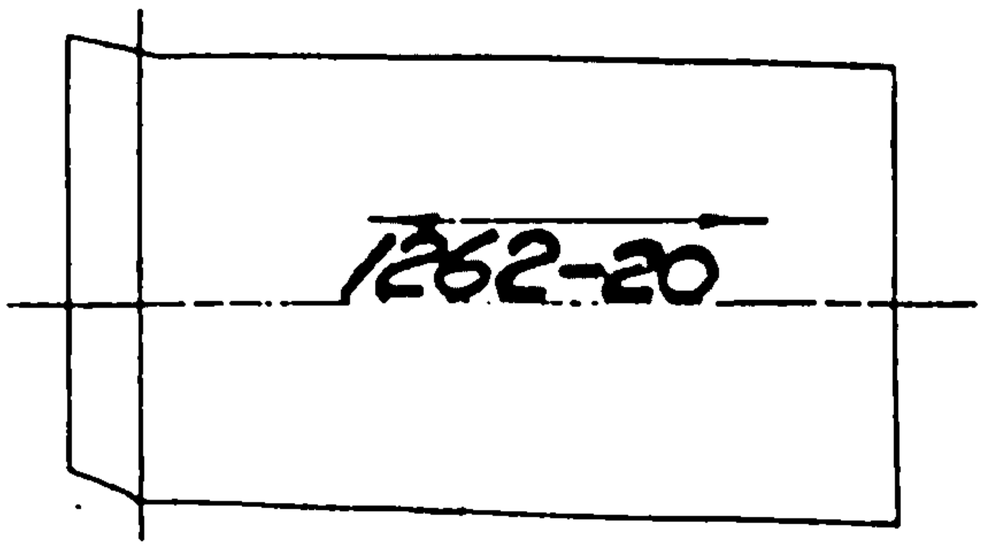
1262-20

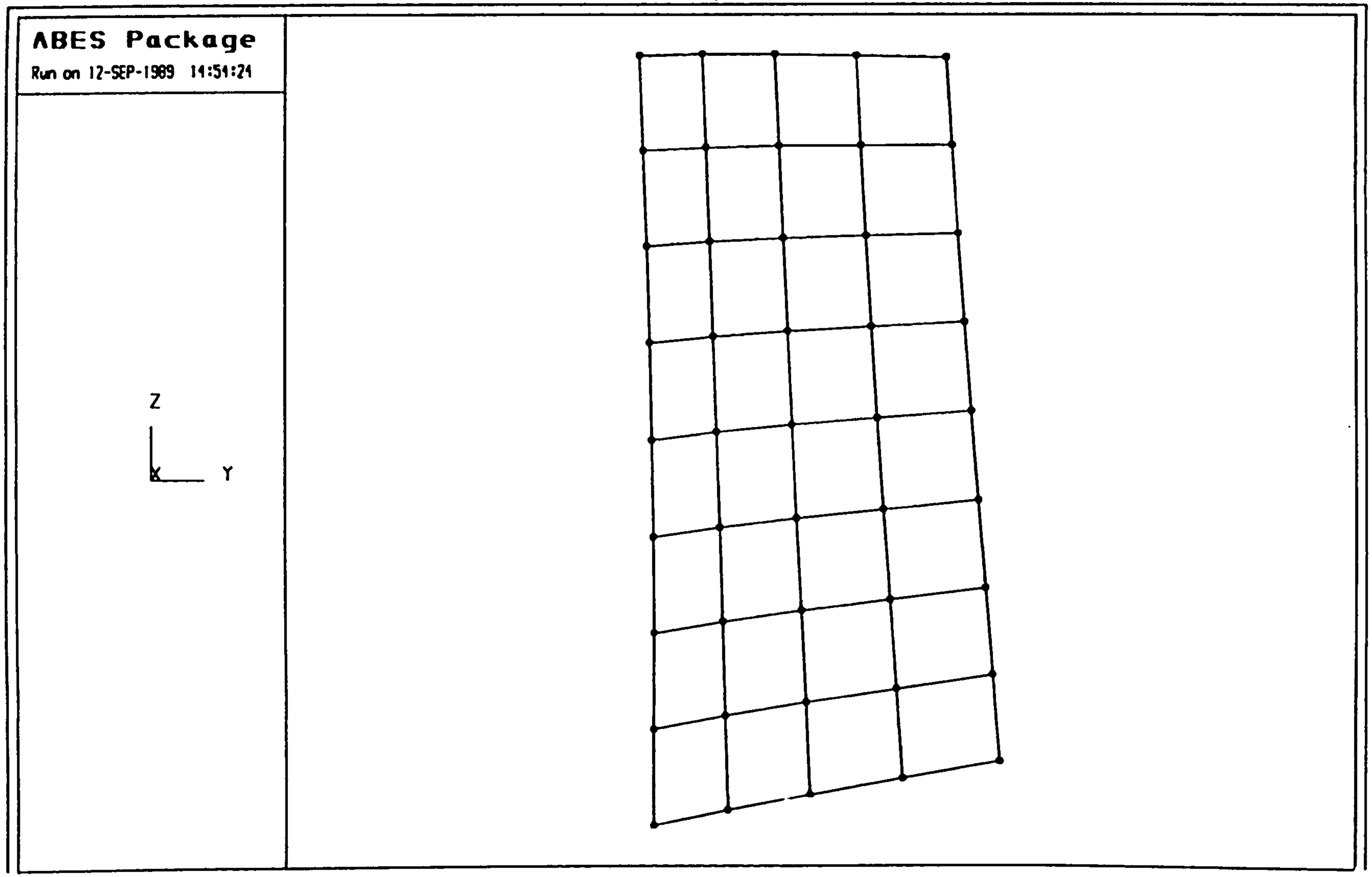

Fig.9.17 2-D Mesh Generated, Using 4-Noded Quadrilateral Elements, For The Analysis Of An RB162 Composite Blade

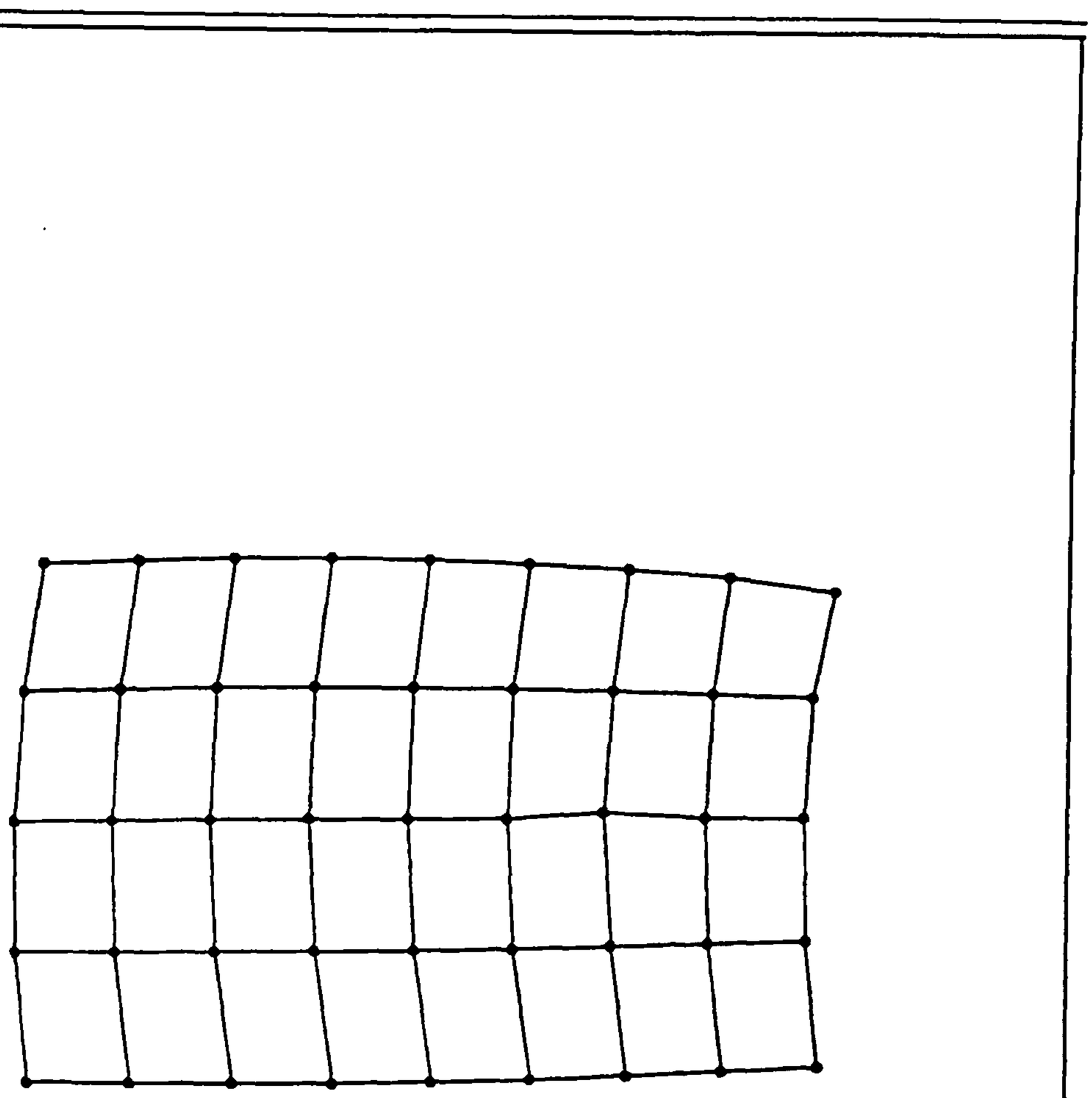

Fig.9.18 3-D Mesh Generated, Using 4-Noded Quadrilateral Elements, For The Analysis Of An RB162 Composite Blade

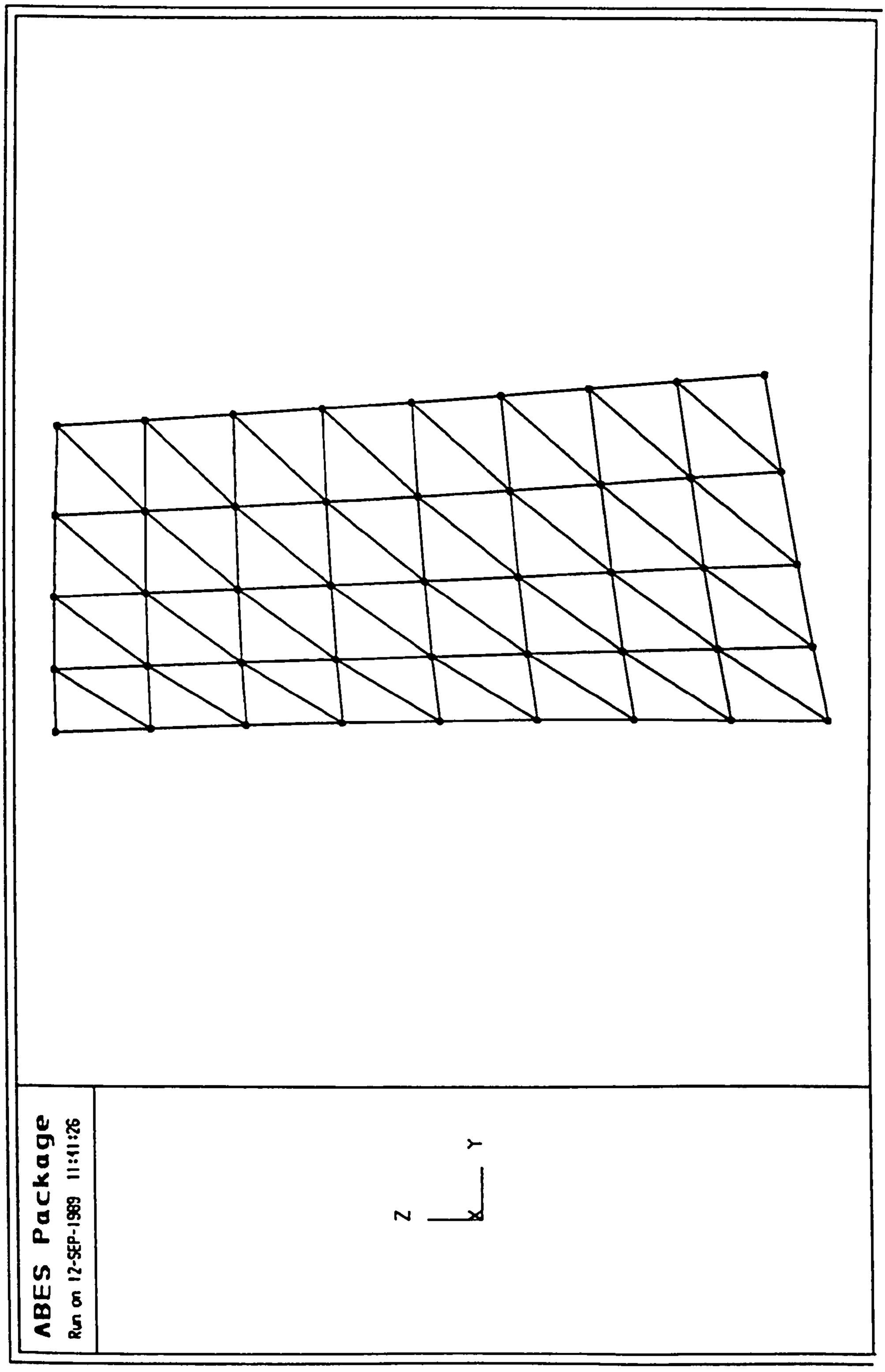

Fig.9.19 2-D Mesh Generated, Using 3-Noded Triangular Composite Elements, For The Analysis Of An RB162 Compressor Blade

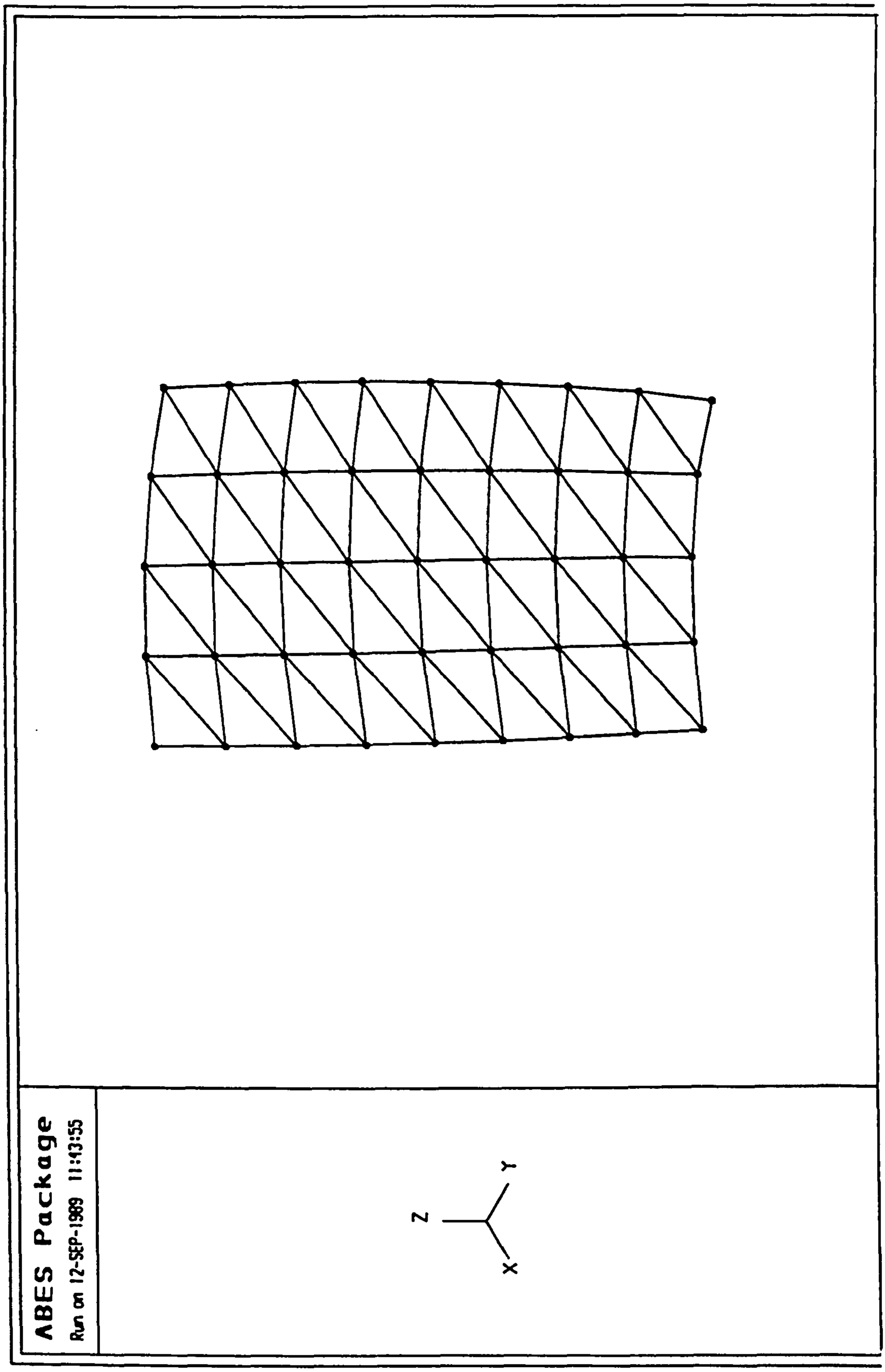

Fig.9.20 3-D Mesh Generation, Using 3-Noded Triangular Element, For The analysis of RB162 Blade.

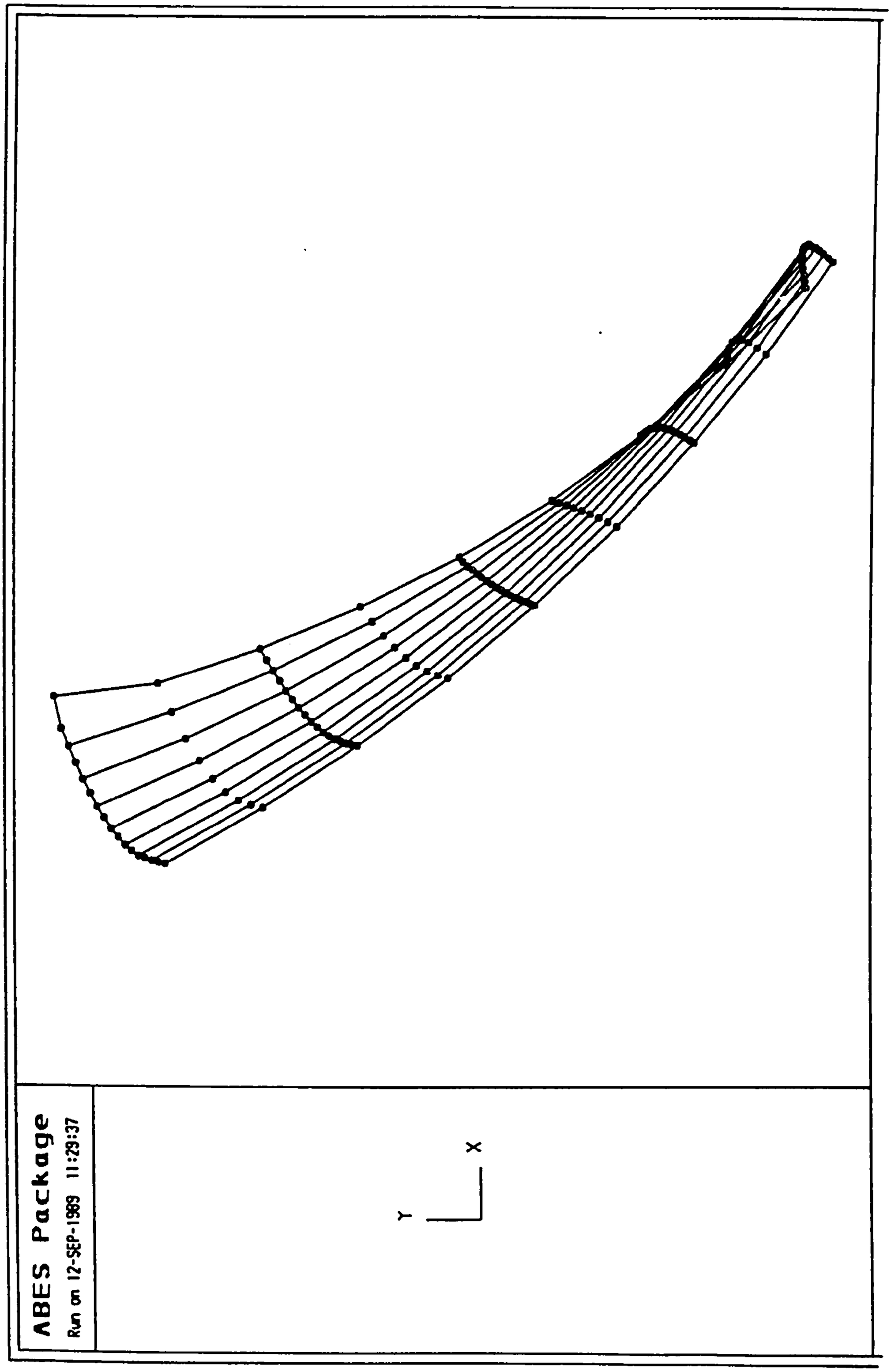

Fig.9.21 2-D Mesh Generation, Using 8-Noded Quadrilateral Element, For the Analysis of RB162 Blade.

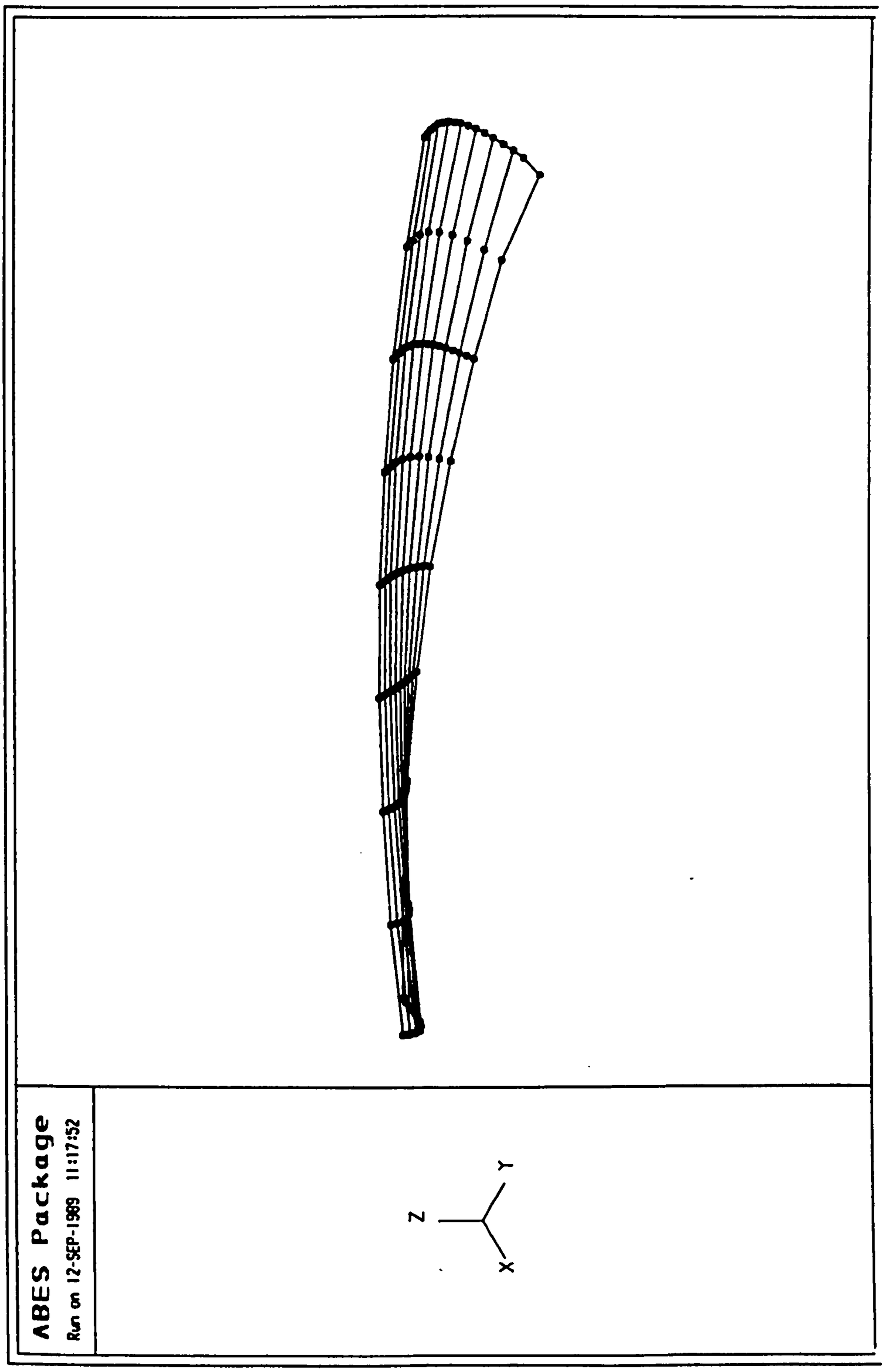

Fig.9.22 3-D Mesh Generated, Using 8-Noded Quadrilateral Elements, For The Analysis Of An RB162 Composite Blade

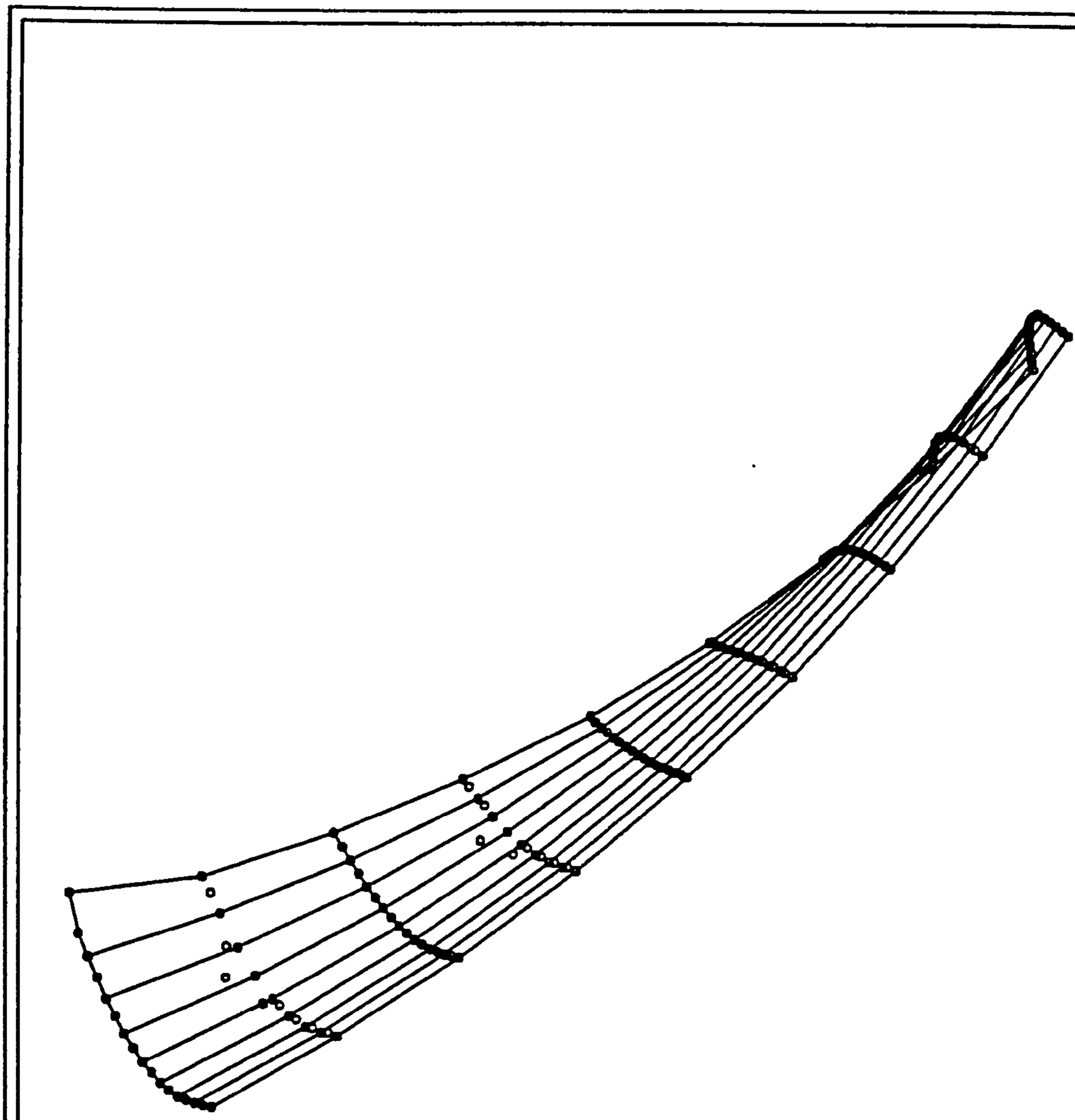

Fig.9.23 2-D Mesh Generated, Using 9-Noded Quadrilateral Elements, For The Analysis Of An RB162 Composite Blade

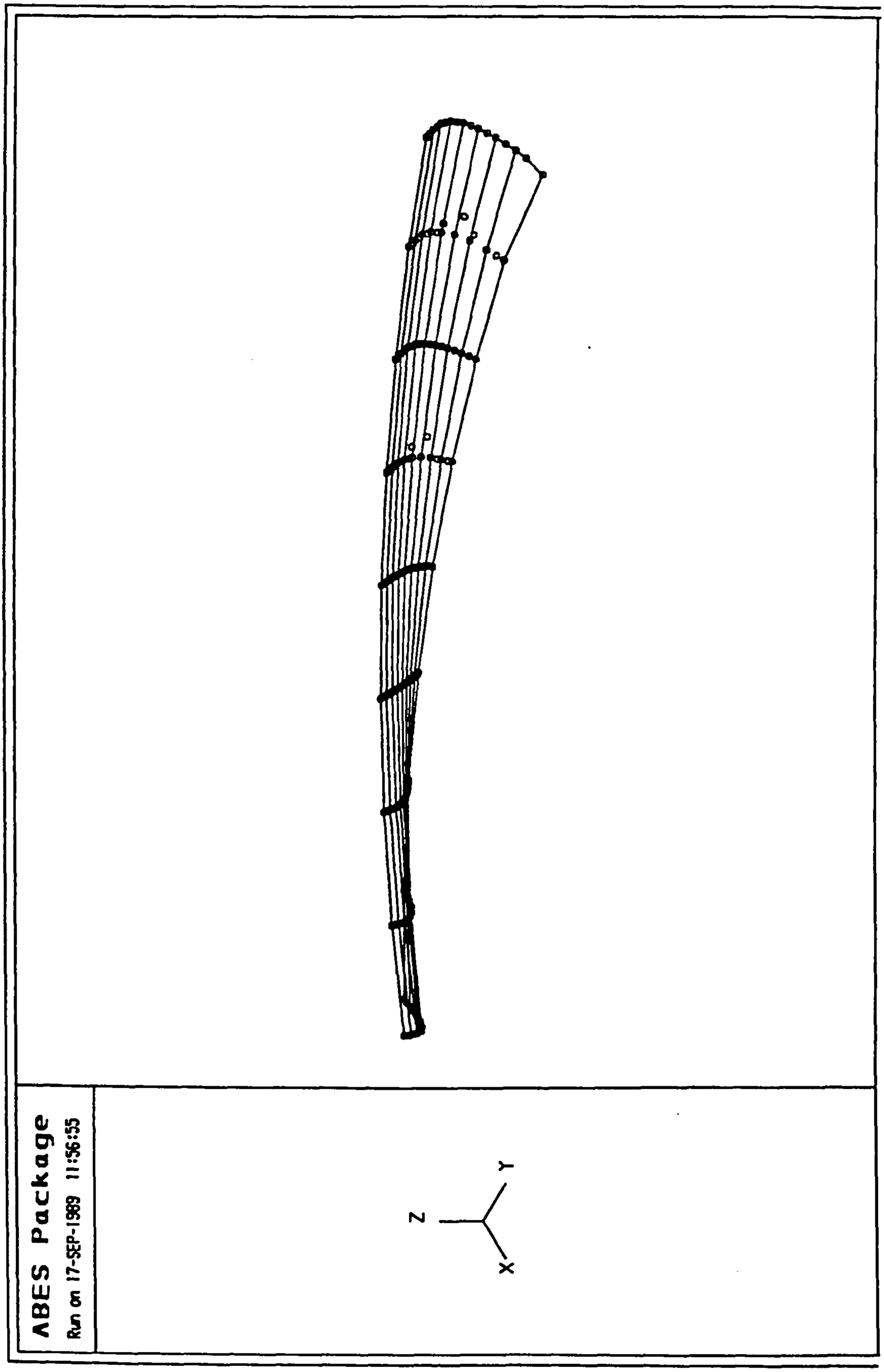

Fig.9.24 2-D Mesh Generated, Using 9-Noded Quadrilateral Elements, For The Analysis Of An RB162 Composite Blade

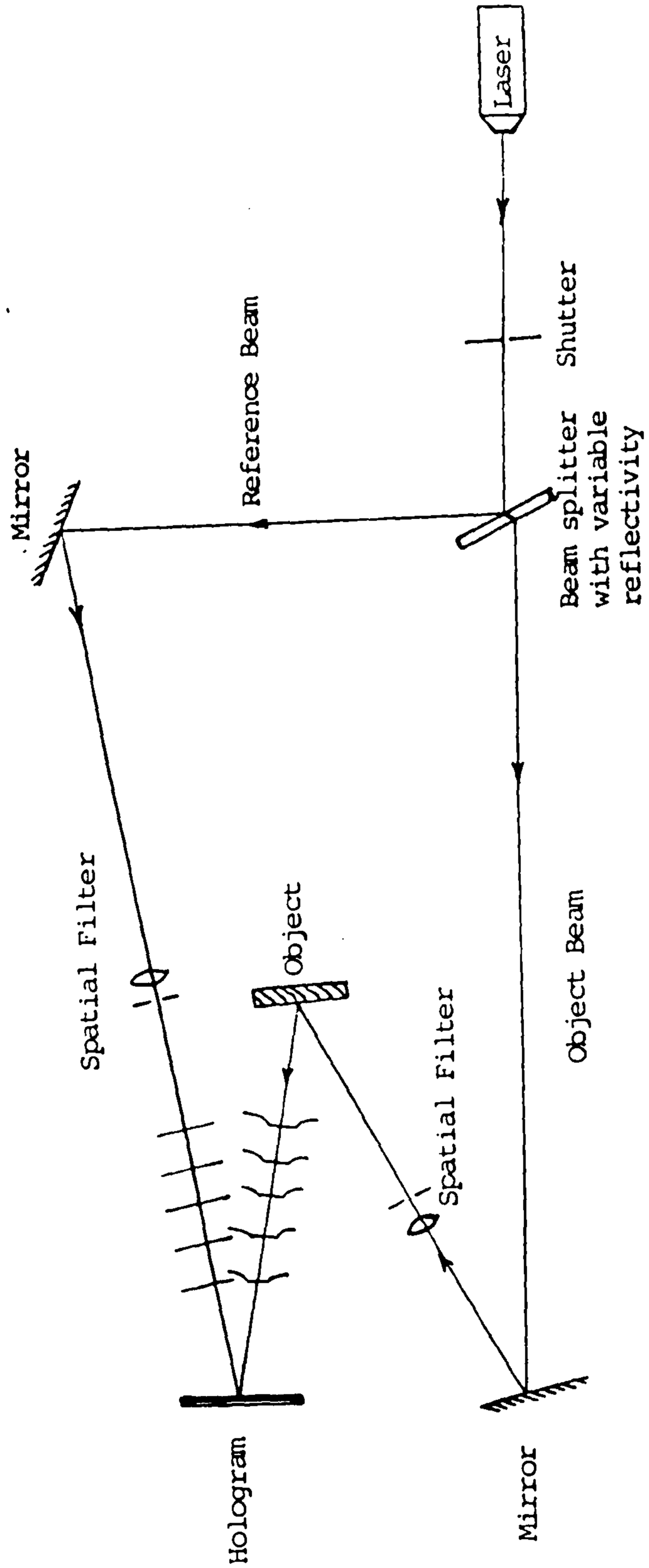

Fig.9.25 Set Up For Hologram Recording System.

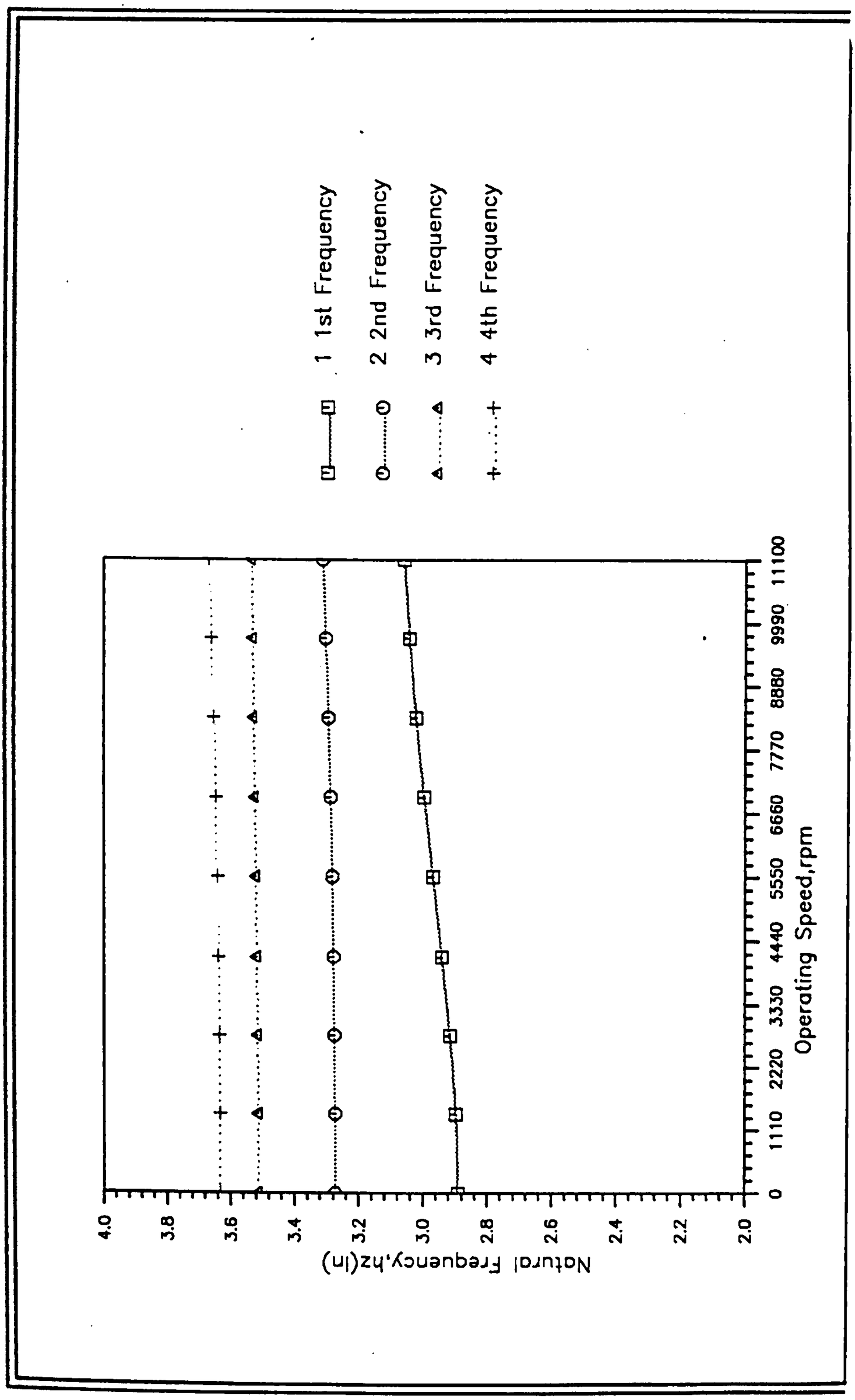

Fig.9.26 Plot Showing Natural Frequencies Of Composite Blade At Various Speeds.

9.27 Holographic Representation of 1st Frequency(1F) obtained through experiments.

FIG.9.28 Holographic Representation of 2nd Frequency(1T) Obtained by Experiments.

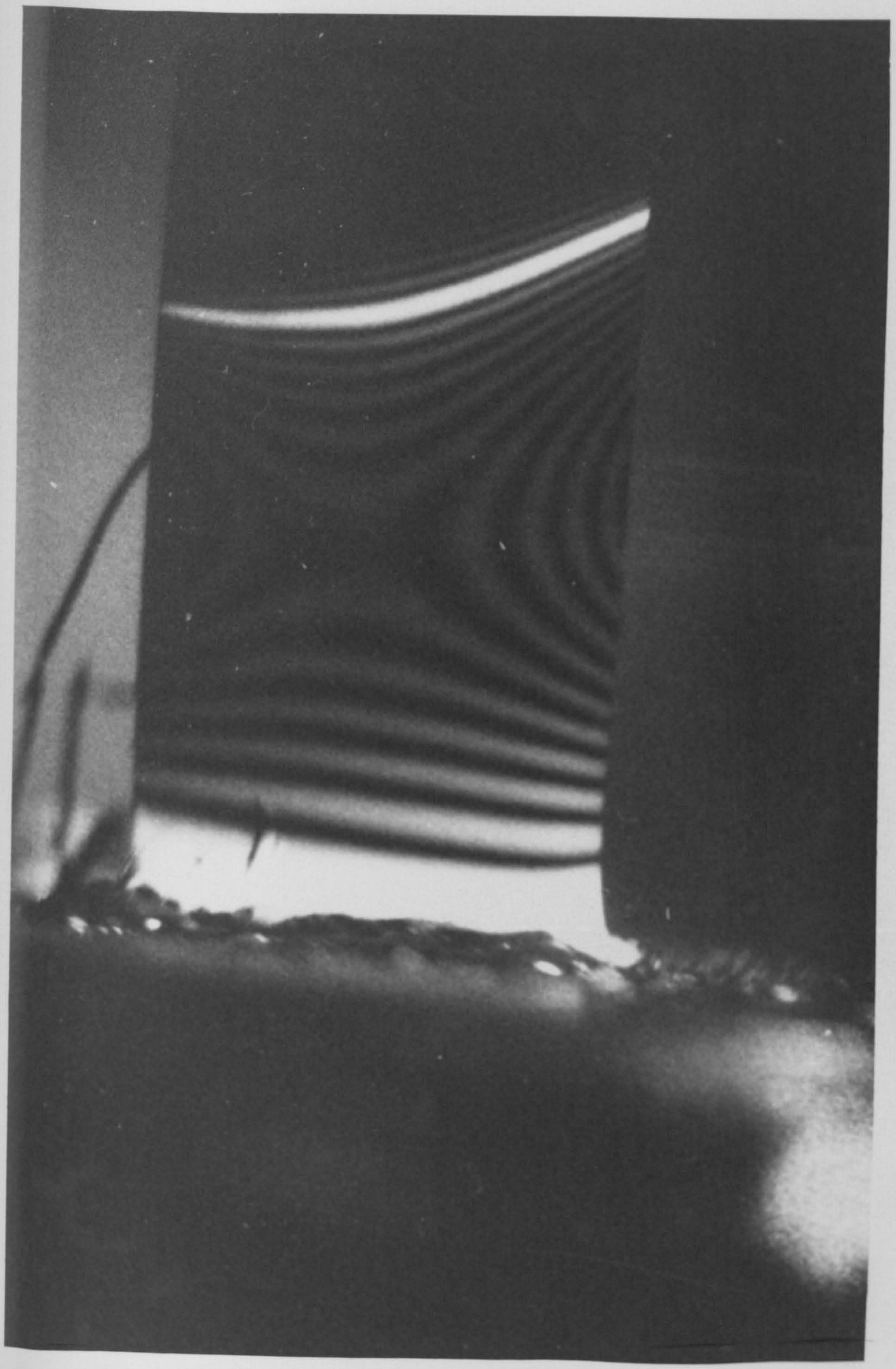

FIG.9.29 Holographic Representation of 3rd Frequency(2F) Obtained by Experiments.

	PACKAGE RESULTS			ANALYTICAL SOLUTION
VALUE (ω)	FACET SHELL ELEMENT	CURVED SHELL ELEMENT	HIGHER ORDER ELEMENT	
FIRST BEND.	23.01	23.01	23.01	25.04
SECOND BEND.	160.5	160.5	159.7	156.5

Table 9.1A Comparison of The Package Results With The Analytical Solution For The Case of a Cantilever Plate, Employing 3-Noded Triangular Elements.

NATURAL FREQ.	FIRST ORDER FACET SHELL	FIRST ORDER CURVED SHELL	HIGHER ORDER CURVED SHELL	EXPERIMENTAL RESULTS
ω1	741	741	417	455
ω2	1503	1503	1446	1955
ω3	4989	4989	2762	2500

Table 9.1 Results Obtained Using Developed Package For RR Isotropic Material Blade(at ω=0), Using 3-noded Triangular Elements With Selective Integration (NQ=2,2,1,2,2) vs Results Provided By RR.

	FIRST ORDER FACET SHELL	FIRST ORDER CURVED SHELL	HIGHER ORDER CURVED SHELL	EXPERIMENT RESULTS
ω1	649	649	418	455
ω2	1433	1433	1444	1965
ω3	4531	4531	2742	2500

Table 9.2 Results Obtained Using Developed Package For RR Isotropic Material Blade(at ω=0), Using 3-noded Triangular Elements With Full Integration vs Results Provided By RR.

NATURAL FREQ. (HZ)	SPEED (RPM)	0	2720	3440	6880	10320	13760
ω1		417	512	561	848	1132	1148
ω2		1444	1443	1443	1435	1433	1603
ω3		2741	2743	2744	2746	2716	2609

TABLE 9.3 Package Results Obtained, Using Higher Order Element, Employing 3-noded Triangular Elements With Full Integration, For The Centrifugal Stiffening Effects

NATURAL FREQUENCIES	FIRST ORDER FACET SHELL ELEMENT	FIRST ODRER CURVED SHELL ELEMENT	EXPER. RESULTS
ω1	1144	1076	874
ω2	2011	1951	1935
ω3	4650	4850	3855
ω4	5866	5817	----
ω5	6628	6461	----

Table 9.4 Results Obtained Using Developed Package For RR Composite Material Blade (ω=0), Using 4-noded Quadrilateral Elements With Full Integration

NATURAL FREQUENCIES	FIRST ORDER FACET SHELL ELEMENT	FIRST ORDER CURVED SHELL ELEMENT
ω1	1144	1075
ω2	2011	1950
ω3	4650	4650
ω4	5866	5816
ω5	6628	6461

Table 9.5 Results Obtained Using Developed Package For RR composite Material Blade(at ω=0), Using 4-noded Quadrilaateral Elements With Selective Integration (NQ=3,3,2,3,3).

NATURAL FREQUENCIES	FIRST ORDER FACET SHELL ELEMENT	FIRST ORDER CURVED SHELL ELEMENT
ω1	1144	1075
ω2	2011	1952
ω3	4650	4850
ω4	5868	5819
ω5	6627	6461

Table 9.6 Results Obtained Using Developed Package For RR Composite Material Blade(at ω=0), Using 4-noded Quadrilateral Elements With Reduced Integration (NQ=2,2,2,2,2).

NATURAL FREQUENCIES	FIRST ORDER FACET SHELL ELEMENT	FIRST ORDER CURVED SHELL ELEMENT
ω1	802	728
ω2	1790	1740
ω3	3050	3017
ω4	4074	3999
ω5	5236	5244

Table 9.7 Results Obtained Using Developed Package For RR composite Material Blade(at ω=0), Using 4-noded Quadrilateral Elements With Selective Reduced Integration (NQ=2,2,1,2,2).

NATURAL FREQUENCIES	FIRST ORDER FACET SHELL ELEMENT	FIRST ORDER CURVED SHELL ELEMENT
ω1	989	1076
ω2	2024	2189
ω3	3258	3142
ω4	3892	4563
ω5	5506	5016

Table 9.8 Results Obtained Using Developed Package For RR Composite Material Blade(at ω=0), Using 8-noded Quadrilateral Elements With Full Integration (NQ=3,3,3,3,3).

NATURAL FREQUENCIES	FIRST ORDER FACET SHELL ELEMENT	FIRST ORDER CURVED SHELL ELEMENT
ω1	968	1021
ω2	1950	2116
ω3	3163	2854
ω4	3498	3378
ω5	5048	4703

Table 9.9 Results Obtained Using Developed Package For RR Composite Material Blade(at ω=0), Using 8-noded Quadrilateral Elements With Selective Integration (NQ=3,3,2,3,3).

NATURAL FREQUENCIES	FIRST ORDER FACET SHELL ELEMENT	FIRST ORDER CURVED SHELL ELEMENT
ω1	933	945
ω2	1913	2036
ω3	3150	2789
ω4	3664	3396
ω5	5253	4038

Table 9.10 Results Obtained Using Developed Package For RR composite Material Blade(at ω=0), Using 8-noded Quadrilateral Elements With Reduced Integration (NQ=2,2,2,2,2).

NATURAL FREQUENCIES	FIRST ORDER FACET SHELL ELEMENT	FIRST ORDER CURVED SHELL ELEMENT
ω1	816	889
ω2	1924	2094
ω3	3151	3149
ω4	4260	4251
ω5	5400	5060

Table 9.11 Results Obtained Using Developed Package For RR Composite Material Blade(at ω=0), Using 9-noded Quadrilateral Elements With Selective Integration (NQ=3,3,2,3,3).

NATURAL FREQUENCIES	FIRST ORDER FACET SHELL ELEMENT	FIRST ORDER CURVED SHELL ELEMENT
ω1	805	841
ω2	1840	1951
ω3	3068	2758
ω4	4192	4028
ω5	5322	4704

Table 9.12 Results Obtained Using Developed Package For RR composite Material Blade(at ω=0), Using 9-noded Quadrilateral Elements With Reduced Integration (NQ=2,2,2,2,2).

NATURAL FREQUENCIES	FIRST ORDER FACET SHELL ELEMENT	FIRST ORDER CURVED SHELL ELEMENT	HIGHER ORDER FACET SHELL ELEMENT	EXPERI. RESULTS
ω1	1082	1082	777	874
ω2	4356	4347	1866	1935
ω3	6020	6018	3242	3855
ω4	6630	6627	----	----
ω5	11728	11687	----	----

Table 9.13 Results Obtained Using Developed Package For RR Composite Material Blade(at ω=0), Using 3-noded Triangular Elements With Reduced Integration (NQ=2,2,2,2,2)

NATURAL FREQUENCIES	FIRST ORDER FACET SHELL ELEMENT	FIRST ORDER CURVED SHELL ELEMENT	HIGHER ORDER FACET SHELL ELEMENT	EXPERI. RESULTS
ω1	876	876	762	874
ω2	3336	3336	1839	1935
ω3	4209	4209	3186	3855
ω4	6165	6165	4198	----
ω5	8407	8407	5684	----

Table 9.14 Results Obtained Using Developed Package For RR Composite Material Blade(at ω=0), Using 3-noded Triangular Elements With Reduced And Selective Integration (NQ=2,2,1,2,2).

NATURAL FREQUENCIES	FIRST ORDER FACET SHELL ELLMENT	FIRST ORDER CURVED SHELL ELEMENT	HIGHER ORDER FACET SHELL ELEMENT
ω1	1082	1082	777
ω2	4357	4357	1867
ω3	6020	6020	3242
ω4	6630	6630	4276

Table 9.15 Results Obtained Using Developed Package For RR Composite Material Blade(at ω=0), Using 3-noded Triangular Elements With Full Integration (NQ=3,3,3,3,3).

NATURAL FREQUENCIES	FIRST ORDER FACET SHELL ELLMENT	FIRST ORDER CURVED SHELL ELEMENT	HIGHER ORDER FACET SHELL ELEMENT
ω1	1082	1082	777
ω2	4346	4346	1866
ω3	6015	6015	3242
ω4	6626	6626	4276
ω5	11680	11680	--------

Table 9.16 Results Obtained Using Developed Package For RR Composite Material Blade(at ω=0), Using 3-noded Triangular Elements With Selective Integration (NQ=3,3,2,3,3).

NATURAL FREQUENCIES	FIRST ORDER FACET SHELL ELEMENT	FIRST ORDER CURVED SHELL ELEMENT
ω1	1362	1201
ω2	2054	2002
ω3	4723	4720
ω4	5934	5916
ω5	6681	6503

Table 9.17 Results Obtained Using Developed Package For RR Composite Material Blade, Using 4-noded Quadrilateral Elements With Full Integration For The Centrifugal Stiffening Effects At The Speed of Engine(ω) 11100 RPM.

NATURAL FREQUENCIES	FIRST ORDER FACET SHELL ELEMENT	FIRST ORDER CURVED SHELL ELEMENT
ω1	1228	1165
ω2	2046	1987
ω3	4702	4700
ω4	5918	5887
ω5	6667	6490

Table 9.18 Results Obtained Using Developed Package For RR composite Material Blade, And Using 4-noded Quadrilateral Elements With Full Integration For The Centrifugal Stiffening Effects At The Speed Of Engine(ω) 9300 RPM.

NATURAL FREQUENCIES	FIRST ORDER FACET SHELL ELLMENT	FIRST ORDER CURVED SHELL ELEMENT	HIGHER ORDER FACET SHELL ELEMENT
ω1	1207	1199	1130
ω2	4439	4434	2025
ω3	6059	6057	3379
ω4	6670	6667	4639

Table 9.19 Results Obtained Using Developed Package For RR Composite Material Blade, And Using 3-noded Triangular Elements With Full Integration For the Centrifugal Stiffening Effects At The Engine Speed(ω) Of 11100 RPM

NATURAL FREQUENCIES	FIRST ORDER FACET SHELL ELLMENT	FIRST ORDER CURVED SHELL ELEMENT	HIGHER ORDER FACET SHELL ELEMENT
ω1	1171	1165	1075
ω2	4415	4411	1974
ω3	6047	6046	3352
ω4	6658	6658	4526

Table 9.20 Results Obtained Using Developed Package For RR Composite Material Blade, And Using 3-noded Triangular Elements With Selective Integration For The Centrifugal Stiffening Effects At The Engine Speed(ω) Of 9300 RPM

NATURAL FREQUENCIES	FIRST ORDER FACET SHELL ELEMENT	FIRST ORDER CURVED SHELL ELEMENT
ω1	1228	1197
ω2	2046	2231
ω3	4702	3245
ω4	5918	4590
ω5	6667	5037

Table 9.21 Results Obtained Using Developed Package For RR composite Material Blade, And Using 8-noded Quadrilateral Elements With Full Integration For The Centrifugal Stiffening Effects At The Engine Speed(ω) Of 11100 RPM.

NATURAL FREQUENCIES	FIRST ORDER FACET SHELL ELEMENT	FIRST ORDER CURVED SHELL ELEMENT
ω1	1089	1165
ω2	2054	1987
ω3	3345	4700
ω4	3925	5887
ω5	5542	6490

Table 9.22 Results obtained using developed package for RR Composite Material Blade, And Using 8-noded Quadrilateral Elements With Full Integration For The Centrifugal Stiffening Effects At The Engine Speed(ω) Of 9300 RPM

NATURAL FREQUENCIES	FIRST ORDER FACET SHELL ELEMENT	FIRST ORDER CURVED SHELL ELEMENT
ω1	963	993
ω2	1934	2007
ω3	3206	2890
ω4	4262	4118
ω5	5375	4754

Table 9.23 Results Obtained Using Developed Package For RR Composite Material Blade, And Using 9-noded Quadrilateral Elements With Full Integration For The Centrifugal Stiffening Effects At The Engine Speed(ω) Of 11100 RPM.

NATURAL FREQUENCIES	FIRST ORDER FACET SHELL ELEMENT	FIRST ORDER CURVED SHELL ELEMENT
ω1	919	950
ω2	1922	1990
ω3	3166	2852
ω4	4241	4092
ω5	5360	4739

Table 9.24 Results Obtained Using Developed Package For RR composite Material Blade, And Using 9-noded Quadrilateral Elements With Full Integration For The Centrifugal Stiffening Effects At The Engine Speed(ω) Of 9300 RPM.

NATURAL FREQ. (HZ)	SPEED (RPM)	0	1387	2775	4162	5550	6937	8325	9712	11100
ω1		776	787	819	866	922	981	1038	1088	1129
ω2		1866	1868	1874	1885	1901	1922	1950	1984	2025
ω3		3242	3245	3255	3270	3290	3312	3335	3358	3379
ω4		4275	4280	4296	4322	4360	4410	4473	4549	4639

TABLE 9.25 Package Results Obtained, Using Higher Order Element Analysis, Employing 3-noded Triangular Elements With Full Integration, For The Centrifugal Stiffening Effects On RB162 Blade.

APPENDIX A-1 MODULE STATIC-MASTER

-MASTER

-SUBROUTINE ASSEMBLER

-SUBROUTINE REDUCER

-SUBROUTINE SOLVER

-SUBROUTINE OLD SOLVER

-SUBROUTINE DISP

-SUBROUTINE REACT

APPENDIX A-2 MODULE STATIC-FRONT

-MASTER

-SUBROUTINE INITIATION

-SUBROUTINE FRONT

-SUBROUTINE SOLVER

-SUBROUTINE STIFF

-SUBROUTINE DISP

APPENDIX A-3 MODULE DYNAMIC-BAND

-MASTER

-SUBROUTINE REDUCER

-SUBROUTINE DISP

-SUBROUTINE SUBSPACE

-SUBROUTINE SOLVER

-SUBROUTINE TPRODUCT

-SUBROUTINE TRANSF

-SUBROUTINE DCOMP

-SUBROUTINE EITR

-SUBROUTINE LPKS

-SUBROUTINE SHIFT

-SUBROUTINE ASSEMBLER

-SUBROUTINE GAUSOL

-SUBROUTINE REACT

-SUBROUTINE INITIATE

-SUBROUTINE SOLV

-SUBROUTINE BAND PRODUCT

-SUBROUTINE EIGENV

-SUBROUTINE CHOLES

-SUBROUTINE SWEEP

-FUNCTION SPR

-SUBROUTINE OUTPUT

APPENDIX A-4 MODULE DYNAMIC-FRONT

-MASTER

-SUBROUTINE XMAT

-SUBROUTINE FPRODUCT

-SUBROUTINE EIGENV

-SUBROUTINE CHOLES

-SUBROUTINE SWEEP

-FUNCTION SPR

-SUBROUTINE INITIATION

-SUBROUTINE SOLVER

-SUBROUTINE STIFF

-SUBROUTINE OUTPUT

-SUBROUTINE SUBSI

-SUBROUTINE TPRODUCT

-SUBROUTINE TRANSF

-SUBROUTINE DCOMP

-SUBROUTINE EITR

-SUBROUTINE LPKS

-SUBROUTINE SHIFT

-SUBROUTINE FRONT

-SUBROUTINE S-SOLVER

-SUBROUTINE MASS

-SUBROUTINE DISP

APPENDIX A-5 MODULE FACET-UT/VT

-SUBROUTINE DATA -SUBROUTINE INFORM -SUBROUTINE STRESS

-SUBROUTINE ESMG -SUBROUTINE ESMGIN -SUBROUTINE ESMGB

-SUBROUTINE ESMGS -SUBROUTINE ESMGINB -SUBROUTINE CARTD

-SUBROUTINE BMATRIXM -SUBROUTINE JACOB -SUBROUTINE BMATRIXB

-SUBROUTINE LOCAL -SUBROUTINE BMATRIXS -SUBROUTINE NFVG

-SUBROUTINE NODEF -SUBROUTINE LACC -SUBROUTINE RVECTOR

-SUBROUTINE EMMG -SUBROUTINE EMMG11 -SUBROUTINE EMMG12

-SUBROUTINE EMMG22 -SUBROUTINE NMATRIX11 -SUBROUTINE NMATRIX22

-SUBROUTINE CSMADD -SUBROUTINE CSEMG1 -SUBROUTINE CSEMG2

-SUBROUTINE CSEMG3 -SUBROUTINE CSEMG4 -SUBROUTINE GMAT1

-SUBROUTINE GMAT2 -SUBROUTINE SMATM11 -SUBROUTINE SMATM12

-SUBROUTINE SMATB11 -SUBROUTINE SMATB12

APPENDIX A-6 MODULE AHMAD-UT/VT

-SUBROUTINE DATA	-SUBROUTINE INFORM	-SUBROUTINE STRESS
-SUBROUTINE ESMG	-SUBROUTINE ESMGM	-SUBROUTINE ESMGB
-SUBROUTINE ESMGS	-SUBROUTINE ESMGINB	-SUBROUTINE BMATRIXS
-SUBROUTINE BMATRIXM	-SUBROUTINE JACOB	-SUBROUTINE BMATRIXB
-SUBROUTINE NFVG	-SUBROUTINE CMATRIX	-SUBROUTINE AVECTOR
-SUBROUTINE EMMG	-SUBROUTINE EMMG11	-SUBROUTINE EMMG12
-SUBROUTINE EMMG22	-SUBROUTINE NMATRIX11	-SUBROUTINE NMATRIX22
-SUBROUTINE CSMADD	-SUBROUTINE CSEMG1	-SUBROUTINE CSEMG2
-SUBROUTINE GMATRIX	-SUBROUTINE SMATM	-SUBROUTINE SMATB

APPENDIX A-7 MODULE FACET-HER

-SUBROUTINE DATA -SUBROUTINE INFORM -SUBROUTINE STRESS

-SUBROUTINE ESMG -SUBROUTINE ESMGIN -SUBROUTINE ESMGT

-SUBROUTINE ESMGB -SUBROUTINE ESMGS -SUBROUTINE ESMGBT

-SUBROUTINE BMATRIXM -SUBROUTINE BMATRIXB -SUBROUTINE BMATRIBS

-SUBROUTINE LOCAL -SUBROUTINE NFVG -SUBROUTINE NODEF

-SUBROUTINE LACC -SUBROUTINE RVECTOR -SUBROUTINE EMMG

-SUBROUTINE EMMGIN -SUBROUTINE EMMGS -SUBROUTINE EMMGB

-SUBROUTINE EMMGW -SUBROUTINE EMMGBS -SUBROUTINE NMATRIXIN

-SUBROUTINE NMATRIXB -SUBROUTINE NMATRIXW -SUBROUTINE CSMADD

-SUBROUTINE CSEMGM -SUBROUTINE CSEMGS -SUBROUTINE CSEMGB

-SUBROUTINE CSEMGW -SUBROUTINE CSEMGBS -SUBROUTINE GMATM

-SUBROUTINE GMATB -SUBROUTINE GMATW -SUBROUTINE SMATM

-SUBROUTINE SMATS -SUBROUTINE SMATW -SUBROUTINE SMATB

-SUBROUTINE SMATBS

APPENDIX A-8 MODULE COMMON-UT/VT

-SUBROUTNE MATI

-SUBROUTINE MATV

-SUBROUTINE MATSV

-SUBROUTINE MATS

-SUBROUTINE MATM

-SUBROUTINE MATT

-SUBROUTINE INTRCO

-SUBROUTINE INTRD

-SUBROUTINE SHAPE

-SUBROUTINE GET GAUSS

-SUBROUTINE BWF

APPENDIX A-9 MODULE COMMON-HER

-MODULE COMMON-UT/VT

-SUBROUTINE CARTD

-SUBROUTINE JACOB

-SUBROUTINE HCARD1

-SUBROUTINE HCARTD2

-SUBROUTINE JACOB2

-SUBROUTINE HSHAPE

-SUBROUTINE HINTRD1

-SUBROUTINE HINTRD2

APPENDIX A-10 MODULE MATERIAL-UT/VT

-SUBROUTINE DMATRIX

-SUBROUTINE LAYERD

-SUBROUTINE AMATRIX

-SUBROUTINE BEMATRIX

-SUBROUTINE QMATRIX

-SUBROUTINE DR11

-SUBROUTINE DR12

-SUBROUTINE DR22

-SUBROUTINE PZ (for VT only)

APPENDIX A-11 MODULE MATERIAL-HER

-SUBROUTINE DMATRIX
-SUBROUTINE LAYERD
-SUBROUTINE LAYERDM
-SUBROUTINE DMATRIXIN
-SUBROUTINE DMATRIXT
-SUBROUTINE DMATRIXB
-SUBROUTINE DMATRIXBT
-SUBROUTINE DMATRIXS
-SUBROUTINE ROWIN
-SUBROUTINE ROWB
-SUBROUTINE ROWS
-SUBROUTINE ROWBS
-SUBROUTINE PZ
-SUBROUTINE HVECTORM
-SUBROUTINE HVECTORB
-SUBROUTINE HVECTORS
-SUBROUTINE HVECTORBS